

HYDROPROCESSING OF BIOMASS DERIVED OILS TO TRANSPORTATION FUELS

Ph.D. THESIS

by

MUKESH KUMAR PODDAR



DEPARTMENT OF CHEMISTRY
INDIAN INSTITUTE OF TECHNOLOGY ROORKEE
ROORKEE – 247 667 (INDIA)
JUNE, 2019

HYDROPROCESSING OF BIOMASS DERIVED OILS TO TRANSPORTATION FUELS

A THESIS

*Submitted in partial fulfilment of the
requirements for the award of the degree*

of

DOCTOR OF PHILOSOPHY

in

CHEMISTRY

by

MUKESH KUMAR PODDAR



DEPARTMENT OF CHEMISTRY
INDIAN INSTITUTE OF TECHNOLOGY ROORKEE
ROORKEE – 247 667 (INDIA)
JUNE, 2019

**©INDIAN INSTITUTE OF TECHNOLOGY ROORKEE, ROORKEE-2019
ALL RIGHTS RESERVED**

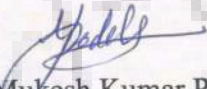


INDIAN INSTITUTE OF TECHNOLOGY ROORKEE
ROORKEE

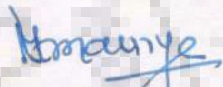
CANDIDATE'S DECLARATION

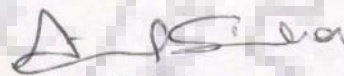
I hereby certify that the work which is being presented in the current thesis entitled "HYDROPROCESSING OF BIOMASS DERIVED OILS TO TRANSPORTATION FUELS" in partial fulfilment of the requirements for the award of the Degree of Doctor of Philosophy and submitted in the Department of Chemistry of the Indian Institute of Technology Roorkee is an authentic record of my own work carried out during a period from July, 2013 to June, 2019 under the supervision of Dr. Mannar Ram Maurya, Professor, Department of Chemistry, Indian Institute of Technology Roorkee, Roorkee and Dr. Anil Kumar Sinha, Sr. Principal Scientist Bio Fuel Division, CSIR-Indian Institute of Petroleum, Dehradun.

The matter presented in the thesis has not been submitted by me for the award of any other degree of this or any other Institute.

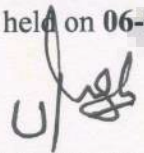

Mukesh Kumar Poddar
Signature of the Candidate

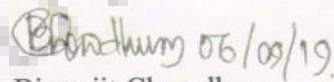
This is to certify that the above statement made by the candidate is correct to the best of my knowledge.


(M. R. Maurya)
Signature of Supervisor

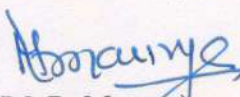

(A. K. Sinha)
Signature of Supervisor

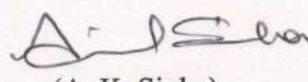
The Ph.D. Viva-Voce Examination **Mr. Mukesh Kumar Poddar**, Research Scholar, has been held on **06-09-2019**.



(U. P. Singh)
Chairman, SRC


Biswajit Chowdhury
Signature of External Examiner

This is to certify that the student has made all the corrections in the thesis.


(M. R. Maurya)
Supervisor


(A. K. Sinha)
Supervisor


K. R. Justin Thomas
Head of the Department

Dated: 06/09/2019

डा. के. आर. जस्टिन थॉमस
Dr. K. R. Justin Thomas
प्रोफेसर एवं विभागाध्यक्ष / Prof. & Head
रसायन विभाग / Chemistry Deptt.
भा. प्रौद्योगिकी संस्थान / I.I.T. Roorkee

ABSTRACT

Energy is the foundation of economic and infrastructure development. Environmental concerns, global energy requirement, and declining fossil fuel reserves have boosted energy research on alternative source from conventional fossil fuels to an alternative renewable and sustainable sources. Based on the availability of biomass feedstock, first generation, second generation, and third generation are the classification of biofuels.

First generation biofuels are bio-ethanol and bio-diesel, which are produced by using biological process (fermentation) and chemical-process (trans-esterification) from edible sources like sugar, starch and plant seeds oils (vegetable oils) etc. The production of first-generation biofuels is very less in comparison to the requirement in terms of conventional refineries/fossil fuels, so there is an issue with demand vs. supplies, i.e. competition with the food industry and fuels, which may raise ethical questions. It also doesn't give the drop-in-fuel quality. Research now strongly focuses on the so-called second-generation biofuels.

Second generation biofuels give attention to the thermal conversion of non-edible biomass sources. The thermal conversion has mainly four processes: combustion, gasification, hydrothermal liquefaction and pyrolysis. Combustion is already widely practiced. Gasification has higher efficiency as compared to combustion. It has a high level of interest, to produce bio-syngas to generate methanol or transportation fuels like gasoline, kerosene and diesel. Hydrothermal liquefaction (HTL) of biomass has been done in presence of solvents at various temperature and pressure. Pyrolysis process decomposes the biomass in the absence of oxygen to generate vapors (pyrolysis vapor) and aerosols with some char/coke (bio-char) at high temperature, on condensation of pyrolysis vapor a liquid has been obtained, called pyrolysis oil/bio oil.

The Third-generation biofuels concern about fast-growing feedstokes, requires less maintenance/nutrient and low cost for production. It has tendency to regenerate in the less fertile soil, and resistance to extreme weather conditions. The third-generation

biomass includes microalgae and macroalgae. Marine biomass such as seaweed, hyacinth, caltrop diatoms, duckweed, and algae have a strong domain for the production of biofuels. In recent year Aquatic biomass (microalgae) is considered third-generation biomass and advanced biofuel feedstock due to their perennial and inherent growth, high growth rate and areal productivity as well as no competency with arable land and crops for space, sunlight, and nutrients.

Algal biomass can produce different types of biofuels, including bioethanol, biodiesel, syngas, gasoline, kerosene/jet oil and diesel (green diesel). Some of them biofuels, like gasoline, kerosene/jet oil and diesel (green diesel) can produce by hydroprocessing, a refinery technique for upgradation of biomass derived oil (pyrolysis oil/bio oil and algae oil/lipids) by using batch reactor as well as continuous fixed bed (microchannel) reactor.

For convenience, the work embodied in the thesis has been divided into the following chapters:

First chapter

This chapter is introductory one and presents general remarks on first, second, and third generation biofuels. This chapter also deals with hydroprocessing of biomass-derived oil to transportation fuels. Updated literature survey has also been included here.

Second chapter

This chapter deals with the production of transportation fuels (gasoline, kerosene, and diesel) by hydroprocessing of mixture of gas oil (GO) with heavy, dark viscous pyrolysis oil/ bio oil liquid (BO) obtained from waste de-oiled jatropha curcas seeds cake (JCC). A sulfided cobalt–molybdenum phosphorus/aluminum oxide ($\text{CoMoP/Al}_2\text{O}_3$) catalyst was studied in the hydroprocessing of bio-oil (BO) obtained from the pyrolysis of de-oiled *Jatropha curcas* seed cake. Hydroprocessing was carried out with different ratios of GO and BO with sulfided cobalt–molybdenum phosphorus/aluminum oxide ($\text{S-CoMoP/Al}_2\text{O}_3$) catalyst. The oxygen content in the products was reduced to trace amounts after hydroprocessing. A clear liquid product having 2–16 % gasoline, 30–35 %

kerosene/jet oil and 35–44 % diesel has been produced by co-processing of BO with refinery GO in various ratios. This liquid have 50–60 % alkanes, 10–45 % cycloalkanes, and 1–10 % aromatics with negligible amount of char. Hydroprocessing of 100 % BO produce 10 % gasoline, 30 % kerosene/jet oil and 30 % diesel. This liquid has 15 % of alkanes, 15% cycloalkanes, and 45 % aromatics. A maximum amount of kerosene (41%) was obtained at 375°C and 75 bar from 100 % BO, with a small amount of char (1.5%) deposited on the catalyst. In comparison, over sulfided CoMo/Al₂O₃ catalyst (without P promoter) only 31% of kerosene was produced, with 17% char, using similar reaction conditions. The advantage of this work is that transportation fuels can be produced by using a single catalyst instead of other expensive multi-catalyst processes such as hydrodeoxygenation with noble metals followed by cracking.

Third chapter

This chapter discusses the production of transportation fuels (gasoline, kerosene, and diesel) by hydroprocessing of aqueous-phase of pyrolysis oil obtained from de-oiled jatropha curcas seeds cake (JCC), by using sulfided NiMo/SiO₂-Al₂O₃ catalyst coated in a microchannel reactor. The oxygen contents of the dissolved organic compound in the aqueous-phase were reduced to trace amount after hydroprocessing. Clear organic hydrocarbon phase product obtained after hydroprocessing contained 5-45% gasoline (<C₉), 5-60% kerosene (C₉-C₁₄), 15-40% diesel (C₁₅-C₁₈). This liquid has 15-65% alkanes, 0-5% polyaromatic hydrocarbons (PAH) with negligible amount of cycloalkanes and aromatics. The unreacted feedstock and residues was 30-75%. Maximum hydrocarbon yield (~65%) was obtained at 375°C, 0.25 LHSV, and 70 bar. The water obtained after hydroprocessing contained little organics (<5%).

Microchannel reactor has the advantages of portability, easy scale-up, better heat and mass transfer characteristics, high reaction throughputs, precise control of hydrodynamics. The good thing about this work is that transportation fuels can be produced by using small modular microchannel reactors (with catalyst coating inside the channels) compared to using largely fixed bed reactors. Additionally, this process improves the economics of processing bio-oils by utilizing its aqueous-phase (containing

~30% inseparable soluble organics) to produce hydrocarbon fuels.

Fourth Chapter

This chapter deals with the production of transportation fuels from triacylglycerides neutral lipids (TAGs) extracted from marine microalgae algae *Nannochloropsis* sp by hydroprocessing over sulfided cobalt molybdenum phosphorus/aluminum oxide (S-CoMoP/Al₂O₃) catalyst in a batch reactor at 300–375 °C with H₂ at 50–120 bar. A clear light yellowish green product was obtained, containing 6–26 % gasoline, 35-50 % kerosene, 8–40 % diesel. This liquid having 10–80 % alkanes, 1–10 % cycloalkanes, and 5–35 % aromatics, with a maximum of 10% char formation. Power law kinetic model was validated with experimental results. A kinetic study shows a pseudo 1st order reaction with respect to the neutral algae lipids oil concentration, with the activation energy for algal oil conversion was 14.96 kJ/mol. Activation energies for the formation of diesel (125 kJ/mol) and kerosene (146 kJ/mol) were higher than for the heavy hydrocarbons such as PAH (7 kJ/mol) and alkanes (64 kJ/mol) products. This study investigates for the first time the hydroprocessing of crude lipids extracted from the commercially relevant marine microalga *Nannochloropsis* sp. over a sulphided form of CoMoP/Al₂O₃ catalyst.

Finally, summary and conclusions based on the achievements are presented.

ACKNOWLEDGEMENTS

“There is nothing I believe in more strongly than getting young people interested in science and engineering, for a better tomorrow, for all humankind”

Bill Nye

I want to take opportunity first to thanks and express my sincere gratitude to the parents and god like mother (Sushila Devi) to give strength and motivate to move ahead in any kind of circumstances and believing in myself.

I would like to express my deepest gratitude and reverence to the persons also helped me directly and indirectly to support me to start and continue the PhD work.

I would like express my sincere gratitude and thanks from bottom of my heart to my supervisors Dr. Anil. K. Sinha and Prof. Mannar R. Maurya for their continuous support and guidance for their patience with me, constant motivation, enthusiasm and immense knowledge. They always supported and guided me to do extra which laid the foundation for execution of the research work embodied in this thesis. His constant desire to learn and ability to be self-motivated has influenced me both in my professional and personal way. I consider myself extremely blessed to have worked under their guidance.

I would like to acknowledge Director, CSIR-Indian Institute of Petroleum, Dehradun. This work was supported by the Council of Scientific & Industrial Research (CSIR) under OLP 134919 (OLP 893) project Agreement

I would like to express my sincere gratitude to Dr. Dillip K. Adhikari, Dr. D.V. Naik to help like friend and moral supporter, Dr. Rajaram Bal, Dr. Neeraj Atray, and Mr. S. P. Nautiyal to support while I need any kind of supports. I will be always obliged to all of them.

I would like thanks to the all Hydroporcessing staff members for their support and cooperation during entire thesis work.

I would like also thank Mr. Vivek and all Engineering Service Division (ESD), Analytical Science Division (ASD) and Advance Crude lab members for kind support. I am also very thankful to the CSIR-IIP family members.

I am thankful to the Head, Institute Instrumentation Centre of Indian Institute of technology Roorkee (IIC-IITR) for providing me necessary instrumentation facilities for my research work.

I am very thankful to my Student Research Committee (SRC) members Prof. Kaushik Ghosh, Prof. Prakash Biswas, Prof. Udai P. Singh, Prof. Rama Krishna Peddinti and HoD Prof. K. R. Justin Thomas for their valuable suggestions and assistance from time to time.

I express my heartily gratitude to the my previous faculty members of my graduation time from IITK and undergraduate faculty from Zakir Hussain College, Delhi University, Delhi, and my school (G.D. College Begusarai, Bihar and Shri Ramdhari Singh Dinkar, High School, Bihar) teachers.

I owe a heartily thanks and express my love and gratitude to my beloved daughter Gauravi Poddar (Pullu).

Finally, I wish to acknowledge all those whose names have not figured above, but have helped me in any form till now.

Mukesh Kumar Poddar

LIST OF FIGURES

- Figure 1.1.** Partial complex structure of cellulose
- Figure 1.2.** The Monomer of hemicellulose.
- Figure 1.3.** The complex structure of lignin.
- Figure 1.4.** The schematic reaction mechanism for the removal of oxygen from triglyceride (TAGs) by hydrotreating
- Figure 1.5.** n-Alkane hydroconversion (hydroisomerization and dehydrogenation) mechanism over Pt catalyst on an acidic support
- Figure 2.1.** Schematic flow diagram for slow pyrolysis set-up.
- Figure 2.2.** FT-IR of *Jatropha curcas cake* and its fast pyrolysis biochar
- Figure 2.3.** SEM of *Jatropha curcas cake* (a and b) and its fast pyrolysis biochar (c and d).
- Figure 2.4.** XRD of *Jatropha curcas cake* and its fast pyrolysis biochar.
- Figure 2.5.** A TEM micrograph of sulfided CoMoP/Al₂O₃ catalyst.
- Figure 2.6.** Yield (%) of products for the reaction of 25% of bio-oil (BO) in gas-oil (GO) at various temperatures.
- Figure 2.7.** Yield (%) of products from the reaction of feeds with 25%, 50 % and 100 % of bio-oil (BO) in gas-oil (GO) at 375 °C.
- Figure 2.8.** Distribution of hydrocarbons (■ gasoline (<C9); ● kerosene (C9-C14); ▲ diesel (C15-C18); and ▼ heavy residue (>C18)) in the products from feed containing 25 % bio-oil (BO) in gas-oil (GO) at various temperatures and 50 bar of H₂ pressures.

Figure 2.9. Distribution of hydrocarbons □ gasoline (<C9); Δ kerosene (C9-C14); ▽ diesel (C15-C18); and ◇ heavy residue (>C18)) in the products from feeds containing 25 %, 50 % and 100 % of bio-oil (BO) in gas-oil (GO) (at 375 °C, 50 bar of H₂ pressures, 10 wt% of catalyst, 5h).

Figure 2.10. Distribution of hydrocarbon types (■ alkanes; ● cycloalkanes; ▼ aromatics; and ▲ polynuclear aromatics) in hydroprocessed products for the reaction of 25% bio-oil (BO) in gas-oil (GO) at various temperatures (50 bar of H₂ pressures; 10 wt% of catalyst, 5h).

Figure 2.11. Distribution of hydrocarbon types (○ alkanes; Δ cycloalkanes; ◇ aromatics; and ▽ polynuclear aromatics) in hydroprocessed products for the reaction of 25%, 50 % and 100% of bio-oil (BO) in gas-oil (GO) at 375 °C (50 bar of H₂ pressures; catalyst: 10wt%, 5h).

Figure 3.1.

- Microchannel plate, (bottom)
- microchannel reactor experimental set-up.

Figure 3.2. Microchannel plate dimensions and specification

Figure 3.3. Nitrogen sorption isotherm of NiMo SiO₂-Al₂O₃

Figure 3.4. Ammonia TPD of NiMo SiO₂-Al₂O₃.

Figure 3.5. Diffractogram of fresh NiMo/SiO₂-Al₂O₃ catalyst.

Figure 3.6. Distribution of hydrocarbons [■gasoline (<C9), ●kerosene (C9-C14), and ▲diesel (C15-C18) in the products at various temperature (pressure 70 bar, LHSV 1.0, H₂/feed 1000nL/L) at various temperature.

- Figure 3.7.** Distribution of hydrocarbons [■gasoline (<C9), ●kerosene (C9-C14), and ▲diesel (C15-C18)] in the products (pressure 70 bar, LHSV 1.0, H₂/feed 500nL/L) at various temperature.
- Figure 3.8.** Distribution of hydrocarbons [■gasoline (<C9), ●kerosene (C9-C14), and ▲diesel (C15-C18)] in the products (pressure 70 bar, temperature 375 °C, H₂/feed 1000nL/L) at various LHSV.
- Figure 3.9.** Distribution of hydrocarbons [(■gasoline (<C9), ●kerosene (C9-C14), and ▲diesel (C15-C18)] in the product (pressure 70 bar, LHSV 1.0, temperature 325 °C) at various H₂/feed.
- Figure 3.10.** Distribution of hydrocarbons types (● alkanes, ▲cycloalkanes, ▼aromatics, ◀ PAH, ▶residue and ■ unreacted) in the products (pressure 70 bar, H₂: feed 1000nL/L, temperature 375 °C) at various LHSV.
- Figure 3.11.** Distribution of hydrocarbons types (● alkanes, ▲cycloalkanes, ▼aromatics, ◀ PAH, ▶residue and ■ unreacted) in the products (pressure 70 bar, H₂: feed 1000nL/L, LHSV 1.0) at various temperature.
- Figure 3.12.** Distribution of hydrocarbons types (● alkanes, ▲cycloalkanes, ▼aromatics, ◀ PAH, ▶residue and ■ unreacted) in the products (pressure 70 bar, LHSV 1.0, temperature 325 °C) at various H₂: feed.
- Figure 4.1.** Batch reactor (M/S Parr instrument US) used for hydroprocessing of a mixture of BO & GO and Nannochloropsis sp. micro marine algae extracted lipids (TAGs).
- Figure 4.2.** Nitrogen sorption isotherm and pore size distribution of mesoporous CoMoP/Al₂O₃

- Figure 4.3.** TPR of CoMoP/Al₂O₃.
- Figure 4.4.** Algal oil and its hydroprocessed product.
- Figure 4.5.** Distribution of hydrocarbons [▪ gasoline (<C9), • kerosene (C9–C14), ▲ diesel (C15–C18), and ▼ heavy residue (>C18)] in the products at various temperatures (cat: feed ratio 1:10; pressure 50 bar).
- Figure 4.6.** Yield (%) of the products (liquid, gases and solid char) at various H₂ pressures at 375 °C (reaction time of 5 h; cat: feed ratio of 1:10).
- Figure 4.7.** Distribution of hydrocarbons [▪ gasoline (<C9), • kerosene (C9–C14), ▲ diesel (C15–C18), and ▼ heavy residue (>C18)] in the products at various H₂ pressures (temp. 375 °C; cat: feed ratio 1:10; reaction time 5 h).
- Figure 4.8.** Distribution of hydrocarbon types (▪ alkanes, • cycloalkanes, ▲ aromatics, and ▼ polynuclear aromatics) in hydroprocessed products at various H₂ pressures (temp. 375 °C; cat: feed ratio 1:10; reaction time 5 h).
- Figure 4.9.** Distribution of hydrocarbons [▪ gasoline (<C9), • kerosene (C9–C14), ▲ diesel (C15–C18), and ▼ heavy residue (>C18)] in the products at various reaction times (temp 325 °C; cat: feed ratio 1:10; pressure 50 bar).
- Figure 4.10.** Distribution of hydrocarbons [▪ gasoline (<C9), • kerosene (C9–C14), ▲ diesel (C15–C18), and ▼ heavy residue (>C18)] in the products at various reaction times (temp. 350 °C; cat: feed ratio 1:10; pressure 50 bar).

LIST OF TABLES

- Table 1.1.** The physical property of bio-oil
- Table 2.1.** Ultimate and structural analysis of JCC.
- Table 2.2.** GC -MS analysis of pyrolysis-oil.
- Table 2.3.** Elemental analysis of gas-oil (GO), bio-oil (BO) and hydroprocessed Products (reaction time: 5h; feed/catalyst: 10(wt/wt)).
- Table 2.2.** Distribution of normal (n) and iso (i) -alkanes and i/n ratios in kerosene range (C9-C14) hydrocarbons. [Catalyst: 10wt%; pressure 50 bar].
- Table 3.1.** GC-MS result of the representative product.
- Table 3.2.** Physicochemical properties of mesoporous supports and catalysts
- Table 4.1.** Compositional details of lipids

LIST OF PUBLICATIONS

1. M. K. Poddar, A. Rai, M. R. Maury and A. K. Sinha, Co-processing of bio-oil from de-oiled *Jatropha curcas* seed cake with refinery gas-oil over sulfided CoMoP/Al₂O₃ catalyst, *RSC Adv.*, 6 (2016) 113720-113726.
2. M. K. Poddar, S. Kumar, P. K. Das, M. R. Maurya, A.K. Sinha, Hydroprocessing of Aqueous phase of Pyrolysis oil over NiMo/Al₂O₃-SiO₂ in microchannel reactor, *Catalysis in Green Chemistry and Engineering* 1(3) (2018) 1–10.
3. M. K. Poddar, M. Anand, S. A. Farooqui, G. J. O. Martin, M. R. Maurya, A. K. Sinha, Hydroprocessing of lipids extracted from marine microalgae *Nannochloropsis* sp. over sulfided CoMoP/Al₂O₃ catalyst, *Biomass and Bioenergy*, 119 (2018) 31–36

Other related publications

4. D. V. Naik, V. Kumar, B. Prasad, M. K. Poddar, B. Behera, R. Bal, O. P. Khatri, D. K. Adhikari and M. O. Garg, Catalytic cracking of jatropha-derived fast pyrolysis oils with VGO and their NMR characterization, *RSC Adv.* 5 (2015) 398-409.
5. P. K. Kanaujia, D. V. Naik, D. Tripathi, R. Singh, M. K. Poddar, L.N. S. K. Konathal, Y. K. Sharma, Pyrolysis of *Jatropha Curcas* seed cake followed by optimization of liquid-liquid extraction procedure for the obtained bio-oil, *Journal of Analytical and Applied Pyrolysis*, 118 (2016) 202–224.
6. R. K. Singh, A. Kukrety, O. P. Sharma, M. K. Poddar, N. Atray, G. D. Thakre, S. S. Ray, Evaluation of a Novel Hindered Phenolic Triazine Schiff Base as Multifunctional Additive in Biolube and Biodiesel, *Waste and biomass valorization* 7, 6 (2016) 1437–1445.
7. R. K. Singh, A. Kukrety, O. P. Sharma, M. K. Poddar, N. Atray, S. S. Ray, Synthesis of a Novel Efficient Antioxidant for Use in Lubes and Biodiesel, *Petroleum Chemistry* 57 (1) (2017) 100–105.

CONTENTS

Page No.

CONDIDATE’S DECLEARATION

ABSTRACT **i**

ACKNOWLEDGEMENT **v**

LIST OF FIGURES **vii**

LIST OF TABLES **xi**

LIST OF PUBLICATIONS **xii**

CHAPTER 1: General Introduction and Literature Survey **1**

1.1. Introduction and literature survey 1

1.1.1. Cellulose Pyrolysis..... 4

1.1.2. Hemicellulose Pyrolysis 5

1.1.3. Lignin Pyrolysis 6

1.1.4. Jatropha 7

1.1.5. Fuel applications of bio-oils 11

1.1.6. Upgrdation 11

1.1.7. Reaction mechanisms under hydroprocessing 14

1.1.7.1. Olefin Saturation 15

1.1.7.2. Cracking/ Hydrocracking 15

1.1.7.3. Heteroatom removal 16

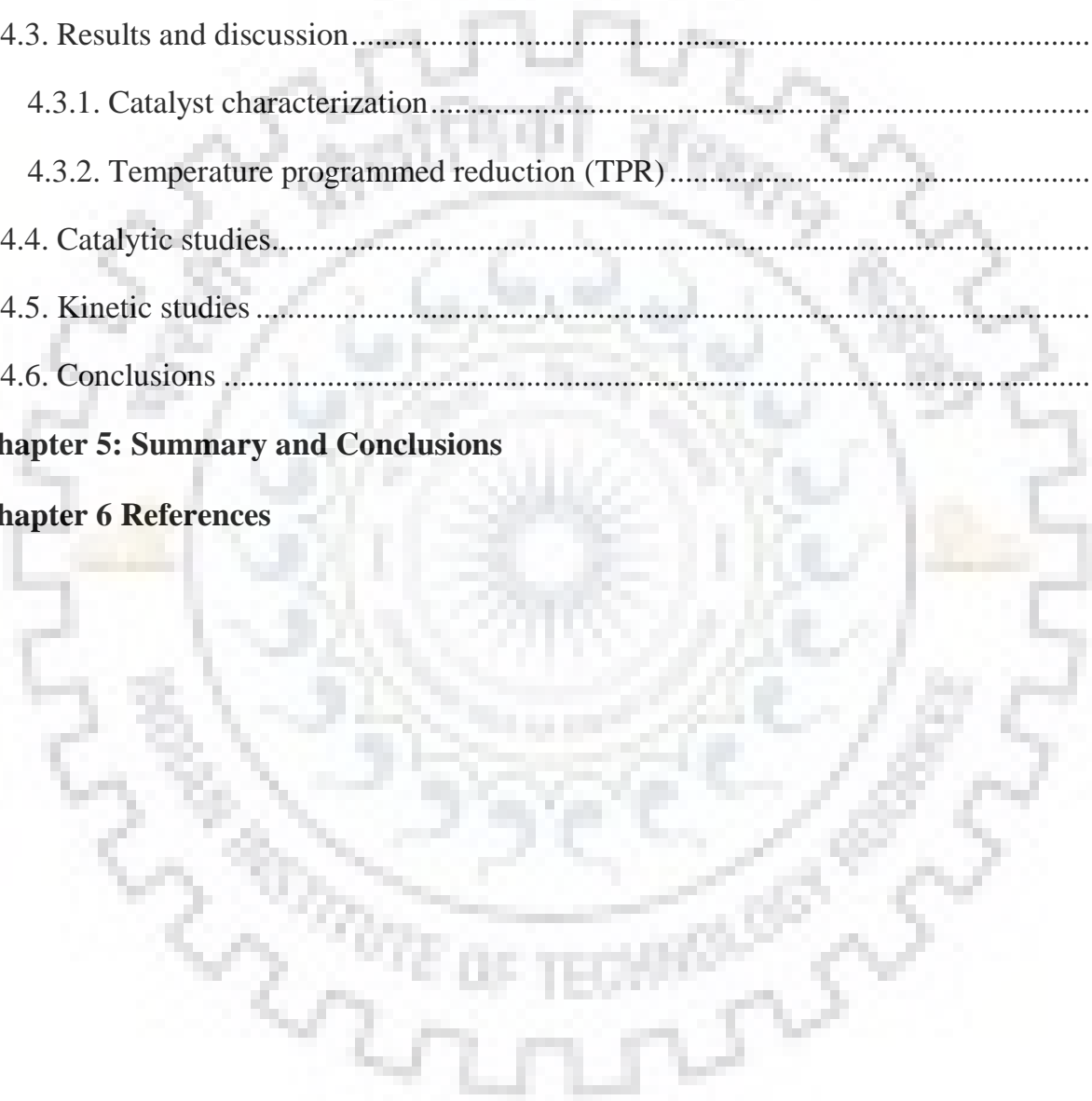
1.1.7.4. Isomerization/ Hydroisomerization..... 17

1.1.8. Hydroprocessing catalysts 18

1.1.8.1. Metal phosphides.....	21
1.1.8.2. Metal nitrides.....	22
1.1.8.3. Supports.....	23
1.1.8.4. Promoters.....	24
1.1.9. Kinetic modeling methods.....	24
1.2. Motivation.....	25
1.3. Objective.....	25
Chapter 2: Co-processing of bio-oil from de-oiled jatropha curcas seeds cake with refinery gas-oil over sulphided CoMoP/Al₂O₃ catalyst	27
2.1. Introduction.....	27
2.2. Experimental details.....	29
2.2.1. Materials.....	29
2.2.2 Catalyst preparation.....	29
2.2.3. Characterization methods.....	29
2.3. Reaction procedure.....	30
2.3.1. Pyrolysis.....	30
2.3.2 Biochar analysis.....	31
2.3.2.1. FTIR Analysis.....	31
2.3.2.2. SEM Analysis.....	33
2.3.2.3. XRD Analysis.....	35
2.3.2.4. CHNO Analysis.....	36
2.3.3. Sulfidation of catalyst.....	36
2.3.4. Catalytic reaction conditions.....	36
2.4. Analysis.....	37

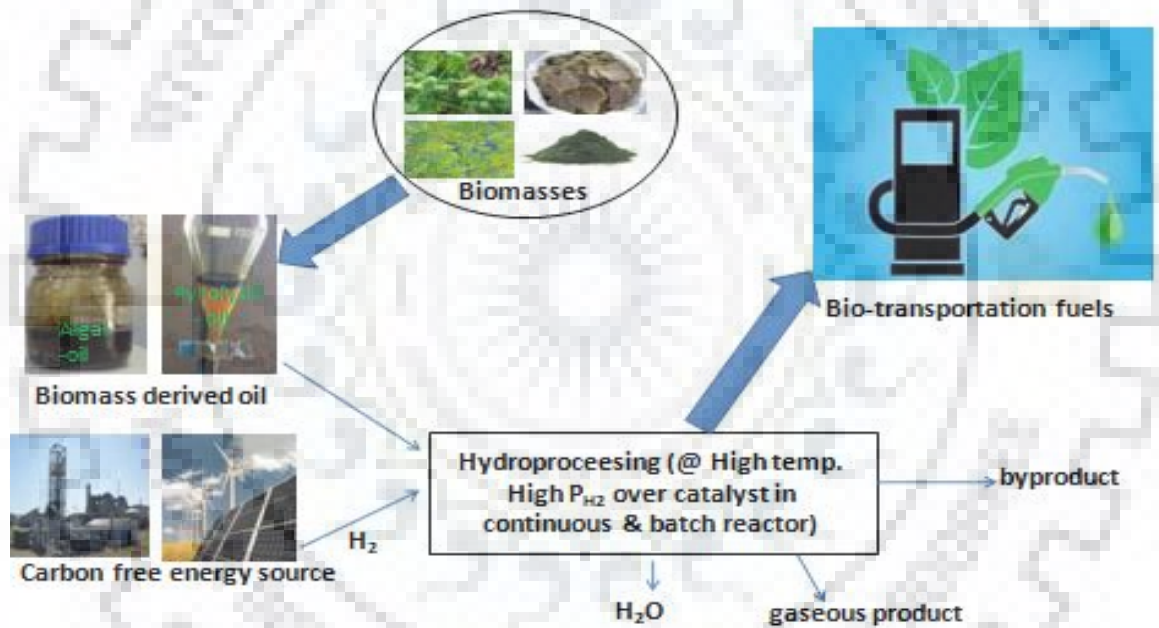
2.4.1. Gas Chromatography	37
2.4.2. Two-dimensional gas chromatography (GC x GC-MS)	38
2.4.3. CHNS analysis	38
2.4.4. Total acid number (TAN)	38
2.5. Results and Discussion	39
2.5.1. Catalyst characterization	39
2.5.2. Catalytic studies	41
2.6. Conclusions	52
Chapter 3: Hydroprocessing of aqueous-phase of pyrolysis oil over NiMo/Al₂O₃-SiO₂ in the microchannel reactor	53
3.1. Introduction	53
3.2. Experimental details	55
3.2.1. Materials	55
3.2.2. Catalyst preparation	55
3.2.3. Catalyst coating in the microchannel reactor	56
3.2.4. Experimental setup	57
3.3. Results and Discussion	61
3.3.1. Physicochemical Properties of Catalyst	61
3.3.1.1. BET NH ₃ -TPD (acidity) and XRD analysis	61
3.3.2. Catalytic studies	64
3.4. Conclusions	71
Chapter 4: Hydroprocessing of lipids extracted from marine microalgae <i>Nannochloropsis</i> sp. over sulfided CoMoP/Al₂O₃ catalyst	73
4.1. Introduction	73

4.2. Experimental details	75
4.2.1. Catalyst preparation	75
4.2.2. Lipid (TAGs) extraction from ruptured microalgae biomass	76
4.2.3. Lipid Conversion	76
4.3. Results and discussion.....	79
4.3.1. Catalyst characterization.....	79
4.3.2. Temperature programmed reduction (TPR).....	81
4.4. Catalytic studies.....	82
4.5. Kinetic studies	89
4.6. Conclusions	90
Chapter 5: Summary and Conclusions	91
Chapter 6 References	93



Chapter 1

General Introduction and Literature Survey



Chapter 1: General Introduction and Literature Survey

1.1. Introduction and literature survey

Energy is the foundation of economic and infrastructure development. Environmental concerns, global energy requirement, and declining fossil fuel reserves have boosted energy research on alternative source from conventional fossil fuels to alternative renewable and sustainable sources [1–7]. Biomass is a carbon-neutral renewable feedstock source which can be used for transportation fuels production/generation. It is a promising alternative and renewable source of energy that could be the key component for the future sustainable energy supply, with significant benefits in environmental protection, utility energy demand and regional development [8–13]. Apart from energy independence, there will be economic and social benefits as well, by the implementation of bio-refineries. U.S. Department of Energy (DOE) has declared the replacement of 30% transportation fuel with biofuels and 25% of organic chemicals with renewable biochemical by 2025 [14]. Biomass is an organic matter derived from plants through photosynthesis. Based on the availability of biomass feedstocks, biofuels have been defined as first, second, and third generation biofuels.

The first-generation biomass comprises of edible food crops such as wheat, food grains, corn, and sugarcane. First generation bio-fuels concern the production of bio-ethanol from carbohydrates (sugar, starch, etc.), and bio-diesel from trans-esterification of plant seeds oils (vegetable oils) with methanol, and it creates food-versus-fuel controversies [3]. Presence of C=O (carbonyl) and C=C (unsaturation) bonds in fatty acid methyl ester (FAME) gives low antioxidation stability and high flash point. Worldwide biohydrogenated diesel (green diesel) has also been studied as an alternative to transesterification product (bio-diesel) of vegetable oil. Generally, long-chain alkanes can be synthesized via catalytic hydrogenation reactions of waste cooking oil containing a great extent of free fatty acids [15]. Heteroatoms, sulfur, and nitrogen are most effectively removed (>99%), while oxygen can be removed from waste cooking oil by applying hydrotreating temperature [16,17]. Saturation of double bond gets enhanced by increasing the hydrogenation temperature, which is confirmed by the decreasing bromine number and increasing H₂ consumption during the reaction. iso-Paraffins amount increases with an

Chapter 1: General Introduction and Literature Survey

increase in the temperature. Isomerization reactions are favored by increasing temperature due to hydrocracking reaction; it is confirmed by the decrease in n-paraffins and the increase in iso-paraffins [18]. Diesel production favored at lower hydrotreating temperatures, and it is selectively formed with yield 90%.

The production of first-generation biofuels is very limited in comparison to the requirement in terms of conventional refinery oils, so there is an issue with demand vs. supply, which is mainly due to the competition of food. For this reason, second-generation biofuels have become the main aspect of research [19].

Various agricultural crop residues such as mustard stalk, apricot pits, wheat straw, barley straw, paddy straw, corn stover, corncob, cotton stalk, almond shell, canola meal, canola hull, flax fiber, jute blast, plum pits, coconut coir, coconut shell, palm seeds, rice husk, olive pits, walnut shell, cashew nut shell, sugarcane bagasse, peanut shell, peach pits, hazelnut shell, flax straw, etc. are available in plenty. The forest residue from softwood and hardwood type biomass (include barks, cones, stems, twigs, and needles) are obtained throughout the world as a result of agricultural activities [20].

Second generation biofuels give attention to the thermal conversion of lignocellulosic biomass [21]. The thermal conversion has mainly four processes: combustion, gasification, hydrothermal liquefaction, and pyrolysis. Combustion is already widely practiced; gasification has a high level of interest, to produce bio-syngas to generate methanol or gasoline and diesel. Gasification has higher efficiency as compared to combustion [22]. Hydrothermal liquefaction of biomass needs temperature (250-350 °C) and pressure (10-50 bar) in the presence of various organic solvents [23]. Pyrolysis process decomposes the biomass in the inert atmosphere (N_2), and it generates pyrolysis vapor and char/coke (biochar) at high temperature (350-550 °C). The vapor get condensed to the liquid product, which is called pyrolysis oil the gas generated during the process is recirculated or vented off [24,25].

The third-generation biofuels deal with fast-growing feedstocks with minimal requirement of maintenance/nutrient; the tendency for the regeneration of these feedstocks

Chapter 1: General Introduction and Literature Survey

is very high, along with the low cost of feed production in all weather conditions, with the high growth rate. Algae (microalgae and macroalgae), marine biomasses such as caltrop diatoms, seaweed, hyacinth, kelp, duckweed, and salvinia have candidacy for the production of biofuels [26]. In recent years, these feedstocks are considered third-generation biomass [27,28]. The productivity of algae is 61,000 l/ha for biofuels [29].

Third generation biofuels source, algae may produce biodiesel, bioethanol, syngas by trans-esterification, fermentation, and gasification, respectively[30]. The energy costs for a downstream process, extraction of lipids (TAGs) from the cells can be significant, and the processing cost of microalgae biomass should be minimized to enable economical viability to produce biofuels and lipids feeds [4,31–38].

Co-production of higher value-added chemicals/petrochemicals might help offset the high capital and operational costs for microalgal biofuel production via refinery processes; Microalgal biomass also contains animal livestock materials (essential amino acids) [4,39–42]. Transportation fuels produced by using algal oil should be distilled out/separated to the various end products. [43]. There are several steps involved before extraction of the lipid from harvested algal biomass, like drying, cell rupture, etc., The extracted lipids are transesterified or hydroprocessed to their respective products like biodiesel or transportation fuels (gasoline, kerosene, and diesel). This processing is energy-intensive steps [44]. It should be aimed to increase the energy efficiency of the produced biofuels, and it is only possible by minimizing energy consumption during each step [27,36,44–50]. Harvesting of algal biomass is done on a very small scale (0.5 g/L). However, it can be improved by mechanical dewatering (25–30% solids) [30]. Conventionally, lipids get extracted using dry biomass (algae), and drying is an energy-intensive process and does not contribute to minimizing the cost-saving steps [30]. Lipids are stored inside the algae and to extract the lipids from inside the cell, walls of algae biomass needs to be ruptured mechanically [50]. There are several techniques to rupture the algae cell walls, such as microwave (MW), high-pressure homogenization (HPH), ultrasonics (US), hydrodynamic cavitation (HC), bead beating (BB), and heat/sulfuric acid treatment, etc. [37]. It was observed that only the high-pressure homogenization (HPH)

Chapter 1: General Introduction and Literature Survey

technique demonstrated to be energy efficient, scalable. By this process, maximum microalgae, biomass gets ruptured, and concentrated slurries (~20% solids) could be achieved from the biomass [38,43,46,51]. Ultrasonication is an alternative way for the extraction of lipids. Commercially sonication systems are available currently in biorefinery process [52].

This thesis mainly covers the production of transportation fuels by hydroprocessing of biomass pyrolysis oil and algae extracted lipids (Triacylglycerides; TAGs). A dark brown viscous liquid with the distinctive smoky smell is obtained by condensing the pyrolysis vapor. Biomass has various components; among them, cellulose, hemicellulose, and lignin are the major. Cellulose is mainly responsible for volatiles and oxygen-containing compounds in pyrolysis liquid. Lignin (aromatics) is the main precursor for char formation by aromatization/cyclization, while hemicellulose is responsible for char as well as the formation of oxyhydrocarbons [53,54].

1.1.1. Cellulose Pyrolysis

The cellulose individually decomposes at low temperature 150°C, cellulose get depolymerized below 300°C temperature, it results, in reduction of the degree of polymerization (DP), formation of reactive free radicals (needs rapid quenching/freezing to avoid further reaction), carboxyl, hydroperoxide, and carbonyl groups, along with evolution of CO, CO₂ and H₂O [55,56]. The unit cell of cellulose is shown in Figure 1.1. Pyrolysis of cellulose initially forms activated cellulose (low degree of polymerization) [57]. After that, two parallel pathways are involved, i.e., depolymerization, and the fragmentation by ring breaking/scission.

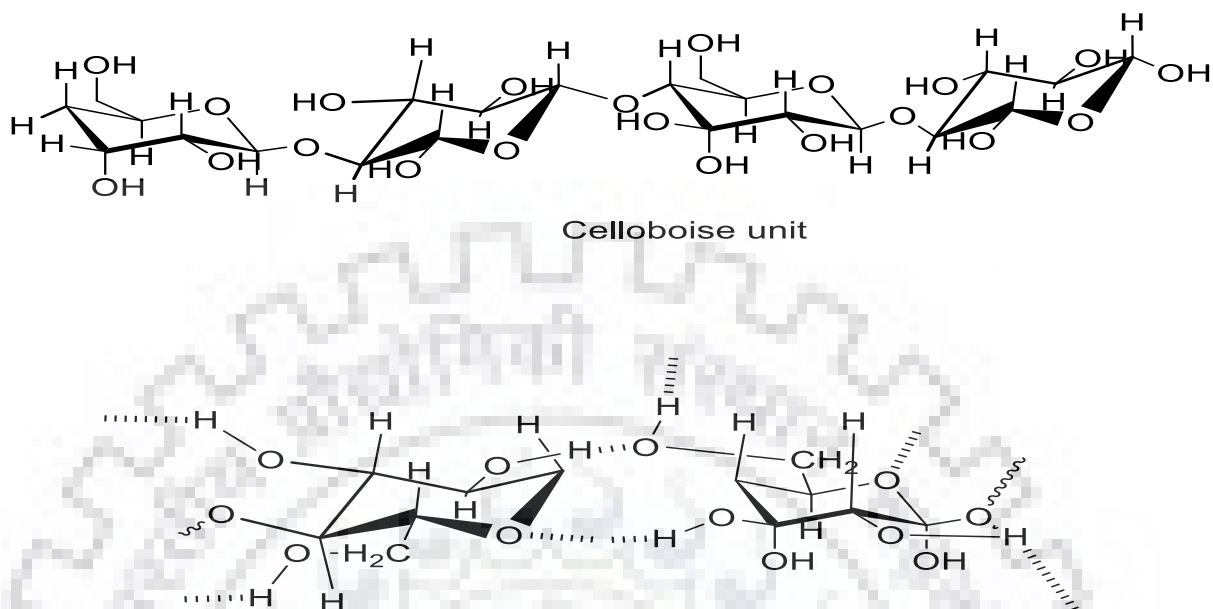


Figure 1.1. Partial complex structure of cellulose.

Anhydro-oligosaccharides, levoglucosenone, levoglucosan, levoglucosan, and other monomeric cyclopentanones, anhydrosugars, pyrans, and furans form by depolymerization, and acetol (HA), hydroxy acetaldehyde (HAA), other linear carbonyls, alcohols, furfural, and esters form by fragmentation of ring scission [4,58–61].

1.1.2. Hemicellulose Pyrolysis

Hemicelluloses are amorphous polysaccharides of hexoses (D-glucose, D-galactose and D-mannose) and/or pentoses (L-arabinose and D-xylose). Hemicelluloses (due to the lack of crystallinity) are less thermally stable than cellulose. [62]. The unit cell of hemicellulose is shown in Figure 1.2. Generally, xylan gives higher char yield than that obtained from cellulose depolymerization [63].

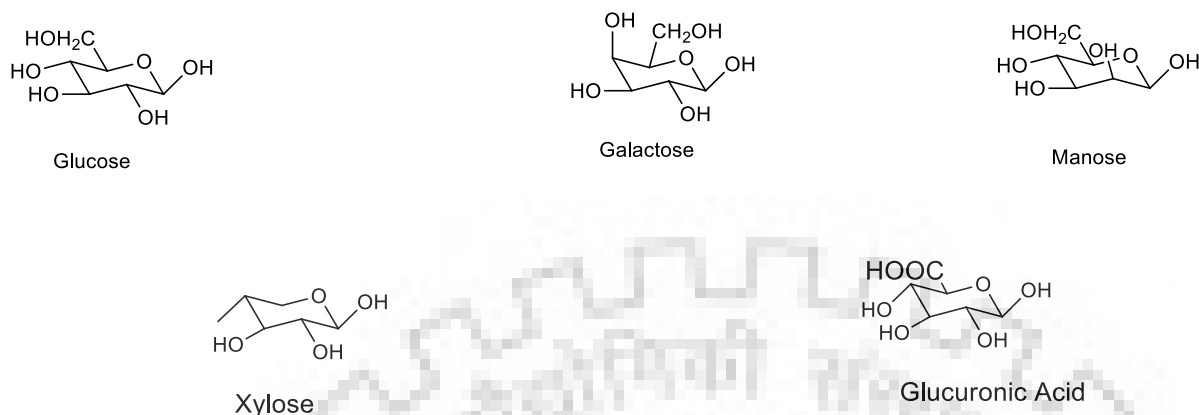


Figure 1.2. The monomer of hemicellulose.

Cellulose pyrolysis generates glucosyl cation by scission of glucans that - gives a stable 1, 6-anhydride C-6 alcohol, which ultimately results in the volatile levoglucosan. Xylosyl cation is more likely to follow non-specific dehydration pathways that may form char rather than volatiles material by stabilization of intermolecular xylosyl cation.

1.1.3. Lignin Pyrolysis

Lignin is an amorphous material in the building blocks of biomass cell. It is the heterogeneous polymer of three monomers, p-coumaryl alcohol (3-Hydroxyprop-1-enylphenol), coniferyl alcohol, sinapyl alcohol (4-(3-hydroxyprop-1-enyl)-2, 6-imethoxyphenol and (4-(3-hydroxy-1-propenyl)-2-methoxyphenol). The complex structure of lignin is shown in Figure 1.3. [64]. Lignin in biomass is more thermally stable component than cellulose or hemicellulose. Pyrolysis of lignin starts from 200°C by thermal softening. Most of the lignin pyrolysis occurs at higher temperatures than cellulose decomposition, resulting in lower liquid yield and higher char yield than holocellulose (cellulose and hemicellulose).

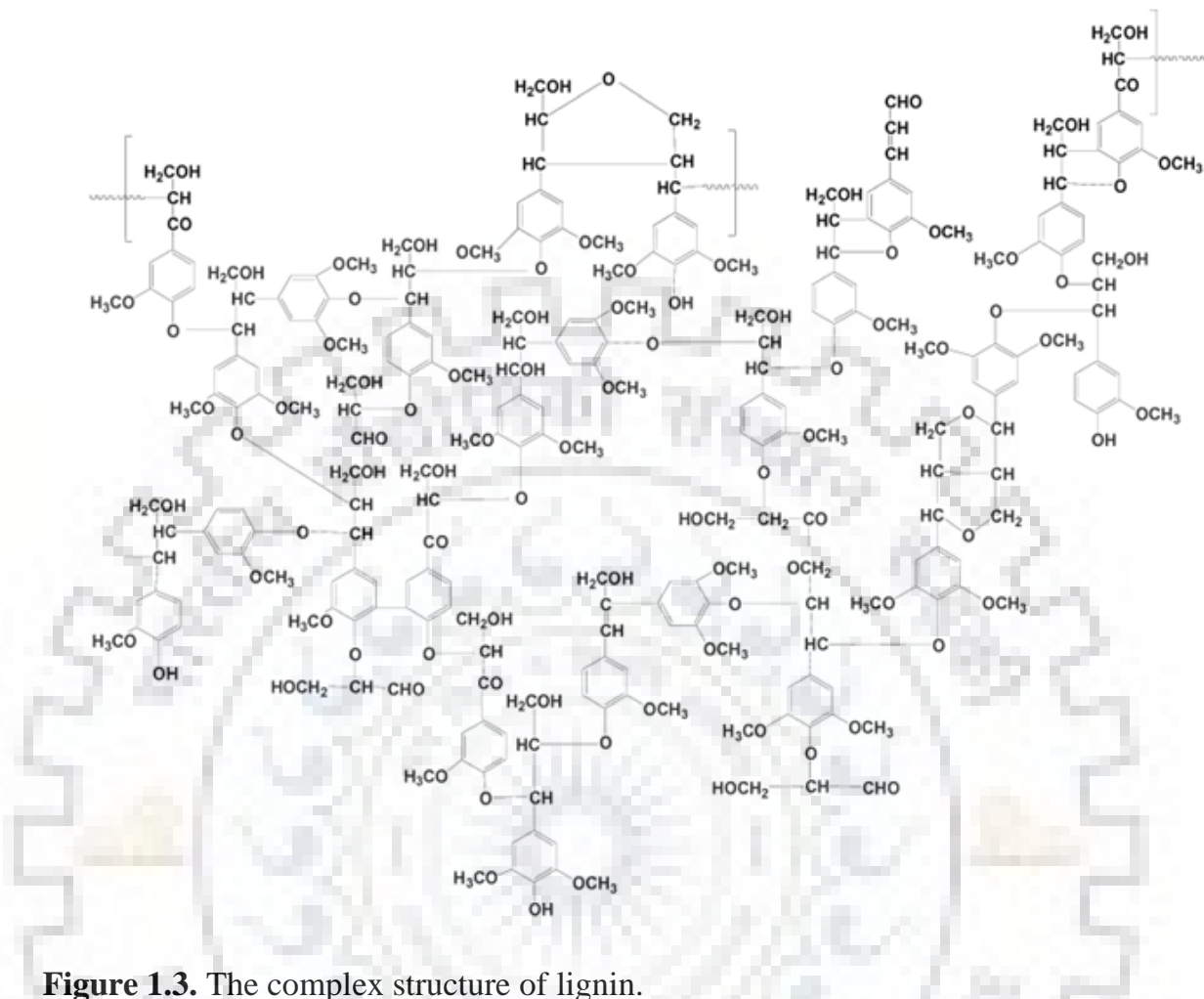


Figure 1.3. The complex structure of lignin.

1.1.4. Jatropha

We have opted for Jatropha and marine microalgae *Nannochloropsis* sp., biomass for our study over hydroprocessing reaction to get transportation fuels. Jatropha seeds are a small, oleaginous, tropical plant of Euphorbiaceae family. A single Jatropha plant will continue to bear fruit up to 50 years after adulthood. Most of the Jatropha fruit gets mature in only 90 days after flowering [65].

Jatropha curcas can grow with a minimal supply of nutrients in a wide range of atmospheric conditions from dry regions to humid region in a variety of soils with ample supply of hot weather and medium to low rainfall. Jatropha curcas can be grown from either the direct planting of cuttings or from seeds [66]. Jatropha seed has phorbol esters and curcin protein, which gives toxicity.

Chapter 1: General Introduction and Literature Survey

Worldwide pyrolysis liquid has been reformed by names like pyrolysis-oil, bio-oil (BO), bio-crude-oil, bio-fuel-oil, liquid fuels, wood liquids, wood oil, liquid smoke, pyroligneous tar, pyroligneous acid, etc.

The de-oiled *Jatropha curcas* seed cake (JCC), with average particle size 1.4 mm and bulk density 0.56 g/ml, contains 45.0, 7.0 and 45.0% of C, H, and O, respectively with a heating value (HHV) approx. 17 MJ/kg [3].

Pyrolysis product of biomass deoiled *jatropha-curcas* seeds cake (JCC) has 50-70 (wt. %) of liquid, 25-35 (wt. %) gases and 10-25 (wt. %) of char products [1,3,8,9,67]. Liquid products (Bio-oil) have a mixture of more than 300 different hydrocarbons and oxyhydrocarbons having a wide range of functional groups [68]. The wide range of chemicals obtained due to the presence of polymer of C5 and C6 carbohydrate (cellulose and hemicellulose) and polymers of phenolic compounds (lignin). On heating, these polymers first get depolymerized to the lower degree of polymer, and on further heating, get cracked to the mixture of various hydrocarbons.

The bio-oil has two phases. One is water soluble aqueous-phase; 50-60 wt. %, and the other one is non-aqueous bio-crude 40-50 wt. % [69]. The bio-oil appeared as dark brown emulsion form of aqueous as a well organic phase which was thick at the bottom. The quality of bio-oil (pyrolysis product) deteriorates rapidly due to the reaction in atmospheric condition and presence of higher oxygen content.

The detail chemical composition, along with carbon content in aqueous-phase and the non-aqueous phase of bio-oil, is provided in chapter 2 [4]. Aqueous phase oil contains aldehydic and ketonic compounds in major (~ 28%) followed by acids (~ 17%) in lower amounts. The minor compounds are guaiacols (10%), phenols (9%), hydrocarbons (8%), furan (7%), esters (1%), alcohols (7%), sugars (1%) and others (12%) of the total organics. Additionally, the nitrogen-containing compounds, mainly alkyl, hydroxyl or carbonyl substituted pyridine, pyrazine, pyrrole, indole, piperidine, etc.

The presence of water in bio-oils (BO) results in the dehydration reactions during pyrolysis and partly due to the presence of moisture in the biomass [63]. Therefore, variation in

Chapter 1: General Introduction and Literature Survey

water content is over a wide range of 15-45 (wt. %), depending on the feedstock and pyrolysis conditions. In the case of *Jatropha curcas* cake (JCC), the moisture content varies 30-45 (wt. %), maximum 10 Wt % due to moisture and remaining due to pyrolysis reaction [70].

Pyrolysis liquid usually contains pyrolytic lignin, monomeric phenolic compounds and light compounds like methanol, various acids (acetic, propanoic, formic) acid, aldehydes (acetaldehyde, hydroxy acetaldehyde), sugars (glucose, xylose, fructose), ketones (hydroxyacetone, hydroxybutanone, acetone, acetol hydroxyketones), guaiacols, syringols, furans, furfurals etc. along with 35-50 (wt. %) water, which is one of the major component of the pyrolysis-oil, and this amount is good enough to dissolve the oligomeric lignin-derived components and carbohydrates pyrolysis products (low carbon chain compounds of alcohols, acids, hydroxy aldehydes, and ketones), due to solubilizing effect [64]. Liquid yield decreases by increasing the pyrolysis temperature, due to severe cracking of the biomass and formed vapors, which gives less organic liquid with a small amount of oxygen content. Approx. 13 - 28 (wt. %) water present in pyrolysis oil is just because of moisture associated with biomass, and the rest of the water is mainly due to dehydration reactions during pyrolysis [71–73].

Based on GPC-HPLC, the average molecular weight of water free pyrolysis-oil/bio-oil (BO) obtained was 650 – 1300 g/mol; it consists of mainly biphenyl, phenyl coumarin, diphenyl ethers, stilbene, and resinol, etc. [71,74–77].

Many researchers have studied the physical properties of bio-oils of various feedstocks, including *Jatropha Curcas* Cake (JCC) [78,79]. It was observed that there is a significant difference between pyrolysis oil/ bio-oils and petroleum fossil oils [80]. Pyrolysis oil has many drawbacks due to the presence of soluble water oxygen-containing hydrocarbons [14]. The pyrolysis oil has lowered heating value 17-20MJ/Kg, which is almost 50% of the existing fossil fuels, low flame temperature, and lower immiscibility in hydrocarbon fuels [80]. Presence of water and oxygenated compound in bio-oil (BO) increases ignition delay, and decrease in combustion rate (thermal stability) compared to

Chapter 1: General Introduction and Literature Survey

fossil [81]. Bio-oils have high viscosity and high acidity (pH 2-3); acidity might be due to the presence of organic acid components, due to which they have corrosion properties and can affect some sealing materials. Some of the physical properties are listed in Table 1.1.[3,64,81–86].

Upon longer storage, due to the presence of active species, in such as free radicals and active oxygenates compounds, the further reaction may occur, resulting in the formation of heavier compounds. For example, phenol-formaldehyde polymerization reactions may happen by condensation reactions of these functional groups by longer storage; however, this solid is very useful for plastic material Bakelite even though vacuum distillation of pyrolysis oil generates solid coke by polymerization reactions involving polyhydroxyphenols or methoxyphenols [87,88].

Table 1.1. The physical property of bio-oil [89]

Physical Property	Values	Physical Property	Values
Lower heating value (LHV)	17–20 (MJ/kg)	Oxygen	35–40 (wt %)
Higher heating value (HHV)	13–18 (MJ/kg)	Carbon	50–60 (wt %)
Kinematic viscosity@40°C	15–42 (mm ² /s)	Hydrogen	7–8 wt (%)
Density at 15 °C	1.10–1.30 (kg/dm ³)	Sulfur	<0.05 (wt %)
Pour point	–9.0 -36 (°C)	Nitrogen	<0.5 (wt %)
Flash point	40–110 °C	Ash	<0.3 (wt %)
TAN	70–100 (mg KOH/g)	Solids (char)	17–23 (wt %)
pH	2–3	Water	20–35 (wt %)

Chapter 1: General Introduction and Literature Survey

Bio-oil/pyrolysis oil is a microemulsion of the aqueous part (continuous phase), formed by the decomposition of holocellulose (cellulose and hemicellulose) and organic part (discontinuous phase) formed by pyrolytic lignin macromolecules. This emulsion may form through hydrogen bonding.

1.1.5. Fuel applications of bio-oils

Diesel engines have high efficiency (45%), so pyrolysis oil is not suitable for a diesel engine as such. This can be utilized for heat and power generation devices like boilers, turbines, sterling engines, medium, slow speed engines, and all combined heat and power process (CHP) unit [3]. This device contains a modified flameless oxidation burner (air pressure atomizer). CHPs is known as a small-scale power generation device/unit which is mostly used to generate heat by using economically as well as financially low-grade fuels. CHPs mostly used diesel engines on behalf of pyrolysis oils/bio-oils, due to some of the reason like difficult ignition, high corrosion value, less thermal stability, resulting cocking. These problems arise due to the presence of high water content and oxygen content [90].

The other way to use bio-oil is in transportation fuels and blends with existing hydrocarbons. Pyrolysis oils are not miscible with hydrocarbons; surfactants can help to emulsify with diesel fuels. Ikura (CANMET Canada) Diebold and Baglioni, developed surfactant to emulsify pyrolysis oil / bio-oil with 5- 90 % with diesel [91].

The drawback of this approach is process economics. The cost of surfactants is very high, and using this process gives high corrosion than using pure bio-oil or diesel in the engine. Therefore, we have to look for other ways to use bio-oil for transportation fuels.

1.1.6. Upgradation

The pyrolysis-oil/bio-oil (BO) needs to upgrade to convert them into existing transportation fuels, either by a chemical or physical method. Physically as discussed earlier, another way is using bio-oil in CHP unit by mixing surfactants. There are several ways in the refinery process to improve the quality of pyrolysis/bio-oils, like fluid catalytic cracking (FCC), hydroprocessing, reforming, and heavy oil processing. Hydroprocessing

Chapter 1: General Introduction and Literature Survey

involves hydrotreating, hydrocracking, and hydrogenation reaction; it gives partial or total elimination of the oxygen and unsaturation. Oxygen gets eliminated in the form of water, carbon dioxide, and carbon monoxide, either by catalytic cracking or by deoxygenation of pyrolysis/bio-oils (BO) or both by using hydrogen [92,93]. This process, commonly being referred as hydrodeoxygenation, hydrotreating, hydroprocessing and/or hydrocracking, and may include any of these reactions where hydrogen is used to transform into the transportation fuel, either diesel or jet oil/jet fuel or gasoline. Hydrotreating of bio-oil is carried out at high hydrogen pressure and temperature [[92,94–98].

Catalytic cracking refers to the fluid catalytic cracking (FCC) using zeolite-containing catalysts that lead to the formation of gasoline at high temperatures (300-600°C) and atmospheric pressure. The advantage of this process is, it does not need any H₂ and is cost-effective [99,100]. However, a major disadvantage of this process is the coke formation, which deactivates the catalyst, and it needs to be regenerated [101].

Hydrodeoxygenation of lignin follows two steps. The first step includes the breaking of phenolic C–O–C bonds without breaking of C–C bonds, and the second step is the hydrogenation of benzene based ring followed by hydrogenolysis of the C–O bonds to produce compounds C₉ and C_{14–18} [102,103].

The development of technology to convert biomass pyrolysis oil/bio-oil to fossil fuels is a global challenge for researchers using hydroprocessing refinery process. A technical research center of Finland (VTT) and Pacific Northwest national laboratory (PNNL) Finland developed the process for hydroprocessing of bio-oil produced from pine wood in two-stage continuous fixed bed reactor, over a sulphided catalyst, including both ruthenium (Ru) and promoted molybdenum (Mo). [104].

Molybdenum sulfide (MoS₂) catalyst was used for the removal of heteroatom from bio-oil and fossil fuels [105]. However, RuS catalyst hydrogenates the sugars and polyols without forming methane [106,107]. The Process parameter was optimized to get a liquid hydrocarbons product having oxygen-free or trace amount of oxygen content with a low

Chapter 1: General Introduction and Literature Survey

acid number (TAN) [92,108]. Conventional hydrotreating processes cannot be directly applied to the upgradation of pyrolysis oil [109].

Conventional hydrotreating is economically not viable, although this process is extremely effective for fuels, due to the need for high hydrogen requirement and high energy [76]. It may be viable if hydrogen is readily available, as in the case of refinery industries [3].

Typically, sulphided CoMo or NiMo supported on γ -Al₂O₃ are used for hydrotreating of fossil fuel [110,111]. One of the disadvantages of these catalysts is the requirement of the sulfur on metal to remain active. Presence of sulfur in transportation fuels has a drawback. There are several mechanisms for catalyst deactivation, like sintering of the active metals, poisoning of the catalyst (presence of nitrogen compounds), blockage of catalyst pores and active sites, structural degradation of the support, active sites, coking and metal deposition [112]. The catalyst gets deactivate due to coke formation, which may result in blockage of the catalyst pores and disturb the access of reactants over the active pores [80,88,92,113,114].

Based on several studies, it was found that acidic support like alumina promotes the coke formation, along with that, the phenol is the precursor for coke formation, along with this it was also observed that carbohydrate fraction pyrolysis oil is also responsible for coke formation [88,109,114,115]. Bridgwater reviewed the upgradation of bio-oil (BO) by hydrotreating [109,115].

Catalytic hydroprocessing is the removal of heteroatom (sulfur, nitrogen, oxygen, metals) and saturation of olefinic bond (C=C) present in straight and aromatics chain, along with isomerization and cracking reaction.

The refinery streams are subjected to hydrogen in the downstream process to improve product quality (straight-run naphtha, diesel, kerosene, and gas-oils, etc.) by using conventional CoMo and NiMo supported γ -Al₂O₃ [116]. Quality of petroleum products is dependent on the improvement of catalyst to convert heavier and lower quality feedstocks. Catalytic hydroprocessing of liquid biomass technology has possibility to fulfill the

Chapter 1: General Introduction and Literature Survey

demand of biofuels market as it can convert a wide range of liquid biomass, such as waste cooking oils, vegetable oils, pyrolysis oil, non-edible seeds oils, animal fats and algal oils (microalgae or macroalgae), solvents extracted lipid into biofuels (gasoline, jet oil/kerosene, and diesel) with high conversion yields.

Aqueous-phase reforming (APR) of oxygenated hydrocarbons of pyrolysis oil/ bio-oil forms hydrogen (H₂) or light alkanes (primary methane) by fragmentation of C–C bonds, as well as C–H and/or O–H bonds over supported metal catalysts of Group VIII metals such as Pt and Ni catalytic [117–120]. Rh preferably gives C–O scission, as opposed to a C–C bond breaking [88].

Aqueous phase processing of sugars and polyols results in H₂ and alkanes products [119]. Hydrogen is a major feedstock for the majority of refinery processes to the production of transportation fuel [120]. C can produce hydrogen–C bond cleavage (to produce CO) followed by the water gas shift reaction, which is endothermic reaction over supported metal catalysts in the APR process [121,122]. The overall reaction for APR of sorbitol is shown in equation (1).



Paraffin (C1-C6) can be produced by dehydration/hydrogenation (APD/H) in APR; also a subset of APP by using a bifunctional catalyst containing metal and acidic sites such as Pt supported on silica-alumina, as shown in equation (2).



1.1.7. Reaction mechanisms under hydroprocessing

Hydrotreating process of bio-oil involves three-step; in the first step, preheated liquid feed trickles down over the solid catalyst bed in the presence of high-pressure H₂ gas. Hydrogenation reaction of the unsaturated/olefinic bond (C=C), followed by oxygen removal from C–O and C=O bonds, via hydrocracking through three different pathways: decarboxylation, decarbonylation, and hydrodeoxygenation to produce saturated alkanes. Third and final step involves the isomerization and cracking (hydro/thermal) to produce

Chapter 1: General Introduction and Literature Survey

different saturated straight chain hydrocarbons via hydrocracking; refinery gas product (<C6), gasoline (C6-C9), middle distillates like kerosene/jet oils (C9-C14) and diesel (C15-C18) with some degree of branching hydrocarbons and heavy hydrocarbons (>C18). The details of major reactions involve in this process are given below [20,123].

1.1.7.1. Olefin Saturation

Saturation reactions need to catalytic hydrotreating in excess H₂ environment to allow the breakage of C=C bonds and their conversion to their respective single bonds containing compounds, e.g., the double bond of unsaturated carboxylic acid converts into saturated carboxylic acid in lipids (TAGs), as mentioned in equation 3. Furthermore, in addition to the hydrogenation of C=C bonds, other saturation reactions of unsaturated cyclic compounds and aromatic compounds are likely to occur in pyrolysis oil to form naphthenes, during the upgrading of pyrolysis oils, which are mentioned in equations 4 and 5, respectively.

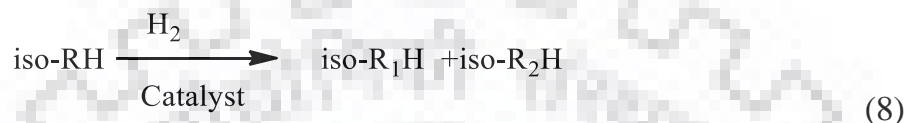
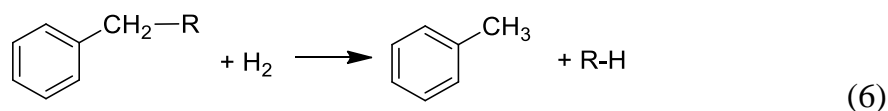


1.1.7.2. Cracking/ Hydrocracking

Biomass-derived liquid has relatively large and complicated molecules; cracking process converts them into small molecules, and low boiling range conventional transportation fuels hydrocarbons (gasoline, kerosene/jet oil, and diesel). Triglycerides (TAGs) of algae lipids crack into fatty acids (carboxylic acids) and propane [27]. Based on boiling point, TAGs have higher boiling range (IBP 600 °C) compounds, which convert to mid-distillate range hydrocarbons (naphtha, kerosene, and diesel) by cracking. The long chain hydrocarbons of pyrolysis oil which include polyaromatic and aromatic compounds convert into the lower range of aromatics hydrocarbons along with deoxygenation of

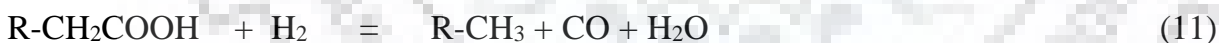
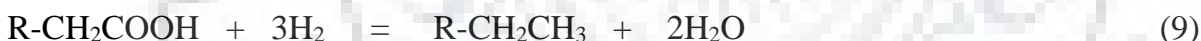
Chapter 1: General Introduction and Literature Survey

oxygenated hydrocarbons of pyrolysis oil leading to smaller chain paraffin, during the upgradation, which is mentioned in equations 6, 7 and 8, respectively.



1.1.7.3. Heteroatom removal

Biomass-based oil has extremely low heteroatoms, sulfur (S), and nitrogen (N). However, it has an extremely large quantity of heteroatom, oxygen (O). Particularly O₂ removal is most important for upgradation. The drawback in biofuels has been discussed earlier. The oxygen is removed in the form of CO₂, CO, and H₂O by decarboxylation/decarbonylation dehydration. Removals of oxygen are mentioned in equations 9, 10, and 11, respectively [124].

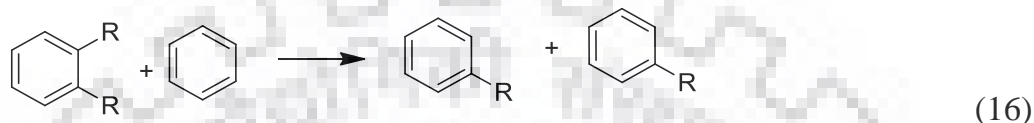


Hydrotreated products are paraffinic. The other heteroatom, i.e., S and N are removed in the form of gaseous H₂S and NH₃, respectively as shown in equation 12, 13 and 14.



1.1.7.4. Isomerization/ Hydroisomerization

Isomerized hydrocarbons containing biofuels, improve the cetane number, oxidation stability, cold flow properties, and heating value. The isomerization reactions are mentioned in equations 15, 16, and 17, respectively.



Hydroprocessing, mechanism, and kinetics are still under investigation, due to its complexity. The all possible mechanism of cleavage the C-O/C-C bond of three different carboxylic esters in TAGs is schematically represented in Figure 1.4. [27].

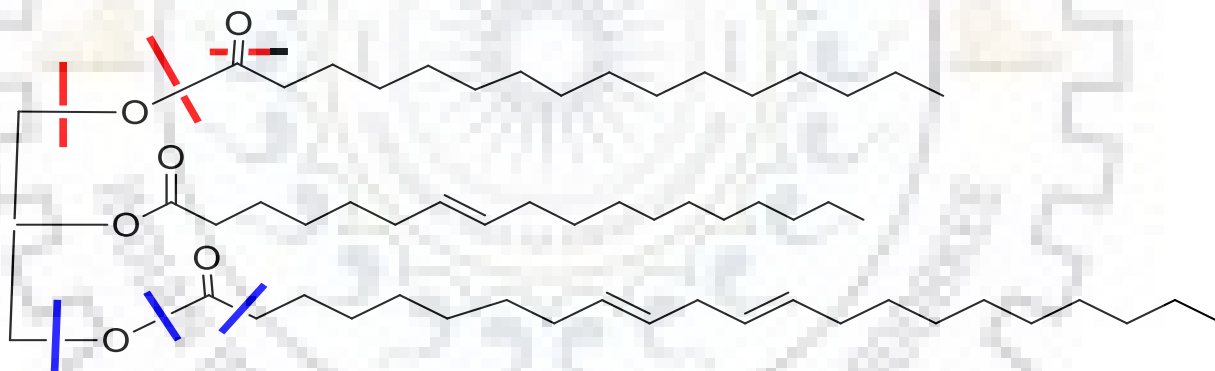


Figure 1.4.. The schematic reaction for the removal of oxygen from triglyceride (TAGs) by hydrotreating

The expected pathway for hydroprocessing of TAGs is shown above in Figure 1.2. Oxygen gets removed as water (H_2O) during hydrogenation/hydrodeoxygenation (HDO) reaction, which is represented in red color. Another mechanism, i.e., decarboxylation or decarbonylation, converts the TAG into CO_2 , propane, and/or CO and n-alkane with one C-atom shorter than the total length of the fatty acid. Blue dotted lines represent this. Heavy hydrocarbon compounds are cracked into paraffin and olefins followed by the thermal

Chapter 1: General Introduction and Literature Survey

cracking and oxygen removal via HDO reaction of the triglyceride (TAGs) molecule, results in the thermal and catalytic mechanisms. During isomerization, an n-alkane can be hydroisomerized with some extent of branching, which is described in Figure 1.5. To understand the mechanism, it involves methyl group branches [28,125].

Carbon dioxide is one of the greenhouse gases, which leads to environmental pollution. To prevent environmental pollution, various methodologies are developed for the chemical fixation of carbon dioxide to valuable chemicals, and the synthesis of five member cyclic carbonates via coupling of carbon dioxide with an epoxide is one of the promising reaction in this direction [126].

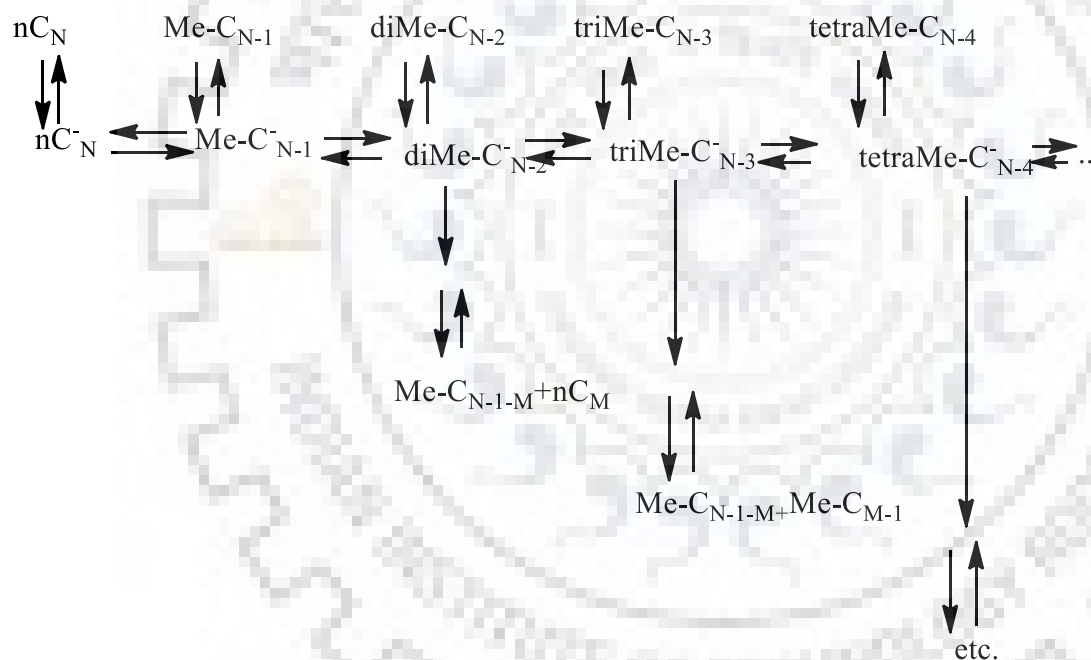


Figure 1.5. n-Alkane hydroconversion (hydroisomerization and dehydrogenation) mechanism over Pt catalyst on an acidic support

1.1.8. Hydroprocessing catalysts

Catalytic hydroprocessing of liquid biomass (agriculture and marine algae) is still developing in the field of biofuels/ transportation fuels. There are many parameters to be developed of optimization for hydroprocessing. Hydrodeoxygenation (HDO),

Chapter 1: General Introduction and Literature Survey

hydrodecarbonylation, hydrocarboxylation, hydrocracking, and hydrogenation are the major steps involved in biomass-derived oils conversion transportation fuels by removing oxygen [19]. These reactions mentioned are together called hydroprocessing reactions. This reaction is defined as catalytic high-pressure hydrotreatment or hydrodeoxygenation accompanied by hydrocracking [20].

The most known commercial catalysts for hydroprocessing (refinery streams) are Group VIB and VIII metals, e.g., cobalt and molybdenum (CoMo) or nickel and molybdenum (NiMo) on alumina support (Al_2O_3). These catalysts functioned well in the typical hydroprocessing reaction environment for oxygen-containing organic precursor feedstock, by which high concentrations of H_2O are generated/removed [21]. The concentration of base metals varies from 1- 6 wt % for Ni and from 8-20 wt % for W, which is needed to be maintain in their sulphided form in order to be active at process conditions, to maintain activity, therefore, a small amount of H_2S is commonly added with feed. However, novel metal gets deactivated in the presence of sulfur; besides it is also not good for environmental reasons.

Hydrocracking catalysts are bimetallic, containing both hydrogenation and cracking/isomerization reactions. Hydrogenation needs active metals like cobalt (Co), nickel (Ni), palladium (Pd) platinum (Pt), etc. [33–38,127–130]. However, there are several disadvantages to using these catalysts. Noble metal catalysts are not economically viable and more sensitivity towards catalyst poison due to the presence of impurities like sulfur, heavy metals, and oxygenated compounds [39,40].

Many hydroprocessing catalysts use amorphous mixed oxides of $\text{SiO}_2 - \text{Al}_2\text{O}_3$ as the support, due to its low cost and high acidity. The metallic sites are involved in hydrogenation and dehydrogenation reactions and the acidic supports, such as crystalline zeolites (γ -zeolites), amorphous oxides ($\text{SiO}_2\text{-Al}_2\text{O}_3$), and mixtures of zeolite having amorphous oxides are involved in cracking as well as in isomerization reaction, to enhance the cetane number. The catalyst activity decreases by the deposition of coke over active metals. Coke formation is due to the presence of acidic support. [42–47,49–52,131–135].

Chapter 1: General Introduction and Literature Survey

Zeolites have acidic properties and have major application properties for petroleum refining and fine chemical industries. Zeolites (microporous) give diffusion constraints for reactant and product molecules for fine chemical industries application [8,9]. Zeolites having intracrystalline or intercrystalline mesoporosity have attracted significant attention because of their catalytic activity, improved diffusion, selectivity, and retardation against deactivation [136].

Temperature and hydrogen partial pressure (P_{H_2}) affect the catalyst deactivation rate. Higher temperature and higher acidity of support may lead to cracking, resulting in catalyst deactivation. However, high hydrogen partial pressure tends to mitigate/suppress the catalyst deactivation rate. Amorphous oxide supported catalysts give less cracking activities than the zeolite-containing catalysts.

The commercial catalysts are designed for conventional crude fossil fuel feedstocks, which have high sulfur concentration. The catalyst for hydroprocessing of renewable feedstocks like algae extracted lipids, non edible biomass and other intermediates of products of biomass conversion processes (e.g., pyrolysis bio-oil) are under development, because, the character of biomass-based oil (pyrolysis oil/bio-oil or algae oil; TAGs/lipids) feed is different from the existing fossil-based fuel [137].

Therefore, it is very important to design the acidic sites as well as metal components and tailor the balance between the metal and acid for the product selectivity, catalyst activity, and stability.

Worldwide research has been done for HDO over various catalysts, keeping in mind that, the catalyst should have better selectivity, activity, and resistance to deactivation. The catalytic species have various derivatives of metals, like sulfides, phosphides, nitrides, and carbides. These have been used on various supports, and in general, the acidic supports catalyze the transformation of a methyl group and lead to catalyst deactivation by coke formation on the catalyst surface. Noble metals, such as platinum, offer high activities for HDO reactions, that lead to the hydrogenation of aromatic rings by consuming H_2 [138–141]. The use of noble metal and the consumption of H_2 have an economic disadvantage.

Chapter 1: General Introduction and Literature Survey

Many researchers have studied the supported non-noble transition metals (e.g., ZrO₂, SiO₂, and MgO), which are less expensive than noble metals and offer resistant to coke formation [106,113,142–144].

It was found that the activity for guaiacol HDO decreased in the following order (equation 15) [140]:



Conversion of guaiacol, over bimetallic active metal, combinations of Rh, Pt, and Pd lead to much better results than were observed with monometallic platinum (Pt), palladium (Pd) and Rhodium (Rh) based catalysts. Hydroprocessing of anisole over Ni–Cu/ Al₂O₃ catalysts showed higher conversions than monometallic Ni/Al₂O₃ catalyst. The higher activity of the bimetallic catalysts may be due to the incorporation of less nickel in the bulk Al₂O₃, while the copper, results in less formation of nickel spinel than in the monometallic nickel catalyst. MoS₂ and supported catalyst that incorporates cobalt and molybdenum or nickel and molybdenum (abbreviated as CoMoS and NiMoS) are widely used in hydroprocessing reactions [113,138,145–155].

1.1.8.1. Metal phosphides

Hydroprocessing of various model compounds of bio-oil has been studied over transition metal phosphide catalysts. Guaiacol is one of the model compounds. It was observed that metal phosphide gave higher conversion than metal sulfide, but CoMo/Al₂O₃ catalysts underwent rapid deactivation. However, in the conversion of guaiacol, more coke formed on the phosphide than on the sulfide catalyst, due to higher existence of Lewis acid sites/ Brønsted acid sites, which favor the demethylation pathway [156–158].

The observed trend for phosphide of transition metals for hydroprocessing/hydrodeoxygenation (HDO) of guaiacol was observed as in mentioned order: Ni₂P > Co₂P > Fe₂P > WP > MoP.

Chapter 1: General Introduction and Literature Survey

1.1.8.2. Metal nitrides

In recent years, the researchers gave attention to metal carbides and nitrides of some of the transition metals for the hydrotreating process. The metal carbides and nitrides have comparatively better catalytic activity than conventional hydrotreating bimetallic sulphided catalysts. These type of catalysts have similar activity to the noble metals based catalysts, due to the presence of carbon or nitrogen in the lattice of the transition metals, and it increases the lattice parameter and leads to an increase in the d-electron density [159,160]. Mono- and bimetallic carbides and nitrides catalysts have been successfully applied in place of metal sulfide catalyst for upgradation of petroleum oil, and it produced branched diesel-like hydrocarbons [161–164]. Mono and bimetallic carbides and nitrides catalysts also show high activity and selectivity for one-step conversion of lipids (TAGs) extracted from algae biomass.

Nitrides of metals like tungsten (W), molybdenum (Mo), and vanadium (V) supported on γ -Al₂O₃ have been used for hydrodeoxygenation of oleic acid and canola oil. The oxygen content was removed > 90%, for a reaction time of 450 h. It gives 38-48 wt% yields of the middle distillate of refinery hydrocarbons. It also improves the cetane number of diesel.

Metal nitrides give both acidic as well as basic sites for reaction due to the electronegativity differences between the metal and nitrogen atoms; they drew attention as hydroprocessing catalysts. The potential advantages of metal nitride catalysts have their low-cost resistance, ease of preparation, and oxidation reaction. Doing HDO reactions on nitride catalysts, nitrogen may be released from the bulk lattice and create surface sites for adsorption and activation of hydrogen.

For metal carbides and nitrides of transitions metal (Mo and W), the hydrogen absorption amount increases with increasing particle size. The activity of this catalyst for hydrodesulfurization, hydrogenation, and hydrodenitrogenation exhibits similar trend. Carbides and nitrides of transitions metal (Mo and W) catalysts are stable under typical hydroprocessing conditions [162].

Chapter 1: General Introduction and Literature Survey

Bimetallic nitride catalyst CoMoN gave a higher yield of deoxygenated products than the monometallic nitride (MN) catalyst; although, the overall activities was higher for bimetallic than for monometallic metal nitrides catalyst [163].

1.1.8.3. Supports

Support species disperse the active metal for better accessibility and reactivity of feed material; alumina is one of the most commonly applied supports for hydroprocessing reaction. A major disadvantage of the acidic support is the formation of coke in high yield. Weak Lewis acid leads to coke formation [113]. Researchers now have focused on developing new supports for less H₂ consumption, increasing selectivity for direct oxygen removal, and minimizing coke formation. There are many supports like Ni–W, active carbon, SiO₂, SiO₂–Al₂O₃, and nitric acid treated carbon black, mesoporous silica (SBA-15 and SBA-16), ZrO₂, and TiO₂, SiO₂–ZrO₂ for upgradation of bio-oil and its model compounds [151,152,158,165].

Researchers have studied several supports like alumina, silica, titania, and zirconia on molybdenum (Mo) based catalysts for hydroprocessing applications [166]. High activity and selectivity are usually provided by the compounding of two or more functionalities like hydrogenolysis activity, and acidity on the same material [167–169].

Various mixed oxides such as TiO₂–ZrO₂, TiO₂–Al₂O₃, SiO₂–ZrO₂, and TiO₂–SiO₂ also have been applied to many reactions like dehydrocyclization, isomerization, dehydration, selective reduction of NO_x, etc. [166,170–174].

A catalyst having a high content of ZrO₂ showed very less activity and less stability under hydrotreating reaction condition. In contrast, the mixed oxides having high content of TiO₂ show better activity than single TiO₂ oxide, or conventional Al₂O₃ supported catalysts. A wide pore TiO₂–ZrO₂ catalyst showed better activity for hydrodesulfurization of dibenzothiophene after impregnating it with MoS₂ [175].

The following conclusions have been observed throughout the studies. The TiO₂ – ZrO₂ mixed oxide support calcined at 500 °C has amorphous nature and exhibits a high specific surface area (SA). The amorphous TiO₂ –ZrO₂ converted into ZrTiO₄ on

Chapter 1: General Introduction and Literature Survey

calcination beyond 600 °C, and this is thermally more stable even up to 800 °C in the absence of molybdenum. It indicates that to convert more ordered crystalline compound from the amorphous phase by inter-diffusion of ions requires high temperature. The most interesting theory of promoter activity in the heterogeneous catalytic reaction is the role of interface between two surfaces of different compositions [176].

1.1.8.4. Promoters

The promoter has a great role in improving the activity of metal deposited on the support. In the petroleum industry, cobalt or nickel in the presence of MoS₂ supported on Al₂O₃, promote as ions in the layer structure of MoS₂. The promoter increased the activity under hydroprocessing condition. Ni–Mo sulfides were more active than nickel or molybdenum sulfides alone, and the maximum activity was obtained at a Ni/ (NiMo) atomic ratio of 0.3[177].

There is no direct application of noble metals for the production of jet fuel from lipid extracted from marine algae or biomass-derived oil or vegetable oil via hydroprocessing reaction. Hydroprocessing conditions generally include temperatures range 250°C- 400°C and H₂ pressure of 50 bar – 150 bar. Transportation fuels have certain limitations, such as lower allowable limits for toxic elements such as sulfur (S) and nitrogen (N), the application of metallic nitride and carbide catalysts for hydroprocessing has been attracting a lot of researchers' attention [178].

1.1.9. Kinetic modeling methods

Kinetic studies are critical to connecting the microscopic picture of molecules undergoing reactions, to the macroscopic picture of reaction engineering, which extends to commercial scale. Kinetics is one of the key disciplines in the field of catalysis. Even a simple model based on power-law kinetics could predict the dependence of the individual components of algae oil (lipid) on the rate of a chemical process. These are the critical information to predict how a reactor behaves in a given range of temperature and pressures [179].

Chapter 1: General Introduction and Literature Survey

1.2. Motivation

In spite of several studies on co-processing at laboratory and pilot plant levels, the understanding of the influence of various types presence of a type of pyrolysis oil components on the hydroprocessing product distribution remains limited. Also, there is a lack supply on *Jatropha curcas* cake-derived pyrolysis oil (indigenous feedstock) and microalgae-based oil (lipids) for hydroprocessing with or without refinery gas oil (GO) to get drop-in liquid hydrocarbons or transportation fuels like gasoline, kerosene/jet oils and diesel. The same holds for the understanding on ways to optimize the process parameters, to obtain the limitations on hydroprocessing of biomass-based oil with petroleum-derived fraction, i.e., GO and specific effect of type of oil (pyrolysis and lipids oil) compound on hydroprocessing product distribution.

1.3. Objective

The objective of the present work is to pursue and describe the studies on hydroprocessing/ co-processing of non-edible biomass-based oil (pyrolysis oil and algae oil/lipid) with or without refinery gas oil (GO). It is an effective way to find renewable fuels. These studies will help in understanding the blending limitations of GO with organic phase (BO) of pyrolysis oil of *Jatropha curcas* seeds cake (JCC) and influence of various reactions parameters like temperature, pressure space velocity, activation energy and catalyst, etc. on biomass-derived oils (pyrolysis oil; aqueous phase as well as organic phase and algae oil/lipid).

The specific objectives of the present study are as follows:

- a. Production of pyrolysis oil from de-oiled *jatropha curcas* seeds cake biomass (JCC) in continuous fixed bed reactor set-up.
- b. Separation of the aqueous and organic phase of pyrolysis oil.
- c. Extraction of lipid (TAGs) from marine microalgae *Nannochloropsis* sp. algae biomass.
- d. Compositional analysis of pyrolysis oil (organic phase, aqueous phase), and lipid (TAGs).

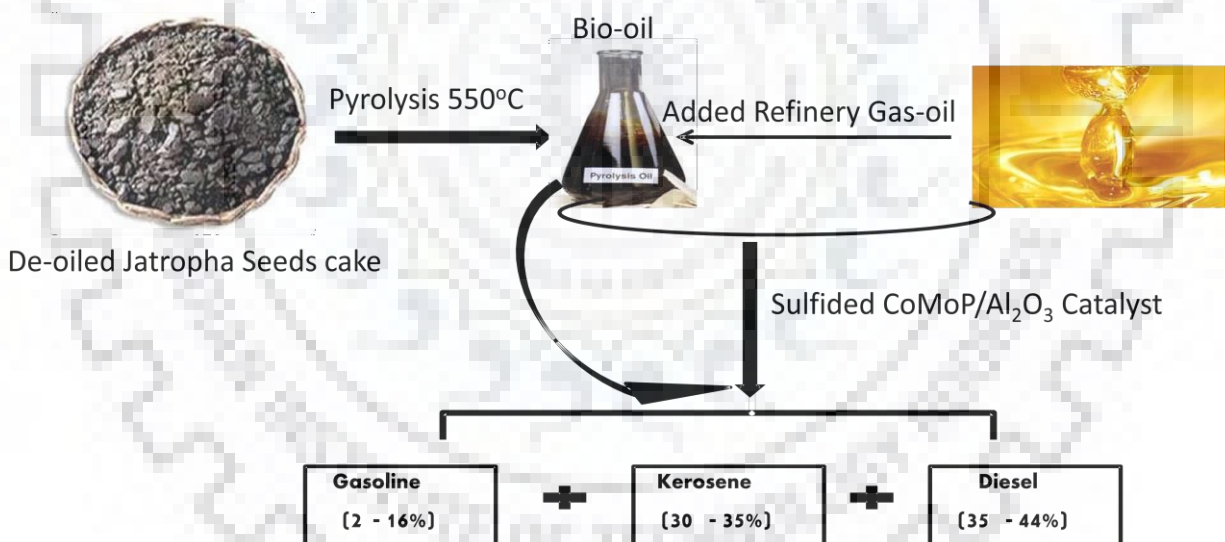
Chapter 1: General Introduction and Literature Survey

- e. Catalysts preparation
- f. Optimization of process conditions like temperature, pressure, blending ratio, reaction time, etc. for hydroprocessing reaction to produce transportation fuel like gasoline, jet fuel, and diesel in a batch reactor.
- g. Reactor set-up and catalyst loading in channels of continuous microchannel reactor (MCR).
- h. Optimization of process parameters (temperature, pressure, space velocity (LHSV) and H_2 : feed, etc.) for hydroprocessing to produce transportation fuel like gasoline, jet fuel, and diesel in a MCR.
- i. Kinetic parameters study for reactions involved in hydroprocessing of lipids.
- j. Optimization of process conditions like temperature, pressure, blending ratio, reaction time, etc. for hydroprocessing of algae oil to produce transportation fuels (gasoline, jet fuel, and diesel) in a batch reactor.



Chapter 2

Co-processing of bio-oil from de-oiled jatropha curcas seeds cake with refinery gas-oil over sulphided CoMoP/Al₂O₃ catalyst



This work has been published in RSC Adv., 6 (2016) 113720-113726.

Chapter 2: Co-processing of bio-oil from de-oiled jatropha curcas seeds cake with refinery gas-oil over sulphided CoMoP/Al₂O₃ catalyst

2.1. Introduction

Liquid transportation fuels; gasoline, kerosene (jet oil) and diesel, from biomass, are renewable alternatives to the current fossil derived fuels. The first generation has been investigated for the conversion of biomass (edible component) into liquid fuels (biodiesel and bioethanol). Biodiesel has been produced from edible plant oils and bio-ethanol from carbohydrate-rich resources by biological process (fermentation) and chemical process (trans-etherification). First generation biofuels have problem with food versus fuel demands, so these biofuels are not encouraged socially and industrially, and new options are being developed. Second generation biofuel platforms are thermochemical conversion processes like pyrolysis, gasification, and hydrothermal liquefaction of non-edible biomass sources like agricultural wastes, forestry wastes, and municipal wastes, etc. [180]. High abundance, availability, and low procurement cost are the advantages of considering biomass as a source. The potential for successful deployment of technologies to produce liquid biofuel from biomass and their cost reductions [181].

Liquid product yields from pyrolysis of deoiled jatropha (non-edible) curcas seeds cake are up to 60-70 wt% and the product (bio-oil) consists a wide range of functional groups containing oxygenate and heavy compounds having a wide range of molecular weights [68]. Classes of the compounds in bio-oil (BO) are organic acids, aldehydes, ketones, phenolics, and alcohols. The bio-oil (BO) requires upgrading because as such it is not suitable as a biofuel for high-speed internal combustion engines, due to large amounts of water (up to 30 wt. %) and corrosive organic acids (up to 10 wt. %) present in it [69,84]. It shows limited storage stability and undesirable physical properties.

Catalytic bio-oil upgrading presently seems to be an economic techno process toward the production of fuel-like components. A major aim of upgrading bio-oils is to convert the oxygen-rich, high molecular weight components into hydrocarbons that are similar to petroleum-derived fuels (drop-in fuels). Upgradation is done by chemical (such as cracking etc.), and physical methods (such as distillation, etc.) [84]. Catalytic hydrotreatment is considered a promising upgrading technology to produce kind drop-in

Chapter 2: Co-processing of bio-oil from de-oiled jatropha curcas seeds cake with refinery gas-oil over sulphided CoMoP/Al₂O₃ catalyst

fuels from bio-oils [182]. This process involves the treatment of bio-oil (BO) with hydrogen in the presence of a heterogeneous catalyst. However, the selection of stable and productive catalyst(s) towards refinery products with low coke formation is a great challenge. The primary aim is the minimization of the oxygen content and reduction of the chain length by a process called hydroprocessing (catalytic high-pressure hydrotreating or hydrodeoxygenation accompanied by hydrocracking). Hydrodeoxygenation is a chemical conversion that takes place at high H₂ partial pressures (as high as 75-300 bar) and high temperatures (300–450 °C) to remove oxygen primarily in the form of water or CO₂ [183,184].

Hydrodeoxygenation of bio-oils gives hydrocarbons and oxygen-containing organic compounds in addition to water and CO₂, and the classes of reactions include decarboxylation, hydrogenation, hydrogenolysis, hydrocracking, and dehydration leading to gasoline, kerosene, and diesel like products. Research activities on the hydrodeoxygenation of pyrolysis oil started in 1984 with the pioneering work of Elliott and Baker on commercial hydrodesulfurization (HDS) catalysts, i.e., sulphided NiMo/Al₂O₃ and CoMo/Al₂O₃[185]. The primary issue interfering with long-term operation of these systems has been the fouling of the catalyst bed by carbonaceous deposits. Deactivation of these catalysts as a function of time on stream is reported [186,187]. Deactivation might be due to blockage of catalyst pores and active sites, sintering of the active metals, poisoning of the catalyst, structural degradation of the support and active sites, coking and metal deposition [112].

This chapter intends to report the production of transportation fuel (gasoline, kerosene, and diesel) by hydroprocessing of heavy, dark viscous organic phase (bio-oil) obtained from pyrolysis of non-edible jatropha curcas seeds cake (JCC), as such or with refinery streams, by using economically viable catalyst sulfided CoMoP/Al₂O₃. The advantage of this work is that transportation fuels can be produced by using a single catalyst compared to other expensive multi-catalyst processes such as hydrodeoxygenation with noble metals followed by cracking. It is demonstrated that optimization of process

Chapter 2: Co-processing of bio-oil from de-oiled jatropha curcas seeds cake with refinery gas-oil over sulphided CoMoP/Al₂O₃ catalyst

conditions resulted in the suppression of carbonaceous deposits by minimizing the formation of the polynuclear aromatic, which are the precursors for carbonaceous deposits.

2.2. Experimental details

2.2.1. Materials

Co (NO₃)₂·6H₂O, (NH₄)₆Mo₇O₂₄·4H₂O and orthophosphoric acid (85% of aq. H₃PO₄) were obtained from Sigma Aldrich. γ -alumina was obtained from Sasol. HPLC grade water was used as a solvent for synthesis. Bio-oil (BO) was produced in a tubular reactor (SS 314) (shown in Figure 2.1.). Gas-oil (GO) was obtained from Mathura Refinery, India.

2.2.2 Catalyst preparation

The catalyst was prepared by the incipient wet-impregnation method. Mo metal precursor (NH₄)₆Mo₇O₂₄·4H₂O (1.89 g) in liq. NH₃ was added dropwise with continuous stirring to 7.9 g of dried γ -alumina to obtain the required Mo (16 wt %) loading on the support. Then calculated amount of Co metal precursor (Co (NO₃)₂·6H₂O, 1.55 g) dissolved in water was added dropwise with continuous stirring to obtain the required Co amount (4 wt %). The solution was dried at 393 K for 4h. After drying, 85% aq. H₃PO₄ (0.16 g), was added dropwise with continuous stirring to obtain the required P amount (1 wt %). The sample was dried at 100 °C and calcined at 550 °C for 6 h (heating rate, 1 °C min⁻¹).

2.2.3. Characterization methods

The surface area of catalyst was measured using the Brunauer–Emmett–Teller (BET) method by nitrogen adsorption isotherm at -196 °C using BELSORP-max, Japan apparatus. Before analysis catalyst sample was degassed at 250 °C under vacuum. The pore size was calculated from desorption isotherm using the BJH (Barrett, Joyner, and Hallender) method.

Chapter 2: Co-processing of bio-oil from de-oiled jatropha curcas seeds cake with refinery gas-oil over sulphided CoMoP/Al₂O₃ catalyst

Samples for Transmission Electron Microscopy (TEM) were prepared by deposition of the catalyst on a copper grid by suspension in isopropanol. TEM images were recorded using FEI, series Tecnai G2 operating at 200 kV. Deposited metals (Co 4%; Mo 16% and P 1%) were determined by Inductively Coupled Plasma-atomic emission spectroscopy (ICP-AES) method on a Leeman Labs, Inc (U.S.A.) (model no PS3000 UV (DRE) equipment.

2.3. Reaction procedure

2.3.1. Pyrolysis

A tubular reactor (inner diameter 7.5 cm and length 85 cm) electrically heated with a furnace around it was used for the pyrolysis of deoiled Jatropha curcas cake (10-35 mesh), at 550 °C temperature (heating rate 10 °C/min) and ambient pressure in N₂ atmosphere. N₂ gas was used to maintain an inert medium in the reaction system, to dilute the formed pyrolysis vapors, to minimize char formation and to prevent further reactions. Biomass (1kg deoiled Jatropha curcas cake) was used for the reaction, and N₂ gas (825 ml/min) was passed continuously through a gas-meter, and pyrolysis vapors were carried into a series of two condensers to condense the pyrolysis vapor to obtain the pyrolysis liquid (bio-oil), and the non-condensable gases were vented off. The schematic diagram of the pyrolysis unit is shown in Figure 2.1. The detailed composition of bio-oil has been reported recently [4]

Chapter 2: Co-processing of bio-oil from de-oiled *Jatropha curcas* seeds cake with refinery gas-oil over sulphided CoMoP/Al₂O₃ catalyst

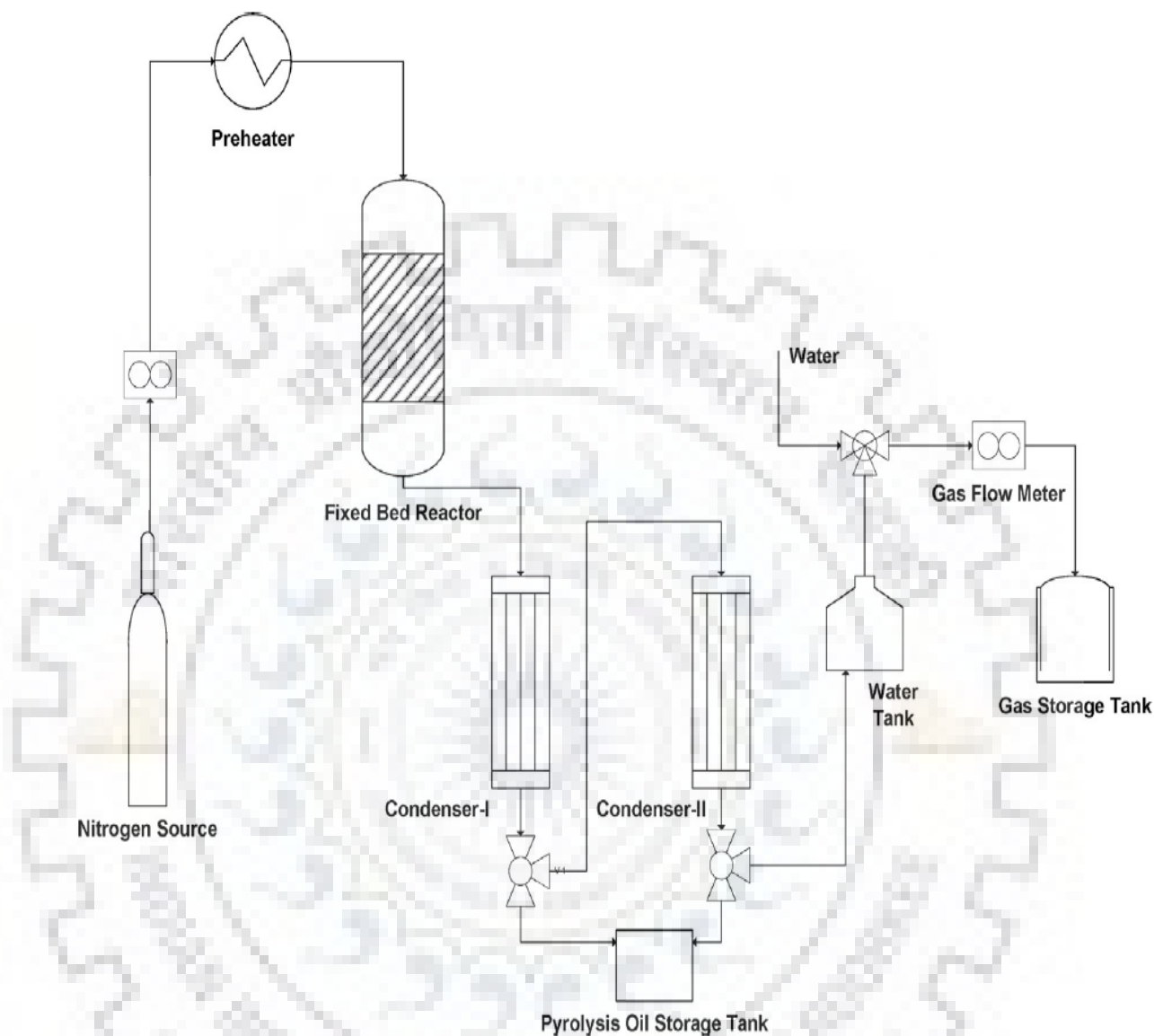


Figure 2.1. Schematic flow diagram for slow pyrolysis set-up.

2.3.2 Biochar analysis

2.3.2.1. FTIR Analysis

The FTIR spectra of *Jatropha curcas* cake and char are shown in Figure 2.2. For *Jatropha curcas* cake, the band at 3420 cm^{-1} represent the stretching vibration of -OH hydroxyl groups of phenol. The -CH stretching band of methylene group was detected at a wave number of 2929 cm^{-1} . The of O-CH_3 band and C=O band of aldehyde group were

Chapter 2: Co-processing of bio-oil from de-oiled *Jatropha curcas* seeds cake with refinery gas-oil over sulphided CoMoP/Al₂O₃ catalyst

found around 2845 cm⁻¹ and at 1647 cm⁻¹ respectively [188]. The bands at 1452, 1419, 1403, and 1378 cm⁻¹ were assigned mainly to CH₂ units in biopolymers [189]. The peak at 1154 cm⁻¹ is assigned to C-O stretching vibration of ester bonds. The band due to aliphatic C-O-C and alcohol -OH (1154-1030 cm⁻¹) represents oxygenated functional groups of cellulose [190]. The peak at 1544 cm⁻¹ represents the C=C ring stretching vibration of lignin. The band at 1272 cm⁻¹ was assigned to the aromatic CO and phenolic -OH stretching [191]. Methyl or amine groups were shown a peak at around 1381 cm⁻¹.

The band from 1200 to 1000 cm⁻¹ is the fingerprint of syringyl alcohol units. Aldehyde groups and derivatives of benzene were detected by peaks at 897 and 775 cm⁻¹[188]. The FTIR spectrum of char showed an increasing drift in the baseline at high wavenumbers, which is an indication of an increase in the carbonaceous component content of chars [192]. All these bands experience different changes after the fast pyrolysis reaction, which can be clearly seen in pyrolysis char. The absorbance peaks in the range of 1740 and 1100 indicated the presence of hemicelluloses components, which became weak and broadened due to the structural collapse of the holocellulose. The band intensities were dramatically decreased at 3420 cm⁻¹ (-OH) and 1154-1030 cm⁻¹ (C-O). The intensity of the absorbance of -OH hydroxyl decreased due to the decrease in hydrogen-bonded -OH stretching after fast pyrolysis of *Jatropha curcas cake*. It may be due to the loss of phenolic or alcoholic groups since the oxygen/carbon (O/C) ratio of the biochar also decreased.

The same was confirmed from the SEM-EDAX analysis. The broadband at 3340-3570 cm⁻¹ and 3230-3310 cm⁻¹ are generally assigned to hydrogen bonded OH groups in intramolecular and intermolecular cellulose, respectively. The symmetric CH₃ stretch of the O-CH₃ group in *Jatropha curcas cake* and its intensity got decreased after fast pyrolysis. It indicated that the CH₃ groups had been removed from the substituted aromatic rings after fast pyrolysis. The loss of ether groups leads to a more ordered carbon structure. The presence of peaks at 1510, 1425 and 1270 cm⁻¹ in the *Jatropha curcas cake* clearly showed that the carbon framework of lignin components are present in the cake and the same is absent in the *Jatropha curcas cake*, due to the amorphous nature of lignin

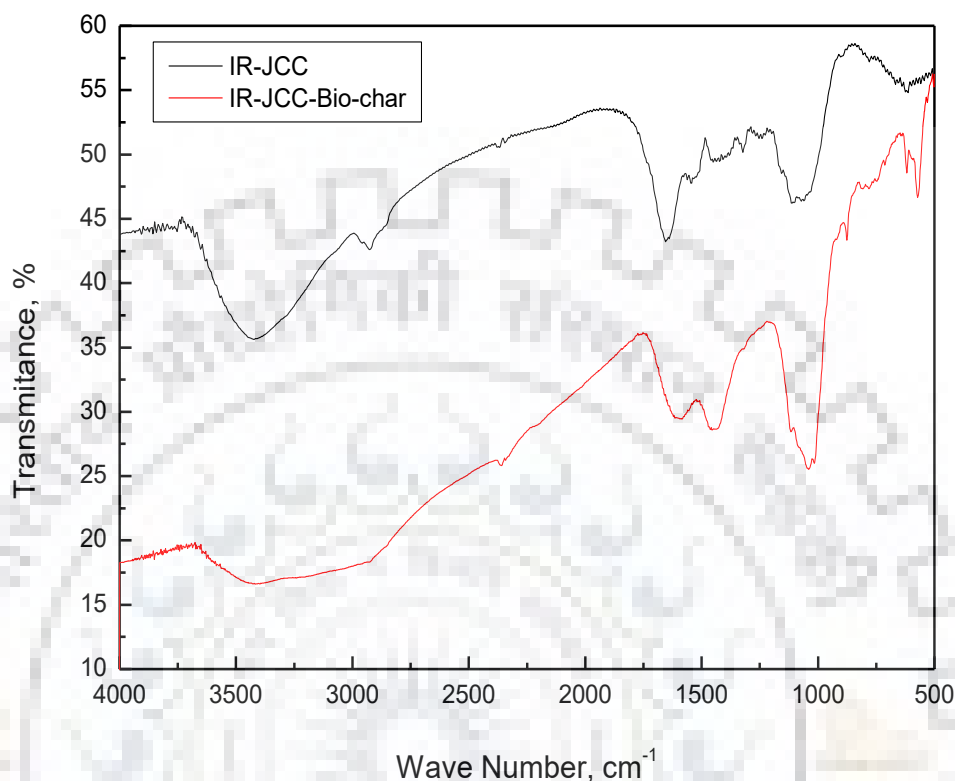


Figure 2.2. FT-IR of *Jatropha curcas* cake and its fast pyrolysis biochar

2.3.2.2. SEM Analysis

The morphology of *Jatropha curcas* cake and JCC-derived fast pyrolysis char was investigated using SEM analysis and presented in Figure 2.3. (a and b) and Figure 2.3. (c and d). It can be seen that surface of *Jatropha* char is smooth as well as cracked and pitted morphology and the presence of macropores (varies from 1.82 to 4.28 μm) on the surface leads to develop an elementary pore network. The shape of the particles varies, and many long fibrous particles were observed. The average diameter of macropore size was greater than 50 nm, according to IUPAC (International Union of Pure and Applied Chemistry).

The typical observations were: various sizes of round holes were found in the smooth areas which suggest a melt formation and volatile gas release during fast pyrolysis; precipitation of potassium, magnesium, phosphorous and sulfur was also observed along

Chapter 2: Co-processing of bio-oil from de-oiled jatropha curcas seeds cake with refinery gas-oil over sulphided CoMoP/Al₂O₃ catalyst

with the carbonaceous deposits; a large number of vesicles presence was observed along the surface of fast pyrolysis char. Even though the well developed porous structure was seen in the various resolutions of the cake images, the decomposition of biomass components was not uniform as the bigger particles break apart into several particles sequentially during the condensation and decomposition reaction of components. The elemental analysis or chemical characterization of fast pyrolysis char is shown in Table 2.1. It can be seen that the carbonaceous content of fast pyrolysis char is 88.03 wt % and the same was also confirmed by EDAX analysis, while that of JCC is 68.11 wt%. The amount of oxygen content in fast pyrolysis char is (11.07 wt %) less as compared to JCC (30.58 wt %).

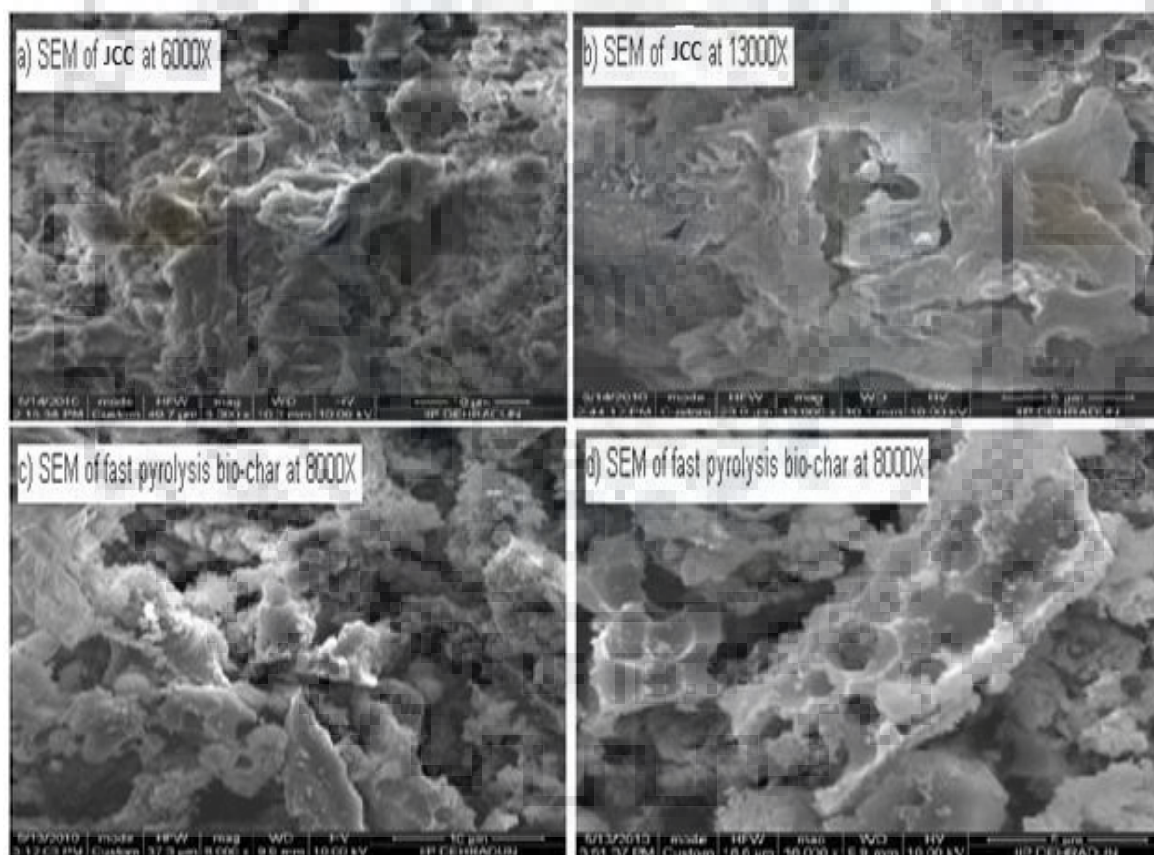


Figure 2.3. SEM of *Jatropha curcas* cake (a and b) and its fast pyrolysis biochar (c and d).

Chapter 2: Co-processing of bio-oil from de-oiled *Jatropha curcas* seeds cake with refinery gas-oil over sulphided CoMoP/Al₂O₃ catalyst

2.3.2.3. XRD Analysis

The image of *Jatropha curcas* cake and fast pyrolysis char X-ray diffractograms (XRD) are displayed in Figure 2.4. The X-ray diffraction pattern of *Jatropha* seed cake has a wide halo in the 2θ range from 5 to 16° , which is characteristics of multi-component carbon-containing materials [193]. The two bands were observed at $2\theta \approx 22.5^\circ$ and 44° , which correspond to the diffuse graphite (002) and (100) bands, respectively in biochar. Further, it can be seen a broad peak centered at $2\theta \approx 28^\circ$ in the X-ray diffractogram of biochar, which showed the presence of silica. The peaks at $15, 17,$ and 22.7° are derived from cellulose[192,193].

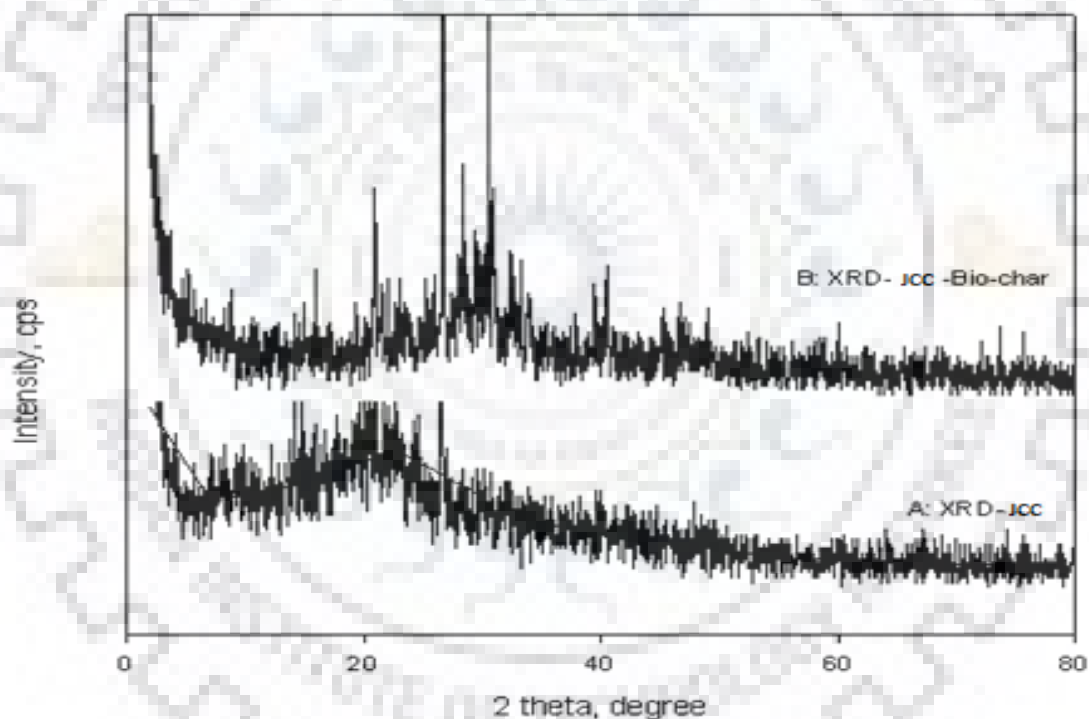


Figure 2.4. XRD of *Jatropha curcas* cake and its fast pyrolysis biochar.

Chapter 2: Co-processing of bio-oil from de-oiled jatropha curcas seeds cake with refinery gas-oil over sulphided CoMoP/Al₂O₃ catalyst

Table 2.1. Ultimate and structural analysis of JCC.

Ultimate analysis, wt.% (Dry Basis)		Structural analysis, wt.% (Dry & Extractive)	
Carbon	45.50	Cellulose	26.00
Hydrogen	6.70	Hemicellulose	45.55
Nitrogen	2.47	Total lignin	16.16
Oxygen	45.33	Ash	9.42
		Moisture	7.20

2.3.2.4. CHNO Analysis

The ultimate and structural analysis of *Jatropha curcas* cake feedstock is shown Table 2.2. It can be seen that the carbon content of JCC-derived pyrolysis char is very high, 88 wt. %, as compared to the JCC biomass feedstock, which is 45 wt. % on a dry basis.

The ash content of JCC is about 9% on a weight basis from trace metal analysis, and as a result, some of the trace metals were also seen in the pyrolysis char and pyrolysis oil fractions.

2.3.3. Sulfidation of catalyst

Catalytic reactions were carried out in a stirred batch reactor (Parr, USA) with vessel size of 25 ml (alloy C276), and with K type thermocouple (calibrated to the accuracy of ± 1 °C) in the reactor. Sulfidation of catalysts was carried out in the same reactor before reactions. Sulfidation was done using 2.5 wt % of dimethyl disulfide (DMDS) mixed in refinery gas oil (GO) at 40 bar of hydrogen pressure by gradually raising the temp from 100 °C to 350 °C (10 °C min^{-1}) and heating for 13 h.

2.3.4. Catalytic reaction conditions

Bio-oil (BO) from deoiled *Jatropha curcas* cake was hydroprocessed, in the same reactor used for sulfidation, in the presence of a sulfided form of prepared catalyst CoMoP/Al₂O₃. The same reactor set-up have been used for hydroprocessing of marine microalgae *Nannochloropsis* sp. over sulfided CoMoP/Al₂O₃ catalyst (will discuss in

Chapter 2: Co-processing of bio-oil from de-oiled jatropha curcas seeds cake with refinery gas-oil over sulphided CoMoP/Al₂O₃ catalyst

chapter 4 figure 4.1) Reaction feed mixtures (BO or mixtures of BO and GO) with 10 wt % of sulfided CoMoP/Al₂O₃ catalyst was used for hydroprocessing. The reaction system containing feed BO or a mixture of BO and GO with sulfided catalyst was purged with H₂ 4-times and then pressurized to the desired pressure (50 and 75 bar) with H₂. The desired temperature was achieved by heating gradually (10 °C/min). A constant stirring rate of 680 rpm was maintained till completion of the reaction. After cooling down the reaction system, the liquid product was filtered with 0.2 µm filter paper. The viscous residue which was considered as a mixture of unprocessable bio-oil, catalyst and deposited coke (char) was dissolved in tetrahydrofuran (THF) followed by toluene to separate the catalyst from unreacted feed and deposited hydrocarbon. The amounts of liquid products, char, and unprocessable bio-oil were determined by weighing, with the repeatability of weighing balance as ±0.00025 g. The catalyst weight was subtracted from the weight of the final solid containing char and catalyst to determine the amount of char formed. The amount of gas formed after the reaction was determined from the difference in the weights of reaction vessel containing the solid and liquid reaction mixtures, before and after the reaction. Errors up to ±5 % for liquid products, ±4 % for char and ±2 % for gas products was observed. The errors are included in the final results.

2.4. Analysis

2.4.1. Gas Chromatography

Liquid products filtered with a cellulose membrane filter (pore size 0.22 µm) were analyzed using gas chromatography. A Varian 3800-GC with vf-5 ms column (30 m × 0.25 mm, 0.25 µm) and FID, was used for the analysis of hydrocarbons. The oven temperature program was 35-150 °C (3 °C min⁻¹; hold time: 5 min), 150- 300 °C (10 °C min⁻¹; hold time: 5 min), and 300-320 °C (15 °C min⁻¹; hold time: 15 min). The yields of various liquid product components were calculated on a relative basis, considering the entire range of liquid products formed as 100 %. Word, the relative yield has been used to mean the relative amounts of gas, liquid, and char produced during co-processing.

Chapter 2: Co-processing of bio-oil from de-oiled jatropha curcas seeds cake with refinery gas-oil over sulphided CoMoP/Al₂O₃ catalyst

As in petroleum refinery practice, the product distributions were quantified based on hydrocarbons size (carbon numbers): gasoline (<C₉ hydrocarbons), kerosene (C₉-C₁₄ hydrocarbons), diesel (C₁₅-C₁₈ hydrocarbons) and heavy oil (>C₁₈ hydrocarbons). Errors up to ±4 % were observed and included in the final results.

2.4.2. Two-dimensional gas chromatography (GC x GC-MS)

Two dimensional (2D) GC from Agilent Technologies (Model No.7890B), with flow modulation (G3440B), FID and mass detector (5977A, single quadrupole) and 2D GC software from Zoex Corp. was used to analyze the components of the liquid products. The 2D GC was able to group alkanes, cycloalkanes, oxygenates, aromatics, and polyaromatics. Two columns system was used to separate various components present in the product. The columns were 1st and 2nd dimension columns. The 1st-dimensional column was a proprietary non-polar column (PAC Corp.) with dimensions 30 m x 320 mm x 0.10 mm, the 2nd dimension column (PAC corp.) was a proprietary polar column with dimensions 10 m x 250 mm x 0.25 mm. Errors up to ±3 % were observed and included in the final results.

2.4.3. CHNS analysis

Carbon, hydrogen, nitrogen, and sulfur analysis of the feed, hydroprocessed products and the used catalyst containing char was performed using a CHNS analyzer equipped with TCD (for CHN) and IR detector (for ppm level of S analysis) (elementar, model - vario MICRO cube) and XP6 Automated-S Microbalance (Mettler-Toledo) with 0.6-0.8 µg repeatability. The analyses were repeated thrice for each sample. For carbon, nitrogen and hydrogen analysis the results with two significant digits after decimal were repeatable and hence reported accordingly (the error was up to 0.5 %), while for sulfur analysis the results with four significant digits were repeatable (with error up to 5 %) and reported accordingly.

2.4.4. Total acid number (TAN)

Total acidity number (TAN) of filtered liquid products was determined by the amount of potassium hydroxide (in mg) that is needed to neutralize the acids in one gram

Chapter 2: Co-processing of bio-oil from de-oiled jatropha curcas seeds cake with refinery gas-oil over sulphided CoMoP/Al₂O₃ catalyst

of oil, using Mettler Toledo G20 potentiometric titrator following ASTM D664-11a method. Alcoholic KOH was used as titrant; standardization of the titrant has been done by the standard solution of potassium hydrogen phthalate. A mixture of toluene, 2- propanol and a small amount of water, in the volume ratio of 500: 495: 5 was used as a solvent for the titration. For titration of each sample, a blank titration of the solvent was also done, to obtain the relative TAN value of hydroprocessed bio-oil concerning the solvent. For each analysis, 125 ml of solvent was taken. The weights of samples to be analyzed were 0.25-1.85 g with the repeatability of weighing balance as ± 0.00025 g. The total acid number (TAN) was determined thrice for each sample, and the variation in TAN was $\pm 1-2$ mg KOH/g.

2.5. Results and Discussion

2.5.1. Catalyst characterization

The surface area (BET) of catalyst support was $298 \text{ m}^2/\text{g}$ with a pore volume of 0.5 ml/g and mean pore size (BJH) of 7 nm . A transmission electron microscopy (TEM) image of the sulfided CoMo/Al₂O₃ catalyst is shown in Figure 2.5. The well-dispersed densely populating straight and curved CoMo-S nanoslabs of width $1-2 \text{ nm}$ and length $20-60 \text{ nm}$ are seen by TEM.

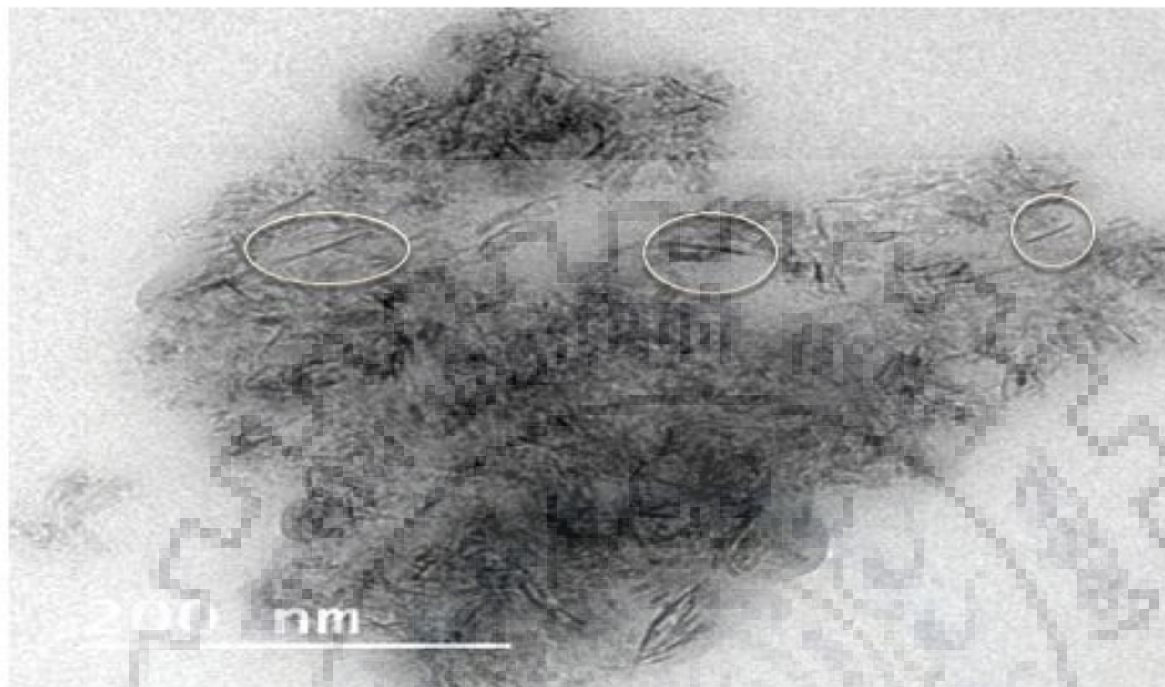


Figure 2.5. A TEM micrograph of sulfided CoMoP/Al₂O₃ catalyst.

Considering an interlayer spacing of 0.65 nm, CoMo-S nanoslabs consist of about 2 to 3 layers [194]. For CoMoS/Al₂O₃ catalyst the typical CoMoS particle size is 5–8 nm long [194,195] This indicates that P used during impregnation has resulted in better active metal dispersion with smaller nanoslab sizes.

Chapter 2: Co-processing of bio-oil from de-oiled jatropha curcas seeds cake with refinery gas-oil over sulphided CoMoP/Al₂O₃ catalyst

2.5.2. Catalytic studies

The detailed composition of bio-oil has been reported in Table 2.2. Elemental analysis (carbon, hydrogen, and nitrogen) of the feeds & hydroprocessed products are listed in Table 2.3. [4]

Table 2.2. GC -MS analysis of pyrolysis-oil.

Bio-oil composition	Wt (%)	Bio-oil composition	Wt (%)
Hydrocarbons	48	Esters	8
Aldehydes/Ketones	12	Acids	2
Phenols	10	Furans	2
Guaiacols	9	Alcohols	1
		Others	8

Chapter 2: Co-processing of bio-oil from de-oiled jatropha curcas seeds cake with refinery gas-oil over sulphided CoMoP/Al₂O₃ catalyst

Table 2.3. Elemental analysis of gas-oil (GO), bio-oil (BO) and hydroprocessed Products (reaction time: 5h; feed/catalyst: 10(wt/wt)).

Feed composition		Conditions		Elemental composition		
BO (wt%)	GO (wt%)	Temp. (°C)	Pressure (bar)	C (wt%)	H (wt%)	N (wt%)
Reactants						
100	0	-	-	64.52	8.83	6.65
0	100	-	-	76.60	13.27	0.04
Products						
25	75	300	50	78.15	11.84	0.70
25	75	350	50	81.58	12.26	0.92
25	75	375	50	80.04	12.21	0.76
25	75	400	50	81.44	13.10	0.70
50	50	375	50	81.56	11.98	0.92
100	0	375	50	65.55	7.90	3.43

De-oiled jatropha seed-cake contains 3-7% remnant triglyceride after expeller extraction. Carbon content in the product increased slightly from 78 % to 80 % and hydrogen content increased from 12 % to 13 % on increasing reaction temperature from 300 °C to 400 °C for the feed with 25 % BO in GO. Nitrogen content reduced from 7 % to 3 % for 100 % BO hydroprocessing and it reduced further down to ~1 % for 25 % and 50 % BO in GO. Remaining 10 and 20% in GO and BO, respectively are predominantly O, and some S. Higher O content in gas-oil could be due to oxidation, dissolved oxygen and moisture due to prolonged storage under ambient conditions. Sulfur reduction from feed (2300-2500 ppm S) was 50-80% (down to 400-1000 ppm S) during this co-processing study. In comparison, S removal is 80-90% for catalytic upgraded pristine GO. During co-

Chapter 2: Co-processing of bio-oil from de-oiled jatropha curcas seeds cake with refinery gas-oil over sulphided CoMoP/Al₂O₃ catalyst

processing of oxygenated feeds with gas-oil, deoxygenation reactions do not adversely affect the hydrodesulfurization reactions, as also reported earlier by us [194]. Oxygen content in the bio-oil was 19%, which reduced to trace amounts after hydroprocessing of all the feeds.

Product (liquid, solid and gases) distributions (yield %) of the hydroprocessing reactions of feeds with 25 %, 50 % and 100 % of bio-oil (BO) mixed with refinery gas oil (GO) at various temperatures (300-400 °C) and feed compositions (25 %, 50 % and 100 % of BO in GO), over CoMoP/Al₂O₃, are given in figure 2.6 and figure 2.7 respectively. If we see the liquid product yields for 25 % BO in GO (Figure 2.6.) at various temperatures and 50 bar of hydrogen pressure, we get maximum liquid yield (63.4 %) at 400 °C, which reduces to 18.2 % at a lower temperature of 300 °C. On the other hand, a little change in the yields of gases with temperature is observed (maximum 23.5% at 400 °C and 21.2 % at 300 °C). Char yield increases monotonously from 0 to 12 % with increasing temperature from 300 °C to 400 °C. The liquid yield for pure GO is 85-95%. The unprocessable bio-oil content was very high at a lower reaction temperature of 300 °C (~60%), which reduced drastically (2-5%) at higher reaction temperatures (375-400 °C). These results indicate that at the intermediate reaction temperature, the undesirable char formation is suppressed while obtaining nearly complete bio-oil conversion.

Chapter 2: Co-processing of bio-oil from de-oiled jatropha curcas seeds cake with refinery gas-oil over sulphided CoMoP/Al₂O₃ catalyst

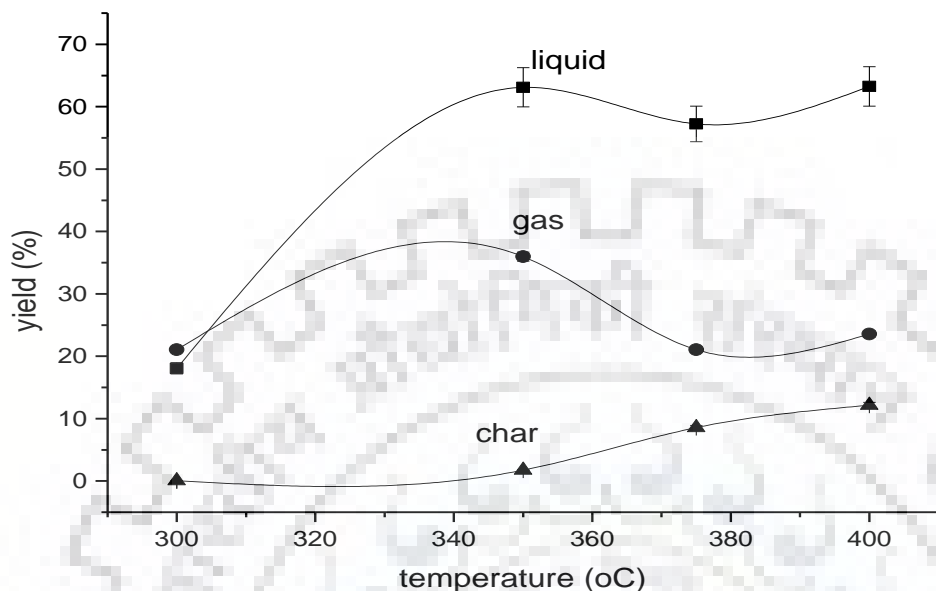


Figure 2.6. Yield (%) of products for the reaction of 25% of bio-oil (BO) in gas-oil (GO) at various temperatures.

Figure 2.7. shows the yield distributions of the product (char, liquid, and gases) for the reaction of feeds of various compositions (25 %, 50 % and 100 % BO in GO) at a temperature of 375 °C. Maximum liquid product yield (63.4 %) was obtained with 100 % BO feed which also gave maximum char (12.2 % yield), while maximum gases (40 % yield) were observed for feed with 50 % BO in GO. The hydroprocessed product, a transparent liquid, obtained as a phase separate from water, is composed of light and heavy fractions.

Chapter 2: Co-processing of bio-oil from de-oiled jatropha curcas seeds cake with refinery gas-oil over sulphided CoMoP/Al₂O₃ catalyst

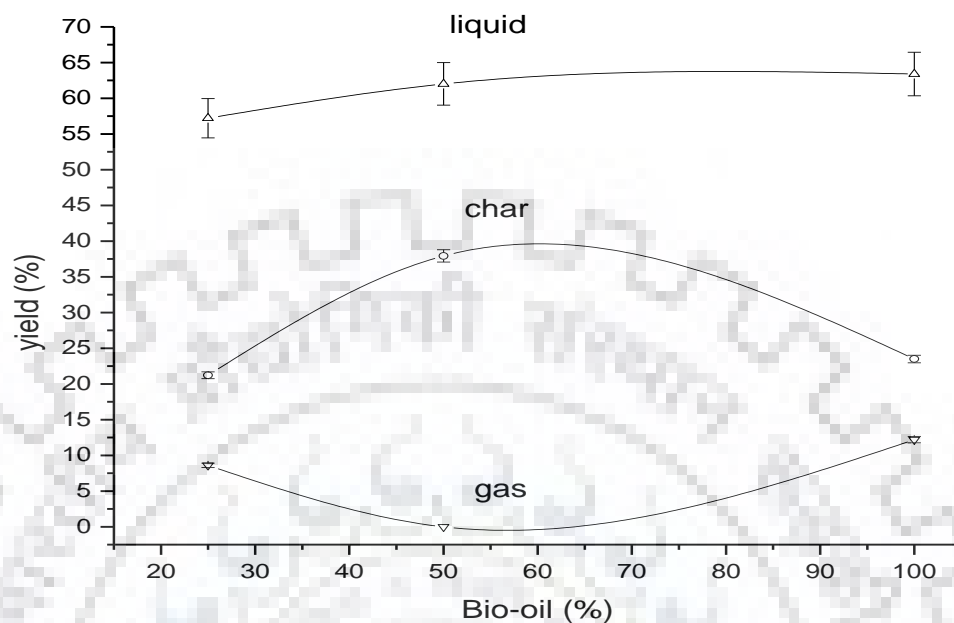


Figure 2.7. Yield (%) of products from the reaction of feeds with 25%, 50 % and 100 % of bio-oil (BO) in gas-oil (GO) at 375 °C.

The product yield distributions for 25 % bio-oil (BO) in gas-oil (GO) at various temperatures and 50 bar of hydrogen pressure are shown in Figure 2.8. The diesel yield increases with reaction temperature from 300 °C to 400 °C due to increasing reaction severity which favors cracking of bio-oil components. At reaction temperature of 400 °C, maximum gasoline (<C₉) (16 %) and maximum diesel (C₁₅-C₁₈) (45 %) are produced, while heavy oil (> C₁₈) yield is minimum (9 %), due to severe cracking conditions.

As the reaction severity increased with increase in temperature, the diesel yield increased monotonously (because deoxygenation reactions are favored). The longer chain components (>C₁₈) undergoes cracking with increasing temp, and hence their yield decreased monotonously from 33% at 300 °C to 9 % at 400 °C.

Chapter 2: Co-processing of bio-oil from de-oiled jatropha curcas seeds cake with refinery gas-oil over sulphided CoMoP/Al₂O₃ catalyst

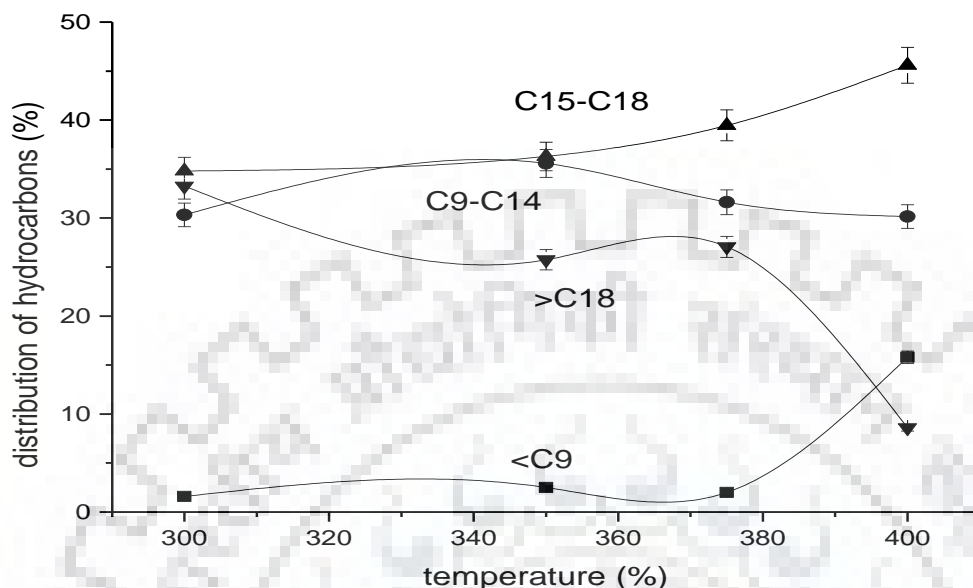


Figure 2.8. Distribution of hydrocarbons (■ gasoline (<C9); ● kerosene (C9-C14); ▲ diesel (C15-C18); and ▼ heavy residue (>C18)) in the products from feed containing 25 % bio-oil (BO) in gas-oil (GO) at various temperatures and 50 bar of H₂ pressures.

Gasoline (<C9) product yield showed little increase with increasing temp from 300 to 375 °C. Beyond 375 °C there was a rapid increase in gasoline yield from 2 % (at 375 °C) to 16 % (at 400 °C) due to increased severity leading to more cracking. In contrast, the heavier products (>C18 hydrocarbons) decreased little with increasing temperature (300-375 °C), but there were sharp decreases in yield from 27 % at 375 °C to 9 % at 400 °C. These results indicate that at 400 °C the heavier hydrocarbons (>C18) crack selectively into gasoline range (<C9) hydrocarbons. Maximum aviation kerosene (C9-C14 hydrocarbons) yield (36 %) is obtained at an intermediate temperature of 350 °C. At higher temperature (375-400 °C), the kerosene yield decreased by about 5 %. for 100 % BO hydroprocessing, high char content after the reaction was a major problem (Figure 2.7.). Higher reaction pressures generally suppress char formation. We observed that at higher pressures, not only more kerosene (41 %) was obtained (at 375 °C and 75 bar) from 100 % BO, but also char formation was also suppressed (1.5%). These results indicate that it is necessary to operate at higher pressures for hydroprocessing pure BO to obtain desired products and to

Chapter 2: Co-processing of bio-oil from de-oiled jatropha curcas seeds cake with refinery gas-oil over sulphided CoMoP/Al₂O₃ catalyst

minimize undesired coking to prolong the catalyst life. In comparison, CoMo/Al₂O₃ catalyst (without P promoter) showed only 31 % kerosene and 17 % char was obtained at similar reaction conditions. This indicates that P as promoter suppresses char formation and hence improves the catalyst life. Catalyst life is dependent on char/coke deposition rate. Catalyst deactivation is mainly due to coke deposition over the catalyst. Char/coke formation over P promoted catalyst was nearly 10-times lower than that over catalyst without P as a promoter, which indicates that phosphorous promoted catalyst has better catalyst life. Catalyst modified by phosphorus work in two ways: increase in active sites by enhanced metal dispersion and increase in Brönsted acidity; molybdenum interacts preferentially with the P–OH groups on phosphorus-added γ -alumina and also other surface hydroxyls become more reactive with molybdenum in the presence of phosphorus. It was also observed that catalysts prepared by impregnating P, on CoMo/Al₂O₃ (co-impregnation) are more active than the P-free catalyst [196]. Earlier work on bio-oil hydrotreatment with NiMo(S)/Al₂O₃ has reported that at 375-450 °C and 70 bar polynuclear aromatics formation was rapid, which prevented long-term operation under these conditions [194,197].

Isomerization is required to produce aviation kerosene with desirable freezing point. Table 2.3 shows that the kerosene range product had high isomer selectivity with isomers- and normal alkanes ratio (i/n ratio) varying between 1 - 2. Highest iso-alkanes yield (i/n=2) was obtained at the lowest reaction temperature studied (300 °C), for 25% BO in GO feed. Even though CoMoP/Al₂O₃ may not have required Brönsted acidity but the high TAN of the feed is expected to catalyze the isomerization reactions during hydrocracking of BO, as also reported earlier for co-processing of oxygenated biomass-derived oils with GO over CoMo/Al₂O₃ catalyst [198].

Chapter 2: Co-processing of bio-oil from de-oiled jatropha curcas seeds cake with refinery gas-oil over sulphided CoMoP/Al₂O₃ catalyst

Table 2.4. Distribution of normal (n) and iso (i) -alkanes and i/n ratios in kerosene range (C₉-C₁₄) hydrocarbons. [Catalyst: 10wt%; pressure 50 bar].

Conditions		Distribution of alkanes in kerosene		
Temp.(°C)	% BO in GO	n-alkane	i-alkane	i/n
300	25	10.95	19.47	1.77
350	25	18.53	16.97	0.91
350	50	11.62	11.5	0.98
375	25	13.16	18.44	1.40
375	50	12.53	16.94	1.35
375	100	13.98	16.31	1.16

The products yields for the reaction of 25 %, 50 %, and 100 % BO in GO at 375 °C are shown in Figure 2.9. Maximum gasoline (<C₉) (13 %) is obtained from the reaction of 100 % BO at 375 °C. Major Components of BO are short-chain oxygenated compounds, and hence as expected, the lighter components (<C₉) in the product increase with increasing BO % in the feed. There was little change in the product yields with variation in BO content in GO from 25 % to 50 %. With increasing BO in GO, from 50 to 100 % the diesel content reduced to 32 % from 40 %, the kerosene yield showed little variation; the gasoline (<C₉) yield increased from 3 to 13 %, the heavy oil components (>C₁₈) reduced slightly from 28 % to 25 %. These results indicate that pure BO (undiluted with GO) shows a completely different product pattern than the BO mixed with GO.

Chapter 2: Co-processing of bio-oil from de-oiled jatropha curcas seeds cake with refinery gas-oil over sulphided CoMoP/Al₂O₃ catalyst

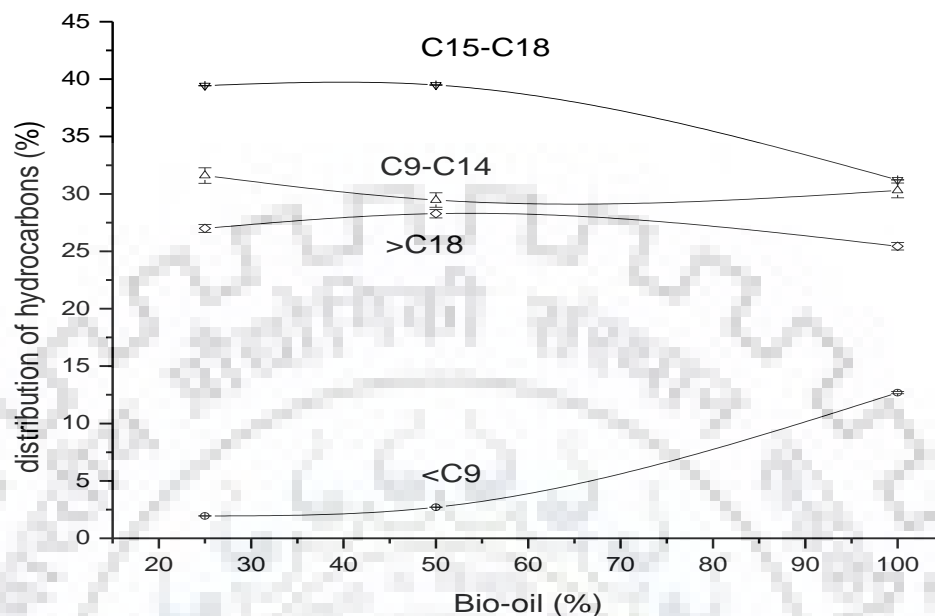


Figure 2.9. Distribution of hydrocarbons ◻ gasoline (<C9); Δ kerosene (C9-C14); ▽ diesel (C15-C18); and ◊ heavy residue (>C18) in the products from feeds containing 25 %, 50 % and 100 % of bio-oil (BO) in gas-oil (GO) (at 375 °C, 50 bar of H₂ pressures, 10 wt% of catalyst, 5h).

This may also be correlated with the large differences in the total acid number (TAN) of pure BO (52 mg_{KOH}/g) and a mixture of BO and GO (12 mg_{KOH}/g for 25 % mixture and 23 mg_{KOH}/g for 50 % mixture). Higher TAN for pure BO results in more acidity in the reaction mixture which would catalyze the cracking reactions. Hence higher cracked products (gasoline) yield and lower diesel range hydrocarbons yields are observed. Higher TAN for pure BO results in more acidity in the reaction mixture which would catalyze the cracking reactions; hence higher cracked products (gasoline) yield and lower diesel range hydrocarbons yields are observed. Higher TAN (acidity) feeds have been reported to show more cracking activity [198,199]. Which have been correlated to the acidity of the feed, the catalyst used has very low acidity.

Chapter 2: Co-processing of bio-oil from de-oiled jatropha curcas seeds cake with refinery gas-oil over sulphided CoMoP/Al₂O₃ catalyst

The distribution of alkanes, cycloalkanes, aromatics, and polynuclear aromatics in hydroprocessed products obtained from GC x GC-MS analysis are shown in Figure 2.10. and 2.11. GCXGC-MS analysis showed the absence of any observable oxygenated compounds indicating complete oxygen removal from the bio-oil components during hydroprocessing. Figure 2.10 shows hydrocarbon type distribution for the feed with 25 % of bio-oil (BO) in gas oil (GO) at various temperatures and 50 bar of hydrogen pressure. The trend for the formation of cycloalkanes showed that maximum cycloalkanes (45 %) were formed at 400 °C temperature. Maximum alkanes (63 %) was formed at 375 °C. Alkanes yield at 400 °C was minimum (55 %). Aromatics yield was zero at 400 °C.

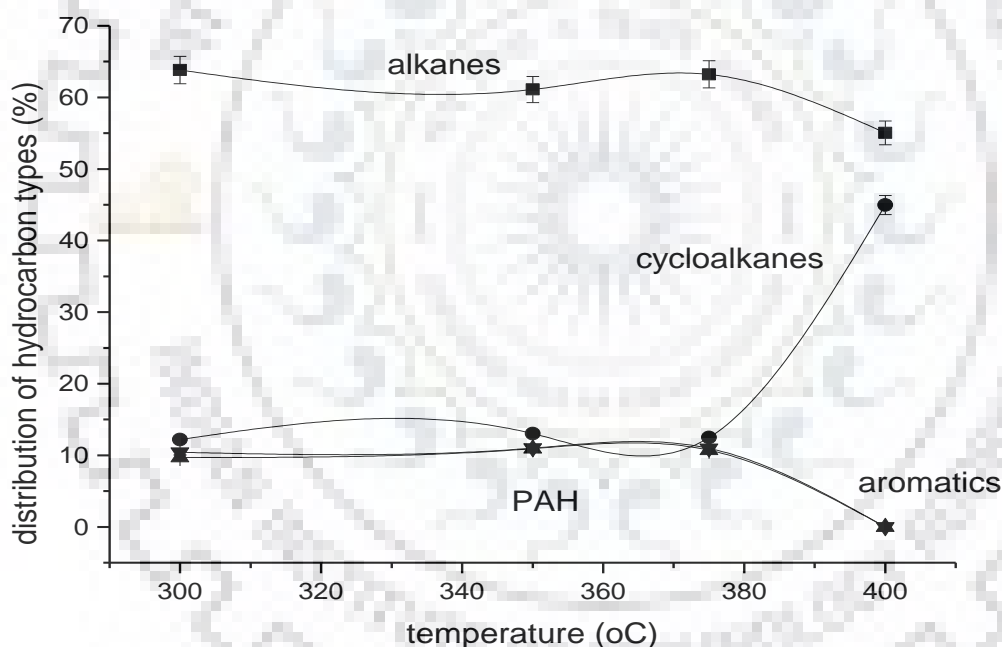


Figure 2.10. Distribution of hydrocarbon types (■ alkanes; ● cycloalkanes; ▼ aromatics; and ▲ polynuclear aromatics) in hydroprocessed products for the reaction of 25% bio-oil (BO) in gas-oil (GO) at various temperatures (50 bar of H₂ pressures; 10 wt% of catalyst, 5h).

There is a little variation in the yield of various hydrocarbons at temperatures from 300 °C to 375 °C. Aromatics are thermodynamically controlled product, and hence their

Chapter 2: Co-processing of bio-oil from de-oiled jatropha curcas seeds cake with refinery gas-oil over sulphided CoMoP/Al₂O₃ catalyst

yield minimized at higher reaction temp of 400 °C. More cracking was favored at a higher temperature (400 °C), and hence the cycloalkanes yield was enhanced while alkanes yield was reduced. Lower aromatics and polynuclear aromatics at higher temperature give a very useful insight that we can avoid rapid coking of catalyst at this temperature because the precursors for coke (polynuclear aromatics) are completely suppressed. Earlier work has shown that temperature drastically affected the coke formation during hydrotreating of bio-oils [198]. Increasing temperature favors the polymerization for the formation of coke. The authors reported that at very high temperature (450 °C), the coke formation could be so severe that the reactor was blocked.

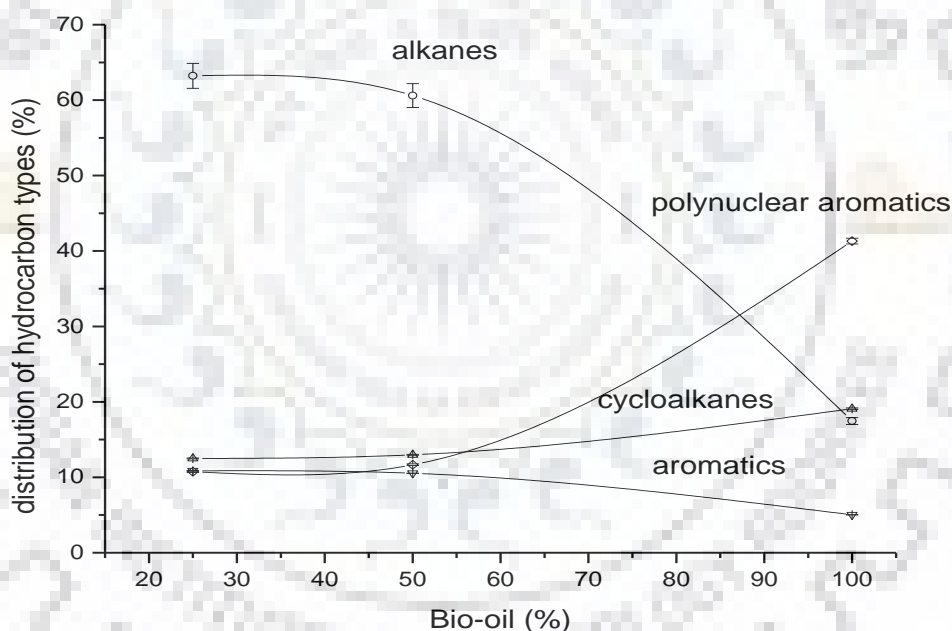


Figure 2.11. Distribution of hydrocarbon types (\circ alkanes; Δ cycloalkanes; \diamond aromatics; and ∇ polynuclear aromatics) in hydroprocessed products for the reaction of 25%, 50 % and 100% of bio-oil (BO) in gas-oil (GO) at 375 °C (50 bar of H₂ pressures; catalyst: 10wt%, 5h).

If we see Figure 2.11. for hydrocarbon types in hydroprocessed products for 25 %, 50 % and 100 % of bio-oil (BO) at 375 °C, we get maximum cycloalkanes (19 %) for 100

Chapter 2: Co-processing of bio-oil from de-oiled jatropha curcas seeds cake with refinery gas-oil over sulphided CoMoP/Al₂O₃ catalyst

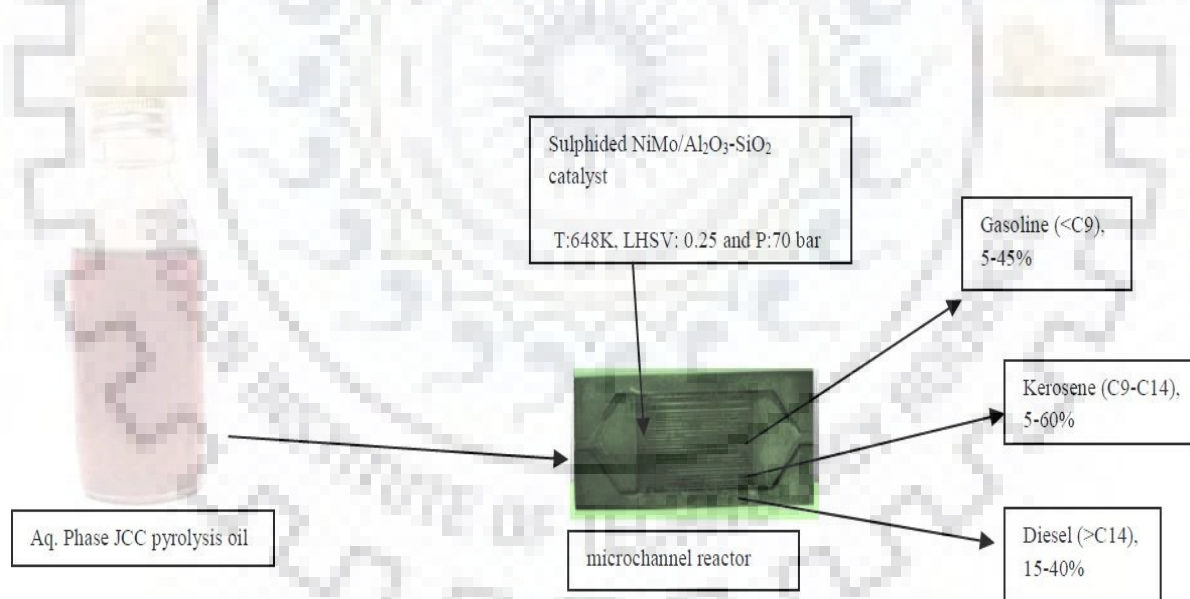
% of bio-oil (BO), while alkanes are very less (17 %) compared to others feed percentage of bio-oil at that temperature. The alkanes yield decreased rapidly from the feed with 50 % BO in GO to feed with 100 % BO. Surprisingly, though the aromatics yield was lower (5%) 100% BO feed the polynuclear aromatics yield was rapidly enhanced (nearly 4-times) compared to the feeds with 25 % and 50 % BO. These results indicate that polynuclear aromatics formation by condensation reactions are selectively favored for the 100 % BO most likely due to its high TAN value via the Diels–Alder reaction and also via secondary reactions of oxygenated compounds such as phenols [200].

2.6. Conclusions

The results indicate that co-hydroprocessing of bio-oils with sulphided CoMoP/Al₂O₃ catalyst is a promising route for producing transportation fuels. Products obtained from co-processing 25 % and 50 % of bio-oil (BO) with gas-oil (GO) contained 2-16 % gasoline, 30-35 % kerosene, 35-44 % diesel, with negligible oxygenates and char. Hydroprocessing of 100% BO at 375 °C and 50 bar produced 10 % gasoline, 30 % kerosene, and 30 % diesel with a large amount (40 %) of undesirable polynuclear aromatics. But at 75 bar (375 °C) for 100 % BO, polynuclear aromatics formation was suppressed (<2 %) and kerosene yield was maximum (41 %), with very small amount of char (1.5 %) formation.

Chapter 3

Hydroprocessing of aqueous-phase of pyrolysis oil over NiMo/Al₂O₃-SiO₂ in the microchannel reactor



*This work has been published in Catalysis in Green Chemistry and Engineering
1(3) (2018) 1–10.*

Chapter 3: Hydroprocessing of aqueous-phase of pyrolysis oil over NiMo/Al₂O₃-SiO₂ in the microchannel reactor

3.1. Introduction

Environmental concerns and possible future demand have turned the research on derived fossil fuels. Biomass is supposed to be the best alternative due to abundance worldwide, easy availability, renewability, low environmental footprint, and low procurement costs are some of the major reasons for considering biomass as a fuel source [201,202]. Thermochemical biomass conversion routes like pyrolysis, gasification, and hydrothermal liquefaction of agricultural wastes, forestry wastes, and municipal wastes, etc. are proposed for alternative technologies [184].

The yield of liquid products from pyrolysis of deoiled jatropha-curcas seeds cake is ~60-70 wt % and consists of a wide range of functional groups, mostly oxygenates [68]. The bio-oil has two phases. One is water soluble aqueous-phase (50-60%), and the other one is non-aqueous bio-crude (40-50 %) [69].

The detail chemical composition, along with a carbon range of aqueous-phase bio-oil, was provided in an earlier publication [4]. Aqueous phase oil contains aldehydic and ketonic compounds in major (28 %) followed by acids (17 %). The minor compounds are guaiacols (10 %), phenols (9 %), hydrocarbons (8 %), furan (7 %), alcohols (7 %), esters (1 %), sugars (1 %) and others (12 %) of the total organics. Additionally, the nitrogen-containing compounds, mainly alkyl, hydroxyl or carbonyl substituted pyridine, pyrrole, pyrazine, piperidine, indole, etc. are also present in bio-oils.

The bio-oils require upgrading because as-such they are not suitable as a fuel for internal-combustion engines, due to water and organic acids present in them [84]. They have limited storage stability and also have undesirable physical properties. Several technologies have been used for upgradation of bio-oil, such as thermal treatment, high-pressure thermal treatment, thermal hydrotreating, catalytic hydrotreating, catalytic emulsion, and catalytic cracking [183,203–206]. Catalytic hydroprocessing is also the most widely used technique in petroleum refining [69]. Elliott et al. studied hydroprocessing of phenolic oils in stage reactor using sulfided CoMo and platinum-group over carbon

Chapter 3: Hydroprocessing of aqueous-phase of pyrolysis oil over NiMo/Al₂O₃-SiO₂ in the microchannel reactor

catalysts. Platinum-Group catalysts resulted in more saturated products [207].

Catalytic bio-oil upgrading produces hydrocarbons that are similar to petroleum-derived fuels predominantly by deoxygenation process. Upgradation is done by chemical (such as cracking and hydrocracking, etc.), and physical (such as liquid-liquid separation and distillation, etc.) methods [69]. Catalytic hydrotreatment is a viable upgrading technology to convert bio-oils into fuels [183,203–207]. Bio-oil is treated with H₂, with the presence of a sulphided heterogeneous catalyst (NiMo, CoMo) on the support of γ -Alumina by catalytic hydrotreatment process. Selection of stable and economically viable and productive catalyst(s) for refinery hydrocarbons with low coke formation is a great challenge. Minimization of oxygen content and increasing of H/C ratio with reduction of the chain length by hydroprocessing (catalytic high-pressure hydrotreating or hydrodeoxygenation accompanied by hydrocracking) is the primary aim. Hydrodeoxygenation is a chemical conversion that takes place at high H₂ partial pressures (as high as 75-250 bar) and high temperatures (250 – 400 °C) to remove oxygen primarily in the form of water or CO₂ [161,183].

Hydrodeoxygenation of bio-oils produces hydrocarbons along with water and CO₂, and the classes of reactions include decarboxylation, hydrogenation, hydrogenolysis, hydrocracking, and dehydration leading to gasoline, kerosene, and diesel like products. Deactivation of these catalysts as a function of time on stream is reported [112,187,208]. Blockage of catalyst pores and active sites, sintering of the active metals, poisoning of the catalyst, structural degradation of the support and active sites, coking and metal deposition are may be the likely reason for catalyst deactivation [112,199,209].

The present chapter discusses the production of transportation fuels (gasoline, kerosene, and diesel) by hydroprocessing of aqueous-phase of pyrolysis oil obtained from de-oiled jatropha curcas seeds cake (JCC), by using sulfided NiMo/SiO₂-Al₂O₃ catalyst coated in a microchannel reactor. Microchannel reactors have the advantages of portability, easy scale-up, better heat and mass transfer characteristics, high reaction throughputs, precise control of hydrodynamics [210]. The good thing about this work is that

Chapter 3: Hydroprocessing of aqueous-phase of pyrolysis oil over NiMo/Al₂O₃-SiO₂ in the microchannel reactor

transportation fuels can be produced by using small modular microchannel reactors (with catalyst coating inside the channels) compared to using largely fixed bed reactors. Additionally, this process improves the economics of processing bio-oils by utilizing its aqueous-phase (containing ~30 % inseparable soluble organics) to produce hydrocarbon fuels.

3.2. Experimental details

3.2.1. Materials

Ammonium heptamolybdate tetrahydrate (NH₄)₆Mo₇O₂₄·4H₂O, Nickel nitrate hexahydrate (Ni(NO₃)₂·6H₂O, Aluminum isopropoxide, Aluminum acetylacetonate, Polyvinyl alcohol, Dimethyldisulfide (DMDS), Nitric acid and ethyl alcohol were purchased from Aldrich. HPLC grade water (Merck) was used as a solvent for synthesis. Refinery gas oil was used for sulfidation from Mathura refinery, UP, India. Bio-oil (BO) was produced in a tubular reactor (SS 314) as described earlier [4,20].

3.2.2. Catalyst preparation

The sol-gel method was used to synthesize a silica-alumina support solution. Water and isopropanol were mixed in 10:1 molar ratio at 45 °C by constant stirring for 15 min. Then, colloidal silica and alumina suspended in isopropanol were added slowly with constant stirring for 45 min at 80 °C, polyvinyl alcohol (3 %, as a binding agent) were added consecutively added, and stirring was continued for another 15 min. Mo metal precursor dissolved in (NH₄)₆Mo₇O₂₄·4H₂O (3.31 g) and Ni precursor (Ni(NO₃)₂·6H₂O, 1.98 g) were added to the above-prepared alumina support solution to obtain a final catalyst composition of 80 % SiO₂-Al₂O₃, 18 % MoO₃, and 2 % NiO (wt %). Finally, Nitric acid was added drop-wise to peptize the silica-alumina sol, and the pH was adjusted to 4 [211]. The final solution was stirred for 24 h at 80 °C. The solution was dried at 120 °C and calcinated at 550 °C for 6 h (heating rate, 10 °C min⁻¹).

Chapter 3: Hydroprocessing of aqueous-phase of pyrolysis oil over NiMo/Al₂O₃-SiO₂ in the microchannel reactor

3.2.3. Catalyst coating in the microchannel reactor

The 10-plate microchannel reactor was made of SS314. Each plate had 28 channels (each channel of size 50 mm x 0.5 mm x 0.25 mm) (Figure 3.1a and Figure 3.1b). Synthesized catalyst was ball-milled and dispersed in ethanol to obtain the wash-coat solution and coated inside the channels of each plate only followed by calcination at 500 °C.

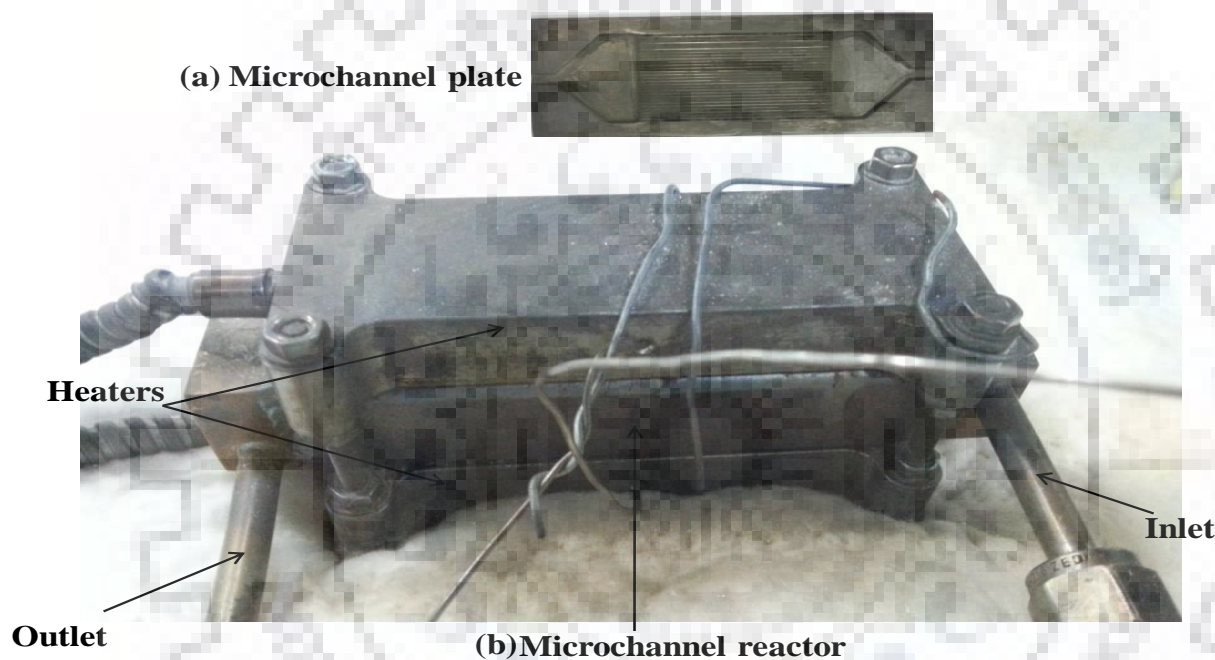


Figure 3.1 a. Microchannel plate (top), b microchannel reactor experimental set-up (bottom).

Synthesized catalyst was ball-milled and dispersed in ethanol to obtain the wash-coat solution and coated inside the channels of each plate (with ~0.25 mm thickness). Adhesion test of the catalyst was done by the drop test method. The plates were assembled using laser welding [210,212]. The microchannel plates were pretreated, and drop-test was conducted after catalyst coating to minimize the possibility of catalyst/metal leaching from the plates during the reaction.

Chapter 3: Hydroprocessing of aqueous-phase of pyrolysis oil over NiMo/Al₂O₃-SiO₂ in the microchannel reactor

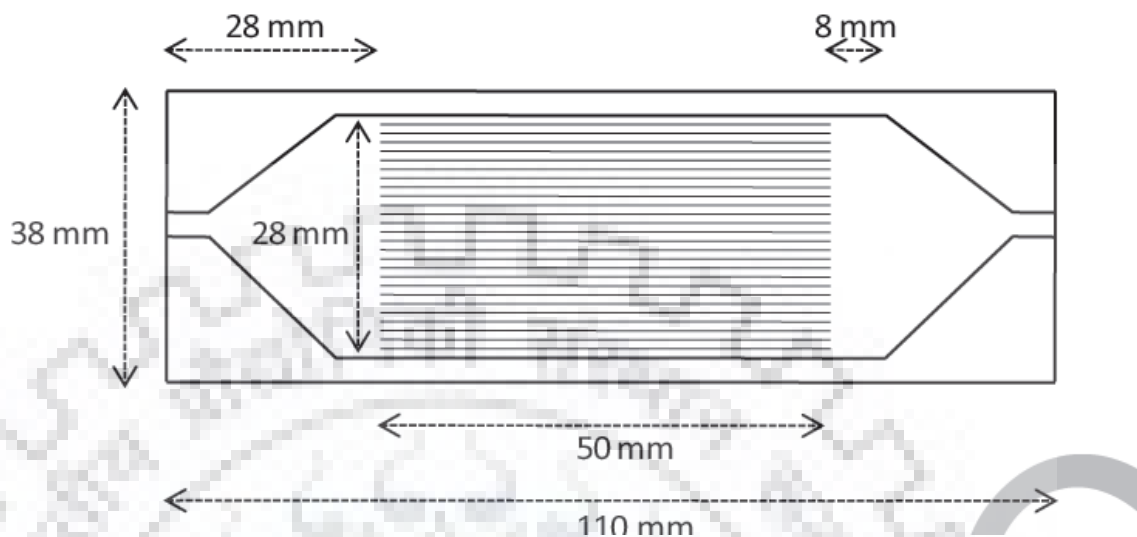


Figure 3.2. Microchannel plate dimensions and specification.

3.2.4. Experimental setup

The microchannel reactor was assembled with 10 microchannel plates (Figure 3.1 a and Figure 3.1 b). The plates were welded together by laser welding. The inlet and outlet of the reactor were welded to SS316 tubes ($\frac{1}{4}$ ”). Heating blocks with temperature controller were placed on both sides of the reactor assembly. Thermocouples were used to measure the reaction temperature.

During catalytic experiments, precise control of the operating parameters such as temperature, pressure, and the feed flow rate was maintained using the calibrated equipment. The activities were studied at different temperatures and space velocities. A back pressure regulator was used to control the pressure of the system. The pressure of the reactor was measured using pressure gauges. Mass flow controller (MFC) was used to measure H₂ flow in the reactor. The gas-liquid product mixture from the reactor was separated using a liquid separator.

Sulfidation of the catalyst was carried out in the same microchannel reactor before reactions by using 2.5 wt% of dimethyl disulfide (DMDS) mixed in refinery gas oil (GO) at 30 bar of hydrogen pressure by gradually raising the temp., from ambient to 320 °C (10 °C

Chapter 3: Hydroprocessing of aqueous-phase of pyrolysis oil over NiMo/Al₂O₃-SiO₂ in the microchannel reactor

min⁻¹). Aqueous-phase of bio-oil obtained from deoiled Jatropha seed-cakes was filtered and hydroprocessed in the presence of the sulfided form of coated catalyst Ni–Mo(S)/SiO₂–Al₂O₃.

Liquid products were filtered with cellulose membranes (pore size 0.22 μm), before analysis in gas chromatography (GC). A Varian 3800 GC (Agilent) with a J&W VF-5ms column (Agilent: 30 m X 0.25 mm, 0.25 μm) and flame ionization detection (FID) was used for the analysis of hydrocarbons. Errors up to ±8% were observed and included in the final results. Detailed hydrocarbon in liquid products (paraffins, naphthenes, aromatics and poly-aromatic hydrocarbon) were analysed by an Agilent 7890B 2D-GC (GC × GC; first dimension–nonpolar, DB-5 ms column, 30 m × 0.25 mm, 0.25 μm; second dimension polar, PAC column, 5 m × 0.25 mm, 0.15 μm), with FID, MS, capillary flow modulator and ZOEX software. The relative yields of liquid hydrocarbon component were calculated and identify the products (Table 3.1). Errors up to ±5% were observed and included in the final results.

Chapter 3: Hydroprocessing of aqueous-phase of pyrolysis oil over NiMo/Al₂O₃-SiO₂ in the microchannel reactor

Table 3.1. GC-MS result of the representative product.

Hexane: solvent				
Hydrocarbons Name	R.T.	Area	Pct Max	Pct Total
Undecane, 5-methyl-	20.559	246462	53.22	2.765
Dodecane	23.707	353987	76.44	3.971
Undecane, 2,8-dimethyl-	26.556	371653	80.25	4.17
Dodecane, 2,6,11-trimethyl-	33.607	288495	62.3	3.237
3,5-Dimethyldodecane	33.681	389924	84.2	4.375
Decane, 6-ethyl-2-methyl-	35.558	239231	51.66	2.684
: Undecane, 4-ethyl-	35.631	377989	81.62	4.241
Nonane, 3-methyl-5-propyl-	37.433	305498	65.97	3.427
Hexadecane	37.506	446578	96.43	5.01
Heptadecane,2,6,10,15-tetramethyl-	40.81	334594	72.25	3.754
DCM: solvent				
Nonane, 2-methyl-5-propyl-	26.705	251650	76.38	4.09
Pentadecane	29.256	327360	99.36	5.321
Decane, 2,4,6-trimethyl-	31.508	205103	62.25	3.334
Hydroxylamine, O-decyl-	31.581	209444	63.57	3.404
Nonane, 2-methyl-5-propyl-	35.632	216480	65.71	3.519

Chapter 3: Hydroprocessing of aqueous-phase of pyrolysis oil over NiMo/Al₂O₃-SiO₂ in the microchannel reactor

Ether: solvents				
Undecane, 4,7-dimethyl-	20.559	300744	54.22	1.378
Tridecane	23.706	378923	68.31	1.736
Tetradecane	26.63	449482	81.03	2.06
Decane, 5-propyl-	29.109	297939	53.71	1.365
3,5-Dimethyldodecane	29.256	523201	94.32	2.397
Pentadecane, 7-methyl-	31.581	467923	84.35	2.144
Tridecane	33.608	308767	55.66	1.415
Pentadecane, 2,6,10-trimethyl-	33.754	501852	90.47	2.3
Eicosane, 10-methyl-	33.828	293163	52.85	1.343
Dodecane, 2,7,10-trimethyl-	35.631	314725	56.74	1.442
Heptadecane, 2,6-dimethyl-	35.705	467212	84.22	2.141
Pentadecane, 2,6,10-trimethyl-	35.778	466688	84.13	2.138
Eicosane, 10-methyl-	37.579	482012	86.89	2.209
Eicosane	39.306	481704	86.84	2.207
Tridecane, 7-propyl-	39.38	290449	52.36	1.331
Naphthalene, 1-methyl-	39.604	311709	56.19	1.428
Tridecane, 5-propyl-	40.957	339977	61.29	1.558
Naphthalene, 2,3-dimethyl-	42.079	200157	36.08	0.917
Naphthalene, 1,7-dimethyl-	42.304	375586	67.71	1.721

Bio-oil (BO) containing water-soluble aqueous-phase and non-aqueous bio-crude was produced in a tubular reactor made up of SS 314 (inner diameter 7.5cm and length

Chapter 3: Hydroprocessing of aqueous-phase of pyrolysis oil over NiMo/Al₂O₃-SiO₂ in the microchannel reactor

85cm) by using slow pyrolysis technology (shown in Figure 2.1 of Chapter 2). Pyrolysis reactor was electrically heated with a furnace around it, at 550 °C temperature (heating rate 10 °C/min) and ambient pressure in N₂ atmosphere. N₂ gas was used to maintain an inert medium in the reaction system, to dilute the formed pyrolysis vapors, to minimize char formation and to prevent further reactions. Biomass (1kg deoiled *Jatropha curcas* cake) was used for the reaction, and N₂ gas (825 ml/min) was passed continuously through a gas-meter, and pyrolysis vapors were carried into a series of two condensers to condense the pyrolysis vapor to obtain the pyrolysis liquid (water-soluble aqueous-phase and non-aqueous bio-crude), and the non-condensable gases were vented off. The schematic diagram of the pyrolysis unit is shown in Figure 2.1 of Chapter 2 [20].

3.3. Results and Discussion

3.3.1. Physicochemical Properties of Catalyst

3.3.1.1. BET NH₃-TPD (acidity) and XRD analysis

Physicochemical properties (surface area, pore diameter, pore volume, and surface acidity) of the prepared SiO₂-Al₂O₃ support and Ni-Mo/SiO₂-Al₂O₃ catalysts used in the microchannel for the study of Hydroprocessing of aqueous-phase of pyrolysis oil are given in Table 3.2. Surface area, mean pore diameter, and pore volume of SiO₂-Al₂O₃ support was 377 m²/g, 8.6 nm, and 0.85 ml/g, respectively. After impregnation of Mo and Ni and calcination at 500 °C, both surface area and pore size were reduced.

Chapter 3: Hydroprocessing of aqueous-phase of pyrolysis oil over NiMo/Al₂O₃-SiO₂ in the microchannel reactor

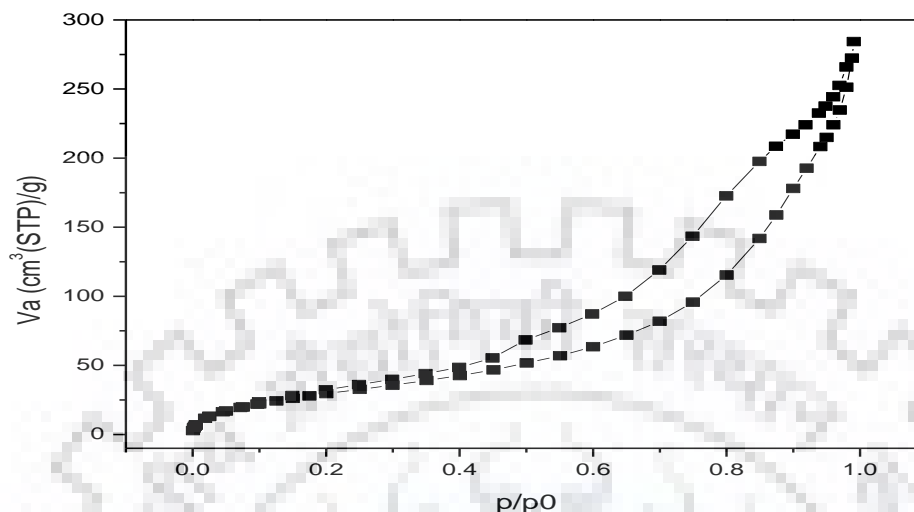


Figure 3.3. Nitrogen sorption isotherm of NiMo SiO₂-Al₂O₃

Table 3.2. Physicochemical properties of mesoporous supports and catalysts

Physicochemical properties	Al ₂ O ₃	SiO ₂ -Al ₂ O ₃	Ni-Mo/SiO ₂ -Al ₂ O ₃
Surface Area (m ² .g ⁻¹)	243	236	202
Total Pore Volume (ml.g ⁻¹)	0.9	0.39	0.5
Mean Pore Diameter (nm)	12.9	8.6	10.6
Surface Acidity NH ₃ (mmol.g ⁻¹ cat)	0.11	0.77	0.46

After impregnation, surface area, mean pore diameter, and pore volume was 202 m²/g, 10.6 nm, and 0.5 ml/g, respectively (Figure 3.3.). The mesoporous SiO₂- Al₂O₃ support has a total acidity of 0.77 mmol of NH₃ g⁻¹ catalyst, the acidity was measured by NH₃-temperature programmed desorption (NH₃-TPD), which is mentioned in figure 3.4.. Acidity of support is expected to result in different product yield and selectivity due to cracking activity. Ni-Mo/SiO₂-Al₂O₃ catalysts had a composition similar to the commercial hydrotreating catalyst, which was used in the present study.

Chapter 3: Hydroprocessing of aqueous-phase of pyrolysis oil over NiMo/Al₂O₃-SiO₂ in the microchannel reactor

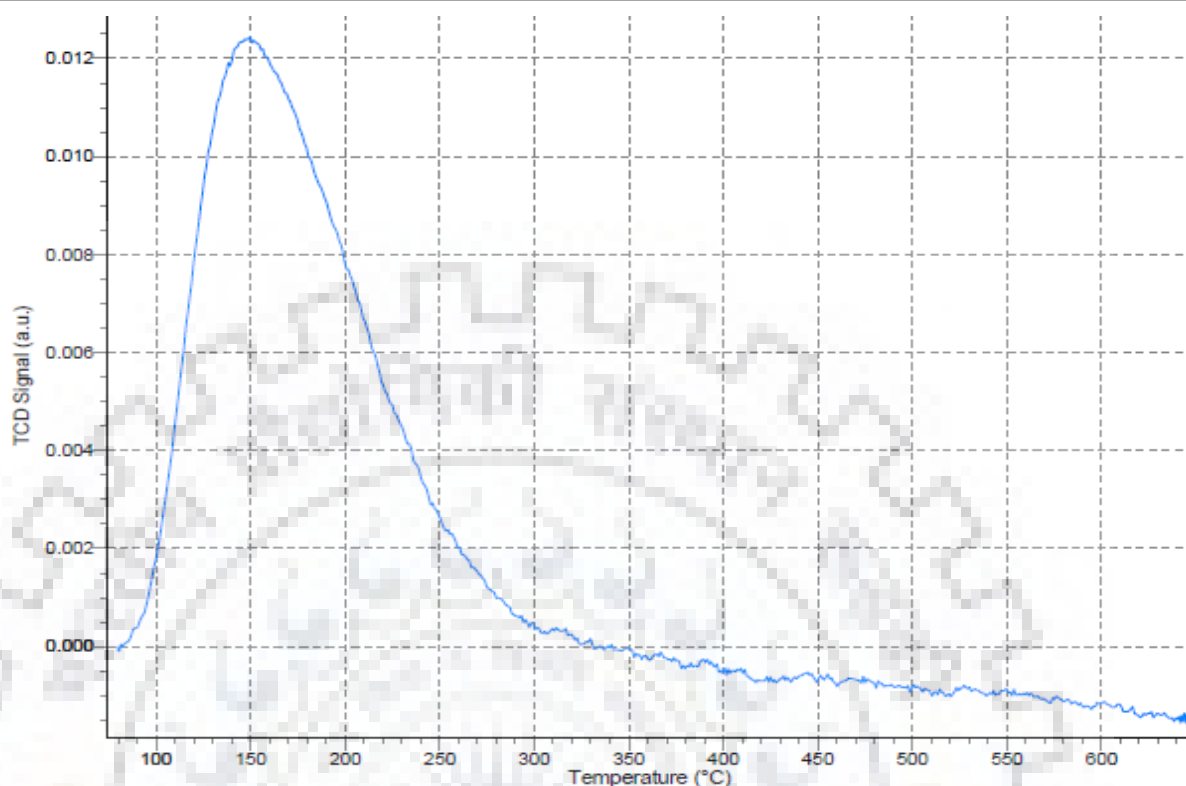


Figure 3.4. Ammonia TPD OF NiMo SiO₂-Al₂O₃.

X-ray diffraction (XRD) patterns were recorded using a PROTO XRD benchtop powder diffraction X-ray Diffractometer with monochromatic radiation Cu K α ($\lambda=1.5418$ Å) by applying operating voltage of 34.6 kV used during the analysis, and a current of 14.3 mA, in the step scanning mode in the range $10^\circ < 2\theta < 80^\circ$ with a continuous scan rate of 2.0 °C/min.

The powder XRD of NiMo/SiO₂-Al₂O₃ catalyst (Figure 3.5) shows that SiO₂-Al₂O₃ is amorphous while characteristics peaks of MoO₃ and NiO are not observed. A broad hump between $2\theta=10-20^\circ$ is ascribed to amorphous silica. Orthorhombic MoO₃ peaks are not seen between $2\theta=26-31^\circ$, indicating that the oxides are highly dispersed on the support, and the sizes are smaller than the detection limit of XRD (< 3 nm). [3 1 1], [4 0 0], [4 4 0] peaks corresponding to γ -alumina phase are observed [213,214].

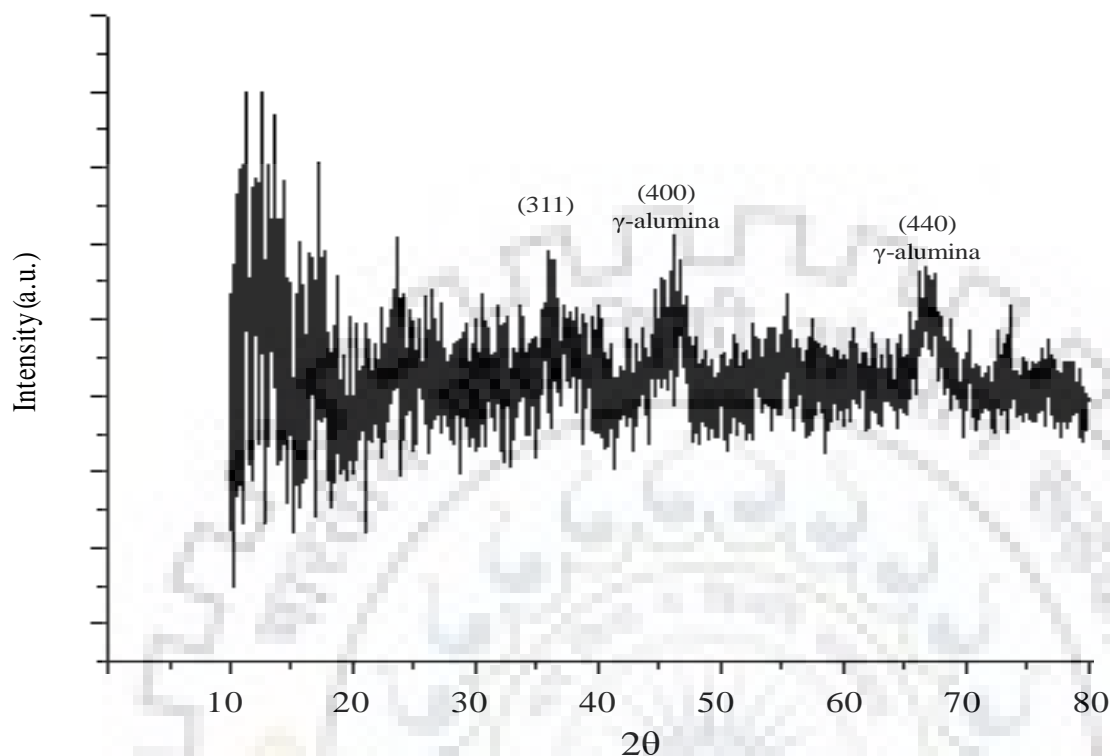


Figure 3.5. Diffractogram of fresh NiMo/SiO₂-Al₂O₃ catalyst.

3.3.2. Catalytic studies

The oxygen content of the organics in the aqueous-phase was reduced to trace amount after hydroprocessing. The water obtained after hydroprocessing contained a small amount of organic (<5 %). Stable activity during the study indicated that there was no significant catalyst leaching from the plates. Product distributions (yield %) for the hydroprocessing reactions of the aqueous phase of bio-oil at various temperatures (250-400 °C), 70 bar pressure, space-velocity (LHSV) of 1.0 and H₂/ feed ratio of 1000 are given in Figure 3.6. The yield of gasoline (<C₉) range hydrocarbons increased rapidly from 3% to 4% by changing temp., from 250 °C to 300 °C, to a maximum of 60 % at 350 °C. Gasoline (<C₉) further decreased to 10-15 % at higher temperatures (375 °C, 400 °C). Kerosene yield (C₉ - C₁₄) decreased from 28 % to 15 % by changing the temperature from 250 °C to 300 °C, and it increased from 35 to 40 % by increasing temperature from 350 °C to 400 °C.

Chapter 3: Hydroprocessing of aqueous-phase of pyrolysis oil over NiMo/Al₂O₃-SiO₂ in the microchannel reactor

The yield of diesel hydrocarbons (C₁₅-C₁₈) increased rapidly from 5 % to 50 % by changing the temperature from 250 °C to 325 °C.

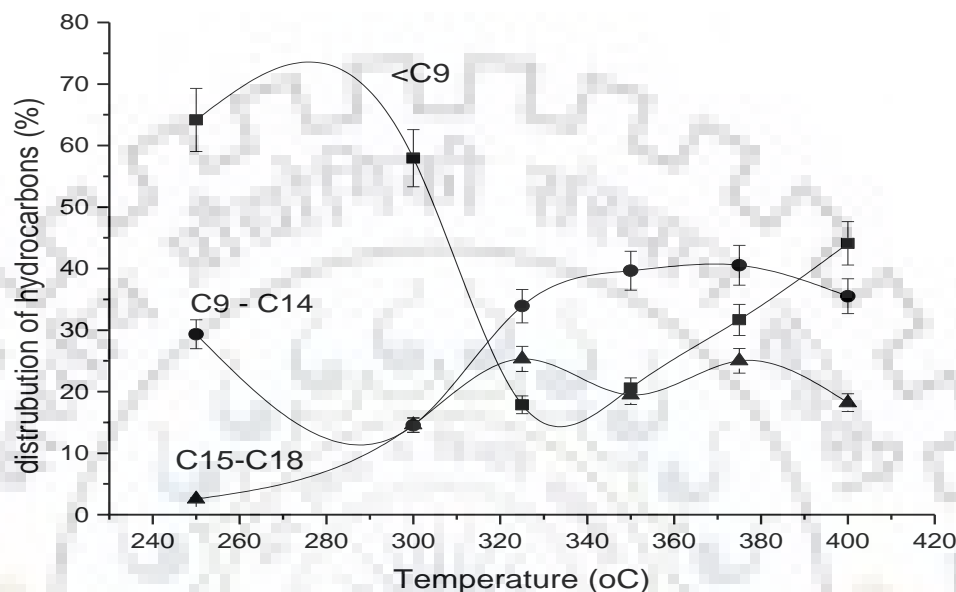


Figure 3.6. Distribution of hydrocarbons [■gasoline (<C₉), ●kerosene (C₉-C₁₄), and ▲diesel (C₁₅-C₁₈) in the products at various temperature (pressure 70 bar, LHSV 1.0, H₂/feed 1000nL/L) at various temperature.

However, a further increase in temperature diesel yield decreased rapidly to 20 % at 400 °C. As the reaction severity increased due to increasing reaction temperature, the longer chain diesel range hydrocarbons cracked more, resulting in their reduced yields, while the yield of shorter chain gasoline and kerosene increased. Due to several interconversion reactions of bio-oil molecules, increasing and decreasing trends are observed with the change in reaction temperature. At a lower H₂/feed ratio of 500, the trends of conversion were haphazard (Figure 3.7.), which could be due to lower hydrogen content in the reaction system due to which inter-conversion and oligomerization reactions are predominant. At this condition, the product qualities are poor, and reactor operation was difficult.

Chapter 3: Hydroprocessing of aqueous-phase of pyrolysis oil over NiMo/Al₂O₃-SiO₂ in the microchannel reactor

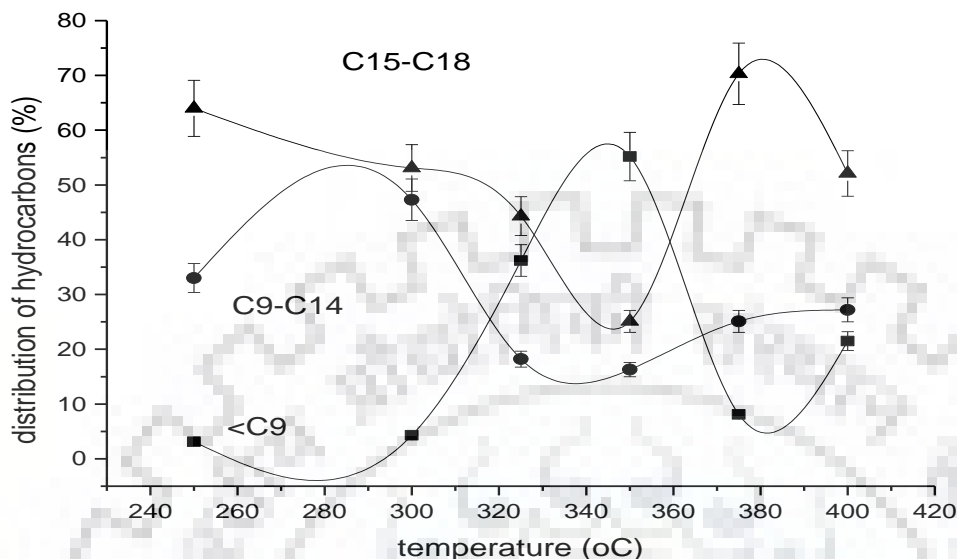


Figure 3.7. Distribution of hydrocarbons [■gasoline (<C9), ●kerosene (C9-C14), and ▲diesel (C15-C18)] in the products (pressure 70 bar, LHSV 1.0, H₂/feed 500nL/L) at various temperature.

Figure 3.8. shows the distribution of hydrocarbons (gasoline (<C9), kerosene (C9–C14) and diesel (C15-C18) in the products at various liquid hourly space velocities (LHSV) (Pressure 70 bar; temperature 375 °C and H₂/feed ratio of 1000 nL/L). With increasing space velocities the yield of gasoline (<C9) range hydrocarbons increased from 5% (at 0.25 LHSV) to 35-60% (at 0.5 - 1.25 LHSV). Maximum yield of gasoline (<C9) range hydrocarbons (60 %) was obtained at 0.75 LHSV, as aqueous bio-oil has oxygen-containing smaller hydrocarbons predominantly. At lower LHSV, i.e., at higher contact time may favor intermolecular oligomerization reactions and hence the gasoline yields are lower. The yield of kerosene (C9-C14) range hydrocarbons reached maximum (45 %) at the highest studied LHSV of 1.25, from 30 % at 0.25 LHSV. Additionally, with increasing space velocity (0.25 to 1.25), the longer chain hydrocarbons (C15-C18) yield decreases from 65% (at 0.25 LHSV) to ~20% at 0.75-1.25 LHSV. These differences in the distribution patterns of various products are due to differences in the relative rates of

Chapter 3: Hydroprocessing of aqueous-phase of pyrolysis oil over NiMo/Al₂O₃-SiO₂ in the microchannel reactor

formation of various products. The oligomerization of smaller bio-oil molecules may obtain the diesel range product (C₁₅-C₁₈).

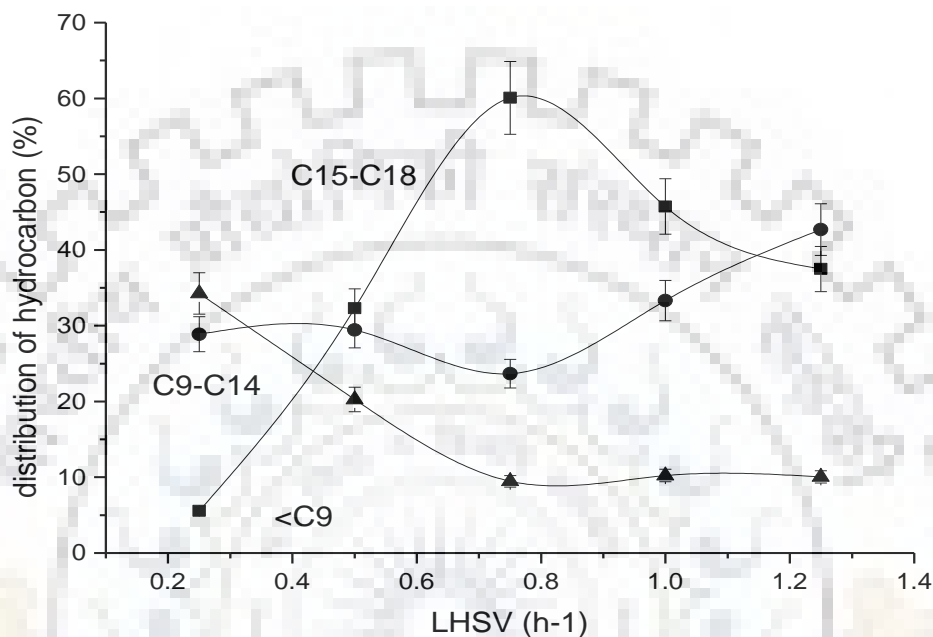


Figure 3.8. Distribution of hydrocarbons [■gasoline (<C₉), ●kerosene (C₉-C₁₄), and ▲diesel (C₁₅-C₁₈)] in the products (pressure 70 bar, temperature 375 °C, H₂/feed 1000nL/L) at various LHSV.

Figure 3.9. shows the distribution of hydrocarbons (gasoline (<C₉), kerosene (C₉ – C₁₄) and diesel (C₁₅-C₁₈) in the products at various hydrogen/feed ratios (Pressure 70 bar; temperature 325 °C; LHSV 1.0). The yield of diesel (C₁₅-C₁₈) range compounds decreased from ~50% at H₂/feed ratio of 500, 1000 to ~2-5% at H₂/feed ratio of 2500, 4000. This drastic decrease could be due to the high linear velocity of feed and hydrogen in the reactor. The kerosene (C₉ - C₁₄) range hydrocarbons increased from 40 % to 50 % with an increase in H₂/feed ratio from 500 to 4000. The gasoline (<C₉) range hydrocarbons increased from 7 % to 95 % with an increase in H₂/feed ratio from 500 to 2500, this could be due to the hydrocracking of higher oxygenated hydrocarbons to the lower one. Such a large variation in the product yields with a change in H₂/feed ratio could be due to a large

Chapter 3: Hydroprocessing of aqueous-phase of pyrolysis oil over NiMo/Al₂O₃-SiO₂ in the microchannel reactor

change in linear velocity of the reactants (H₂ and feed) in the very narrow microchannels. As the catalyst is coated inside microchannels the flow conditions are not completely plug-flow type (unlike packed bed reactors) and hence such prominent effect of hydrogen flow is observed, unlike in case of fixed bed reactors [212].

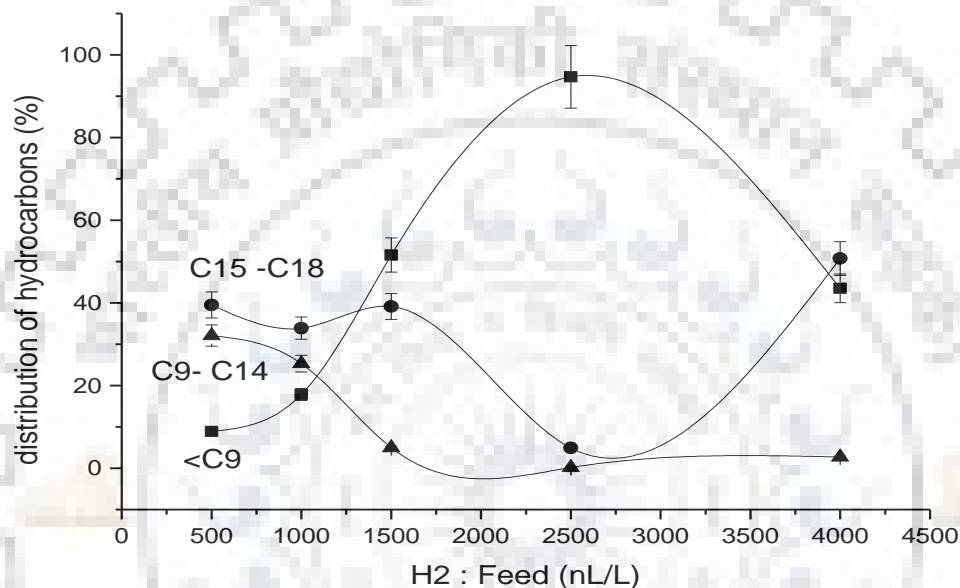


Figure 3.9. Distribution of hydrocarbons [(■gasoline (<C9), ●kerosene (C9-C14), and ▲diesel (C15-C18)] in the product (pressure 70 bar, LHSV 1.0, temperature 325 °C) at various H₂/feed.

Figure 3.10. shows the distribution of hydrocarbon types (alkanes, cycloalkanes, aromatics, PAH, residue and unreacted feed) in hydroprocessed products at various space velocities (LHSV) (Pressure, 70 bar; H₂/feed ratio, 1000; temperature, 375 °C). The alkanes yield decreases rapidly from 65 % (at 0.25 LHSV) to 20 % (at 1.25 LHSV) when LHSV is reduced. Simultaneously the unreacted compounds increase from 0 to 70 % as the LHSV increases from 0.25 to 1.25. The results indicate that very low space velocity is required for complete conversion of the compounds present in the aqueous phase of bio-oil. The residues in the product decrease from 30 % to 10 % with an increase in LHSV from 0.25 to

Chapter 3: Hydroprocessing of aqueous-phase of pyrolysis oil over NiMo/Al₂O₃-SiO₂ in the microchannel reactor

1.25. The PAH formation remains below 5 % at all studied space velocities, while the formation of aromatics and cycloalkanes is negligible.

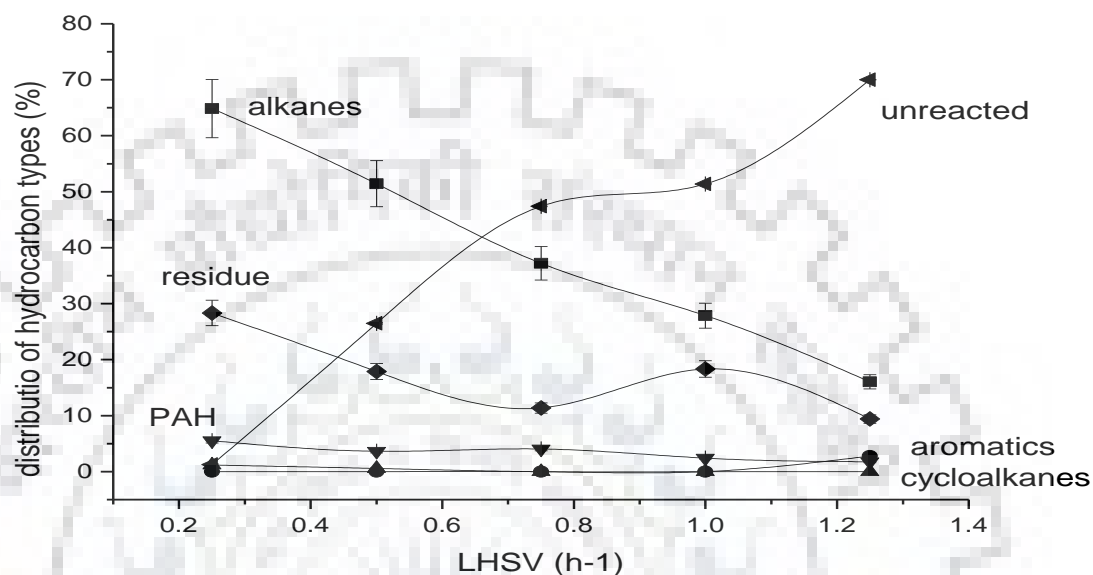


Figure 3.10. Distribution of hydrocarbons types (● alkanes, ▲ cycloalkanes, ▼ aromatics, ◀ PAH, ▶ residue and ■ unreacted) in the products (pressure 70 bar, H₂: feed 1000nL/L, temperature 375 °C) at various LHSV.

Figure 3.11. Shows the distribution of hydrocarbon type (alkanes, cycloalkanes, aromatics, PAH, residue, and unreacted compound) in the liquid product. Maximum conversion of feed (75 %) is observed at 300 °C, but the formation of undesired PAH (10%) and residues (20%) are very high. Maximum alkane formation (50%) is observed at 324 °C. The results indicate that the feed conversion is maximum in a very narrow temperature range around 300 °C.

Chapter 3: Hydroprocessing of aqueous-phase of pyrolysis oil over NiMo/Al₂O₃-SiO₂ in the microchannel reactor

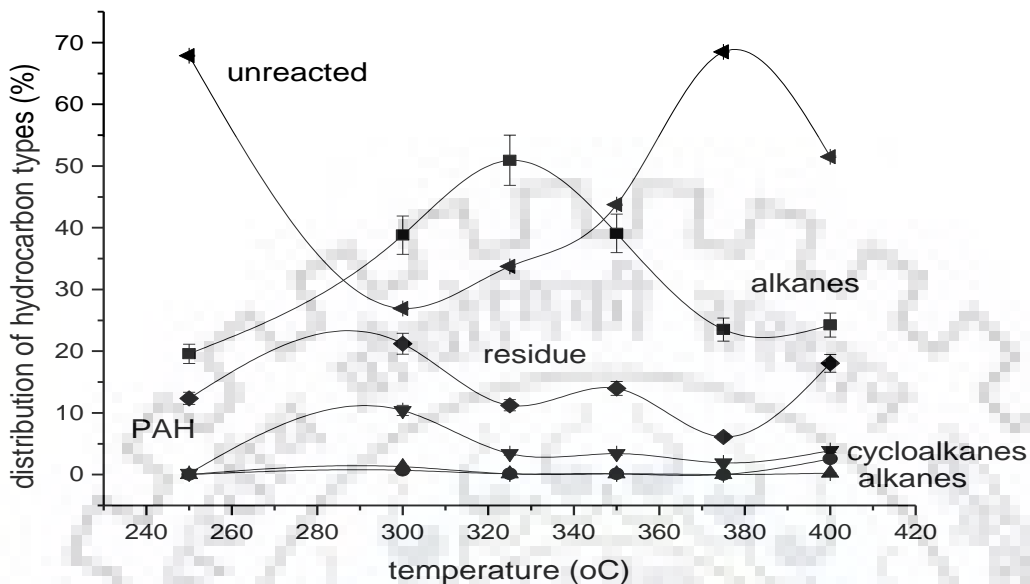


Figure 3.11. Distribution of hydrocarbons types (● alkanes, ▲ cycloalkanes, ▼ aromatics, ◀ PAH, ▶ residue and ■ unreacted) in the products (pressure 70 bar, H₂: feed 1000nL/L, LHSV 1.0) at various temperature.

Figure 3.12. shows the distribution of hydrocarbon types (alkanes, cycloalkanes, aromatics, PAH, residue and unreacted compounds) in the hydroprocessed product at various H₂/feed ratios (pressure 70 bar; LHSV 1.0; temperature 325 °C). The figure shows that at 1500 and higher H₂/feed ratios, the conversion is very low (>80 % unreacted compounds). Only at 1000 H₂/feed ratio, the conversion is ~65 %. As the catalyst is coated inside microchannels, the flow conditions are not completely plug-flow type, and hence hydrogen flow increase (higher H₂/feed ratio) would reduce the effective utilization of catalyst for conversions [212].

Chapter 3: Hydroprocessing of aqueous-phase of pyrolysis oil over NiMo/Al₂O₃-SiO₂ in the microchannel reactor

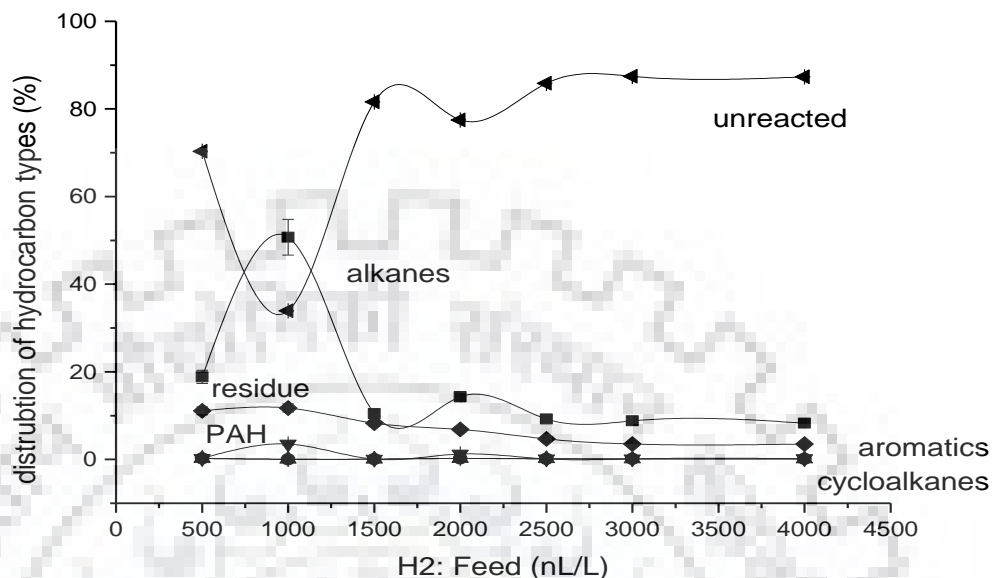


Figure 3.12. Distribution of hydrocarbons types (● alkanes, ▲ cycloalkanes, ▼ aromatics, ◀ PAH, ▶ residue and ■ unreacted) in the products (pressure 70 bar, LHSV 1.0, temperature 325 °C) at various H₂: feed.

3.4. Conclusions

Hydroprocessing of aqueous-phase of bio-oil (BO) obtained from pyrolysis of de-oiled jatropha curcas seeds cake (JCC) with sulphided NiMo catalyst supported on mesoporous silica-alumina and coated in a microchannel reactor is a promising route for producing transportation fuels. Complete deoxygenation of the organics in the aqueous-phase was achieved. The water obtained after hydroprocessing contained <5 % organics indicating that >95 % of organics in the aqueous-phase of bio-oil was converted into desirable products. Products obtained from hydroprocessing contained 5-45 % gasoline (<C₉), 5-60 % kerosene (C₉-C₁₄), 15-40 % diesel (C₁₅-C₁₈), with 15-65 % alkanes, 0-5 % polyaromatic hydrocarbons (PAH), negligible cycloalkanes and aromatics, with 30-75 % unreacted and residues under reaction condition of temperature 250- 400 °C, LHSV 0.25-1.25, H₂:feed ratio 500-4000 and at fixed pressure of 70 bar. Maximum hydrocarbon yield

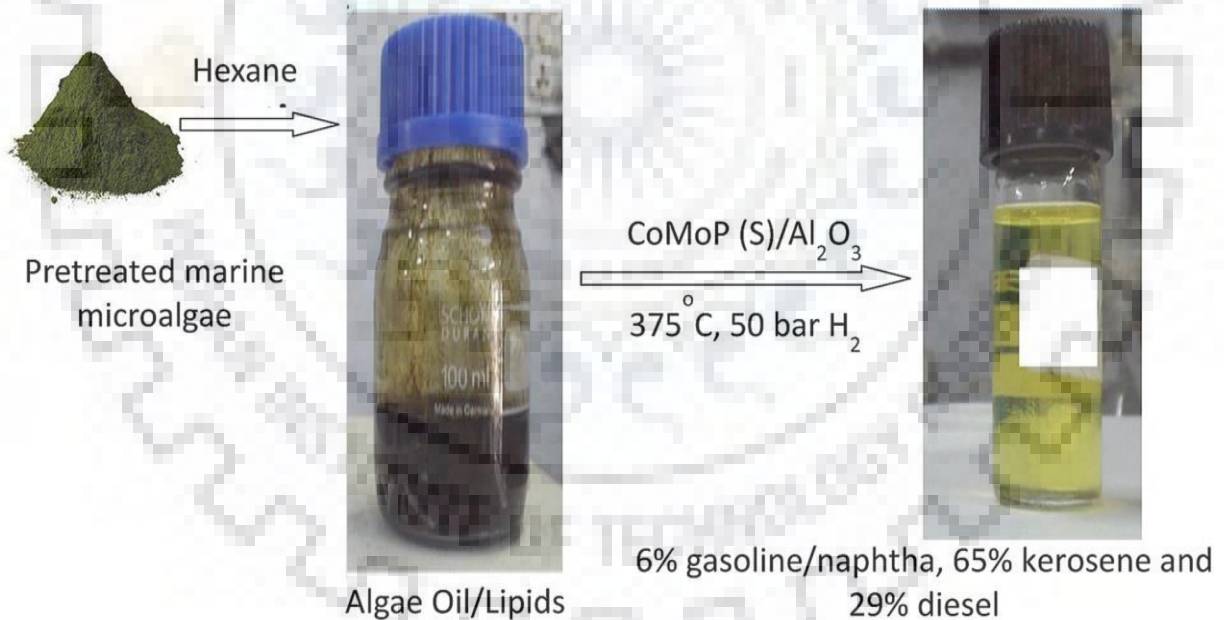
Chapter 3: Hydroprocessing of aqueous-phase of pyrolysis oil over NiMo/Al₂O₃-SiO₂ in the microchannel reactor

(~65 %) was obtained at 375 °C, 0.25 LHSV, and 70 bar, with 35 % undesired residues and PAH.



Chapter 4

Hydroprocessing of lipids extracted from marine microalgae *Nannochloropsis* sp. over sulfided CoMoP/Al₂O₃ catalyst



This work has been published in Biomass and Bioenergy, 119 (2018) 31–36.

Chapter 4: Hydroprocessing of lipids extracted from marine microalgae *Nannochloropsis* sp. over sulfided CoMoP/Al₂O₃ catalyst

4.1. Introduction

There is much-continued interest to produce sustainable renewable energy sources to replace fossil fuels. These renewable sources are set to develop keeping in mind two key factors; it should not use food utility sources, and it should produce drop-in-fuel or need small changes in infrastructure either in production or utilization [215,216]. First-Generation biofuels, i.e., ethanol and biodiesel from sugar or starch and vegetable oils, respectively, require the cultivation of crops on land that could be otherwise used for food production [216]. In contrast, second-generation biofuels can be produced either from crop or food wastes. These include biodiesel from waste oil or tallow and lignocellulosic ethanol from forestry or crop wastes. The details for second-generation biofuels/ transportation fuels production have been discussed in an earlier chapter (2nd and 3rd).

More recently, algae have been considered as a promising feedstock for third generation biofuels, as they can be produced at high productivity on otherwise non-arable land by using less amount of nutrients and low cost for production. Moreover, many algae can be cultivated to have high oil (lipids; triacylglyceride) content and can produce oil at a much higher productivity than other land-based oil-crops [217,218]. These are a hydrophyte containing chlorophyll without stems and roots and are categorized into two variants based on size, i.e., macroalgae (seaweed) and microalgae [219]. Algae can be cultivated in nonagricultural land by using any water (brackish, salty, west water, open ponds or in closed photobioreactors), with ample nutrients. They grow rapidly compared to other crops and plant and its volume and size doubles in just 24 h by consuming CO₂ as feed [218,219]. Unfortunately, the conventional biofuels produced from these crops, ethanol, and biodiesel, require engine modifications for their use in present vehicular engines. There is a need to develop second and third generation biofuels that are compatible with the current infrastructure.

Currently, mainly, three approaches are being used to produce algae-based biofuels. The first process involves extracting lipids from algal cells, followed by the transesterification of triglycerides (TAGs) and alcohol into fatty acid alkyl esters

Chapter 4: Hydroprocessing of lipids extracted from marine microalgae *Nannochloropsis* sp. over sulfided CoMoP/Al₂O₃ catalyst

(biodiesel). The second technique employs hydrothermal liquefaction (HTL) at high pressure (50–200 bar) and temperature (250–450 °C) to produce water-insoluble bio-crude oil. The third technique is pyrolysis, which thermally degrades biomass at 300–700°C in the absence of oxygen, resulting in the production of bio-oils (aqueous and organic phase), solid residues (biochar), and gases (biogas). All of these processes require the final bio-oil/crude to be upgraded using hydrogen, before being used in conventional transportation engines. Hydroprocessing of the bio-oil/crude may produce drop-in biofuels which are compatible with engines and can be used directly without any upgrading.

Many researchers have studied the hydroprocessing of bio-crude produced via hydrothermal liquefaction of algae over various catalysts including sulfide CoMo/ γ -alumina, HZSM-5 at temperatures between 400-500 °C. Refined oil yields of between 55-85% have been obtained, with yields being reduced at increased temperatures. The highest reported yields were achieved using a combination of Ru/C and Raney/Ni catalysts [220–223].

Today, the direct conversion of algal lipids to drop-in fuels has yet to be investigated. In comparison to hydrothermal liquefaction, the extraction of algal lipids allows the other valuable biomass components, in particular, the proteins, pigments, and long-chain polyunsaturated fatty acids, to be recovered [224]. The direct conversion of these lipids to a drop-in fuel would be a major improvement over the conventional approach of conversion to biodiesel via transesterification.

The lipids extracted from microalgae using a wet extraction process are predominantly triacylglycerides, but also contain waxes, sterols, free fatty acids, monoglycerides, diglycerides, phospholipids, glycolipids and chlorophyll as impurities. It is therefore of interest to determine whether a catalytic process can be developed that can successfully convert this complex feedstock to a suitable drop-in fuel. This study investigates for the first time, the hydroprocessing of crude lipids extracted from the commercially relevant marine microalga *Nannochloropsis* sp. over a sulphided form of CoMoP/Al₂O₃ catalyst [20].

Chapter 4: Hydroprocessing of lipids extracted from marine microalgae *Nannochloropsis* sp. over sulfided CoMoP/Al₂O₃ catalyst

4.2. Experimental details

4.2.1. Catalyst preparation

The catalysts CoMoP/Al₂O₃ was prepared by conventional wet impregnation on commercial mesoporous extrudates of γ -Al₂O₃ (BET surface area = 298 m²g⁻¹, BJH pore size = 6.1 nm, pore volume = 1.1 ml g⁻¹). 1.89g of (NH₄)₆Mo₇O₂₄·4H₂O, as molybdenum precursor, 1.55 g Co (NO₃)₂·6H₂O as cobalt metal precursor and 0.16 g of 85 % aqH₃PO₄ as Phosphorous precursor was used during catalyst synthesis. An ammonical solution of molybdenum precursor, an aqueous solution of cobalt and phosphorous precursor, were added over 7.9 g of moisture-free γ -alumina to prepare 16 % Mo, 4 % Co, 1 % P. Each metal precursor was added sequentially after overnight drying at 120 °C. After drying the final prepared catalyst was calcined at 550 °C for 6 h in a muffle furnace with a heating rate of 1 °C min⁻¹ [20]. All precursors, toluene, and DMDS were purchased from (Sigma Aldrich). Refinery gas oil was collected from Mathura refinery. High-performance liquid chromatography (HPLC) grade water was taken as a solvent for synthesis [20].

The surface area of the catalyst was measured using the Brunauer– Emmett–Teller (BET) method with nitrogen (N₂) adsorption isotherm at -196°C using BELSORP-max Microtrac (Japan) apparatus. Before analysis, the catalyst sample was degassed at 250 °C under vacuum. The pore size was calculated from the desorption isotherm using the Barrett, Joyner, and Hallender (BJH) method. Samples for transmission electron microscopy (TEM) were prepared by deposition of the catalyst, suspended in isopropanol, on a copper grid. TEM images were recorded using a Tecnai G2 (FEI) operating at 200 kV. Deposited metals (Co 4%, Mo 16%, and P 1%) were determined using an inductively coupled plasma atomic emission spectroscopy method on a PS 3000 UV (DRE) (Teledyne Leeman Labs, Inc., USA) [20].

Chapter 4: Hydroprocessing of lipids extracted from marine microalgae *Nannochloropsis* sp. over sulfided CoMoP/Al₂O₃ catalyst

4.2.2. Lipid (TAGs) extraction from ruptured microalgae biomass

The feed for the reaction was a neutral lipid extract obtained from multiple batches of *Nannochloropsis* sp. algal biomass [225]. The fatty acid composition of the saponifiable lipids in the extract was mostly palmitic acid (C16:0) and palmitoleic acid (C16:1) and included some longer chain polyunsaturated fatty acids including eicosapentaenoic acid (C20:5n3) as previously presented [225]. The biomass was produced and concentrated to ca. 25% w/w solids as previously described [225]. The cultures were deprived of nitrogen for approximately 10 days to allow accumulation of TAG in the algae. Before lipid extraction, the microalgal cells were weakened by incubated at 37 °C for approximately 24 hr and then ruptured by a single pass through a GEA Panda 2K NS1001L high-pressure homogenizer (GEA NiroSoavi, Parma, Italy) at 1000 bar previously described [225]. The neutral lipids were preferentially extracted by twice contacting with hexane, and the lipid-containing hexane was recovered from the de-lipidated biomass by centrifugation, the hexane was removed from the lipids by evaporation, and the lipids stored at -20 °C [225].

4.2.3. Lipid Conversion

The lipid extract was hydroprocessed in stainless steel cylindrical reactors of 25 ml capacity, with a magnetic drive stirrer (model 4590, Parr Instrument Co., Moline, IL, US), heated by an electric heater and the temperature controlled using a PID controller (Model 4848, Parr Instruments, IL, US) (figure 4.1.). This batch reactor also have been used for Co-processing of bio-oil from de-oiled jatropha curcas seeds cake with refinery gas-oil over sulphided CoMoP/Al₂O₃ catalyst, it was discussed in chapter 2 Typically, 7.0 g of the lipid feedstock was added along with 10 wt% of the sulfide catalyst CoMoP/Al₂O₃ into the reactor. Sulfidation was done in same reactor prior to the reaction, using 2.5 wt% of dimethyl disulphide (Sigma-Aldrich) mixed in refinery gas oil, at a H₂ pressure of 40 bar, by gradually raising the temperature from 100 °C to the final reaction temperature (at 10 °C min⁻¹) which was then maintained for 12 h with constant stirring at 680 rpm [20].

Chapter 4: Hydroprocessing of lipids extracted from marine microalgae *Nannochloropsis* sp. over sulfided CoMoP/Al₂O₃ catalyst



Figure 4.1. Batch reactor (M/S Parr instrument US) used for hydroprocessing of a mixture of BO & GO and *Nannochloropsis* sp. micro marine algae extracted lipids (TAGs).

Before commencing the reaction, high purity hydrogen gas was used to purge the reactor headspace five times, and to build up to a pre-set initial pressure of 10 bar at room temperature. During the reaction, liquid samples were drawn every 2h and cooled before analysis for the kinetic calculations. After the reaction, the reactor was cooled to ambient temperature. The material balance was recorded, which confirmed minimal loss occurred during the experimental measurements. Based on the material balances, an estimated

Chapter 4: Hydroprocessing of lipids extracted from marine microalgae *Nannochloropsis* sp. over sulfided CoMoP/Al₂O₃ catalyst

experimental and measurement uncertainty of 10% has been included in the final results as error bars.

The final reaction temperatures (300 °C, 325 °C, 350 °C, and 375 °C) were achieved by heating gradually (10 °C min⁻¹) while the reaction pressure (50, 75 and 120 bar) was achieved by the addition of external hydrogen gas pressure to maintain desired reaction conditions. The temperature and pressure were increased back to the desired reaction conditions after sample collection. The liquid product was filtered with a 0.2 mm filter paper. The quantity of liquid feed, products, catalyst, and char, were measured using a weighing balance with a precision of ±0.01 g. Catalyst and coke (char) deposited on the catalyst surface was measured after rinsing with toluene to remove unreacted feed and deposited hydrocarbons. The amount of char formed was measured after subtraction of the catalyst amount loaded in the reactor. The amount of gas formed/consumed was determined from the difference in the weights of the reaction vessel, containing the reaction mixtures, before and after the reaction.

Liquid products obtained during the reaction were filtered using cellulose membranes (pore size 220 µm) and then analyzed using gas chromatography (GC). A Varian 3800 GC (Agilent) with a J&W VF-5ms column (Agilent; 30 m × 0.25 mm × 0.25 mm) and flame ionization detection (FID) was used for the analysis of hydrocarbons. A standard calibration sample was produced prior to the analysis of unknown samples for equipment calibration and retention time accuracy. The yields of various liquid product components were calculated on a relative basis considering the entire range of liquid products formed as 100%. Relative yields have been reported based on the relative amounts of gas, liquid, and char produced. Liquid product distributions were quantified on the basis of hydrocarbon chain length: gasoline (<C₉ hydrocarbons), kerosene (C₉-C₁₄ hydrocarbons), diesel (C₁₅-C₁₈ hydrocarbons) and heavy oil (>C₁₈ hydrocarbons).

Detailed hydrocarbon analysis (paraffin, naphthenes, aromatics and poly-aromatic hydrocarbons) was done using an Agilent 7890B 2D-GC (GC × GC; first dimension—nonpolar, DB-5 ms column(30 m × 0.25 mm × 0.25 µm); second dimension

Chapter 4: Hydroprocessing of lipids extracted from marine microalgae *Nannochloropsis* sp. over sulfided CoMoP/Al₂O₃ catalyst

polar, PAC column, 5 m × 0.25 mm, 0.15 μm), with FID, MS, capillary flow modulator and ZOEX software. Two column systems were used to separate various components present in the product.

4.3. Results and discussion

4.3.1. Catalyst characterization

The BET surface area and pore volume of the sulphided catalyst were found to be 298 m²/g and 0.5 ml/g, respectively. BJH analysis (mean pore size) showed a narrow pore size distribution with a mean pore size of 7.0 nm (Figure 4.2).

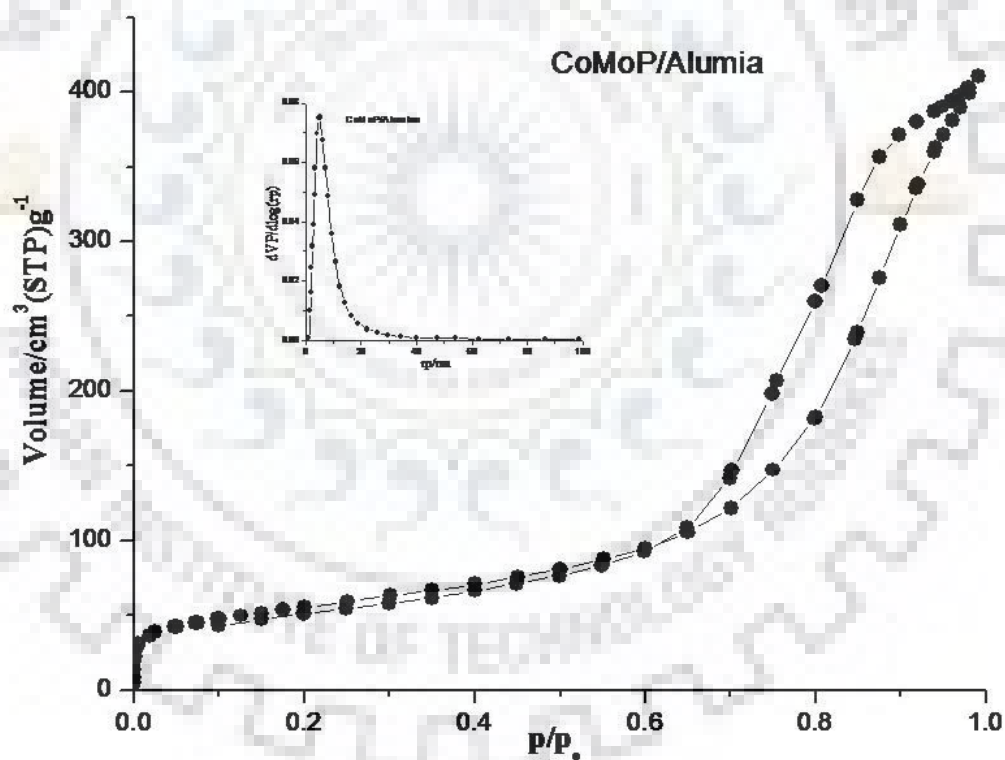


Figure 4.2. Nitrogen sorption isotherm and pore size distribution of mesoporous CoMoP/Al₂O₃

Chapter 4: Hydroprocessing of lipids extracted from marine microalgae *Nannochloropsis* sp. over sulfided CoMoP/Al₂O₃ catalyst

Many researchers have identified the monolayer morphology of MoS₂ slabs with 5-8 nm length visible in micrographs of sulphided CoMo/Al₂O₃ catalyst [195,226]. This indicates that monolayers of CoMoS clusters exist in the active phase, with a slab-like morphology of MoS₂ on Al₂O₃ support [226]. In our case, after doping P on CoMo/Al₂O₃, a multi-layered (3–5 layers) morphology of CoMoS with a 10-50 nm length and ~0.6 nm interlayer spacing can be observed in the TEM images in Figure 2.5 of Chapter 2 (seen a few single black lines in the micrograph) [20]. Our earlier work has shown that CoMoP/Al₂O₃ catalysts are more active than CoMo/Al₂O₃ catalysts [20]. Hence, we have used a CoMoP/Al₂O₃ catalyst in the current study due to its better performance.

The catalyst modified by P works in two ways: there is an increase in active sites by enhanced metal dispersion, and there is an increase in the Brønsted acidity. Mo interacts preferentially with the P–OH groups on P-added γ -alumina, and additionally, the other surface hydroxyls become more reactive with Mo in the presence of P [227–229]. It was also observed that catalysts prepared by impregnating P on CoMo/Al₂O₃ (co-impregnation), were more active than the P-free catalyst [230]. MoP/Al₂O₃ was tested for the catalytic activity in the HDN reaction for some model compounds; it was found that the intrinsic HDN activity of the surface Mo atoms was about 6 times higher than that of Mo edge atoms in MoS₂/Al₂O₃ [228,230]. Deposition of P metal forms Lewis and Brønsted acid sites on the catalyst surface, making the compound accessible for easy reducibility and sulfidation. It increases the Mo dispersion due to enhanced solubility of molybdate by the formation of phosphomolybdate complexes, and it also increases the stacking of MoS₂ crystallites and changes their morphology [227,231].

Chapter 4: Hydroprocessing of lipids extracted from marine microalgae *Nannochloropsis* sp. over sulfided CoMoP/Al₂O₃ catalyst

4.3.2. Temperature programmed reduction (TPR)

The TPR measurements were carried out using Micromeritics Auto Chem II apparatus. Seventy mg of sample was taken in the TPR cell and flushed with argon at 150°C for 30 min. Then the sample was cooled down to room temperature. Finally, the furnace temperature was raised to 1000 °C at 10°Cmin⁻¹ ramp in 40 ml min⁻¹ flow rate with the H₂/Ar mixture (10:90 ratios). The signals of H₂ consumption were monitored by a thermal conductivity detector (TCD) (Figure 4.3).

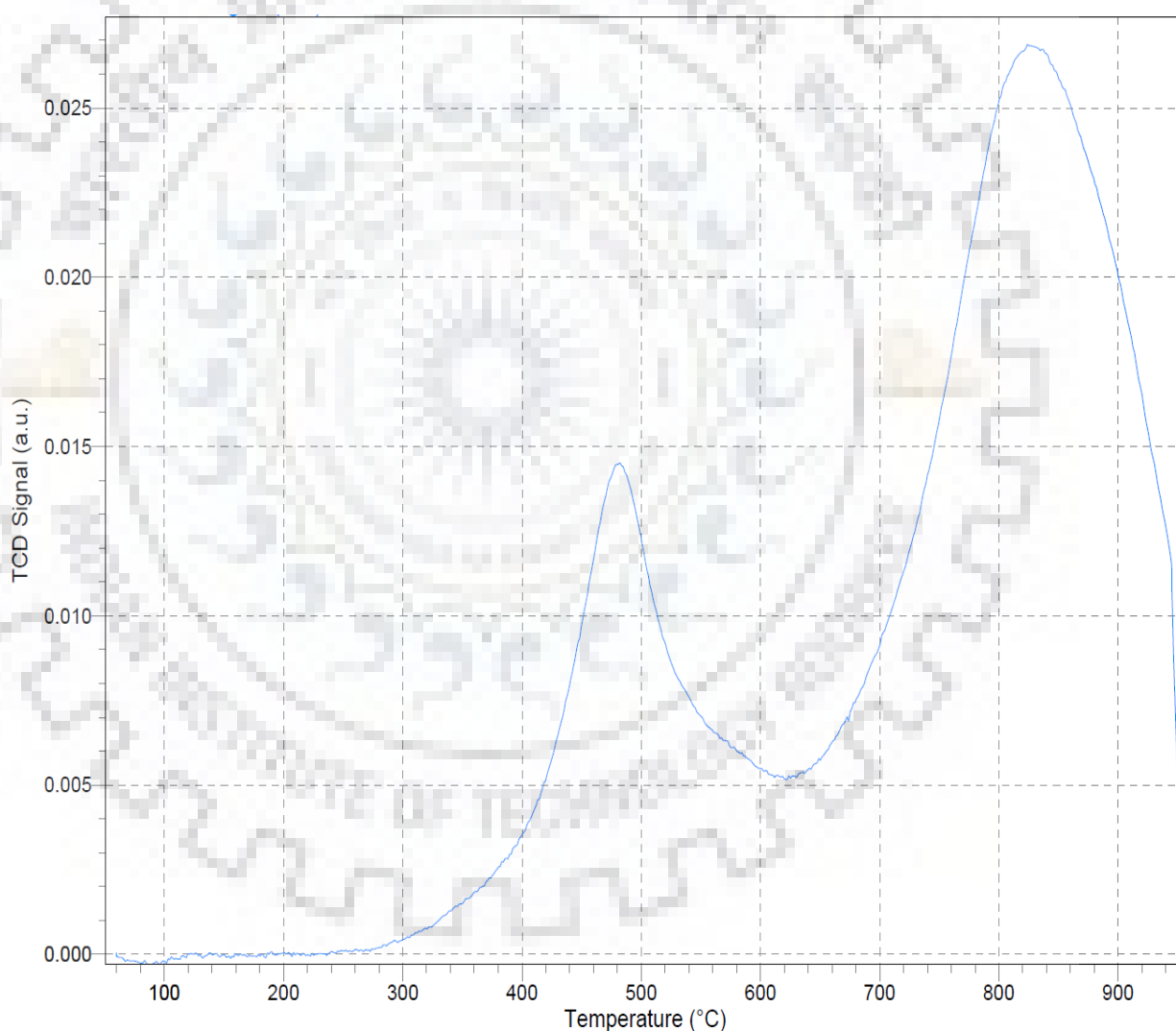


Figure 4.3. TPR of CoMoP/Al₂O₃.

Chapter 4: Hydroprocessing of lipids extracted from marine microalgae *Nannochloropsis* sp. over sulfided CoMoP/Al₂O₃ catalyst

4.4. Catalytic studies

The hydroprocessed product was obtained as a clear transparent liquid after hydroprocessing of the opaque algal oil Figure 4.4.



Figure 4.4. Algal oil and its hydroprocessed product.

Chapter 4: Hydroprocessing of lipids extracted from marine microalgae *Nannochloropsis* sp. over sulfided CoMoP/Al₂O₃ catalyst

Figure 4.5 shows the influence of reaction temperature on the lipid conversion and relative yields of various hydrocarbons. The unconverted lipid was nearly 60% in the liquid product for the reaction at 300 °C, but the concentration of unconverted lipid rapidly decreased to zero at a reaction temperature of 375 °C.

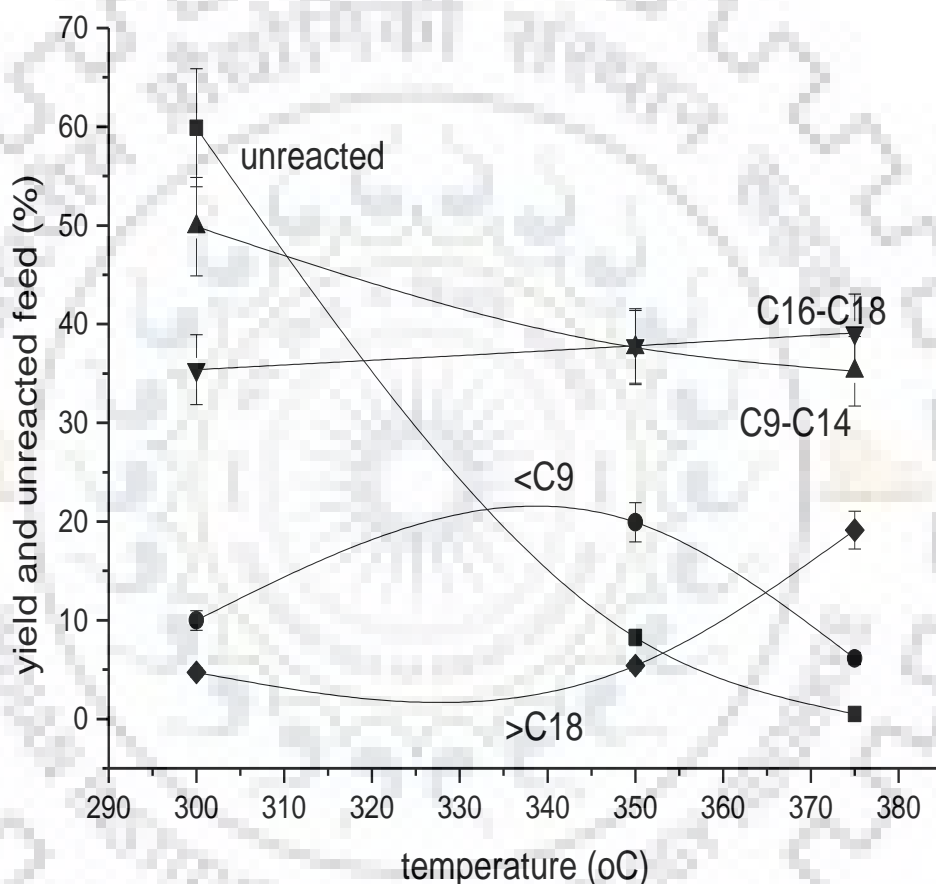


Figure 4.5. Distribution of hydrocarbons [\blacksquare gasoline (<C9), \bullet kerosene (C9–C14), \blacktriangle diesel (C15–C18), and \blacktriangledown heavy residue (>C18)] in the products at various temperatures (cat: feed ratio 1:10; pressure 50 bar).

Figure 4.6 shows the product (liquid, solid and gases) distributions (yield %) as a function of H₂ pressure (50-120 bar) over S-CoMoP/Al₂O₃, at a reaction temperature of 375°C for which the lipid conversion was always >99%. The liquid product yield decreased linearly with pressure, with a maximum liquid yield (78%) obtained at 50 bar H₂ pressure.

Chapter 4: Hydroprocessing of lipids extracted from marine microalgae *Nannochloropsis* sp. over sulfided CoMoP/Al₂O₃ catalyst

This yield decreased to 9% at the higher pressure of 120 bar. The hydrocarbon gas yield increased exponentially from 22% to 80% with an increase in pressure from 50 bar to 120 bar. These results indicate that lower pressures (around 50 bar) are favorable for maximizing liquid hydrocarbons, while higher pressures favor cracking.

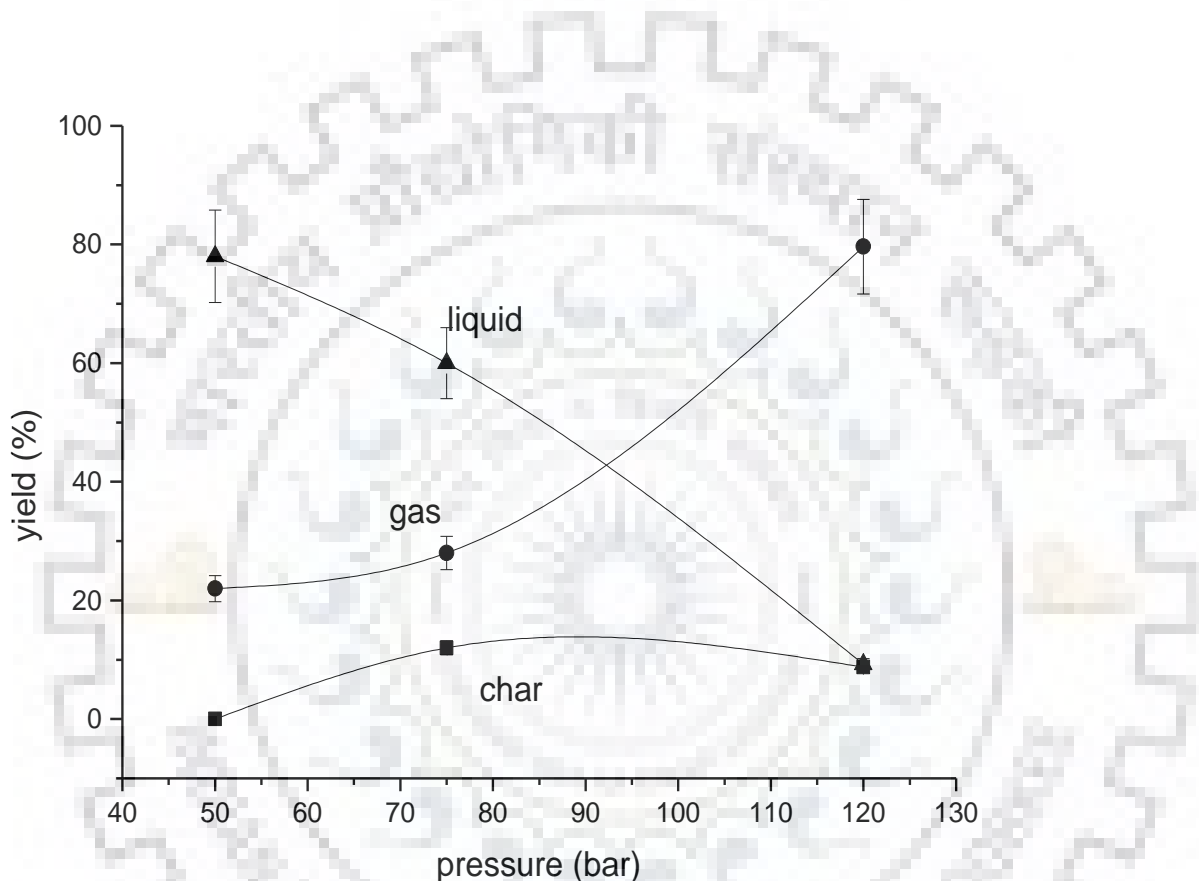


Figure 4.6. Yield (%) of the products (liquid, gases and solid char) at various H₂ pressures at 375 °C (reaction time of 5 h; cat: feed ratio of 1:10).

The influence of pressure on cracking was also observed in the distribution of hydrocarbons, as shown in Figure 4.7. The gasoline (<C₉) yield increased exponentially from 6 to 27 % on increasing the pressure from 50 bar to 120 bar. The kerosene (C₉ - C₁₄) yield changed parabolically from 36 to 50% on increasing the pressure. A minima (at 27 %) can be observed in the kerosene (C₉-C₁₄) yield at around 75 bar. The diesel (C₁₅-C₁₈) and heavier hydrocarbons (>C₁₈) yields increased linearly from 39 to 42% and from 19 to 23%, respectively, on changing the pressure from 50 to 75 bar. The diesel (C₁₅-C₁₈) and

Chapter 4: Hydroprocessing of lipids extracted from marine microalgae *Nannochloropsis* sp. over sulfided CoMoP/Al₂O₃ catalyst

heavier (>C18) hydrocarbons yields decreased sharply from 42 to 8% and 23 to 15% respectively, indicating that severe hydrocracking occurs with an increase in pressure.

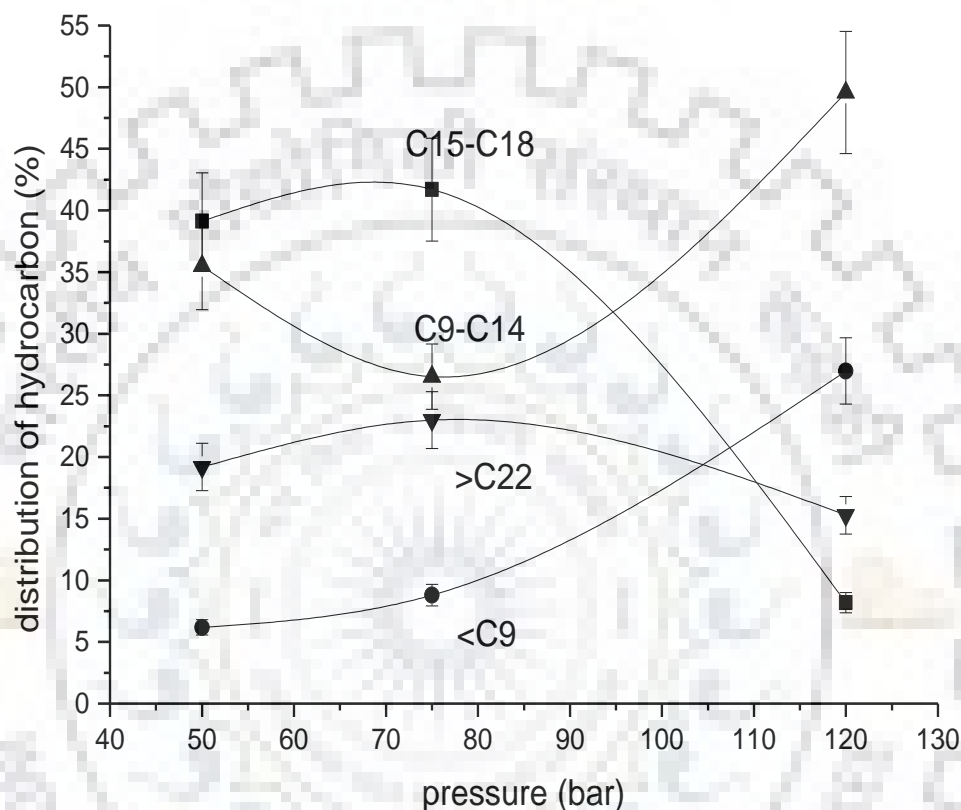


Figure 4.7. Distribution of hydrocarbons [▪ gasoline (<C9), • kerosene (C9–C14), ▲ diesel (C15–C18), and ▼ heavy residue (>C18)] in the products at various H₂ pressures (temp. 375 °C; cat: feed ratio 1:10; reaction time 5 h).

Varying the pressure had a significant impact on the hydrocarbon types in the liquid product (Figure 4.7 and Figure 4.8). The alkane component was >80% at or below 75 bar and then decreased rapidly above this pressure, decreasing to 8% at 120 bar (Figure 4.7). Polyaromatics and aromatics yields were constant at 5% at or below 75 bar, but increased rapidly to 60% and 36%, respectively at 120 bar.

Chapter 4: Hydroprocessing of lipids extracted from marine microalgae *Nannochloropsis* sp. over sulfided CoMoP/Al₂O₃ catalyst

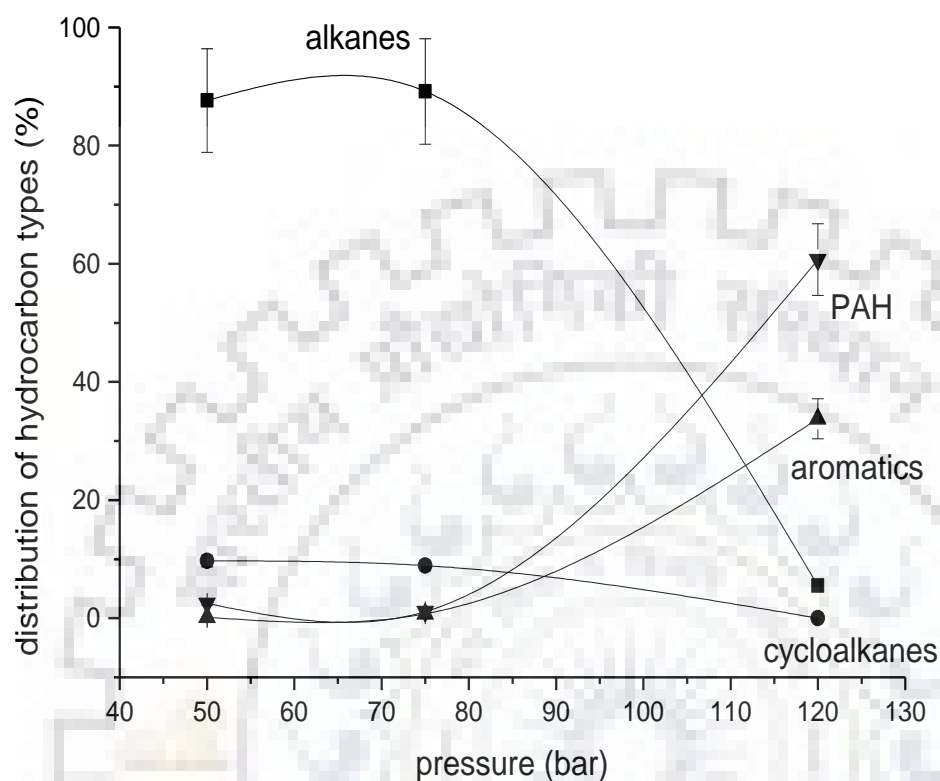


Figure 4.8. Distribution of hydrocarbon types (▪ alkanes, • cycloalkanes, ▲ aromatics, and ▼ polynuclear aromatics) in hydroprocessed products at various H₂ pressures (temp. 375 °C; cat: feed ratio 1:10; reaction time 5 h).

This trend for the polyaromatics and aromatics was similar to that of the <C₉ and C₉ - C₁₅ yields above 75 bar (Figure 4.6). The increase in aromatics may be correlated with the increase in cracking activity, which favors aromatization at higher pressure. The cycloalkanes yield was slightly higher than that of the aromatics and polyaromatics at or below 75 bar pressure, but it decreased to 1 % at 125 bar from 10 % at 75 bar (Figure 4.7). Based on results presented in Figures 4.6, 4.7 and 4.8, it may be concluded that the reaction at 50 bar and 375 °C was the best for product formation, to minimize undesired coking and to prolong the catalyst life. The mechanisms for removal of oxygen content in the lipid are cracking (catalytic cracking), hydrodeoxygenation (HDO), and

Chapter 4: Hydroprocessing of lipids extracted from marine microalgae *Nannochloropsis* sp. over sulfided CoMoP/Al₂O₃ catalyst

decarboxylation/decarbonylation (removal of oxygen to form CO₂/ CO). First double bonds in the alkyl chain are hydrogenated, and then fatty acids and propane are produced through the hydrogenolysis of saturated triglycerides. [227]. A study of hydroprocessing of lipids extracted from *Botryococcus braunii* algae over CoMo/Al₂O₃ catalyst (without P promoter) showed that only 15 % jet fuel (C9 - C14) was obtained even at higher temperatures and pressures (400 °C and 200 bar respectively) that were used in the current study [232]. Catalyst life is dependent on char/coke deposition rate. Catalyst deactivation was mainly due to the deposition of coke on the catalyst. Char/coke formation over the P promoted catalyst was nearly 10 times lower than that over catalyst without P as a promoter, which indicates that the P promoted catalyst has better catalyst life [229].

In the mechanism for direct deoxygenation, vacancy sites are created by the removal of hydrogen sulfide in the presence of H₂. Hydrogen is activated by heterolytic dissociation forming one S-H and one Mo-H group; with oxygen in the feed material adsorbing onto the vacant sites. An adsorbed carbocation is formed after the donation of a proton from an S-H group. This intermediate undergoes direct C-O bond cleavage and generates a deoxygenated product. The vacancy site is recovered by the formation of H₂O from the adsorbed OH and H groups [227].

The distribution of hydrocarbon types (gasoline, kerosene, diesel, and heavy hydrocarbons) at 325°C (Figure 4.8), shows that kerosene (C9 - C14) yield increased as the reaction time progressed, reaching a maximum (up to 56%) after 8 h. However, the gasoline yield formed a maxima (24 %) at a reaction time of 4 h, while the diesel range hydrocarbons formed minima (~ 20 %) at 5 h and the heavy hydrocarbon yield continuously increased with time of reaction. This happened since the conditions were not severe enough for cracking (i.e., low pressure), with only slight cracking leading to the formation of the kerosene range of hydrocarbons.

Chapter 4: Hydroprocessing of lipids extracted from marine microalgae *Nannochloropsis* sp. over sulfided CoMoP/Al₂O₃ catalyst

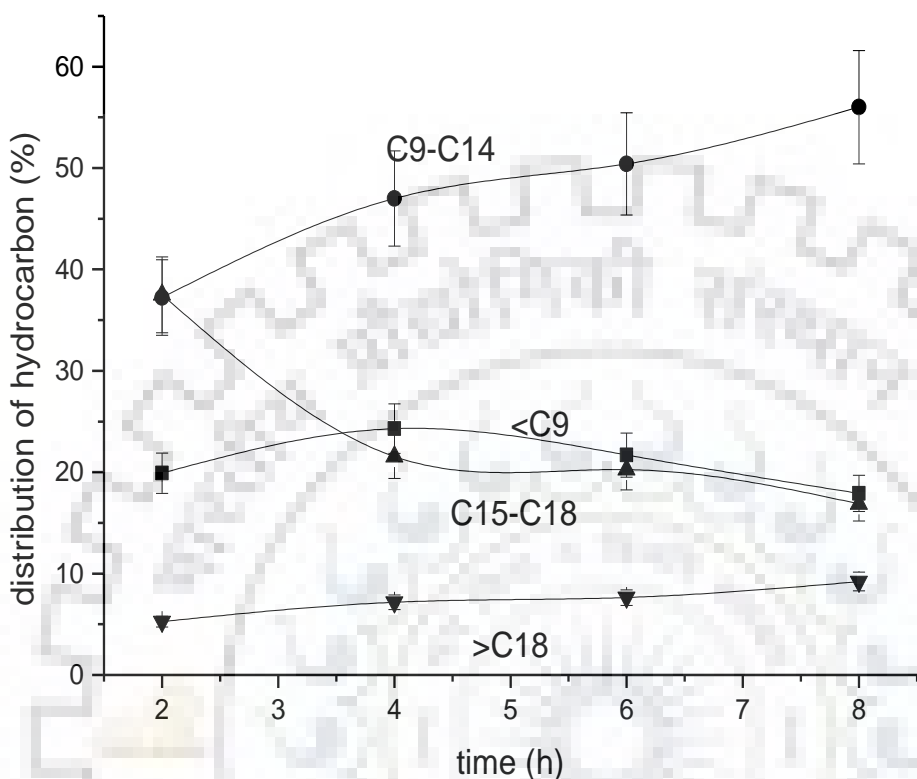


Figure 4.9. Distribution of hydrocarbons [▪ gasoline (<C9), • kerosene (C9–C14), ▲ diesel (C15–C18), and ▼ heavy residue (>C18)] in the products at various reaction times (temp 325 °C; cat: feed ratio 1:10; pressure 50 bar).

The hydrocarbon distribution at 350 °C at various reaction times is shown in Figure 4.9. It can be seen that at a reaction time of 6 h the gasoline (<C9) product formed a minima (46 %). It can also be seen that the gasoline yield was doubled by increasing the reaction temperature by 25 °C (325 to 350 °C); however, the kerosene (C9-C14) yield increased linearly to 41% after a reaction time of 6 h. The higher hydrocarbons (>C18) and diesel (C15-C18) yields, form maxima of 18% and 9% respectively. The higher hydrocarbons yield decreased by almost 4% on increasing the temperature from 325 to 350°C. From Figures 4.9 and 4.10. It may be concluded that a reaction time of 4-6 h is optimal.

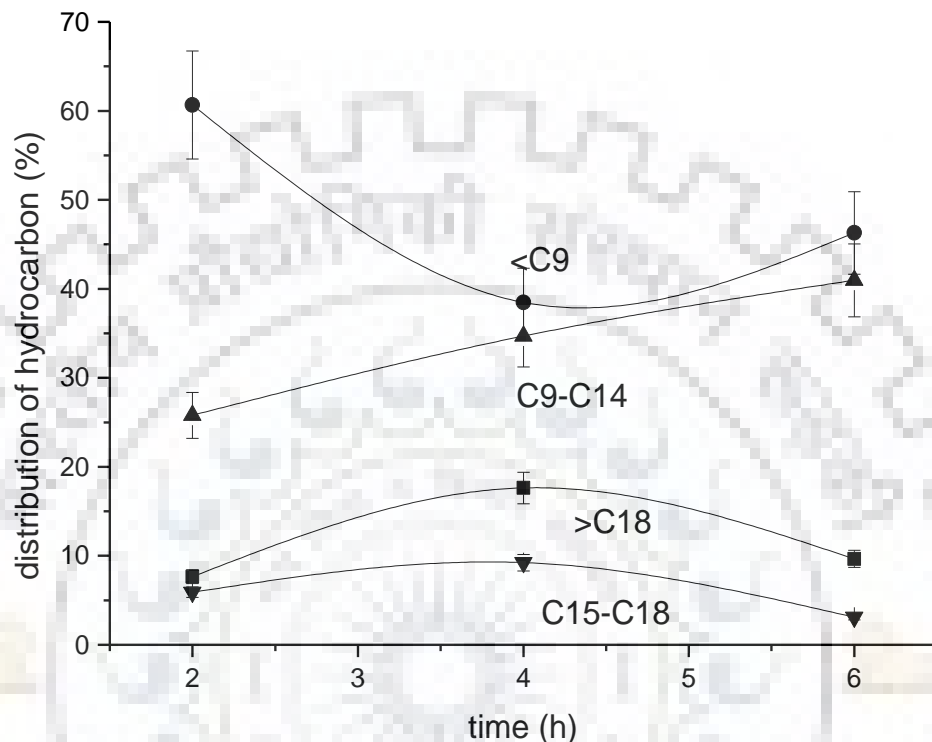


Figure 4.10. Distribution of hydrocarbons [▪ gasoline (<C9), • kerosene (C9–C14), ▲ diesel (C15–C18), and ▼ heavy residue (>C18)] in the products at various reaction times (temp. 350 °C; cat: feed ratio 1:10; pressure 50 bar).

4.5. Kinetic studies

The apparent activation energy for the conversion of algae oil and its hydroprocessed products were calculated by Arrhenius plot [233], and was found that activation energy for the conversion of algae oil was low (in the order of 14.96 KJmol⁻¹ at close to 60 % conversion), as compared to that for the formation of some of the hydroprocessed products.

Chapter 4: Hydroprocessing of lipids extracted from marine microalgae Nannochloropsis sp. over sulfided CoMoP/Al₂O₃ catalyst

Table 4.1. Compositional details of lipids

Compositions	% Fraction	
	Jatropha Oil	Nannochloropsis sp.micro algae
C14:0	<1	2.8
C16:0	19.5	35.7
C16:1	<1	25.9
C18:0	7.9	3.8
C18:1	45.4	26.8
C18:2	27.3	<1

The apparent activation energy for the formation of diesel (125 KJmol^{-1}) is less than kerosene (146 KJmol^{-1}), while apparent activation energy for the formation alkanes and polyaromatics hydrocarbons is 64 KJmol^{-1} and 7 KJmol^{-1} respectively. In comparison, the reported activation energy for jatropha oil hydroprocessing over CoMoP/Al₂O₃ catalyst was 26 kJmol^{-1} and those for kerosene; diesel heavier hydrocarbons are formation was 83, 127 and 47 kJmol^{-1} , respectively. In general activation, energies were lower when using algae oil than those for jatropha oil conversion except for >C18 hydrocarbons.

marine microalgae Nannochloropsis sp. has maximum (~65%) smaller carbon range containing lipids however in case of Jatropha oil lipids has maximum (72%) of higher carbon range containing lipids (Table 1.). So Jatropha oil lipids needs higher activation energy to break down to lower range of hydrocarbons.

4.6. Conclusions

Algal lipids were successfully hydroprocessed over sulfided CoMoP/Al₂O₃ catalyst. The results show that almost complete conversion of lipids was achieved at $375 \text{ }^\circ\text{C}$ and 120 bar of H₂. At these conditions, 26% of gasoline and 50% of kerosene along with 80% of alkanes formation was achieved. The reaction order followed pseudo 1st order kinetics with respect to algae oil concentration. The Activation energy for the conversion of algae oil (14.96 KJmol^{-1}) was lower than Jatropha oil (26 KJmol^{-1}).



Chapter 5

Summary and Conclusions

Chapter 5: Summary and Conclusions

Detailed literature on the various biomasses and classification of biofuels such as first generation, second generation, and third generation, has been discussed. Pyrolysis of non-edible biomass, i.e., jatropha curcas seeds cake (JCC) has been studied by using approx 800 ml min^{-1} of N_2 flow rate at temperature 550°C in continuous fix bed reactor. The pyrolysis-oil is a complex mixture of aldehydes, alcohols, and acids together with more complex carbohydrates and lignin-derived oligomeric materials. Pyrolysis oil has clearly distinguished two phases, one is a very dark viscous liquid having very trace amount of water and an almost equal amount of carbon and oxygen content, called bio-oil (BO) and another one is aqueous phase having 65-75 % of the water in a mixture of organic compounds. Hydroprocessing (refinery technique) has been the best option to upgrade the pyrolysis oil/bio-oil (BO) to bio-transportation fuels by decreasing the oxygen content from 30-40 wt. % to the drop-in-fuels. The BO co-processed with refinery gas oil in the various ratio of refinery gas oil over S- CoMoP/ Al_2O_3 catalyst in a batch reactor.

The results indicate that co-hydroprocessing of bio-oils with sulphided CoMoP/ Al_2O_3 catalyst is a promising route for producing transportation fuels. Products obtained from co-processing 25 % and 50 % of bio-oil (BO) with gas-oil (GO) contained 2-16 % gasoline, 30-35 % kerosene, 35-44 % diesel, with negligible oxygenates and char. Hydroprocessing of 100% BO at 375°C and 50 bar produced 10 % gasoline, 30 % kerosene, and 30 % diesel with a large amount (40 %) of undesirable polynuclear aromatics. But at 75 bar (375°C) for 100 % BO, polynuclear aromatics formation was suppressed (<2 %) and kerosene yield was maximum (41 %), with very small amount of char (1.5 %) formation.

The aqueous phase was hydroprocessed in a continuous microchannel reactor (MCR) over highly dispersed S- NiMo/ Al_2O_3 - SiO_2 catalyst in all channels of the reactor. Reactivity of H_2 gets enhanced due to the presence of a narrow path to travel, so this reactor gives better conversion even though at low reaction parameter than fixed bed continuous reactor.

Chapter 5: Summary and Conclusions

Hydroprocessing of aqueous-phase of bio-oil (BO) obtained from pyrolysis of de-oiled *Jatropha curcas* seeds cake (JCC) with sulphided NiMo catalyst supported on mesoporous silica-alumina and coated in a microchannel reactor is a promising route for producing transportation fuels. Complete deoxygenation of the organics in the aqueous-phase was achieved. The water obtained after hydroprocessing contained <5 % organics indicating that >95 % of organics in the aqueous-phase of bio-oil was converted into desirable products. Products obtained from hydroprocessing contained 5-45 % gasoline (<C9), 5-60 % kerosene (C9-C14), 15-40 % diesel (C15-C18), with 15-65 % alkanes, 0-5 % polyaromatic hydrocarbons (PAH), negligible cycloalkanes and aromatics, with 30-75 % unreacted and residues under reaction condition of temperature 250 – 400°C, LHSV 0.25-1.25, H₂:feed ratio 500-4000 and at fixed pressure of 70 bar. Maximum hydrocarbon yield (~65 %) was obtained at 375°C, 0.25 LHSV, and 70 bar, with 35 % undesired residues and PAH.

Second generation biofuels using thermal conversion followed by hydroprocessing (refinery process to upgrade) is energy as well as the cost-intensive process. We have also studied the third generation bio-fuels feed sources, i.e., algae oil.

The marine microalgae *Nannochloropsis* sp. extracted lipid triglycerides (TAGs) have been hydroprocessed in the batch reactor to produce drop-in-transportation fuels over sulphided CoMoP/Al₂O₃.

Algal lipids were successfully hydroprocessed over sulfided CoMoP/Al₂O₃ catalyst. The results show that almost complete conversion of lipids was achieved at 375 °C and 120 bar of H₂. At these conditions, 26% of gasoline and 50% of kerosene along with 80% of alkanes formation was achieved. The reaction order followed pseudo 1st order kinetics with respect to algae oil concentration. The Activation energy for the conversion of algae oil (14.96 KJmol⁻¹) was lower than *Jatropha* oil (26 KJmol⁻¹).

Finally, it has been concluded that transportation fuels can be generated by hydroprocessing of biomass-derived oil and that can be used as a drop in fuel in the existing transportation engines.

Chapter 6

References

Chapter 6: Reference

References

- [1] Y. Yu, D. Liu, H. Wu, Characterization of water-soluble intermediates from slow pyrolysis of cellulose at low temperatures, *Energy and Fuels*. 26 (2012) 7331–7339. doi:10.1021/ef3013097.
- [2] M. van der Hoeven, IEA. *World Energy Outlook 2011*, International Energy Agency. 2011., (2011) 1–659.
- [3] Anthony V. Bridgwater, *BIOMASS FAST PYROLYSIS*, *Bioresour. Technol.* 85 (2004) 21–49. doi:10.1016/j.biortech.2010.12.075.
- [4] P.K. Kanaujia, D. V. Naik, D. Tripathi, R. Singh, M.K. Poddar, L.N. Siva Kumar Konathala, Y.K. Sharma, Pyrolysis of *Jatropha Curcas* seed cake followed by optimization of liquid-liquid extraction procedure for the obtained bio-oil, *J. Anal. Appl. Pyrolysis*. 118 (2016) 202–224. doi:10.1016/j.jaap.2016.02.005.
- [5] R. Gomes, P. Bhanja, A. Bhaumik, Sulfonated porous organic polymer as a highly efficient catalyst for the synthesis of biodiesel at room temperature, *J. Mol. Catal. A Chem.* 411 (2016) 110–116. doi:10.1016/j.molcata.2015.10.016.
- [6] V.B. Saptal, B.M. Bhanage, Bifunctional Ionic Liquids Derived from Biorenewable Sources as Sustainable Catalysts for Fixation of Carbon Dioxide, *ChemSusChem*. 10 (2017) 1145–1151. doi:10.1002/cssc.201601228.
- [7] S. Samanta, R. Srivastava, A novel method to introduce acidic and basic bi-functional sites in graphitic carbon nitride for sustainable catalysis: cycloaddition, esterification, and transesterification reactions, *Sustain. Energy Fuels*. 1 (2017) 1390–1404. doi:10.1039/C7SE00223H.
- [8] E.M.W. Smeets, A.P.C. Faaij, I.M. Lewandowski, W.C. Turkenburg, A bottom-up assessment and review of global bio-energy potentials to 2050, *Prog. Energy Combust. Sci.* 33 (2007) 56–106. doi:https://doi.org/10.1016/j.peccs.2006.08.001.
- [9] S. Ladanai, J. Vinterbäck, *Global Potential of Sustainable Biomass, Technology*. (2009) 32. doi:ISSN 1654-9406.

Chapter 6: Reference

- [10] S. Sorrell, J. Speirs, R. Bentley, A. Brandt, R. Miller, Global oil depletion: A review of the evidence, *Energy Policy*. 38 (2010) 5290–5295.
doi:10.1016/j.enpol.2010.04.046.
- [11] O.O. James, B. Chowdhury, S. Maity, Comparative TPR and TPD Studies of Cu and Ca Promotion on Fe-Zn- and Fe-Zn-Zr-Based Fischer-Tropsch Catalysts, *Oil Gas Sci. Technol. – Rev. d’IFP Energies Nouv.* 70 (2013) 511–519.
doi:10.2516/ogst/2013114.
- [12] A.A. Lappas, S. Bezergianni, I.A. Vasalos, Production of biofuels via co-processing in conventional refining processes, *Catal. Today*. 145 (2009) 55–62.
doi:10.1016/j.cattod.2008.07.001.
- [13] M. Popova, Á. Szegedi, H. Lazarova, A. Ristić, Y. Kalvachev, G. Atanasova, N. Wilde, N.N. Tušar, R. Gläser, Synthesis of biomass derived levulinate esters on novel sulfated Zr/KIL-2 composite catalysts, *Microporous Mesoporous Mater.* 235 (2016) 50–58. doi:10.1016/j.micromeso.2016.07.047.
- [14] A.J. Ragauskas, C.K. Williams, B.H. Davison, G. Britovsek, J. Cairney, C.A. Eckert, W.J. Frederick, J.P. Hallett, D.J. Leak, C.L. Liotta, J.R. Mielenz, R. Murphy, R. Templer, T. Tschaplinski, The path forward for biofuels and biomaterials, *Science* (80-.). 311 (2006) 484–489. doi:10.1126/science.1114736.
- [15] S. Mondal, R. Singuru, S. Chandra Shit, T. Hayashi, S. Irle, Y. Hijikata, J. Mondal, A. Bhaumik, Ruthenium Nanoparticle-Decorated Porous Organic Network for Direct Hydrodeoxygenation of Long-Chain Fatty Acids to Alkanes, *ACS Sustain. Chem. Eng.* 6 (2018) 1610–1619. doi:10.1021/acssuschemeng.7b02772.
- [16] S. Bezergianni, A. Dimitriadis, A. Kalogianni, P.A. Pilavachi, Hydrotreating of waste cooking oil for biodiesel production. Part I: Effect of temperature on product yields and heteroatom removal, *Bioresour. Technol.* 101 (2010) 6651–6656.
doi:10.1016/j.biortech.2010.03.081.

Chapter 6: Reference

- [17] R.W. Jenkins, C.M. Moore, T.A. Semelsberger, C.J. Chuck, J.C. Gordon, A.D. Sutton, The Effect of Functional Groups in Bio-Derived Fuel Candidates, *ChemSusChem*. 9 (2016) 922–931. doi:10.1002/cssc.201600159.
- [18] S. Bezergianni, A. Dimitriadis, T. Sfetsas, A. Kalogianni, Hydrotreating of waste cooking oil for biodiesel production. Part II: Effect of temperature on hydrocarbon composition, *Bioresour. Technol.* 101 (2010) 7658–7660. doi:10.1016/j.biortech.2010.04.043.
- [19] S.N. Naik, V. V. Goud, P.K. Rout, A.K. Dalai, Production of first and second generation biofuels: A comprehensive review, *Renew. Sustain. Energy Rev.* 14 (2010) 578–597. doi:10.1016/j.rser.2009.10.003.
- [20] M.K. Poddar, A. Rai, M.R. Maurya, A.K. Sinha, Co-processing of bio-oil from de-oiled *Jatropha curcas* seed cake with refinery gas-oil over sulfided CoMoP/Al₂O₃ catalyst, *RSC Adv.* 6 (2016) 113720–113726. doi:10.1039/c6ra20893b.
- [21] R. Lødeng, C. Ranga, T. Rajkhowa, V.I. Alexiadis, H. Bjørkan, S. Chytil, I.H. Svenum, J. Walmsley, J.W. Thybaut, Hydrodeoxygenation of phenolics in liquid phase over supported MoO₃ and carburized analogues, *Biomass Convers. Biorefinery.* 7 (2017) 343–359. doi:10.1007/s13399-017-0252-z.
- [22] R. Kumar, N. Enjamuri, S. Shah, A.S. Al-Fatesh, J.J. Bravo-Suárez, B. Chowdhury, Ketoneization of oxygenated hydrocarbons on metal oxide based catalysts, *Catal. Today.* 302 (2018) 16–49. doi:10.1016/j.cattod.2017.09.044.
- [23] P. Biller, B.K. Sharma, B. Kunwar, A.B. Ross, Hydroprocessing of bio-crude from continuous hydrothermal liquefaction of microalgae, *Fuel.* 159 (2015) 197–205. doi:10.1016/j.fuel.2015.06.077.

Chapter 6: Reference

- [24] S. Raikova, H. Smith-Baedorf, R. Bransgrove, O. Barlow, F. Santomauro, J.L. Wagner, M.J. Allen, C.G. Bryan, D. Sapsford, C.J. Chuck, Assessing hydrothermal liquefaction for the production of bio-oil and enhanced metal recovery from microalgae cultivated on acid mine drainage, *Fuel Process. Technol.* 142 (2016) 219–227. doi:10.1016/j.fuproc.2015.10.017.
- [25] I.P. Boukis, P. Grammelis, S. Bezergianni, A. V. Bridgwater, CFB air-blown flash pyrolysis. Part I: Engineering design and cold model performance, *Fuel*. 86 (2007) 1372–1386. doi:10.1016/j.fuel.2006.11.002.
- [26] M.K. Poddar, M. Anand, S.A. Farooqui, G.J.O. Martin, M.R. Maurya, A.K. Sinha, Hydroprocessing of lipids extracted from marine microalgae *Nannochloropsis* sp. over sulfided CoMoP/Al₂O₃ catalyst, *Biomass and Bioenergy*. 119 (2018) 31–36. doi:10.1016/j.biombioe.2018.08.011.
- [27] B. Donnis, R.G. Egeberg, P. Blom, K.G. Knudsen, Hydroprocessing of bio-oils and oxygenates to hydrocarbons. Understanding the reaction routes, *Top. Catal.* 52 (2009) 229–240. doi:10.1007/s11244-008-9159-z.
- [28] T.L.M. Maesen, S. Calero, M. Schenk, B. Smit, Alkane hydrocracking: Shape selectivity or kinetics?, *J. Catal.* 221 (2004) 241–251. doi:10.1016/j.jcat.2003.07.003.
- [29] M. Nasikin, B. Heru Susanto, M. Adam Hirsaman, A. Wijanarko, Biogasoline from Palm Oil by Simultaneous Cracking and Hydrogenation Reaction over NiMo/zeolite Catalyst, *World Appl. Sci. Journal Environmental Manag. Technol. Towar. Sustain. Dev.* 5 (2009) 74–79. [https://www.idosi.org/wasj/wasj5\(s\)/11.pdf](https://www.idosi.org/wasj/wasj5(s)/11.pdf).
- [30] Q. Smejkal, L. Smejkalová, D. Kubička, Thermodynamic balance in reaction system of total vegetable oil hydrogenation, *Chem. Eng. J.* 146 (2009) 155–160. doi:10.1016/j.cej.2008.09.020.
- [31] W. Charusiri, T. Vitidsant, Kinetic Study of Used Vegetable Oil to Liquid Fuels over Sulfated Zirconia, *Energy & Fuels*. 19 (2005) 1783–1789. doi:10.1021/ef0500181.

Chapter 6: Reference

- [32] T. Rahmes, Status of Sustainable Biofuel Efforts for Aviation, (2004).
- [33] T. Daniel M. Ginosar, Lucia M. Petkovic, conversion of crop seed oil to jet fuel and associated methods, US 2009/0071872 A1, 2009.
- [34] T.A. Wayne A. Seames, method for cold stable biojet fuel, US 2008/0092436 A1, 2008.
- [35] nathan jannasch ramin Abhari, Lynn Tomlinson, Peter havlik, process for co-processing jet fuel and LPG from renewable sources, US2008/0244962 A1, 2008.
- [36] A.C. Donald E. Trimbur, Chung-soon Im, Harrison F. Dillon, Anthony G. Day, Scoot Franklin, Renewable diesel and jet fuel from microbial sources, US2009/0047721 A1, 2009.
- [37] W.D. Morgan, production of fuels with superior low temperature properties from tall oil or fractionated fatty acids, US2009/0049739 A1, 2009.
- [38] edward L. sughrue I. jianhua yao, process for converting triglycerides to hydrocarbons, US 2007/0175795 A1, 2007.
- [39] I.N. Hydroprocessing, Zeolite Catalysis in Hydroprocessing Technology, Catal. Today. (1987) 385–413.
- [40] N. Choudhary, D.N. Saraf, Hydrocracking: A Review, Ind. Eng. Chem. Prod. Res. Dev. 14 (1975) 74–83. doi:10.1021/i360054a002.
- [41] G.E. Dolbear, Hydrocracking catalysts and processes, in: American Chemical Society, Washington, DC (United States), United States, 1995. <https://www.osti.gov/servlets/purl/215000>.
- [42] F. Morel, S. Kressmann, V. Harlé, S. Kasztelan, Processes and catalysts for hydrocracking of heavy oil and residues, (2007) 1–16. doi:10.1016/s0167-2991(97)80003-1.

Chapter 6: Reference

- [43] John W. Ward, Hydrocracking processes and catalysts, *Fuel Process. Technol.* 35 (1993) 55–85.
- [44] P. Mäki-Arvela, I. Kubickova, M. Snåre, K. Eränen, D.Y. Murzin, Catalytic Deoxygenation of Fatty Acids and Their Derivatives, *Energy & Fuels*. 21 (2007) 30–41. doi:10.1021/ef060455v.
- [45] P. Mäki-Arvela, B. Rozmysłowicz, S. Lestari, O. Simakova, K. Eränen, T. Salmi, D.Y. Murzin, Catalytic Deoxygenation of Tall Oil Fatty Acid over Palladium Supported on Mesoporous Carbon, *Energy & Fuels*. 25 (2011) 2815–2825. doi:10.1021/ef200380w.
- [46] K. Murata, Y. Liu, M. Inaba, I. Takahara, Production of Synthetic Diesel by Hydrotreatment of Jatropha Oils Using Pt–Re/H-ZSM-5 Catalyst, *Energy & Fuels*. 24 (2010) 2404–2409. doi:10.1021/ef901607t.
- [47] R. Sotelo-Boyás, Y. Liu, T. Minowa, Renewable Diesel Production from the Hydrotreating of Rapeseed Oil with Pt/Zeolite and NiMo/Al₂O₃ Catalysts, *Ind. Eng. Chem. Res.* 50 (2011) 2791–2799. doi:10.1021/ie100824d.
- [48] G.W. Huber, P.O. Connor, A. Corma, Processing biomass in conventional oil refineries : Production of high quality diesel by hydrotreating vegetable oils in heavy vacuum oil mixtures, 329 (2007) 120–129. doi:10.1016/j.apcata.2007.07.002.
- [49] D.W. soveran wayne k. craig, On the Mechnaism of Rapid Pyrolysis of Cellulose, US4992605, 1991.
- [50] P. Šimáček, D. Kubička, G. Šebor, M. Pospíšil, Hydroprocessed rapeseed oil as a source of hydrocarbon-based biodiesel, *Fuel*. 88 (2009) 456–460. doi:10.1016/j.fuel.2008.10.022.
- [51] G.N. da Rocha Filho, D. Brodzki, G. Djéga-Mariadassou, Formation of alkanes, alkylcycloalkanes and alkylbenzenes during the catalytic hydrocracking of vegetable oils, *Fuel*. 72 (1993) 543–549. doi:10.1016/0016-2361(93)90114-H.

Chapter 6: Reference

- [52] M. Krár, S. Kovács, D. Kalló, J. Hancsók, Fuel purpose hydrotreating of sunflower oil on CoMo/Al₂O₃ catalyst, *Bioresour. Technol.* 101 (2010) 9287–9293. doi:10.1016/j.biortech.2010.06.107.
- [53] H. Yang, R. Yan, H. Chen, D.H. Lee, C. Zheng, Characteristics of hemicellulose, cellulose and lignin pyrolysis, *Fuel*. 86 (2007) 1781–1788. doi:10.1016/j.fuel.2006.12.013.
- [54] L. Wei, S. Xu, L. Zhang, H. Zhang, C. Liu, H. Zhu, S. Liu, Characteristics of fast pyrolysis of biomass in a free fall reactor, *Fuel Process. Technol.* 87 (2006) 863–871. doi:10.1016/j.fuproc.2006.06.002.
- [55] F. Shafizadeh, Introduction to pyrolysis of biomass, *J. Anal. Appl. Pyrolysis*. 3 (1982) 283–305. doi:https://doi.org/10.1016/0165-2370(82)80017-X.
- [56] R.J. Evans, T.A. Milne, Molecular characterization of the pyrolysis of biomass, *Energy & Fuels*. 1 (1987) 123–137. doi:10.1021/ef00002a001.
- [57] O. Boutin, M. Ferrer, J. Lédé, Radiant flash pyrolysis of cellulose - Evidence for the formation of short life time intermediate liquid species, *J. Anal. Appl. Pyrolysis*. 47 (1998) 13–31. doi:10.1016/S0165-2370(98)00088-6.
- [58] J. Piskorz, D. Radlein, D.C. Scott, On the Mechanism of Rapid Pyrolysis of Cellulose, *J. Anal. Appl. Pyrol.* 9 (1986) 121–137.
- [59] D. Radlein, J. Piskorz, D.S. Scott, Fast pyrolysis of natural polysaccharides as a potential industrial process, *J. Anal. Appl. Pyrolysis*. 19 (1991) 41–63. doi:10.1016/0165-2370(91)80034-6.
- [60] R. Lanza, D. Dalle Nogare, P. Canu, Gas Phase Chemistry in Cellulose Fast Pyrolysis, *Ind. Eng. Chem. Res.* 48 (2009) 1391–1399. doi:10.1021/ie801280g.
- [61] Y.-C. Lin, J. Cho, G.A. Tompsett, P.R. Westmoreland, G.W. Huber, Kinetics and Mechanism of Cellulose Pyrolysis, *J. Phys. Chem. C*. 113 (2009) 20097–20107. doi:10.1021/jp906702p.

Chapter 6: Reference

- [62] R. Alén, E. Kuoppala, P. Oesch, Formation of the main degradation compound groups from wood and its components during pyrolysis, *J. Anal. Appl. Pyrolysis*. 36 (1996) 137–148. doi:10.1016/0165-2370(96)00932-1.
- [63] G.R. Ponder, G.N. Richards, Thermal synthesis and pyrolysis of a xylan, *Carbohydr. Res.* 218 (1991) 143–155. doi:10.1016/0008-6215(91)84093-T.
- [64] D. Mohan, C.U. Pittman, P.H. Steele, Pyrolysis of Wood/Biomass for Bio-oil: A Critical Review, *Energy & Fuels*. 20 (2006) 848–889. doi:10.1021/ef0502397.
- [65] energy-outlook-2035-presentation.pdf, in: n.d.
- [66] F. Stirpe, A. Pession-Brizzi, E. Lorenzoni, P. Strocchi, L. Montanaro, S. Sperti, Studies on the proteins from the seeds of *Croton tiglium* and of *Jatropha curcas* . Toxic properties and inhibition of protein synthesis in vitro, *Biochem. J.* 156 (1976) 1–6. doi:10.1042/bj1560001.
- [67] P. Bhanja, A. Bhaumik, Porous nanomaterials as green catalyst for the conversion of biomass to bioenergy, *Fuel*. 185 (2016) 432–441. doi:10.1016/j.fuel.2016.08.004.
- [68] J. Wildschut, I. Melián-Cabrera, H.J. Heeres, Catalyst studies on the hydrotreatment of fast pyrolysis oil, *Appl. Catal. B Environ.* 99 (2010) 298–306. doi:10.1016/j.apcatb.2010.06.036.
- [69] D. V. Naik, V. Kumar, B. Prasad, M.K. Poddar, B. Behera, R. Bal, O.P. Khatri, D.K. Adhikari, M.O. Garg, Catalytic cracking of jatropha-derived fast pyrolysis oils with VGO and their NMR characterization, *RSC Adv.* 5 (2015) 398–409. doi:10.1039/c4ra08128e.
- [70] P.K. Kanaujia, Y.K. Sharma, M.O. Garg, D. Tripathi, R. Singh, Review of analytical strategies in the production and upgrading of bio-oils derived from lignocellulosic biomass, *J. Anal. Appl. Pyrolysis*. 105 (2014) 55–74. doi:10.1016/j.jaap.2013.10.004.

Chapter 6: Reference

- [71] M. Garcia-Perez, S. Wang, J. Shen, M. Rhodes, W.J. Lee, C.-Z. Li, Effects of Temperature on the Formation of Lignin-Derived Oligomers during the Fast Pyrolysis of Mallee Woody Biomass, *Energy & Fuels*. 22 (2008) 2022–2032. doi:10.1021/ef7007634.
- [72] A. Oasmaa, E. Kuoppala, Y. Solantausta, Fast Pyrolysis of Forestry Residue. 2. Physicochemical Composition of Product Liquid, *Energy & Fuels*. 17 (2003) 433–443. doi:10.1021/ef020206g.
- [73] M. Garcia-Perez, A. Chaala, H. Pakdel, D. Kretschmer, C. Roy, Characterization of bio-oils in chemical families, *Biomass and Bioenergy*. 31 (2007) 222–242. doi:10.1016/j.biombioe.2006.02.006.
- [74] D. Meier, J.D. Olson, Characterization of the water-insoluble fraction from pyrolysis oil (pyrolytic lignin). Part I. PY-GC/MS, FTIR, and functional groups, *J. Anal. Appl. Pyrolysis*. 60 (2001) 41–54. doi:10.1016/S0165-2370(00)00110-8.
- [75] B. Scholze, C. Hanser, D. Meier, Characterization of the water-insoluble fraction from fast pyrolysis liquids (pyrolytic lignin) Part II, *J. Anal. Appl. Pyrolysis*. 58–59 (2002) 387–400. doi:10.1016/s0165-2370(00)00173-x.
- [76] R. Bayerbach, V.D. Nguyen, U. Schurr, D. Meier, Characterization of the water-insoluble fraction from fast pyrolysis liquids (pyrolytic lignin). Part III. Molar mass characteristics by SEC, MALDI-TOF-MS, LDI-TOF-MS, and Py-FIMS, *J. Anal. Appl. Pyrolysis*. 77 (2006) 95–101. doi:10.1016/j.jaap.2006.02.002.
- [77] R. Bayerbach, D. Meier, Characterization of the water-insoluble fraction from fast pyrolysis liquids (pyrolytic lignin). Part IV: Structure elucidation of oligomeric molecules, *J. Anal. Appl. Pyrolysis*. 85 (2009) 98–107. doi:10.1016/j.jaap.2008.10.021.

Chapter 6: Reference

- [78] D.C. Elliott, Analysis and comparison of biomass pyrolysis/gasification condensates: Final report, Other Inf. Portions This Doc. Are Illegible Microfich. Prod. Orig. Copy Available until Stock Is Exhausted. (1986) Medium: ED; Size: Pages: 100.
<http://www.osti.gov/bridge/servlets/purl/7049810-1BB610/>.
- [79] L. Fagemas, Chemical and Physical Characterisation of Biomass-Based Pyrolysis Oils Literature Review, 1995.
- [80] A. Oasmaa, S. Czernik, Fuel Oil Quality of Biomass Pyrolysis Oils State of the Art for the End Users, *Energy & Fuels*. 13 (1999) 914–921. doi:10.1021/ef980272b.
- [81] D.C. Elliott, Water, alkali and char in flash pyrolysis oils, *Biomass and Bioenergy*. 7 (1994) 179–185. doi:[https://doi.org/10.1016/0961-9534\(94\)00057-Z](https://doi.org/10.1016/0961-9534(94)00057-Z).
- [82] J. Soltés, S.-C.K. Lin, Hydroprocessing of Biomass Tars for Liquid Engine Fuels, in: D.A. TILLMAN, E.C. JAHN (Eds.), Elsevier, 1984: pp. 1–68.
doi:<https://doi.org/10.1016/B978-0-12-535905-4.50007-2>.
- [83] STEFAN, D.K.J.W. and S.B. CZERNIK, STABILITY OF WOOD FAST PYROLYSIS OIL STEFAN, 7 (1994) 187–192.
- [84] J.P. Diebold, A review of the chemical and physical mechanisms of the storage stability of fast pyrolysis bio-oils, (2000) 1–59. doi:10.2172/753818.
- [85] A. Oasmaa, D. Meier, Norms and standards for fast pyrolysis liquids: 1. Round robin test, *J. Anal. Appl. Pyrolysis*. 73 (2005) 323–334. doi:10.1016/j.jaap.2005.03.003.
- [86] A. Oasmaa, C. Peacocke, S. Gust, D. Meier, R. McLellan, Norms and Standards for Pyrolysis Liquids. End-User Requirements and Specifications, *Energy & Fuels*. 19 (2005) 2155–2163. doi:10.1021/ef040094o.
- [87] E. Laurent, B. Delmon, Study of the hydrodeoxygenation of carbonyl, carboxylic and guaiacyl groups over sulfided CoMo/ γ -Al₂O₃ and NiMo/ γ -Al₂O₃ catalysts: I. Catalytic reaction schemes, *Appl. Catal. A Gen.* 109 (1994) 77–96.
doi:[https://doi.org/10.1016/0926-860X\(94\)85004-6](https://doi.org/10.1016/0926-860X(94)85004-6).

Chapter 6: Reference

- [88] C.A. Fisk, T. Morgan, Y. Ji, M. Crocker, C. Crofcheck, S.A. Lewis, Bio-oil upgrading over platinum catalysts using in situ generated hydrogen, *Appl. Catal. A Gen.* 358 (2009) 150–156. doi:10.1016/j.apcata.2009.02.006.
- [89] A. Oasmaa, B. van de Beld, P. Saari, D.C. Elliott, Y. Solantausta, Norms, Standards, and Legislation for Fast Pyrolysis Bio-oils from Lignocellulosic Biomass, *Energy & Fuels.* 29 (2015) 2471–2484. doi:10.1021/acs.energyfuels.5b00026.
- [90] A. Bandi, F. Baumgart, Stirling Engine with Flax Burner Fuelled with Fast Pyrolysis Liquid, *Prog. Thermochem. Biomass Convers.* (2008) 1459–1467. doi:10.1002/9780470694954.ch120.
- [91] H.S. Michio Ikura, Siamak mirmiran, Maria Stanculescu, *Pyrolysis Liquid-in-Diesel Oil Microemulsions.pdf*, US 5820640, 1998.
- [92] D.C. Elliott, Historical Developments in Hydroprocessing Bio-oils, *Energy & Fuels.* 21 (2007) 1792–1815. doi:10.1021/ef070044u.
- [93] J. Wildschut, F.H. Mahfud, R.H. Venderbosch, H.J. Heeres, Hydrotreatment of fast pyrolysis oil using heterogeneous noble-metal catalysts, *Ind. Eng. Chem. Res.* 48 (2009) 10324–10334. doi:10.1021/ie9006003.
- [94] Q. Zhang, J. Chang, T. Wang, Y. Xu, Review of biomass pyrolysis oil properties and upgrading research, *Energy Convers. Manag.* 48 (2007) 87–92. doi:10.1016/j.enconman.2006.05.010.
- [95] A. V. Bridgwater, Review of fast pyrolysis of biomass and product upgrading, *Biomass and Bioenergy.* 38 (2012) 68–94. doi:10.1016/j.biombioe.2011.01.048.
- [96] Y. Yang, A. Gilbert, C. (Charles) Xu, Hydrodeoxygenation of bio-crude in supercritical hexane with sulfided CoMo and CoMoP catalysts supported on MgO: A model compound study using phenol, *Appl. Catal. A Gen.* 360 (2009) 242–249. doi:10.1016/j.apcata.2009.03.027.

Chapter 6: Reference

- [97] B.K. Sharma, A. Adhvaryu, J.M. Perez, S.Z. Erhan, Effects of hydroprocessing on structure and properties of base oils using NMR, *Fuel Process. Technol.* 89 (2008) 984–991. doi:10.1016/j.fuproc.2008.04.001.
- [98] C.J. Chuck, J. Donnelly, The compatibility of potential bioderived fuels with Jet A-1 aviation kerosene, *Appl. Energy.* 118 (2014) 83–91. doi:10.1016/j.apenergy.2013.12.019.
- [99] M.Á. González-Borja, D.E. Resasco, Anisole and Guaiacol Hydrodeoxygenation over Monolithic Pt–Sn Catalysts, *Energy & Fuels.* 25 (2011) 4155–4162. doi:10.1021/ef200728r.
- [100] X. Zhu, L.L. Lobban, R.G. Mallinson, D.E. Resasco, Bifunctional transalkylation and hydrodeoxygenation of anisole over a Pt/HBeta catalyst, *J. Catal.* 281 (2011) 21–29. doi:10.1016/j.jcat.2011.03.030.
- [101] M.J. Girgis, B.C. Gates, Reactivities, reaction networks, and kinetics in high-pressure catalytic hydroprocessing, *Ind. Eng. Chem. Res.* 30 (1991) 2021–2058. doi:10.1021/ie00057a001.
- [102] N. Yan, C. Zhao, P.J. Dyson, C. Wang, L.T. Liu, Y. Kou, Selective degradation of wood lignin over noble-metal catalysts in a two-step process, *ChemSusChem.* 1 (2008) 626–629. doi:10.1002/cssc.200800080.
- [103] N. Yan, Yuan, R. Dykeman, Y. Kou, P.J. Dyson, Hydrodeoxygenation of lignin-derived phenols into alkanes by using nanoparticle catalysts combined with Brønsted acidic ionic liquids, *Angew. Chemie - Int. Ed.* 49 (2010) 5549–5553. doi:10.1002/anie.201001531.
- [104] E.G.B. Douglas C. Elliott, process for upgrading biomass pyrolyzates, US 4795841, 1989.
- [105] F. Edward, Catalytic hydrodeoxygenation, *Appl. Catal. A Gen.* 199 (2000) 147–190. doi:10.1016/s0926-860x(99)00555-4.

Chapter 6: Reference

- [106] D.C. Elliott, T.R. Hart, Catalytic Hydroprocessing of Chemical Models for Bio-oil, *Energy & Fuels*. 23 (2009) 631–637. doi:10.1021/ef8007773.
- [107] C. Montassier, J.C. Ménézo, L.C. Hoang, C. Renaud, J. Barbier, Aqueous polyol conversions on ruthenium and on sulfur-modified ruthenium, *J. Mol. Catal.* 70 (1991) 99–110. doi:https://doi.org/10.1016/0304-5102(91)85008-P.
- [108] D.C. Elliott, T.R. Hart, G.G. Neuenschwander, L.J. Rotness, M. V. Olarte, A.H. Zacher, Y. Solantausta, Catalytic hydroprocessing of fast pyrolysis bio-oil from pine sawdust, *Energy and Fuels*. 26 (2012) 3891–3896. doi:10.1021/ef3004587.
- [109] A. V. Bridgwater, Production of high grade fuels and chemicals from catalytic pyrolysis of biomass, *Catal. Today*. 29 (1996) 285–295. doi:10.1016/0920-5861(95)00294-4.
- [110] D.C. Elliott, E.G. Baker, Hydrotreating biomass liquids to produce hydrocarbon fuels, in: *United States*, 1987: pp. 765–784. <https://www.osti.gov/servlets/purl/5664873>.
- [111] S. Bezergianni, A. Kalogianni, I.A. Vasalos, Hydrocracking of vacuum gas oil-vegetable oil mixtures for biofuels production, *Bioresour. Technol.* 100 (2009) 3036–3042. doi:10.1016/j.biortech.2009.01.018.
- [112] E. Furimsky, Deactivation of hydroprocessing catalysts, *Catal. Today*. 52 (1999) 381–495. doi:10.1016/s0920-5861(99)00096-6.
- [113] A. Centeno, E. Laurent, B. Delmon, Influence of the Support of CoMo Sulfide Catalysts and of the Addition of Potassium and Platinum on the Catalytic Performances for the Hydrodeoxygenation of Carbonyl, Carboxyl, and Guaiacol-Type Molecules, *J. Catal.* 154 (1995) 288–298. doi:https://doi.org/10.1006/jcat.1995.1170.

Chapter 6: Reference

- [114] and H.J.H. J. Wildschut, J. Arentz, C.B. Rasrendra, R.H. Venderbosch, Catalytic Hydrotreatment of Fast Pyrolysis Oil: Model Studies on Reaction Pathways for the Carbohydrate Fraction, Dep. Chem. Eng. Fac. Chem. Nat. Resour. Eng. Univ. Teknol. Malaysia. 28 (2009) 450–460. doi:10.1002/ep.
- [115] E. Er, A. V Bridgwater, applied catalysis A Catalysis in thermal biomass conversion, Chem. Eng. 116 (1994) 5–47.
- [116] E. Furimsky, Selection of catalysts and reactors for hydroprocessing, Appl. Catal. A Gen. 171 (1998) 177–206. doi:10.1016/S0926-860X(98)00086-6.
- [117] J.W. Shabaker, G.W. Huber, R.R. Davda, R.D. Cortright, J.A. Dumesic, University of Massachusetts - Amherst Aqueous-Phase Reforming of Ethylene Glycol Over Supported Platinum Catalysts, Catal. Letters. 88 (2003) 1–8. doi:10.1023/A:1023538917186.
- [118] J.W. Shabaker, J.A. Dumesic, Kinetics of Aqueous-Phase Reforming of Oxygenated Hydrocarbons: Pt/Al₂O₃ and Sn-Modified Ni Catalysts, Ind. Eng. Chem. Res. 43 (2004) 3105–3112. doi:10.1021/ie049852o.
- [119] R.R. Davda, J.W. Shabaker, G.W. Huber, R.D. Cortright, J.A. Dumesic, A review of catalytic issues and process conditions for renewable hydrogen and alkanes by aqueous-phase reforming of oxygenated hydrocarbons over supported metal catalysts, Appl. Catal. B Environ. 56 (2005) 171–186. doi:10.1016/j.apcatb.2004.04.027.
- [120] G.W. Huber, J.A. Dumesic, An overview of aqueous-phase catalytic processes for production of hydrogen and alkanes in a biorefinery, Catal. Today. 111 (2006) 119–132. doi:10.1016/j.cattod.2005.10.010.
- [121] R.D. Cortright, R.R. Davda, J.A. Dumesic, Hydrogen from catalytic reforming of biomass-derived hydrocarbons in liquid water, Nature. 418 (2002) 964–967. doi:10.1038/nature01009.

Chapter 6: Reference

- [122] P. Rani, R. Srivastava, Cu(I) metal organic framework catalyzed C-C and C-N coupling reactions, *Tetrahedron Lett.* 55 (2014) 5256–5260.
doi:10.1016/j.tetlet.2014.07.118.
- [123] M.K. Poddar, M. Anand, S.A. Farooqui, G.J.O. Martin, M.R. Maurya, A.K. Sinha, Hydroprocessing of lipids extracted from marine microalgae *Nannochloropsis* sp. over sulfided CoMoP/Al₂O₃ catalyst, *Biomass and Bioenergy*. 119 (2018) 31–36.
doi:10.1016/j.biombioe.2018.08.011.
- [124] R. Lødeng, O. Lunder, J.E. Lein, P.I. Dahl, I.H. Svenum, Synthesis of light olefins and alkanes on supported iron oxide catalysts, *Catal. Today*. 299 (2018) 47–59.
doi:10.1016/j.cattod.2017.06.039.
- [125] L. Boda, G. Onyestyák, H. Solt, F. Lónyi, J. Valyon, A. Thernesz, Catalytic hydroconversion of tricaprylin and caprylic acid as model reaction for biofuel production from triglycerides, *Appl. Catal. A Gen.* 374 (2010) 158–169.
doi:10.1016/j.apcata.2009.12.005.
- [126] C. Ranga, R. Lødeng, V.I. Alexiadis, T. Rajkhowa, H. Bjørkan, S. Chytil, I.H. Svenum, J. Walmsley, C. Detavernier, H. Poelman, P. Van Der Voort, J.W. Thybaut, Effect of composition and preparation of supported MoO₃ catalysts for anisole hydrodeoxygenation, *Chem. Eng. J.* 335 (2018) 120–132.
doi:10.1016/j.cej.2017.10.090.
- [127] D. Kim, D.R. Vardon, D. Murali, B.K. Sharma, T.J. Strathmann, Valorization of Waste Lipids through Hydrothermal Catalytic Conversion to Liquid Hydrocarbon Fuels with in Situ Hydrogen Production, *ACS Sustain. Chem. Eng.* 4 (2016) 1775–1784. doi:10.1021/acssuschemeng.5b01768.
- [128] S.R. Jagtap, V.P. Raje, S.D. Samant, B.M. Bhanage, Silica supported polyvinyl pyridine as a highly active heterogeneous base catalyst for the synthesis of cyclic carbonates from carbon dioxide and epoxides, *J. Mol. Catal. A Chem.* 266 (2007) 69–74. doi:10.1016/j.molcata.2006.10.033.

Chapter 6: Reference

- [129] G.G.N. D. C. Elliott, Liquid Fuels by Low-severity Hydrotreating of Biocrude, Dev. Thermochem. Biomass Convers. 1 (1996) 611–621.
- [130] S.B. Jones, C. Valkenburg, C.W. Walton, D.C. Elliott, J.E. Holladay, D.J. Stevens, C. Kinchin, S. Czernik, Production of Gasoline and Diesel from Biomass via Fast Pyrolysis, Hydrotreating and Hydrocracking : A Design Case, in: Energy, Pacific Northwest National Laboratory Richland, Washington 99352 1, 2009: p. 76.
<http://citeseerx.ist.psu.edu/viewdoc/summary?doi=10.1.1.161.1652>.
- [131] A.A. Herod, R. Kandiyoti, A. Megaritis, R. V. Pindoria, A two-stage fixed-bed reactor for direct hydrotreatment of volatiles from the hydrolysis of biomass: effect of catalyst temperature, pressure and catalyst ageing time on product characteristics, Fuel. 77 (1998) 1715–1726. <http://kth.diva-portal.org/smash/searchref.jsf?pid=diva2:8797&searchId=null>.
- [132] S.A. Jagtap, T. Sasaki, B.M. Bhanage, Silica supported palladium phosphine as a robust and recyclable catalyst for semi-hydrogenation of alkynes using syngas, J. Mol. Catal. A Chem. 414 (2016) 78–86. doi:10.1016/j.molcata.2016.01.004.
- [133] G.W. Huber, P. O'Connor, A. Corma, Processing biomass in conventional oil refineries: Production of high quality diesel by hydrotreating vegetable oils in heavy vacuum oil mixtures, Appl. Catal. A Gen. 329 (2007) 120–129.
doi:10.1016/j.apcata.2007.07.002.
- [134] G. Pérot, Hydrotreating catalysts containing zeolites and related materials - Mechanistic aspects related to deep desulfurization, Catal. Today. 86 (2003) 111–128. doi:10.1016/S0920-5861(03)00407-3.
- [135] D. Zuo, D. Li, H. Nie, Y. Shi, M. Lacroix, M. Vrinat, Acid-base properties of NiW/Al₂O₃ sulfided catalysts: Relationship with hydrogenation, isomerization and hydrodesulfurization reactions, J. Mol. Catal. A Chem. 211 (2004) 179–189.
doi:10.1016/j.molcata.2003.10.018.

Chapter 6: Reference

- [136] J. Speight, A review of: “ Hydrotreating Catalysis Science and Technology ”
Topsoe, H., Clausen, B.S., and Massoth, F.E., Springer-Verlag New York, 1996.
ISBN No. 3-540-60380-8 Price not available at time of review , Fuel Sci. Technol.
Int. 14 (2007) 1465–1465. doi:10.1080/08843759608947653.
- [137] T.G. Kaufmann, A. Kaldor, G.F. Stuntz, M.C. Kerby, L.L. Ansell, Catalysis science
and technology for cleaner transportation fuels, Catal. Today. 62 (2000) 77–90.
doi:10.1016/S0920-5861(00)00410-7.
- [138] B. Kaur, M. Tumma, R. Srivastava, Transition-metal-exchanged nanocrystalline
ZSM-5 and metal-oxide- incorporated SBA-15 catalyzed reduction of nitroaromatics,
Ind. Eng. Chem. Res. 52 (2013) 11479–11487. doi:10.1021/ie401059s.
- [139] S. Bezergianni, A. Kalogianni, A. Dimitriadis, Catalyst evaluation for waste cooking
oil hydroprocessing, Fuel. 93 (2012) 638–641. doi:10.1016/j.fuel.2011.08.053.
- [140] A. Gutierrez, R.K. Kaila, M.L. Honkela, R. Slioor, A.O.I. Krause,
Hydrodeoxygenation of guaiacol on noble metal catalysts, Catal. Today. 147 (2009)
239–246. doi:10.1016/j.cattod.2008.10.037.
- [141] D. Procházková, P. Zámotný, M. Bejblová, L. Červený, J. Čejka,
Hydrodeoxygenation of aldehydes catalyzed by supported palladium catalysts, Appl.
Catal. A Gen. 332 (2007) 56–64. doi:10.1016/j.apcata.2007.08.009.
- [142] T.T. Pham, L.L. Lobban, D.E. Resasco, R.G. Mallinson, Hydrogenation and
Hydrodeoxygenation of 2-methyl-2-pentenal on supported metal catalysts, J. Catal.
266 (2009) 9–14. doi:10.1016/j.jcat.2009.05.009.
- [143] V.M.L. Whiffen, K.J. Smith, Hydrodeoxygenation of 4-Methylphenol over
Unsupported MoP, MoS₂, and MoO_x Catalysts, Energy & Fuels. 24 (2010) 4728–
4737. doi:10.1021/ef901270h.

Chapter 6: Reference

- [144] O.I. Şenol, E.M. Ryymin, T.R. Viljava, A.O.I. Krause, Effect of hydrogen sulphide on the hydrodeoxygenation of aromatic and aliphatic oxygenates on sulphided catalysts, *J. Mol. Catal. A Chem.* 277 (2007) 107–112.
doi:10.1016/j.molcata.2007.07.033.
- [145] C. V. Loricera, B. Pawelec, A. Infantes-Molina, M.C. Álvarez-Galván, R. Huirache-Acuña, R. Nava, J.L.G. Fierro, Hydrogenolysis of anisole over mesoporous sulfided CoMoW/SBA-15(16) catalysts, *Catal. Today.* 172 (2011) 103–110.
doi:10.1016/j.cattod.2011.02.037.
- [146] V.N. Bui, D. Laurenti, P. Afanasiev, C. Geantet, Hydrodeoxygenation of guaiacol with CoMo catalysts. Part I: Promoting effect of cobalt on HDO selectivity and activity, *Appl. Catal. B Environ.* 101 (2011) 239–245.
doi:10.1016/j.apcatb.2010.10.025.
- [147] B.S. Gevert, J.-E. Otterstedt, F.E. Massoth, Kinetics of the HDO of methyl-substituted phenols, *Appl. Catal.* 31 (1987) 119–131.
doi:https://doi.org/10.1016/S0166-9834(00)80671-5.
- [148] G. de la Puente, A. Gil, J.J. Pis, P. Grange, Effects of Support Surface Chemistry in Hydrodeoxygenation Reactions over CoMo/Activated Carbon Sulfided Catalysts, *Langmuir.* 15 (1999) 5800–5806. doi:10.1021/la981225e.
- [149] V.N. Bui, D. Laurenti, P. Delichère, C. Geantet, Hydrodeoxygenation of guaiacol, *Appl. Catal. B Environ.* 101 (2011) 246–255. doi:10.1016/j.apcatb.2010.10.031.
- [150] A.L. Jongerius, R. Jastrzebski, P.C.A. Bruijninx, B.M. Weckhuysen, CoMo sulfide-catalyzed hydrodeoxygenation of lignin model compounds: An extended reaction network for the conversion of monomeric and dimeric substrates, *J. Catal.* 285 (2012) 315–323. doi:10.1016/j.jcat.2011.10.006.

Chapter 6: Reference

- [151] P.E. Ruiz, B.G. Frederick, W.J. De Sisto, R.N. Austin, L.R. Radovic, K. Leiva, R. García, N. Escalona, M.C. Wheeler, Guaiacol hydrodeoxygenation on MoS₂ catalysts: Influence of activated carbon supports, *Catal. Commun.* 27 (2012) 44–48. doi:10.1016/j.catcom.2012.06.021.
- [152] S. Boullosa-Eiras, R. Lødeng, H. Bergem, M. Stöcker, L. Hannevold, E.A. Blekkan, Catalytic hydrodeoxygenation (HDO) of phenol over supported molybdenum carbide, nitride, phosphide and oxide catalysts, *Catal. Today.* 223 (2014) 44–53. doi:10.1016/j.cattod.2013.09.044.
- [153] V.N. Bui, G. Toussaint, D. Laurenti, C. Mirodatos, C. Geantet, Co-processing of pyrolysis bio oils and gas oil for new generation of bio-fuels: Hydrodeoxygenation of guaiacol and SRGO mixed feed, *Catal. Today.* 143 (2009) 172–178. doi:10.1016/j.cattod.2008.11.024.
- [154] T.-R. Viljava, A.O.I. Krause, Hydrotreating of compounds and mixtures of compounds having mercapto and hydroxyl groups, (2007) 343–352. doi:10.1016/s0167-2991(97)80032-8.
- [155] E.-M. Turpeinen, Hydrodeoxygenation of methyl heptanoate NiMo and CoMo sulphided supported and phenol over catalysts, University of Groningen the Netherlands, 2011.
- [156] Y.-C. Lin, C.-L. Li, H.-P. Wan, H.-T. Lee, C.-F. Liu, Catalytic Hydrodeoxygenation of Guaiacol on Rh-Based and Sulfided CoMo and NiMo Catalysts, *Energy & Fuels.* 25 (2011) 890–896. doi:10.1021/ef101521z.
- [157] M.K. Huuska, Effect of catalyst composition on the hydrogenolysis of anisole, *Polyhedron.* 5 (1986) 233–236. doi:10.1016/S0277-5387(00)84915-3.
- [158] K. Li, R. Wang, J. Chen, Hydrodeoxygenation of Anisole over Silica-Supported Ni₂P, MoP, and NiMoP Catalysts, *Energy & Fuels.* 25 (2011) 854–863. doi:10.1021/ef101258j.

Chapter 6: Reference

- [159] H.Y. Zhao, D. Li, P. Bui, S.T. Oyama, Hydrodeoxygenation of guaiacol as model compound for pyrolysis oil on transition metal phosphide hydroprocessing catalysts, *Appl. Catal. A Gen.* 391 (2011) 305–310. doi:10.1016/j.apcata.2010.07.039.
- [160] V.M.L. Whiffen, K.J. Smith, S.K. Straus, The influence of citric acid on the synthesis and activity of high surface area MoP for the hydrodeoxygenation of 4-methylphenol, *Appl. Catal. A Gen.* 419–420 (2012) 111–125. doi:10.1016/j.apcata.2012.01.018.
- [161] G.W. Huber, A. Corma, Synergies between bio- and oil refineries for the production of fuels from biomass, *Angew. Chemie - Int. Ed.* 46 (2007) 7184–7201. doi:10.1002/anie.200604504.
- [162] Furimsky E, Metal carbides and nitrides as potential catalysts for hydroprocessing, *Appl. Catal. A Gen.* 240 (2003) 1–28. doi:10.1016/S0926-860X(02)00428-3.
- [163] W. Zhang, Y. Zhang, L. Zhao, W. Wei, Catalytic Activities of NiMo Carbide Supported on SiO₂ for the Hydrodeoxygenation of Ethyl Benzoate, Acetone, and Acetaldehyde, *Energy & Fuels.* 24 (2010) 2052–2059. doi:10.1021/ef901222z.
- [164] B. Diaz, S.J. Sawhill, D.H. Bale, R. Main, D.C. Phillips, S. Korlann, R. Self, M.E. Bussell, Hydrodesulfurization over supported monometallic, bimetallic and promoted carbide and nitride catalysts, *Catal. Today.* 86 (2003) 191–209. doi:10.1016/S0920-5861(03)00411-5.
- [165] S. Ramanathan, S.T. Oyama, New Catalysts for Hydroprocessing: Transition Metal Carbides and Nitrides, *J. Phys. Chem.* 99 (1995) 16365–16372. doi:10.1021/j100044a025.
- [166] H.J.M. Bosman, E.C. Kruissink, J. Vanderspoel, F. Vandenbrink, Characterization of the Acid Strength of SiO₂-ZrO₂ Mixed Oxides, *J. Catal.* 148 (1994) 660–672. doi:https://doi.org/10.1006/jcat.1994.1253.

Chapter 6: Reference

- [167] W. Suprun, M. Lutecki, R. Gläser, H. Papp, Catalytic activity of bifunctional transition metal oxide containing phosphated alumina catalysts in the dehydration of glycerol, *J. Mol. Catal. A Chem.* 342–343 (2011) 91–100.
doi:10.1016/j.molcata.2011.04.020.
- [168] A. Baiker, P. Dollenmeier, M. Glinski, A. Reller, Selective catalytic reduction of nitric oxide with ammonia: II. Monolayers of Vanadia Immobilized on Titania—Silica Mixed Gels, *Appl. Catal.* 35 (1987) 365–380.
doi:https://doi.org/10.1016/S0166-9834(00)82873-0.
- [169] F.E. Massoth, Characterization of Molybdena Catalysts, in: D.D. Eley, H. Pines, P.B. Weisz (Eds.), Academic Press, 1979: pp. 265–310.
doi:https://doi.org/10.1016/S0360-0564(08)60058-9.
- [170] C.R. Lee, J.S. Yoon, Y.W. Suh, J.W. Choi, J.M. Ha, D.J. Suh, Y.K. Park, Catalytic roles of metals and supports on hydrodeoxygenation of lignin monomer guaiacol, *Catal. Commun.* 17 (2012) 54–58. doi:10.1016/j.catcom.2011.10.011.
- [171] B.M. Reddy, A. Khan, Recent advances on TiO₂-ZrO₂ mixed oxides as catalysts and catalyst supports, *Catal. Rev. - Sci. Eng.* 47 (2005) 257–296. doi:10.1081/CR-200057488.
- [172] J. Fling, I. Wang, Dehydrocyclization of C₆C₈ n-paraffins to aromatics over TiO₂ZrO₂ catalysts, *J. Catal.* 130 (1991) 577–587. doi:10.1016/0021-9517(91)90137-S.
- [173] R. Kore, R. Srivastava, B. Satpati, Synthesis of industrially important aromatic and heterocyclic ketones using hierarchical ZSM-5 and Beta zeolites, *Appl. Catal. A Gen.* 493 (2015) 129–141. doi:10.1016/j.apcata.2015.01.002.
- [174] H. Hattori, M. Itoh, K. Tanabe, The nature of active sites on TiO₂ and TiO₂□SiO₂ for the isomerization of butenes, *J. Catal.* 38 (1975) 172–178.
doi:https://doi.org/10.1016/0021-9517(75)90075-5.

Chapter 6: Reference

- [175] L.A. Santillán-Vallejo, J.A. Melo-Banda, A.I. Reyes De La Torre, G. Sandoval-Robles, J.M. Domínguez, A. Montesinos-Castellanos, J.A. De Los Reyes-Heredia, Supported (NiMo,CoMo)-carbide, -nitride phases: Effect of atomic ratios and phosphorus concentration on the HDS of thiophene and dibenzothiophene, *Catal. Today*. 109 (2005) 33–41. doi:10.1016/j.cattod.2005.08.022.
- [176] B.M. Reddy, V.S. Subrahmanyam, Oxygen chemisorption and activity studies on alumina- and carbon-supported hydrodesulphurization catalysts, *Appl. Catal.* 27 (1986) 1–8. doi:https://doi.org/10.1016/S0166-9834(00)81041-6.
- [177] B.M. Reddy, K.V.R. Chary, B.R. Rao, V.S. Subrahmanyam, C.S. Sunandana, N.K. Nag, ESR, oxygen chemisorption and activity studies on MoO₃ □ ZrO₂ catalysts, *Polyhedron*. 5 (1986) 191–194. doi:https://doi.org/10.1016/S0277-5387(00)84907-4.
- [178] S. Tio, B.M. Reddy, B. Chowdhury, P.G. Smirniotis, An XPS study of the dispersion of MoO₃ on, *Appl. Catal.* 211 (2001) 19–30.
- [179] B. Yoosuk, D. Tumnantong, P. Prasassarakich, Amorphous unsupported Ni-Mo sulfide prepared by one step hydrothermal method for phenol hydrodeoxygenation, *Fuel*. 91 (2012) 246–252. doi:10.1016/j.fuel.2011.08.001.
- [180] S.J. Miller, production of biofuels and biolubricants from a common feedstock, US20090084026A1, 2009.
- [181] Y.H.E. Sheu, R.G. Anthony, E.J. Soltes, Kinetic studies of upgrading pine pyrolytic oil by hydrotreatment, *Fuel Process. Technol.* 19 (1988) 31–50. doi:10.1016/0378-3820(88)90084-7.
- [182] D. Otyuskaya, J.W. Thybaut, R. Lødeng, G.B. Marin, Anisole Hydrotreatment Kinetics on CoMo Catalyst in the Absence of Sulfur: Experimental Investigation and Model Construction, *Energy and Fuels*. 31 (2017) 7082–7092. doi:10.1021/acs.energyfuels.7b00519.

Chapter 6: Reference

- [183] F. de Miguel Mercader, M.J. Groeneveld, S.R.A. Kersten, N.W.J. Way, C.J. Schaverien, J.A. Hogendoorn, Production of advanced biofuels: Co-processing of upgraded pyrolysis oil in standard refinery units, *Appl. Catal. B Environ.* 96 (2010) 57–66. doi:10.1016/j.apcatb.2010.01.033.
- [184] F.K.Ã. Forson, E.K. Oduro, Performance of jatropha oil blends in a diesel engine, 29 (2004) 1135–1145. doi:10.1016/j.renene.2003.11.002.
- [185] D.C. Elliott, E.G. Baker, Upgrading Biomass Liquefaction Products Through Hydrodeoxygenation, in: Pacific Northwest Laboratory, 1984. <https://books.google.co.in/books?id=IEqEGwAACAAJ>.
- [186] F. de Miguel Mercader, M.J. Groeneveld, S.R.A. Kersten, N.W.J. Way, C.J. Schaverien, J.A. Hogendoorn, Production of advanced biofuels: Co-processing of upgraded pyrolysis oil in standard refinery units, *Appl. Catal. B Environ.* 96 (2010) 57–66. doi:<https://doi.org/10.1016/j.apcatb.2010.01.033>.
- [187] J.N. Chheda, G.W. Huber, J.A. Dumesic, Liquid-phase catalytic processing of biomass-derived oxygenated hydrocarbons to fuels and chemicals, *Angew. Chemie - Int. Ed.* 46 (2007) 7164–7183. doi:10.1002/anie.200604274.
- [188] S. V. Efremova, Y.M. Korolev, Y.I. Sukharnikov, X-ray diffraction characterization of silicon-carbon nanocomposites produced from rice husk and its derivatives, *Dokl. Chem.* 419 (2008) 78–81. doi:10.1007/s10631-008-3009-1.
- [189] B. Chen, E.J. Johnson, B. Chefetz, L. Zhu, B. Xing, Sorption of Polar and Nonpolar Aromatic Organic Contaminants by Plant Cuticular Materials: Role of Polarity and Accessibility, *Environ. Sci. Technol.* 39 (2005) 6138–6146. doi:10.1021/es050622q.
- [190] R.M. Bustin, Y. Guo, Abrupt changes (jumps) in reflectance values and chemical compositions of artificial charcoals and inertinite in coals, *Int. J. Coal Geol.* 38 (1999) 237–260. doi:[https://doi.org/10.1016/S0166-5162\(98\)00025-1](https://doi.org/10.1016/S0166-5162(98)00025-1).

Chapter 6: Reference

- [191] Y. Chun, G. Sheng, C.T. Chiou, B. Xing, Compositions and Sorptive Properties of Crop Residue-Derived Chars, *Environ. Sci. Technol.* 38 (2004) 4649–4655. doi:10.1021/es035034w.
- [192] M.R. Hajaligol, P.A. Martoglio Smith, J.B. Wooten, V. Baliga, Characterization of Char from Pyrolysis of Chlorogenic Acid, *Energy & Fuels.* 14 (2000) 1083–1093. doi:10.1021/ef000058z.
- [193] P. Fu, S. Hu, J. Xiang, L. Sun, P. Li, J. Zhang, C. Zheng, Pyrolysis of Maize Stalk on the Characterization of Chars Formed under Different Devolatilization Conditions, *Energy & Fuels.* 23 (2009) 4605–4611. doi:10.1021/ef900268y.
- [194] B.S. Rana, R. Kumar, R. Tiwari, R. Kumar, R.K. Joshi, M.O. Garg, A.K. Sinha, Transportation fuels from co-processing of waste vegetable oil and gas oil mixtures, *Biomass and Bioenergy.* 56 (2013) 43–52. doi:10.1016/j.biombioe.2013.04.029.
- [195] G. Li, W. Li, M. Zhang, K. Tao, Morphology and hydrodesulfurization activity of CoMo sulfide supported on amorphous ZrO₂ nanoparticles combined with Al₂O₃, *Appl. Catal. A Gen.* 273 (2004) 233–238. doi:https://doi.org/10.1016/j.apcata.2004.06.038.
- [196] R. de Back, F. Croonenberghs, P. Grange, Influence of phosphorus on the preparation of CoMO/Al₂O₃ hydrotreating catalysts, Elsevier Masson SAS, 2007. doi:10.1016/s0167-2991(98)80218-8.
- [197] M. Gholizadeh, R. Gunawan, X. Hu, F. de Miguel Mercader, R. Westerhof, W. Chaitwat, M.M. Hasan, D. Mourant, C.-Z. Li, Effects of temperature on the hydrotreatment behaviour of pyrolysis bio-oil and coke formation in a continuous hydrotreatment reactor, *Fuel Process. Technol.* 148 (2016) 175–183. doi:https://doi.org/10.1016/j.fuproc.2016.03.002.
- [198] R. Kumar, B.S. Rana, R. Tiwari, D. Verma, R. Kumar, R.K. Joshi, M.O. Garg, A.K. Sinha, Hydroprocessing of jatropha oil and its mixtures with gas oil †, (2010) 2232–2239. doi:10.1039/c0gc00204f.

Chapter 6: Reference

- [199] M. Anand, A.K. Sinha, Temperature-dependent reaction pathways for the anomalous hydrocracking of triglycerides in the presence of sulfided Co-Mo-catalyst, *Bioresour. Technol.* 126 (2012) 148–155. doi:10.1016/j.biortech.2012.08.105.
- [200] M.E. Sánchez, J.A. Menéndez, A. Domínguez, J.J. Pis, O. Martínez, L.F. Calvo, P.L. Bernad, Effect of pyrolysis temperature on the composition of the oils obtained from sewage sludge, *Biomass and Bioenergy*. 33 (2009) 933–940. doi:https://doi.org/10.1016/j.biombioe.2009.02.002.
- [201] A. Demirbas, Progress and recent trends in biofuels, *Prog. Energy Combust. Sci.* 33 (2007) 1–18. doi:https://doi.org/10.1016/j.pecs.2006.06.001.
- [202] A.W. Bhutto, K. Qureshi, R. Abro, K. Harijan, Z. Zhao, A.A. Bazmi, T. Abbas, G. Yu, Progress in the production of biomass-to-liquid biofuels to decarbonize the transport sector-prospects and challenges, *RSC Adv.* 6 (2016) 32140–32170. doi:10.1039/c5ra26459f.
- [203] M. V. Olarte, A.H. Zacher, A.B. Padmaperuma, S.D. Burton, H.M. Job, T.L. Lemmon, M.S. Swita, L.J. Rotness, G.N. Neuenschwander, J.G. Frye, D.C. Elliott, Stabilization of Softwood-Derived Pyrolysis Oils for Continuous Bio-oil Hydroprocessing, *Top. Catal.* 59 (2016) 55–64. doi:10.1007/s11244-015-0505-7.
- [204] F. de Miguel Mercader, M.J. Groeneveld, S.R.A. Kersten, R.H. Venderbosch, J.A. Hogendoorn, Pyrolysis oil upgrading by high pressure thermal treatment, *Fuel*. 89 (2010) 2829–2837. doi:https://doi.org/10.1016/j.fuel.2010.01.026.
- [205] M.C. Samolada, W. Baldauf, I.A. Vasalos, Production of a bio-gasoline by upgrading biomass flash pyrolysis liquids via hydrogen processing and catalytic cracking, *Fuel*. 77 (1998) 1667–1675. doi:https://doi.org/10.1016/S0016-2361(98)00073-8.
- [206] G. Fogassy, N. Thegarid, G. Toussaint, A.C. van Veen, Y. Schuurman, C. Mirodatos, Biomass derived feedstock co-processing with vacuum gas oil for second-generation fuel production in FCC units, *Appl. Catal. B Environ.* 96 (2010) 476–485. doi:https://doi.org/10.1016/j.apcatb.2010.03.008.

Chapter 6: Reference

- [207] D.C. Elliott, H. Wang, M. Rover, L. Whitmer, R. Smith, R. Brown, Hydrocarbon Liquid Production via Catalytic Hydroprocessing of Phenolic Oils Fractionated from Fast Pyrolysis of Red Oak and Corn Stover, *ACS Sustain. Chem. Eng.* 3 (2015) 892–902. doi:10.1021/acssuschemeng.5b00015.
- [208] W. Baldauf, U. Balfanz, M. Rupp, Upgrading of flash pyrolysis oil and utilization in refineries, *Biomass and Bioenergy.* 7 (1994) 237–244. doi:https://doi.org/10.1016/0961-9534(94)00065-2.
- [209] J.E. Otterstedt, S.B. Gevert, S.G. Jääs, P.G. Menon, Fluid catalytic cracking of heavy (residual) oil fractions: a review, *Appl. Catal.* 22 (1986) 159–179. doi:https://doi.org/10.1016/S0166-9834(00)82626-3.
- [210] A.K. Sinha, M. Anand, B.S. Rana, R. Kumar, S.A. Farooqui, M.G. Sibi, R. Kumar, R.K. Joshi, Development of Hydroprocessing Route to Transportation Fuels from Non-Edible Plant-Oils, *Catal. Surv. from Asia.* 17 (2013) 1–13. doi:10.1007/s10563-012-9148-x.
- [211] A.K. Sinha, M.G. Sibi, N. Naidu, S.A. Farooqui, M. Anand, R. Kumar, Process Intensification for Hydroprocessing of Vegetable Oils: Experimental Study, *Ind. Eng. Chem. Res.* 53 (2014) 19062–19070. doi:10.1021/ie502703z.
- [212] A.K. aditya rai Sinha, Intensification of Biobased Processes, n.d.
- [213] G. Escalona, A. Rai, P. Betancourt, A.K. Sinha, Selective poly-aromatics saturation and ring opening during hydroprocessing of light cycle oil over sulfided Ni-Mo/SiO₂-Al₂O₃ catalyst, *Fuel.* 219 (2018) 270–278. doi:10.1016/j.fuel.2018.01.134.
- [214] gloria escalona and anil k sinha aditya rai, mohit anand, saleem faroofui, Hydroprocessing of Light Cycle Oil and Gas Oil Blends over sulfided Ni–Mo/SiO₂–Al₂O₃ Catalyst in Microchannel and Fixed Bed Reactors, 1 (2018) 1–9.
- [215] S.J. Porphy, M.M. Farid, Feasibility Study for Production of Biofuel and Chemicals from Marine Microalgae *Nannochloropsis* sp. Based on Basic Mass and Energy Analysis, *ISRN Renew. Energy.* 2012 (2012) 1–11. doi:10.5402/2012/156824.

Chapter 6: Reference

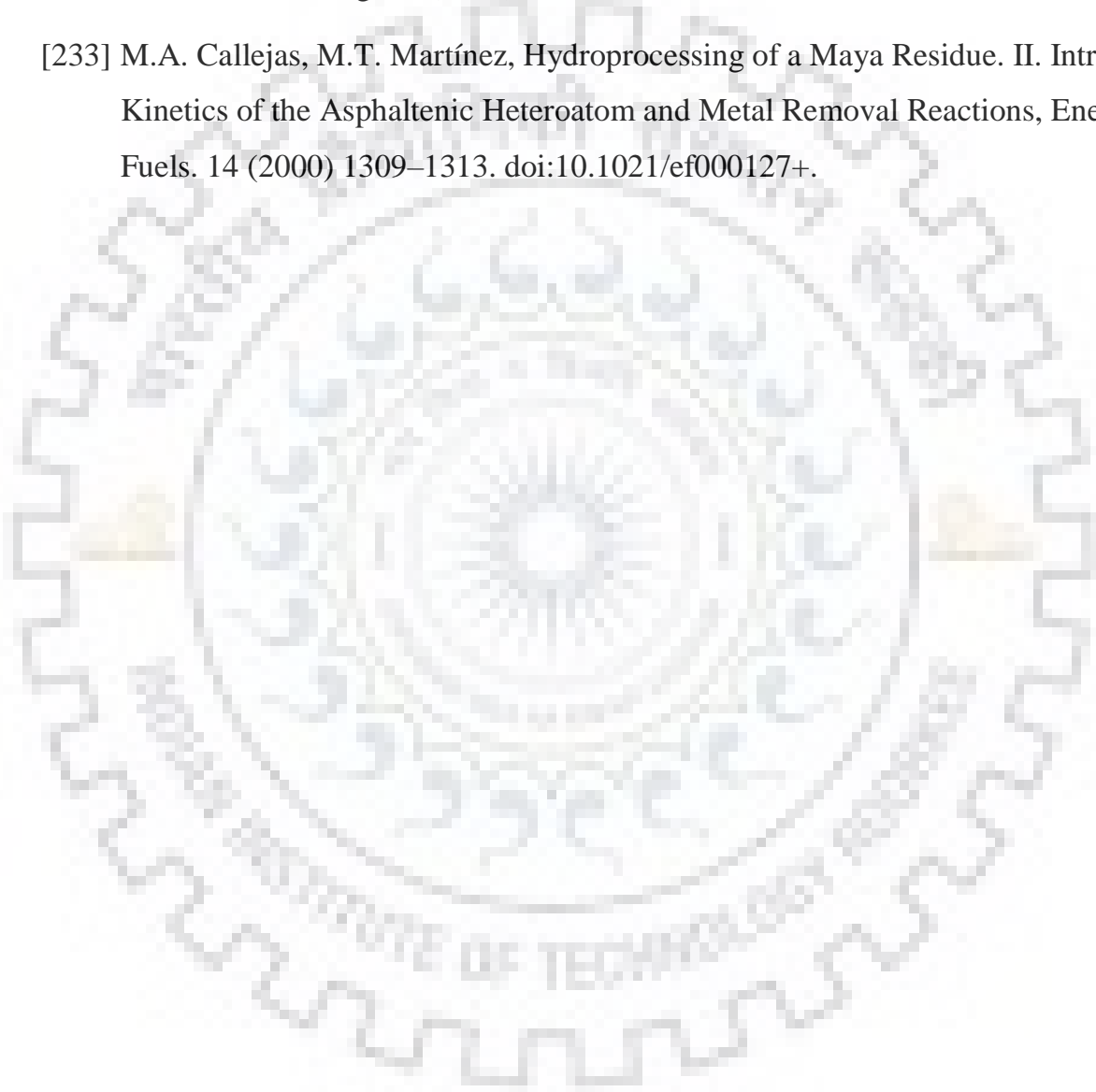
- [216] X. Liu, B. Saydah, P. Eranki, L.M. Colosi, B. Greg Mitchell, J. Rhodes, A.F. Clarens, Pilot-scale data provide enhanced estimates of the life cycle energy and emissions profile of algae biofuels produced via hydrothermal liquefaction, *Bioresour. Technol.* 148 (2013) 163–171. doi:10.1016/j.biortech.2013.08.112.
- [217] D. Zhou, L. Zhang, S. Zhang, H. Fu, J. Chen, Hydrothermal Liquefaction of Macroalgae *Enteromorpha prolifera* to Bio-oil, *Energy & Fuels.* 24 (2010) 4054–4061. doi:10.1021/ef100151h.
- [218] Y. Chisti, Biodiesel from microalgae, *Biotechnol. Adv.* 25. 25 (2007) 294–306.
- [219] J.J. Milledge, B. Smith, P.W. Dyer, P. Harvey, Macroalgae-derived biofuel: A review of methods of energy extraction from seaweed biomass, *Energies.* 7 (2014) 7194–7222. doi:10.3390/en7117194.
- [220] P. Biller, B.K. Sharma, B. Kunwar, A.B. Ross, Hydroprocessing of bio-crude from continuous hydrothermal liquefaction of microalgae, *Fuel.* 159 (2015) 197–205. doi:10.1016/j.fuel.2015.06.077.
- [221] D.C. Elliott, T.R. Hart, A.J. Schmidt, G.G. Neuenschwander, L.J. Rotness, M. V Olarte, A.H. Zacher, K.O. Albrecht, R.T. Hallen, J.E. Holladay, Process development for hydrothermal liquefaction of algae feedstocks in a continuous-flow reactor, *Algal Res.* 2 (2013) 445–454. doi:https://doi.org/10.1016/j.algal.2013.08.005.
- [222] Z. Li, P.E. Savage, Feedstocks for fuels and chemicals from algae: Treatment of crude bio-oil over HZSM-5, *Algal Res.* 2 (2013) 154–163. doi:https://doi.org/10.1016/j.algal.2013.01.003.
- [223] X. Bai, P. Duan, Y. Xu, A. Zhang, P.E. Savage, Hydrothermal catalytic processing of pretreated algal oil: A catalyst screening study, *Fuel.* 120 (2014) 141–149. doi:https://doi.org/10.1016/j.fuel.2013.12.012.

Chapter 6: Reference

- [224] R. Halim, P.A. Webley, G.J.O. Martin, The CIDES process: Fractionation of concentrated microalgal paste for co-production of biofuel, nutraceuticals, and high-grade protein feed, *Algal Res.* 19 (2016) 299–306.
doi:<https://doi.org/10.1016/j.algal.2015.09.018>.
- [225] I.L.D. Olmstead, S.E. Kentish, P.J. Scales, G.J.O. Martin, Low solvent, low temperature method for extracting biodiesel lipids from concentrated microalgal biomass, *Bioresour. Technol.* 148 (2013) 615–619.
doi:[10.1016/j.biortech.2013.09.022](https://doi.org/10.1016/j.biortech.2013.09.022).
- [226] Y. Sakashita, Y. Araki, K. Honna, H. Shimada, Orientation and morphology of molybdenum sulfide catalysts supported on titania particles, observed by using high-resolution electron microscopy, *Appl. Catal. A Gen.* 197 (2000) 247–253.
doi:[https://doi.org/10.1016/S0926-860X\(99\)00488-3](https://doi.org/10.1016/S0926-860X(99)00488-3).
- [227] C. Yang, R. Li, C. Cui, S. Liu, Q. Qiu, Y. Ding, Catalytic hydroprocessing of microalgae-derived biofuels : a review, *Green Chem.* 18 (2016) 3684–3699.
doi:[10.1039/c6gc01239f](https://doi.org/10.1039/c6gc01239f).
- [228] C. Kwak, M.Y. Kim, K. Choi, S.H. Moon, Effect of phosphorus addition on the behavior of CoMoS/Al₂O₃ catalyst in hydrodesulfurization of dibenzothiophene and 4,6-dimethyldibenzothiophene, *Appl. Catal. A Gen.* 185 (1999) 19–27.
doi:[https://doi.org/10.1016/S0926-860X\(99\)00127-1](https://doi.org/10.1016/S0926-860X(99)00127-1).
- [229] J.M. Lewis, R.A. Kydd, The MoO₃-Al₂O₃ interaction: Influence of phosphorus on MoO₃ impregnation and reactivity in thiophene HDS, *J. Catal.* 136 (1992) 478–486.
doi:[https://doi.org/10.1016/0021-9517\(92\)90077-U](https://doi.org/10.1016/0021-9517(92)90077-U).
- [230] C. Stinner, R. Prins, T. Weber, Formation, Structure, and HDN Activity of Unsupported Molybdenum Phosphide, *J. Catal.* 191 (2000) 438–444.
doi:<https://doi.org/10.1006/jcat.1999.2808>.

Chapter 6: Reference

- [231] C. Kwak, M.Y. Kim, K. Choi, S.H. Moon, Effect of phosphorus addition on the behavior of CoMoS / Al₂O₃ catalyst in hydrodesulfurization of dibenzothiophene, 185 (1999) 19–27.
- [232] L.W. Hillen, G. Pollard, L. V Wake, N. White, Hydrocracking of the Oils of, Biotechnol. Bioeng. 24 (1982) 193–205. doi:10.1007/s00253-004-1779-z.
- [233] M.A. Callejas, M.T. Martínez, Hydroprocessing of a Maya Residue. II. Intrinsic Kinetics of the Asphaltenic Heteroatom and Metal Removal Reactions, Energy & Fuels. 14 (2000) 1309–1313. doi:10.1021/ef000127+.



Recommendation

On the basis of the present study, the following recommendations can be made for the future study:

1. It is better to separate the pyrolysis oil into various fractions and then hydroprocess the individual fractions with or without petroleum-derived fractions in refinery units like fluid catalytic cracking (FCC), steam reforming, and hydrocracking unit.
2. Oils/liquid produced from sources other than algae and jatropha seeds cake can also be investigated for hydroprocessing to obtain transportation fuels.
3. Other bimetallic catalyst including noble metal based can also be used for better quality of hydroprocessed liquid.
4. The steam reforming of aqueous fraction of pyrolysis oil unit will be better option for production of hydrogen and the produced hydrogen can be utilized for the refinery process.
5. The lignin-derived monomers or aromatic fraction of pyrolysis oil can be cracked in hydrocracking unit along with petroleum-derived fractions.
6. It is very much essential to develop the specific catalysts for the processing of biomass derived oil in refinery units like FCC, steam reforming and hydrocracking unit.



CrossMark
click for updates

Cite this: *RSC Adv.*, 2016, 6, 113720

Co-processing of bio-oil from de-oiled *Jatropha curcas* seed cake with refinery gas–oil over sulfided CoMoP/Al₂O₃ catalyst†

Mukesh Kumar Poddar,^{ab} Aditya Rai,^a Mannar Ram Maurya^b and Anil Kumar Sinha^{*a}

A sulfided cobalt–molybdenum–phosphorus/aluminium oxide (CoMoP/Al₂O₃) catalyst was studied in the hydroprocessing of bio-oil (BO) obtained from the pyrolysis of de-oiled *Jatropha curcas* seed cake. Hydroprocessing was carried out with different ratios of refinery gas oil (GO) and BO. The oxygen content in the products was reduced to trace amounts after hydroprocessing. A clear product obtained from the co-processing of BO with refinery GO contained 2–16% gasoline, 30–35% kerosene, 35–44% diesel, with 50–60% alkanes, 10–45% cycloalkanes, and 1–10% aromatics, with a negligible amount of char formed in the process. Hydroprocessing of 100% BO produced 30% kerosene and 30% diesel, together with 10% gasoline, with 15% of alkanes and 15% cycloalkanes, and 45% aromatics. A maximum amount of kerosene (41%) was obtained at 648 K and 75 bar from 100% BO, with a small amount of char (1.5%) deposited on the catalyst. In comparison, over sulfided CoMo/Al₂O₃ catalyst (without P promoter) only 31% of kerosene was produced, with 17% char, using similar reaction conditions.

Received 19th August 2016
Accepted 16th November 2016

DOI: 10.1039/c6ra20893b

www.rsc.org/advances

1. Introduction

Liquid transportation fuels (hydrocarbons) from biomass are renewable alternatives to the current fossil derived fuels. Diverse technologies have been investigated for the conversion of biomass into liquid fuels, such as biodiesel from plant oils and bio-ethanol from carbohydrate rich resources.¹ Because of the food *versus* fuel issues, these first generation biofuels were not encouraged and new options are being developed.¹ Second generation biofuel platforms are thermochemical biomass conversion routes such as pyrolysis, gasification and hydro-thermal liquefaction of agricultural wastes, forestry wastes and municipal wastes and so on.¹ High abundance, availability and low procurement cost are the advantages for considering biomass as a source. There is great potential for successful deployment of technologies to produce a liquid biofuel from biomass with cost reductions.²

Liquid product yields from the pyrolysis of de-oiled *Jatropha curcas* cake (non-edible) seeds is up to 60–70 wt% and the product (bio-oil; BO) consists of a wide range of functional groups containing oxygenate and heavy compounds with a wide range of molecular weights.^{3,4} Classes of compounds in BO are organic acids, aldehydes, ketones, phenolics and alcohols. The BO required upgrading because as such it was not suitable as

a biofuel for high speed internal combustion engines, because of large amounts of water (up to 30 wt%) and corrosive organic acids (up to 10 wt%) present in it.^{5,6} It also has limited storage stability and undesirable physical properties.

Catalytic BO upgrading presently seems to be a techno-economic process towards production of fuel-like components. A major aim of upgrading BO is to convert the oxygen-rich, high molecular weight components into hydrocarbons that are similar to petroleum-derived fuels (drop-in fuels). Upgrading is done using chemical methods (such as cracking and so on), and physical methods (such as distillation and so on).^{6,7} Catalytic hydrotreatment is considered to be a promising upgrading technology to produce drop-in kind fuels from BO.⁸ This process involves treatment of BO with hydrogen (H₂) in the presence of a heterogeneous catalyst. However, selection of stable and productive catalyst(s) towards refinery products with low coke formation is a great challenge. The primary aim is minimization of the oxygen content and reduction of the chain length by a process called hydroprocessing (catalytic high pressure hydrotreatment or hydrodeoxygenation accompanied by hydrocracking). Hydrodeoxygenation is a chemical conversion that takes place at high H₂ partial pressures (as high as 75–300 bar) and high temperatures (523–723 K) to remove oxygen primarily in the form of water or carbon dioxide (CO₂).^{9,10}

Hydrodeoxygenation of BO gives hydrocarbons and oxygen containing organic compounds in addition to water and CO₂, and the classes of reactions include decarboxylation, hydrogenation, hydrogenolysis, hydrocracking, and dehydration leading to gasoline, kerosene and diesel like products. Research activities on the hydrodeoxygenation of pyrolysis oil started in

^aCSIR-Indian Institute of Petroleum, Dehradun, India. E-mail: asinha@iip.res.in; Tel: +91-135255842

^bIndian Institute of Technology, Roorkee, India

† Electronic supplementary information (ESI) available. See DOI: 10.1039/c6ra20893b

1984 with the pioneering work of Elliott and Baker on commercial hydrodesulfurization (HDS) catalysts, *i.e.*, sulfided nickel–molybdenum/aluminium oxide (NiMo/Al₂O₃) and cobalt–molybdenum (CoMo)/Al₂O₃.⁸ The primary issue interfering with long-term operation of these systems was the fouling of the catalyst bed by carbonaceous deposits. Deactivation of these catalysts as a function of time on stream is reported.^{11–13} Deactivation might be because of the blockage of catalyst pores and active sites, sintering of the active metals, poisoning of the catalyst, structural degradation of the support and active sites, coking, and metal deposition.^{12,14}

This paper reports the production of transportation fuels (gasoline, kerosene and diesel) by processing a heavy, dark viscous liquid (BO) obtained from waste de-oiled *J. curcas* seeds made into a cake, or with refinery streams, by using the economically viable catalyst sulfided cobalt–molybdenum–phosphorus (CoMoP)/Al₂O₃.¹⁵ The advantage of this work is that transportation fuels can be produced by using a single catalyst instead of other expensive multi-catalyst processes such as hydrodeoxygenation with noble metals followed by cracking. It is demonstrated that the optimization of process conditions in this work has resulted in suppression of carbonaceous deposits by minimizing the polynuclear aromatics formation which are the precursors for carbonaceous deposits.

2. Experimental details

2.1 Materials

Cobalt(II) nitrate hexahydrate (Co(NO₃)₂·6H₂O), ammonium molybdate tetrahydrate [(NH₄)₆Mo₇O₂₄·4H₂O] and orthophosphoric acid (85% of aq. H₃PO₄) were obtained from Sigma-Aldrich. The γ -alumina was obtained from Sasol. High-performance liquid chromatography (HPLC) grade water was used as a solvent for synthesis. BO was produced in a tubular reactor (using Swagelok SS 314 tubing) [shown in Fig. S1; ESI[†]]. Gas-oil (GO) was obtained from Mathura Refinery, India.

2.2 Catalyst preparation

The catalyst was prepared using an incipient wet impregnation method. The calculated amount of the Mo metal precursor (NH₄)₆Mo₇O₂₄·4H₂O (1.89 g) in liquid ammonia was added dropwise, with continuous stirring to 7.9 g of dried γ -alumina to obtain the required amount of Mo (16 wt%) loading on the support. Then the calculated amount of Co metal precursor (Co(NO₃)₂·6H₂O, 1.55 g) solution in water was added dropwise with continuous stirring to obtain the required amount of Co (4 wt%). The solution was dried at 393 K for 4 h. After drying, the calculated amount of 85% aq. H₃PO₄ (0.16 g) was added dropwise with continuous stirring to obtain the required amount of P (1 wt%). The sample was dried at 393 K and calcined at 823 K for 6 h (heating rate, 1 K min⁻¹).

2.3 Characterization methods

The surface area of the catalyst was measured using the Brunauer–Emmett–Teller (BET) method with a nitrogen (N₂) adsorption isotherm at 77 K using BELSORP-max Microtrac

(Japan) apparatus. Before analysis the catalyst sample was degassed at 523 K under vacuum. The pore size was calculated from the desorption isotherm using the Barrett, Joyner and Hallender (BJH) method.

Samples for transmission electron microscopy (TEM) were prepared by deposition of the catalyst, suspended in isopropanol, on a copper grid by TEM images were recorded using a Tecnai G2 (FEI) operating at 200 kV. Deposited metals (Co 4%, Mo 16% and P 1%) were determined using an inductively coupled plasma atomic emission spectroscopy method on a PS 3000 UV (DRE) (Teledyne Leeman Labs, Inc., USA).

2.4 Reaction procedure

2.4.1 Pyrolysis. A tubular reactor (inner diameter 7.5 cm and length 85 cm) electrically heated with a furnace around it was used for the pyrolysis of de-oiled *J. curcas* seed cake (10–35 mesh, C: 45.8 wt%, O: 38.2 wt%, H: 6.2 wt%, N: 3.7 wt%), at a temperature of 823 K (heating rate 10 K min⁻¹) and ambient pressure in a N₂ atmosphere. N₂ gas was used to maintain an inert medium in the reaction system, to dilute the pyrolysis vapors formed, to minimize char formation and to prevent further reactions. Biomass (1 kg de-oiled *J. curcas* seed cake) was used for the reaction and N₂ gas (825 ml min⁻¹) was passed continuously through a gas meter and the pyrolysis vapors were carried into a series of two condensers to condense the pyrolysis vapor to obtain the pyrolysis liquid (BO), and the non-condensable gases were vented off. The schematic diagram of the pyrolysis unit is shown in Fig. S1 (ESI[†]). The detailed composition of BO has been reported recently.¹⁶

2.4.2 Sulfidation of catalyst. Catalytic reactions were carried out in a stirred batch reactor (Parr Instrument Company, USA) with a 25 ml vessel made of INCONEL alloy C-276, with a K type thermocouple (calibrated to the accuracy of ± 1 K) in the reactor. Sulfidation of catalysts was carried out in the same reactor prior to the reactions. Sulfidation was done using 2.5 wt% of dimethyl disulfide mixed in refinery GO at a H₂ pressure of 40 bar, by gradually raising the temperature from 373 K to 623 K (10 K min⁻¹) and heating for 13 h.

2.4.3 Catalytic reaction conditions. Bio-oil from de-oiled *J. curcas* seed cake was hydroprocessed, in the same reactor used for sulfidation, in the presence of the sulfided form of the prepared catalyst CoMoP/Al₂O₃. Reaction feed mixtures (BO or mixtures of BO and GO) with 10 wt% of sulfided CoMoP/Al₂O₃ catalyst were used for hydroprocessing. The reaction system containing feed BO or a mixture of BO and GO with sulfided catalyst were purged four times with H₂ and then pressurized to the desired pressure (50 and 75 bar) with H₂. The desired temperature was achieved by heating gradually (10 K min⁻¹). A constant stirring rate of 680 rpm was maintained until completion of the reaction. After cooling down the reaction system, the liquid product was filtered with 0.2 μ m filter paper. The viscous residue which was considered as mixture of unprocessable BO, catalyst and deposited coke (char) was dissolved in tetrahydrofuran, followed by toluene to separate the catalyst from the unreacted feed and deposited hydrocarbon. The amounts of liquid products, char and unprocessable BO

were determined by weighing, and the repeatability of the weighing balance was ± 0.00025 g. The catalyst weight was subtracted from the weight of final solid containing char and catalyst to determine the amount of char formed. The amount of gas formed after the reaction was determined from the difference in the weights of the reaction vessel containing the solid and liquid reaction mixtures, before and after reaction. Errors up to $\pm 5\%$ for liquid products, $\pm 4\%$ for char and $\pm 2\%$ for gas products was observed. The errors are included in the final results.

2.5 Analysis

2.5.1 Gas chromatography. Liquid products were filtered through a cellulose membrane filter (pore size $0.22 \mu\text{m}$) and were then analyzed using gas chromatography (GC). A Varian 3800 GC (Agilent) with a J&W VF-5ms column (Agilent; $30 \text{ m} \times 0.25 \text{ mm}$, $0.25 \mu\text{m}$) and flame ionization detection (FID), was used for the analysis of hydrocarbons. The oven temperature program was $308\text{--}423 \text{ K}$ (3 min^{-1} , hold time: 5 min), $423\text{--}573 \text{ K}$ (12 K min^{-1} , hold time: 5 min), and $573\text{--}593 \text{ K}$ (15 K min^{-1} , hold time: 15 min). The relative yields of various liquid product components were calculated on a relative basis considering the entire range of liquid products formed as 100%. Relative yields have been reported based on the relative amounts of gas, liquid and char produced during co-processing.

As in normal petroleum refinery practice, the product distributions were quantified on the basis of hydrocarbon size (carbon numbers): gasoline ($< \text{C}_9$ hydrocarbons), kerosene ($\text{C}_9\text{--}\text{C}_{14}$ hydrocarbons), diesel ($\text{C}_{15}\text{--}\text{C}_{18}$ hydrocarbons) and heavy oil ($> \text{C}_{18}$ hydrocarbons). Errors up to $\pm 4\%$ were observed, and are included in the final results.

2.5.2 Two-dimensional gas chromatography (GCxGC-MS). A two-dimensional (2D) 7890B GC (Agilent) was used, with flow modulation (Agilent G3440B), FID and single quadrupole mass detector (Agilent 5977A) and 2D GC software from the Zoex Corporation was used to determine the components of the liquid products. The 2D GC was able to group alkanes, cycloalkanes, oxygenates, aromatics and polyaromatics. Two column systems were used to separate various components present in the product. The columns were designated as 1st and 2nd dimension columns. The 1st dimensional column was a proprietary non-polar column (PAC Corporation) with dimensions of $30 \text{ m} \times 320 \text{ mm} \times 0.10 \text{ mm}$, the 2nd dimension column (PAC Corporation) was a proprietary polar column with dimensions $10 \text{ m} \times 250 \text{ mm} \times 0.25 \text{ mm}$. Errors up to $\pm 3\%$ were observed, and are included in the final results.

2.5.3 CHNS analysis. CHNS analysis of the feed, hydro-processed products and the used catalyst containing char was performed using a vario MICRO cube CHNS (elementar) analyzer equipped with a thermal conductivity detector (for CHN) and an infrared detector (for analysis of ppm levels of S) and an XP6 Automated-S Microbalance (Mettler-Toledo) with $0.6\text{--}0.8 \mu\text{g}$ repeatability. The analyses were repeated three times for each sample. For CHN analysis the results with two significant digits after the decimal point were repeatable and thus, were reported accordingly (error was up to 0.5%), whereas for

the S analysis the results with four significant digits were repeatable (with error up to 5%) and were reported accordingly.

2.5.4 Total acid number (TAN). The total acid number (TAN) of the filtered liquid products was determined by the amount of potassium hydroxide (KOH; in mg) that is needed to neutralize the acids in 1 g of oil, using a G20 Potentiometric Titrator (Mettler-Toledo) following the ASTM D664-11a method. Alcoholic KOH was used as titrant and standardization of the titrant was done using a standard solution of potassium hydrogen phthalate. A mixture of toluene, 2-propanol and a small amount of water, in the volume ratio of 500 : 495 : 5 was used as solvent for the titration. For the titration of each sample, a blank titration of the solvent was also done, to obtain the relative TAN value of hydroprocessed BO with respect to the solvent. For each analysis 125 ml of solvent was taken. The weights of samples to be analyzed were 0.25–1.85 g and the repeatability of the weighing balance was ± 0.00025 g. The TAN was determined three times for each sample, and the variation in TAN was ± 1 to $2 \text{ mg}_{\text{KOH}} \text{ g}^{-1}$.

3. Results and discussion

3.1 Catalyst characterization

The surface area (BET) of the catalyst support was $298 \text{ m}^2 \text{ g}^{-1}$ with a pore volume of 0.5 ml g^{-1} and a mean pore size (BJH) of 7 nm. A TEM image of the sulfided $\text{CoMo}/\text{Al}_2\text{O}_3$ catalyst is shown in Fig. 1. The well dispersed, straight and curved CoMo-S nanoslabs of width 1–2 nm and length 20–60 nm can be seen in the TEM micrograph shown in Fig. 1. If the interlayer spacing is taken to be 0.65 nm, the CoMo-S nanoslabs consist of about two to three layers.¹⁷ For the $\text{CoMoS}/\text{Al}_2\text{O}_3$ catalyst, the typical CoMoS particle size is 5–8 nm long.^{17,18} This clearly indicates that the P used during impregnation has resulted in better active metal dispersion with smaller nanoslab sizes.

3.2 Catalytic studies

Elemental analysis (CHN) of the feeds and hydroprocessed products are listed in Table 1. The detailed composition of BO has been reported in the Table S1 (ESI[†]).¹⁶ De-oiled *Jatropha* seed cake contains 3–7% of triglyceride remnants after expeller extraction. The carbon content in the product was increased slightly from 78% to 80% and the H_2 content increased from 12% to 13% when the reaction temperature was increased from

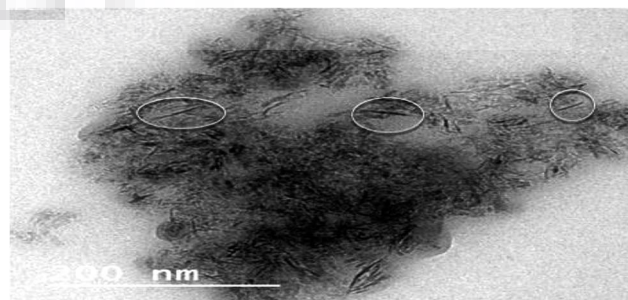


Fig. 1 TEM micrograph of sulfided $\text{CoMoP}/\text{Al}_2\text{O}_3$ catalyst.

Table 1 Elemental analysis of GO, BO and hydroprocessed products [reaction time: 5 h, feed/catalyst ratio: 10 (wt/wt)]

Feed composition		Conditions		Elemental composition		
BO (wt%)	GO (wt%)	Temp. (K)	Pressure (bar)	C (wt%)	H (wt%)	N (wt%)
Reactants						
100	0	—	—	64.5	8.8	6.7
0	100	—	—	76.6	13.3	0.04
Products						
25	75	573	50	78.2	11.8	0.7
25	75	623	50	81.6	12.3	0.9
25	75	648	50	80.0	12.2	0.8
25	75	673	50	81.4	13.1	0.7
50	50	648	50	81.6	12.0	0.9
100	0	648	50	65.6	7.9	3.4

573 K to 673 K for the feed with 25% BO in GO. The nitrogen content was reduced from 7% to 3% for 100% BO hydro-processing and it was reduced further to ~1% for 25% and 50% BO in GO. The remaining 10% and 20% composition in GO and BO, were predominantly O and some S, respectively. The higher O content in GO could be because of oxidation, dissolved oxygen and moisture from prolonged storage under ambient conditions. Sulfur reduction from the feed (2300–2500 ppm S) was 50–80% (down to 400–1000 ppm S) during this co-processing study. In comparison, S removal was 80–90% for catalytic upgraded pristine GO. During the co-processing of oxygenated feeds with GO, deoxygenation reactions do not adversely affect the hydrodesulfurization reactions, as also reported by Rana *et al.*¹⁷ and Tiwari *et al.*¹⁹ The oxygen content in the O was 19% which reduced to trace amounts after hydro-processing of all the feeds.

The product (liquid, solid and gases) distributions (yield%) of the hydroprocessing reactions of the feeds with 25%, 50% and 100% of BO mixed with refinery GO at various temperatures (573–673 K) and feed compositions (25%, 50% and 100% of BO in GO), over CoMoP/Al₂O₃, are given in Fig. 2 and 3, respectively. For the liquid product yields for 25% BO in GO (Fig. 2) at various temperatures and H₂ pressure of 50 bar, a maximum liquid yield (63.4%) was obtained at 673 K, which was reduced to 18.2% at a lower temperature of 573 K. However, little change in the yields of gases with temperature was observed (maximum

23.5% at 673 K and 21.2% at 573 K). Char yield increased monotonously from 0% to 12% as temperature increased from 573 K to 673 K. The liquid yield for pure GO was 85–95%. The unprocessable BO content was very high at a lower reaction temperature of 573 K (~60%) which reduced drastically (2–5%) at higher reaction temperatures (648–673 K). These results indicate that at an intermediate reaction temperature, the undesirable char formation is suppressed but a nearly complete BO conversion is obtained.

Fig. 3 shows the product distributions (char, liquid and gases) for the reaction of feeds of various compositions (25%, 50% and 100% BO in GO) at a temperature of 648 K. A maximum liquid product yield (63.4%) was obtained with 100% BO feed which also gave the maximum char yield (12.2%), whereas the maximum gas yield (40%) were observed for feed with 50% BO in GO. The hydroprocessed product, a transparent liquid, obtained as a phase separate from water, was composed of light and heavy fractions. The product distributions for 25% BO in GO at various temperatures and a of H₂ pressure of 50 bar are shown in Fig. 4. The diesel yield increased with increase of reaction temperature from 573 K to 673 K because of the increasing severity of the reaction which favors cracking of BO components. At a reaction temperature of 673 K, the maximum gasoline (<C₉) (16%) and maximum diesel (C₁₅–C₁₈) (45%) were

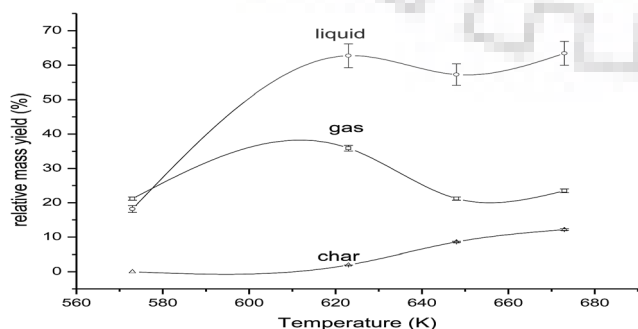


Fig. 2 Yield (%) of the products after reaction of 25% of BO in GO at various temperatures.

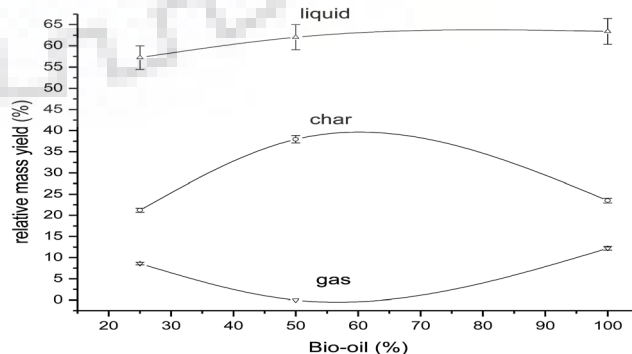


Fig. 3 Yield (%) of products after reaction of feeds with 25%, 50% and 100% of BO in GO at 648 K.

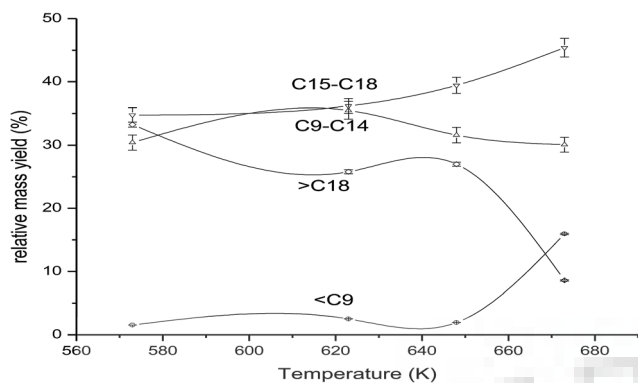


Fig. 4 Distribution of hydrocarbons [O gasoline (<C₉), Δ kerosene (C₉–C₁₄), ∇ diesel (C₁₅–C₁₈), and ◇ heavy residue (>C₁₈)] in the products from feed containing 25% BO in GO at various temperatures and H₂ pressure of 50 bar.

produced, whereas heavy oil (>C₁₈) yield was at its minimum (9%), because of severe cracking conditions.

As the severity of the reaction increased with increase in temperature the diesel yield increased monotonously (because deoxygenation reactions are favored). The longer chain components (>C₁₈) underwent cracking with increasing temperature and thus, their yield decreased monotonously from 33% at 573 K to 9% at 673 K.

Gasoline (<C₉) product yield showed little increase with increasing temperature from 573 K to 648 K. Beyond 648 K there was a rapid increase in gasoline yield from 2% (at 648 K) to 16% (at 673 K) because of increased reaction severity leading to more cracking. In contrast, the heavier products (>C₁₈ hydrocarbons) decreased little with increasing temperature (573–648 K), but there was sharp decrease in yield from 27% at 648 K to 9% at 673 K. These results indicated that at 673 K the heavier hydrocarbons (>C₁₈) crack selectively into the gasoline range (<C₉) hydrocarbons. Maximum aviation kerosene (C₉–C₁₄ hydrocarbons) yield (36%) was obtained at an intermediate temperature of 623 K. At higher temperatures (648–673 K) the kerosene yield decreased by about 5%. For 100% BO hydroprocessing, a high char content after reaction was a major problem (Fig. 3). Higher reaction pressures generally suppress char formation. It was observed that at higher pressures, not only more kerosene (41%) was obtained (at 648 K and 75 bar) from 100% BO but also that char formation was also suppressed (1.5%). These results indicate that it is necessary to operate at higher pressures for hydroprocessing pure BO to obtain desired products and to minimize undesired coking and in order to prolong the catalyst life. In comparison the CoMo/Al₂O₃ catalyst (without P promoter) showed only 31% kerosene and 17% char was obtained at similar reaction conditions. This indicates that P as promoter suppresses char formation and thus, improves the catalyst life. Catalyst life is dependent on char/coke deposition rate. Catalyst deactivation was mainly because of coke deposition over the catalyst. Char/coke formation over the P promoted catalyst was nearly 10 times lower than that over catalyst without P as promoter, which clearly indicates that the P promoted catalyst has better catalyst life. The catalyst modified

by P works in two ways: there is an increase in active sites by enhanced metal dispersion and increase in Brønsted acidity, Mo interacts preferentially with the P–OH groups on P-added γ -alumina and also the other surface hydroxyls become more reactive with Mo in the presence of P.^{20,21} It was also observed that catalysts prepared by impregnating P, on CoMo/Al₂O₃ (co-impregnation) were more active than the P-free catalyst.²² Earlier work on BO hydrotreatment with nickel–molybdenum–sulfur (NiMoS)/Al₂O₃ has reported that at 648–723 K and 70 bar pressure, formation of polynuclear aromatics was rapid which prevented long-term operation under these conditions.^{19,23}

Isomerisation is required to produce aviation kerosene with a desirable freezing point. Table 2 shows that the kerosene range product had high isomer selectivity with isomer and normal alkane ratios (i/n ratio) varying between 1 and 2. The highest iso-alkane yield (i/n = 2) was obtained at the lowest reaction temperature studied (573 K), for 25% BO in GO feed. Even though CoMoP/Al₂O₃ may not have required Brønsted acidity, the high TAN of the feed was expected to catalyze the isomerisation reactions during the hydrocracking of BO, as also reported earlier for the co-processing of oxygenated biomass derived oils with GO over a CoMo/Al₂O₃ catalyst.²⁴

The product yields for reaction of 25%, 50% and 100% BO in GO at 648 K are shown in Fig. 5. The maximum gasoline (<C₉) yield (13%) was obtained from the reaction of 100% BO at 648 K. The major components of BO are short-chain oxygenated compounds, and thus, as expected, the lighter components (<C₉) in the product increase with increasing BO% in the feed. There was little change in the product yields with variation in BO content in GO from 25% to 50%. Increasing BO in GO, from 50 to 100%, caused the diesel content to be reduced to 32% from 40%, whereas the kerosene yield showed little variation, and the gasoline (<C₉) yield increased from 3% to 13%, and the heavy oil components (>C₁₈) reduced slightly from 28% to 25%. These results indicated that pure BO (undiluted with GO) shows a completely different product pattern to the pattern obtained for BO mixed with GO. This may also be correlated with the large differences in the TAN of pure BO (52 mg_{KOH} g⁻¹) and the mixture of BO and GO (12 mg_{KOH} g⁻¹ for the 25% mixture and 23 mg_{KOH} g⁻¹ for the 50% mixture). The higher TAN for pure BO results in more acidity in the reaction mixture which would catalyze the cracking reactions, thus, higher cracked products (gasoline) yield and a lower diesel range hydrocarbons yields are

Table 2 Distribution of normal- (n) and iso- (i) alkanes and i/n ratios in the kerosene range (C₉–C₁₄) hydrocarbons (catalyst: 10 wt%; pressure: 50 bar)

Conditions	Distribution of alkanes in kerosene			
	% of BO (in GO)	n-Alkanes	i-Alkanes	i/n ratio
Temp/K				
573	25	10.95	19.47	2
623	25	18.53	16.97	1
623	50	11.62	11.5	1
648	25	13.16	18.44	1
648	50	12.53	16.94	1
648	100	13.98	16.31	1

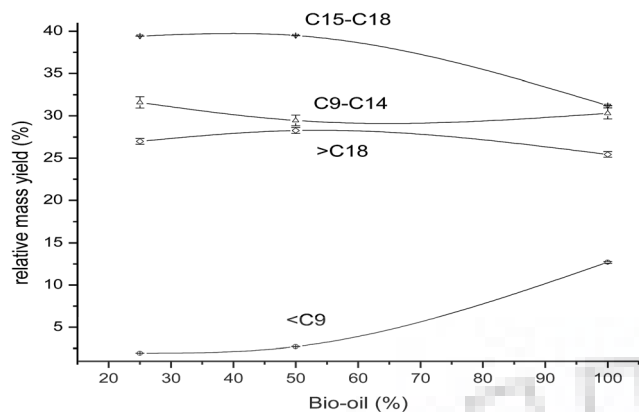


Fig. 5 Distribution of hydrocarbons [\square gasoline ($<C_9$), Δ kerosene (C_9-C_{14}), ∇ diesel ($C_{15}-C_{18}$), and \diamond heavy residue ($>C_{18}$)] in the products from feeds containing 25%, 50% and 100% of BO in GO (at 648 K, H_2 pressure of 50 bar, 10 wt% of catalyst, 5 h).

observed. The higher TAN (acidity) feeds have been reported to show more cracking activity^{15,24} which was clearly correlated to the acidity of the feed, because the catalyst used had a very low acidity.

The distribution of alkanes, cycloalkanes, aromatics and polynuclear aromatics in hydroprocessed products obtained from GCxGC-MS analysis are shown in Fig. 6 and 7. GCxGC-MS analysis showed the absence of any observable oxygenated compounds indicating that there was complete oxygen removal from the BO components during hydroprocessing. Fig. 6 shows the distribution of hydrocarbon type for the feed with 25% of BO in GO at various temperatures and H_2 pressure of 50 bar. The trend for the formation of cycloalkanes showed that the maximum cycloalkane yield (45%) was formed at a temperature of 673 K. The maximum alkane yield (63%) was formed at 648 K and alkane yield at 673 K was minimum (55%). The aromatics yield was zero at 673 K. There was little variation in the yield of various hydrocarbons at temperatures from 573 K to 648 K. Aromatics are thermodynamically controlled product and thus, their yield was minimum at a higher reaction temperature of 673 K. More cracking was

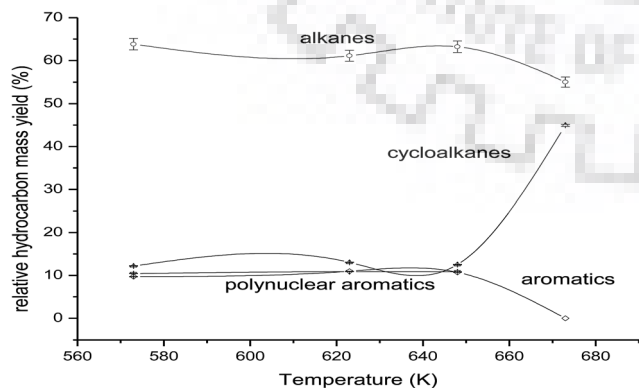


Fig. 6 Distribution of types of hydrocarbon (\square alkanes, Δ cycloalkanes, \diamond aromatics, and ∇ polynuclear aromatics) in hydroprocessed products for the reaction of 25% BO in GO at various temperatures (H_2 pressure of 50 bar, 10 wt% of catalyst, 5 h).

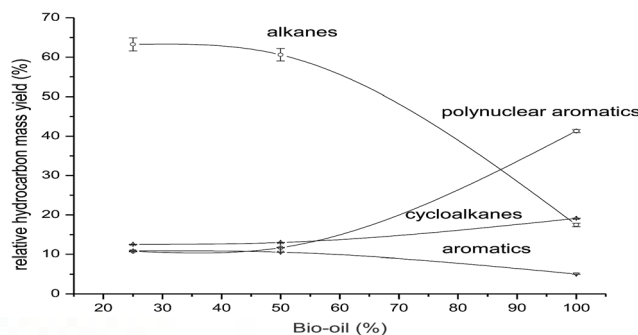


Fig. 7 Distribution of hydrocarbon types (\square alkanes, Δ cycloalkanes, \diamond aromatics, and ∇ polynuclear aromatics) in hydroprocessed products for the reaction of 25%, 50% and 100% of BO in GO (at 648 K (H_2 pressure of 50 bar, 10 wt% of catalyst, 5 h).

favoured at a higher temperature (673 K) and thus, the cycloalkane yield was enhanced whereas the alkane yield was reduced. Lower aromatics and polynuclear aromatics at a higher temperature gives a very useful insight that rapid coking of catalyst at this temperature should be avoided because the precursors for coke (polynuclear aromatics) are completely suppressed. Earlier work has shown that temperature drastically affected the coke formation during hydrotreatment of BOs.²⁴ Increasing temperature favours the polymerisation for the formation of coke. It was found that at a very high temperature (723 K), the coke formation could be so severe that the reactor was blocked.

Fig. 7 shows that for the hydrocarbon types in hydroprocessed products for 25%, 50% and 100% of BO at 648 K, maximum cycloalkane yield was obtained (19%) for 100% of BO, whereas alkane yield was much less (17%) compared to the other feed percentages of BO at that temperature. In fact, the alkane yield decreased rapidly from feed with 50% BO in GO to feed with 100% BO. Surprisingly, although the aromatics yield was lower (5%) with 100% BO feed, with the polynuclear aromatics yield was rapidly enhanced (by nearly four times) compared to the feeds with 25% and 50% BO. These results indicate that polynuclear aromatics formation by condensation reactions are selectively favored for the 100% BO and this is most likely to be because of its high TAN value obtained *via* the Diels–Alder reaction and also *via* secondary reactions of oxygenated compounds such as phenols.²⁵

4. Conclusions

The results indicate that co-hydroprocessing of BO with sulfided CoMoP/ Al_2O_3 catalyst is a promising route for producing transportation fuels. Products obtained from co-processing 25% and 50% of BO with GO contained 2–16% gasoline, 30–35% kerosene, 35–44% diesel, with negligible oxygenates and char. Hydroprocessing of 100% BO at 648 K and a pressure of H_2 of 50 bar produced 10% gasoline, 30% kerosene and 30% diesel with a large amount (40%) of undesirable polynuclear aromatics. But at 75 bar (648 K) for 100% BO, polynuclear aromatics formation was suppressed ($<2\%$) and kerosene yield was maximum (41%), with a very small amount of char (1.5%) formation.

Acknowledgements

The authors would like to thank the Institute Instrumentation Center (IIC) of IIT, Roorkee, India for the TEM analysis. We would also like to thank the Hydroprocessing Laboratory of CSIR-IIP for help with experimental and analytical work.

References

- 1 F. K. Forson, E. K. Oduro and E. Hammond-Donkoh, Performance of *Jatropha* oil blends in a diesel Engine, *Renewable Energy*, 2004, **29**, 1135–1145.
- 2 A. W. Bhutto, K. Qureshi, R. Abro, K. Harijan, Z. Zhao, A. A. Bazmi, T. Abbas and G. Yu, Progress in the production of biomass-to-liquid biofuels to decarbonize the transport sector—prospects and challenges, *RSC Adv.*, 2016, **6**, 32140–32170.
- 3 M. Asadieraghi, W. M. A. W. Daud and H. F. Abbas, Heterogeneous catalysts for advanced bio-fuel production through catalytic biomass pyrolysis vapor upgrading: a review, *RSC Adv.*, 2015, **5**, 22234–32225.
- 4 J. Wildschut, I. Melian-Cabrera and H. J. Heeres, Catalyst studies on the hydrotreatment of fast pyrolysis oil, *Appl. Catal., B*, 2010, **99**, 298–306.
- 5 J. P. A. Diebold, *Chemical and Physical Mechanisms of the Storage Stability of Fast Pyrolysis Bio-Oils: A Review*, Colorado, USA, 2000, NREL/SR-570-27613.
- 6 A. Bridgwater, S. Czernik, J. Diebold, D. Meier, A. Oasmaa and C. Peacocke, *Fast Pyrolysis of Biomass: A Handbook*, CPL Press, Berkshire, 1999, vol. 1.
- 7 D. V. Naik, V. Kumar, B. Prasad and M. K. Poddar, Catalytic cracking of *Jatropha*-derived fast pyrolysis oils with VGO and their NMR characterization, *RSC Adv.*, 2015, **5**, 398–409.
- 8 D. C. Elliott and E. G. Baker, Upgrading biomass liquefaction products through hydrodeoxygenation, *Biotechnol. Bioeng. Symp. Suppl.*, 1984, **14**, 159–174.
- 9 M. F. D. Miguel, M. J. Groeneveld, S. R. A. Kersten, N. W. J. Way, C. J. Schaverien and J. A. Hogendoorn, Production of advanced biofuels: Co-processing of upgraded pyrolysis oil in standard refinery units, *Appl. Catal., B*, 2010, **26**(1–2), 57–66.
- 10 G. Huber and A. Corma, Synergies between bio- and oil refineries for the production of fuels from biomass, *Angew. Chem., Int. Ed. Engl.*, 2007, **46**(38), 7184–7201.
- 11 J. N. Chheda, G. W. Huber and J. A. Dumesic, Liquid-phase catalytic processing of biomass derived oxygenated hydrocarbons to fuels and chemicals, *Angew. Chem., Int. Ed.*, 2007, **46**, 7164–7183.
- 12 E. Furimsky and F. E. Massoth, deactivation of hydroprocessing catalysts, *Catal. Today*, 1999, **52**, 381–495.
- 13 W. Baldauf, U. Balfanz and M. Rupp, Upgrading of Flash Pyrolysis Oil and Utilization in Refineries, *Biomass Bioenergy*, 1994, **7**, 237–244.
- 14 J. E. Otterstedt, S. B. Gevert, S. G. Jaras and P. G. Menon, Fluid Catalytic Cracking of Heavy (residual) Oil Fractions, *Appl. Catal.*, 1986, **22**(2), 159–179.
- 15 M. Anand and A. K. Sinha, Temperature-dependent reaction pathways for the anomalous hydrocracking of triglycerides in the presence of sulfided Co–Mo-catalyst, *Bioresour. Technol.*, 2012, **126**, 148–155.
- 16 P. K. Kanaujia, D. V. Naik, D. Tripathi, R. Singh, M. K. Poddar, L. N. S. K. Konathalaa and Y. K. Sharma, Pyrolysis of *Jatropha* Curcas seed cake followed by optimization of liquid–liquid extraction procedure for the obtained bio-oil, *J. Anal. Appl. Pyrolysis*, 2016, **118**, 202–224.
- 17 B. S. Rana, R. Kumar, R. Tiwari, R. Kumar, R. K. Joshi, M. O. Garg and A. K. Sinha, Transportation fuels from co-processing of waste vegetable oil and gas oil mixtures, *Biomass Bioenergy*, 2013, **56**, 43–52.
- 18 L. Guoran, L. Wei, Z. Minghui and T. Keyi, Morphology and hydrodesulfurization activity of CoMo sulfide supported on amorphous ZrO₂ nanoparticles combined with Al₂O₃, *Appl. Catal., A*, 2004, **273**, 233–238.
- 19 R. Tiwari, B. S. Rana, R. Kumar, D. Verma, R. Kumar, R. K. Joshi, M. O. Garg and A. K. Sinha, Hydrotreating and hydrocracking catalysts for processing of waste soya-oil and refinery-oil mixtures, *Catal. Commun.*, 2011, **12**, 559–562.
- 20 C. Kwak, M. Y. Kim, K. Choi and S. H. Moon, Effect-of-phosphorus-addition-on-the behaviour of CoMoS–Al₂O₃-catalyst-in-hydrodesulfurization-of-dibenzothiophene-and-4,6 dimethyl dibenzothiophene, *Appl. Catal., A*, 1999, **185**, 19–27.
- 21 J. M. Lewis and R. A. Kydd, The MoO₃–Al₂O₃ interaction: influence of phosphorus on MoO₃ impregnation and reactivity in thiophene HDS, *J. Catal.*, 1992, **136**(2), 478–486.
- 22 R. D. Back and F. C. P. Grange, Influence of phosphorus on the preparation of CoMo/Al₂O₃ hydrotreating, *Stud. Surf. Sci. Catal.*, 1998, **118**, 517–531.
- 23 M. Gholizadeh, R. Gunawan, X. Hu, F. D. M. Mercader, R. Westerhof, W. Chaitwat, M. M. Hasan, D. Mourant and C. Z. Li, Effects of temperature on the hydrotreatment behaviour of pyrolysis bio-oil and coke formation in a continuous hydrotreatment reactor, *Fuel Process. Technol.*, 2016, **148**, 175–183.
- 24 R. Kumar, B. S. Rana, R. Tiwari, D. Verma, R. Kumar, R. K. Joshi, M. O. Garg and A. K. Sinha, Hydroprocessing of *Jatropha* oil and its mixtures with gas oil, *Green Chem.*, 2010, **12**, 2232–2239.
- 25 M. E. Sanchez, J. A. Menendez, A. Dominguez, J. J. Pis, O. Martinez, L. F. Calvo and P. L. Bernad, Effect of pyrolysis temperature on the composition of the oils obtained from sewage sludge, *Biomass Bioenergy*, 2009, **33**(6–7), 933–940.

HYDROPROCESSING OF AQUEOUS PHASE OF PYROLYSIS OIL OVER NiMo/Al₂O₃-SiO₂ IN MICROCHANNEL REACTOR

Mukesh K. Poddar,^{1,2} Satyendra Kumar,¹ Pankaj K. Das,¹
Mannar R. Maurya,² & Anil K. Sinha^{1,*}

¹CSIR-Indian Institute of Petroleum, Dehradun, India

²Indian Institute of Technology, Roorkee, India

*Address all correspondence to: Anil K. Sinha, CSIR-Indian Institute of Petroleum, Dehradun, India,
E-mail: asinha@iip.res.in

Original Manuscript Submitted: XX/XX/XXXX; Final Draft Received: XX/XX/XXXX

Sulfided NiMo catalyst supported on mesoporous silica-alumina and coated in a microchannel reactor was studied for the hydroprocessing of aqueous-phase of bio-oil (BO) obtained from pyrolysis of de-oiled jatropha curcas seeds cake (JCC). The oxygen content of the dissolved organic compound in the aqueous phase was reduced to a trace amount after hydroprocessing. A clear organic hydrocarbon phase product obtained after hydroprocessing contained 5%–45% gasoline (< C₉), 5%–60% kerosene (C₉–C₁₄), 15%–40% diesel (> C₁₄), with 15%–65% alkanes, 0%–5% polyaromatic hydrocarbons (PAH), negligible cycloalkanes and aromatics, with 30%–75% unreacted and residues. Maximum hydrocarbon yield (~ 65%) was obtained at 648 K, 0.25 LHSV, and 70 bar, with 35% residues and PAH. The water obtained after hydroprocessing contained few organics (< 5%).

KEY WORDS: jatropha, pyrolysis oil, hydroprocessing, microchannel reactor, catalyst

1. INTRODUCTION

Environmental concerns and increased future demand have shifted the research focus from fossil-derived fuels to other alternatives. Biomass is a suitable alternative due to abundance worldwide, easy availability, renewability, low environmental footprint, and low procurement costs (Demirbas et al., 2007; Bhutto et al., 2016). Thermochemical biomass conversion routes such as pyrolysis, gasification, and hydrothermal liquefaction of agricultural wastes, forestry wastes, and municipal wastes are proposed for alternative technologies (Forson et al., 2004).

The yield of liquid product from pyrolysis of de-oiled jatropha-curcas seeds cake (JCC) is ~ 60–70 wt% and consists of a wide range of functional groups, mostly oxygenates (Wildschut et al., 2010). The bio-oil (BO) has two phases. One is water-soluble aqueous phase (50%–60%), and the other is nonaqueous bio-crude (40%–50%) (Desavath et al., 2015).

A detailed chemical composition, along with the carbon range of aqueous phase bio-oil, were provided in an earlier publication (Pankaj et al., 2016). Aqueous phase oil contains aldehydic and ketonic compounds in major (28%), followed by acids (17%). The minor compounds are guaiacols (10%), phenol (9%), hydrocarbons (8%), furan (7%), alcohols (7%), esters (1%), sugar (1%), and others (12%) of the total organic. Additionally, it contains the nitrogen-containing compounds, mainly alkyl, hydroxyl or carbonyl substituted pyridine, pyrrole, pyrazine, piperidine, and indole.

The bio-oils require upgrading because they are not suitable as a fuel for the internal-combustion engine, due to water and organic acids (Bridgwater et al., 1999; Diebold et al., 2000). They have limited storage stability and also have undesirable physical properties. Several technologies have been used for the upgradation of bio-oil, such as high-pressure thermal treatment, catalytic hydrotreating, catalytic emulsion, and catalytic cracking (Samolada et al., 1998; Fogassy et al., 2010; Mercader et al., 2010a; 2010b; Mariefel, et al., 2016). Catalytic hydroprocessing is also the most

widely used technique in petroleum refining (Desavath et al., 2015). Elliott et al. (2015) studied hydroprocessing of phenolic oils in a two-stage reactor using sulfided CoMo and platinum over carbon catalysts. Platinum (Group VIII) catalysts resulted in more saturated products (Elliott et al., 2015).

The catalytic bio-oil upgrading process produces a hydrocarbon that is similar to petroleum-derived fuels, predominantly by deoxygenation process. The chemical process of cracking results in upgradation and hydrocracking, whereas physical processes lead to liquid–liquid separation and distillation (Bridgwater et al., 1999; Desavath et al., 2015). Catalytic hydrotreatment is a viable upgrading technology to convert bio-oils into transportation fuel (Elliott et al., 1984, 2015; Samolada et al., 1998; Fogassy et al., 2010; Mercader et al., 2010a, 2010b; Mariefel et al., 2016). Bio-oil is treated with H_2 with the presence of a sulfided heterogeneous catalyst (NiMo, CoMo) on the support of gamma-alumina by catalytic hydrotreatment process. Selection of stable economically viable and productive catalyst(s) for refinery hydrocarbons with low coke formation is a great challenge. Minimization of oxygen content and increased H/C ratio with reduction of the chain length by hydroprocessing (catalytic high-pressure hydrotreatment or hydrodeoxygenation accompanied by hydrocracking) is the primary aim. Hydrodeoxygenation is a chemical conversion that takes place at high H_2 partial pressures (as high as 75–250 bar) and high temperatures (523–673 K) to remove oxygen primarily in the form of water (H_2O)/ CO_2 (Huber et al., 2007; Miguel et al., 2010).

The classes of hydrodeoxygenation reactions include decarboxylation, hydrogenation, hydrogenolysis, hydrocracking, and dehydration leading to gasoline, kerosene, and diesel-like products. Deactivation of these catalysts as a function of time on stream is reported (Baldauf et al., 1994; Furimsky et al., 1999; Chheda et al., 2007). Blockage of catalyst pores and active sites, sintering of the active metals, poisoning of the catalyst, structural degradation of the support and active sites, coking and metal deposition cause catalyst deactivation (Otterstedt et al., 1986; Furimsky et al., 1999; Anand et al., 2012).

This report discusses the production of transportation fuels (gasoline, kerosene, and diesel) by hydroprocessing of aqueous-phase of pyrolysis oil obtained from de-oiled jatropha curcas seeds cake (JCC), by using sulfided NiMo/SiO₂-Al₂O₃ catalyst coated in a microchannel reactor. The microchannel reactor has advantages of portability, easy scale-up, better heat and mass transfer characteristics, high reaction throughputs, and precise control of hydrodynamics (Sinha et al., 2013). Transportation fuels can be produced by using small modular microchannel reactors (with catalyst coating inside the channels) rather than using largely fixed bed reactors. Additionally, this process improves the economics of processing bio-oils by utilizing its aqueous phase (containing ~ 30% inseparable soluble organics) to produce hydrocarbon fuels.

2. EXPERIMENTAL DETAILS

2.1 Materials

Ammonium heptamolybdate tetrahydrate ($(NH_4)_6Mo_7O_{24} \cdot 4H_2O$), nickel nitrate hexahydrate ($Ni(NO_3)_2 \cdot 6H_2O$), aluminum isopropoxide, aluminum acetylacetonate, polyvinyl alcohol, dimethyldisulfide (DMDS), nitric acid, and ethyl alcohol were purchased from Aldrich. HPLC grade water (Merck) was used as a solvent for synthesis. Refinery gas oil was used for sulfidation from Mathura Refinery, UP, India. Bio-oil (BO) was produced in a tubular reactor (SS 314) as described earlier (Pankaj et al., 2016; Poddar et al., 2016).

2.2 Catalyst Preparation

The sol-gel method was used to synthesize silica-alumina support. Water and isopropanol (IPA) were mixed in 10:1 molar ratio at 318 K by constant stirring for 15 min. Then, colloidal silica and alumina suspended in isopropanol were added slowly with constant stirring for 45 min at 353 K. Polyvinyl alcohol (PVA) (3%, as a binding agent) was added consecutively, stirring for another 15 min. Mo metal precursor ($(NH_4)_6Mo_7O_{24} \cdot 4H_2O$ (3.31 g) and Ni precursor [$Ni(NO_3)_2 \cdot 6H_2O$, (1.98 g) were added to the above-prepared alumina support solution to obtain a final catalyst composition of 80% SiO₂-Al₂O₃, 18% MoO₃, and 2% NiO (wt %)]. Finally, nitric acid was added drop-wise to peptize/deflocculate the silica-alumina sol, at pH 4 (Sinha et al., 2014). The final solution was stirred continuously for 24 h at 353 K. The catalyst was filtered and dried at 393 K and calcined at 823 K for 6 h (heating rate, 1 K min⁻¹).

2.2.1 Catalyst Coating in the Microchannel Reactor

The 10-plate microchannel reactor was made of stainless steel grade 316 (SS316). Each plate had 28 channels (each channel of size 50 mm × 0.5 mm × 0.25 mm) (Fig. 1). A synthesized catalyst was ball-milled and dispersed in ethanol to obtain the wash-coat solution and coated inside the channels of each plate (with ~ 0.25 mm thickness). Adhesion of the catalyst was tested by the drop test method. The plates were assembled using laser welding (Sinha et al., 2013; 2018). The microchannel plates were pretreated and drop-tested after the catalyst coating to minimize the possibility of catalyst/metal leaching from the plates during the reaction.

2.3 Experimental Setup

The 10 microchannel plates of the microchannel reactor (Fig. 1) were welded together by laser welding. The inlet and outlet of the reactor were welded to SS316 tubes (1/4"). Heating blocks with temperature controller were placed on both sides of the reactor assembly. Thermocouples were used to measure the reaction temperature.

During catalytic experiments, precise control of the operating parameters such as temperature, pressure, and the feed flow rate was maintained using the calibrated equipment. The activities were studied at different temperatures and space velocities. A back pressure regulator was used to control the pressure of the system. The pressure of the reactor was measured using pressure gauges. Mass flow controller (MFC) was used to measure H₂ flow in the reactor. The gas-liquid product mixture from the reactor was separated using a liquid separator.

Sulfidation of catalyst was carried out in the same microchannel reactor before reactions by using 2.5 wt% of dimethyl disulfide (DMDS) mixed in refinery gas oil (GO) at 30 bar of hydrogen pressure by gradually raising the temperature from ambient to 593 K (10 K min⁻¹). The aqueous phase of bio-oil obtained from de-oiled *Jatropha* seed-cakes was filtered and hydroprocessed in the presence of the sulfided form of coated catalyst Ni-Mo(S)/SiO₂-Al₂O₃.

Liquid products were filtered with cellulose membranes (pore size 0.22 μm) before analysis by gas chromatography (GC). A Varian 3800 GC (Agilent) with a J&W VF-5ms column (Agilent: 30 m × 0.25 mm, 0.25 mm) and flame ionization detection (FID) was used for the analysis of hydrocarbons. Errors up to ± 8% were observed and included in the final results. Detailed hydrocarbon in liquid products (paraffins, naphthenes, aromatics, and poly-aromatic hydrocarbon) were analyzed by an Agilent 7890B 2D-GC (GC × GC; first dimension – nonpolar, DB-5 ms column, 30 m × 0.25 mm, 0.25 μm; second dimension polar, PAC column, 5 m × 0.25 mm, 0.15 μm), with FID, MS, capillary flow modulator, and ZOEX software. The relative yields of liquid hydrocarbon component were calculated and the products identified (Table 1). Errors up to ± 5% were observed and included in the final results.

Bio-oil (BO) containing water-soluble aqueous phase and nonaqueous bio-crude was produced in a tubular reactor made up of SS 314 (inner diameter 7.5 cm and length 85 cm) by using slow pyrolysis technology. The pyrolysis reactor was electrically heated by a surrounding furnace, at 823 K temperature (heating rate 10 K/min) and ambient

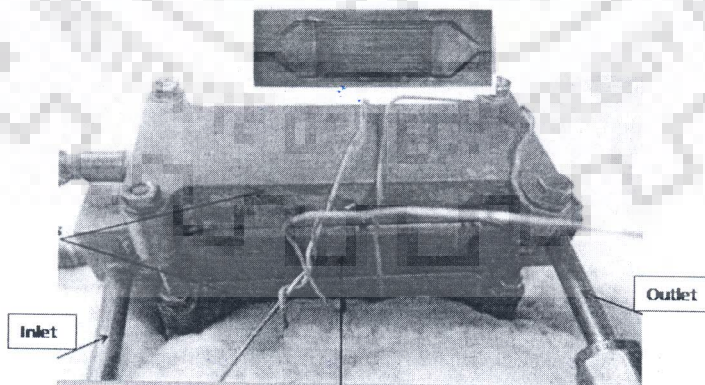


FIG. 1: (Top) Microchannel plate, (bottom) microchannel reactor experimental set-up

TABLE 1: GC-MS result of representative product

Hydrocarbons	R.T.	Area	Pct Max	Pct Total
Hexane: solvent				
Undecane, 5-methyl-	20.559	246462	53.22	2.765
Dodecane	23.707	353987	76.44	3.971
Undecane, 2,8-dimethyl-	26.556	371653	80.25	4.17
Dodecane, 2,6,11-trimethyl-	33.607	288495	62.3	3.237
3,5-Dimethyldodecane	33.681	389924	84.2	4.375
Decane, 6-ethyl-2-methyl-	35.558	239231	51.66	2.684
Undecane, 4-ethyl-	35.631	377989	81.62	4.241
Nonane, 3-methyl-5-propyl-	37.433	305498	65.97	3.427
Hexadecane	37.506	446578	96.43	5.01
Heptadecane, 2,6,10,15-tetramethyl-	40.81	334594	72.25	3.754
DCM: solvent				
Nonane, 2-methyl-5-propyl-	26.705	251650	76.38	4.09
Pentadecane	29.256	327360	99.36	5.321
Decane, 2,4,6-trimethyl-	31.508	205103	62.25	3.334
Hydroxylamine, O-decyl-	31.581	209444	63.57	3.404
Nonane, 2-methyl-5-propyl-	35.632	216480	65.71	3.519
Ether: solvents				
Undecane, 4,7-dimethyl-	20.559	300744	54.22	1.378
Tridecane	23.706	378923	68.31	1.736
Tetradecane	26.63	449482	81.03	2.06
Decane, 5-propyl-	29.109	297939	53.71	1.365
3,5-Dimethyldodecane	29.256	523201	94.32	2.397
Pentadecane, 7-methyl-	31.581	467923	84.35	2.144
Tridecane	33.608	308767	55.66	1.415
Pentadecane, 2,6,10-trimethyl-	33.754	501852	90.47	2.3
Eicosane, 10-methyl-	33.828	293163	52.85	1.343
Dodecane, 2,7,10-trimethyl-	35.631	314725	56.74	1.442
Heptadecane, 2,6-dimethyl-	35.705	467212	84.22	2.141
Pentadecane, 2,6,10-trimethyl-	35.778	466688	84.13	2.138
Eicosane, 10-methyl-	37.579	482012	86.89	2.209
Eicosane	39.306	481704	86.84	2.207
Tridecane, 7-propyl-	39.38	290449	52.36	1.331
Naphthalene, 1-methyl-	39.604	311709	56.19	1.428
Tridecane, 5-propyl-	40.957	339977	61.29	1.558
Naphthalene, 2,3-dimethyl-	42.079	200157	36.08	0.917
Naphthalene, 1,7-dimethyl-	42.304	375586	67.71	1.721

pressure in N₂ atmosphere. N₂ gas was used to maintain inert medium in the reaction system, to dilute the formed pyrolysis vapors, to minimize char formation, and to prevent further reactions. Biomass (1 kg de-oiled *Jatropha curcas* cake) was used for the reaction and N₂ gas (825 ml/min) was passed continuously through a gas meter, and pyrolysis vapors were carried into a series of two condensers to condense the pyrolysis vapor to obtain the pyrolysis liquid (water-soluble aqueous phase and non aqueous bio-crude). The non-condensable gases were vented off (Poddar et al., 2016).

3. RESULTS AND DISCUSSION

3.1 Physicochemical Properties of Catalyst

3.1.1 BET NH₃-TPD (acidity) and XRD analysis

Physicochemical properties (surface area, pore diameter, pore volume, and surface acidity) of the prepared SiO₂-Al₂O₃ support and Ni-Mo/SiO₂-Al₂O₃ catalysts used in the microchannel for the study of hydroprocessing of aqueous phase of pyrolysis oil are listed in Table 2. Surface area, mean pore diameter, and pore volume of SiO₂-Al₂O₃ support was 377 m²/g, 8.6 nm, and 0.85 ml/g, respectively. After impregnation of Mo and Ni and calcination at 500° C, both surface area and pore size were reduced. After impregnation, surface area, mean pore diameter, and pore volume were 202 m²/g, 10.6 nm, and 0.5 ml/g, respectively. The mesoporous SiO₂-Al₂O₃ support has a total acidity of 0.77 mmol of NH₃ g⁻¹ catalyst. Acidity of support is expected to result in different product yield and selectivity due to cracking activity. Ni-Mo/SiO₂-Al₂O₃ catalysts had a composition similar to the commercial hydrotreating catalyst, which was used in the present study.

X-ray diffraction (XRD) patterns were recorded using a PROTO XRD benchtop powder diffraction X-ray diffractometer with monochromatic radiation Cu K α ($\lambda = 1.5418 \text{ \AA}$) by applying operating voltage of 34.6 kV used during the analysis, and a current of 14.3 mA in the step scanning mode in the range $10^\circ < 2\theta < 80^\circ$ with a continuous scan rate of 2.0° C/min .

The powder XRD of NiMo/SiO₂-Al₂O₃ catalyst shows that SiO₂-Al₂O₃ is amorphous while characteristic peaks of MoO₃ and NiO were not observed. A broad hump between $2\theta = 10\text{--}20^\circ$ is ascribed to amorphous silica. Orthorhombic MoO₃ peaks are not seen between $2\theta = 26\text{--}31^\circ$, indicating that the oxides are highly dispersed on the support, and the sizes are smaller than the detection limit of XRD ($< 3 \text{ nm}$). $[3\ 1\ 1]$, $[4\ 0\ 0]$, $[4\ 4\ 0]$ peaks corresponding to γ -alumina phase are observed (Gloria et al., 2018; Rai et al., 2018).

3.2 Catalytic Studies

The oxygen content of the organics in the aqueous phase was reduced to trace amounts after hydroprocessing. The water obtained after hydroprocessing contained a small amount of organic ($< 5\%$). Stable activity during the study indicated that there was no significant catalyst leaching from the plates. Product distributions (yield %) for the hydroprocessing reactions of the aqueous phase of bio-oil at various temperatures (523–673 K), 70 bar pressure, space-velocity (LHSV) of 1.0, and H₂/ feed ratio of 1000 are provided in Fig. 2. The yield of gasoline ($< \text{C}_9$) range hydrocarbons increased rapidly from 3% to 4% by changing temperature from 523 K to 573 K, to a maximum of 60% at 623 K. Gasoline ($< \text{C}_9$) further decreased to 10%–15% at higher temperatures (648 K, 673 K). Kerosene yield (C₉-C₁₄) decreased from 28% to 15% by changing temperature from 523 K to 573 K, and it increased from 35% to 40% by

TABLE 2: Physicochemical properties of mesoporous supports and catalysts

Physicochemical properties	SiO ₂ -Al ₂ O ₃	Ni-Mo/SiO ₂ -Al ₂ O ₃
Surface area (m ² ·g ⁻¹)	236	202
Total pore volume (ml·g ⁻¹)	0.39	0.5
Mean pore diameter (nm)	8.6	10.6
Surface acidity NH ₃ (mmol·g ⁻¹ cat)	0.77	–

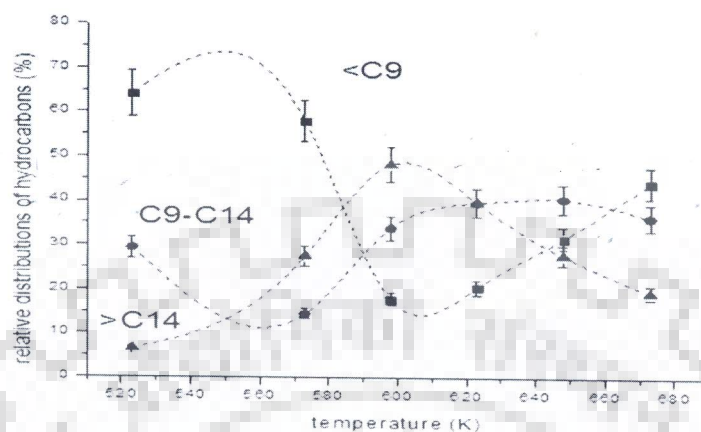


FIG. 2: Distribution of hydrocarbons [■ gasoline (< C9), ● kerosene (C9–C14), and ▲ diesel (> C14)] in the products at various temperatures (pressure, 70 bar; LHSV 1.0; H₂/feed: 1000 nL/L)

increasing temperature from 623 to 673 K. The yield of diesel hydrocarbons (> C14) increased rapidly from 5% to 50% by changing temperature from 523 K to 598 K. However, further increase in temperature caused the diesel yield to decrease rapidly to 20% at 673 K. As the reaction severity increased due to increasing reaction temperature, the longer chain diesel range hydrocarbons cracked more, resulting in their reduced yields, while the yield of shorter chain gasoline and kerosene increased. Due to several interconversion reactions of bio-oil molecules increasing and decreasing trends are observed with change in reaction temperature. At a lower H₂/feed ratio of 500 the trends of conversion were haphazard (Fig. 3), which could be caused by lower hydrogen content in the reaction system due to which inter-conversion and oligomerization reactions are predominant. At this condition the product qualities are poor, and reactor operation was difficult.

Figure 4 shows the distribution of hydrocarbons (gasoline (< C9), kerosene (C9–C14), and diesel (> C14) in the products at various liquid hourly space velocities (LHSV) (Pressure 70 bar; temperature 648 K, and H₂/feed ratio of 1000 nL/L). With increasing space velocities, the yield of gasoline (< C9) range hydrocarbons increased from 5% (at 0.25 LHSV) to 35%–60% (at 0.5–1.25 LHSV). Maximum yield of gasoline (< C9) range hydrocarbons (60%) was obtained at 0.75 LHSV, as aqueous bio-oil has predominantly oxygen containing smaller hydrocarbons.

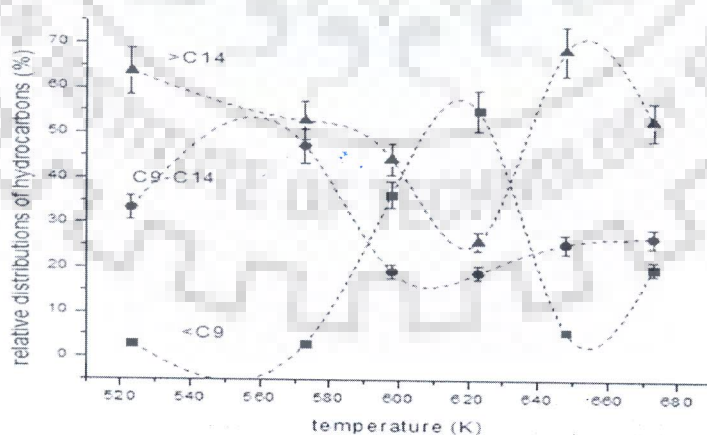


FIG. 3: Distribution of hydrocarbon types (■ alkanes, ▲ cycloalkanes, ● aromatics, ▼ PAH ◀ residue and ▶ unreacted) in hydroprocessed (pressure 70 bar; LHSV 1.0 H₂; feed 1000) at various temperatures

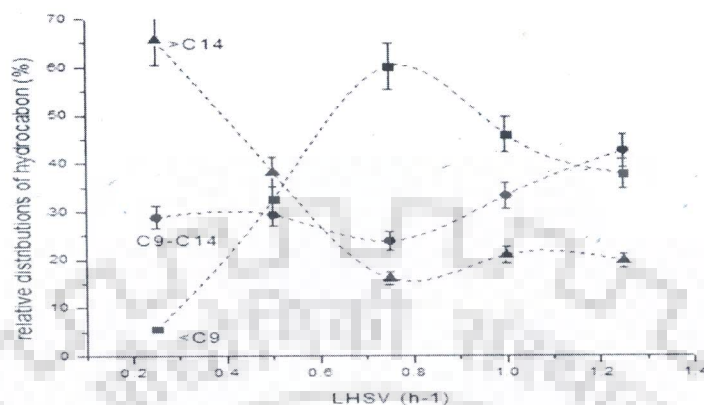


FIG. 4: Distribution of hydrocarbons [■ gasoline (< C9), ● kerosene (C9–C14) and ▲ diesel (> C14)] in the products at various LHSV (pressure 70 bar; temperature 648 K; H₂/feed: 1000 nL/L)

Lower LHSV (i.e., at higher contact time) may favor intermolecular oligomerization reactions and hence the gasoline yields are lower. The yield of kerosene (C9–C14) range hydrocarbons reached maximum (45%) at the highest studied LHSV of 1.25, from 30% at 0.25 LHSV. Additionally, with increasing space velocity (0.25 to 1.25), the longer chain hydrocarbons (> C14) yield decreases from 65% (at 0.25 LHSV) to ~ 20% at 0.75-1.25 LHSV. These differences in the distribution patterns of various products are due to differences in the relative rates of formation of various products. The diesel range product (> C14) may be obtained by the oligomerization of smaller bio-oil molecules.

Figure 5 indicates the distribution of hydrocarbons (gasoline (< C9), kerosene (C9–C14), and diesel (> C14)) in the products at various hydrogen/feed ratios (pressure 70 bar; temperature 598 K; LHSV 1.0). The yield of diesel (> C14) range compounds decreased from ~ 50% at H₂/feed ratio of 500, 1000 to ~ 2-5% at H₂/feed ratio of 2500, 4000. This drastic decrease could be due to the high linear velocity of feed and hydrogen in the reactor. The kerosene (C9–C14) range hydrocarbons increased from 40% to 50% with an increase in H₂/feed ratio from 500 to 4000. The gasoline (< C9) range hydrocarbons increased from 7% to 95% with an increase in H₂/feed ratio from 500 to 2500. This could be due to the hydrocracking of higher oxygenated hydrocarbons to the lower one. Such a large variation in the product yields with a change in H₂/feed ratio could be due to a large change in linear velocity of the reactants (H₂ and feed) in the very narrow microchannels. As the catalyst is coated inside the microchannels, the flow conditions are not completely plug-flow type (unlike packed bed reactors) and hence such prominent effect of hydrogen flow is observed, unlike that of fixed bed reactors (Sinha and Rai, 2018).

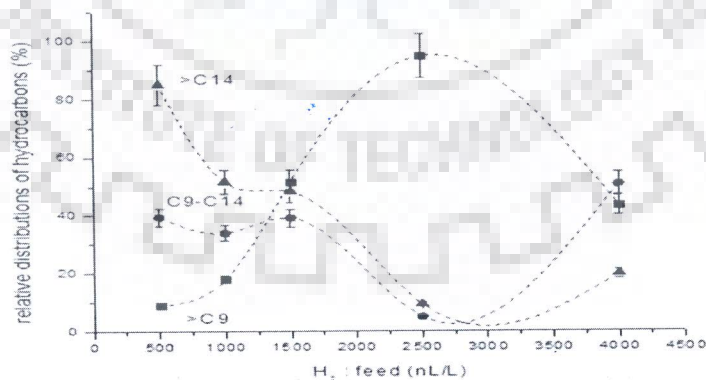


FIG. 5: Distribution of hydrocarbons [■ gasoline (< C9), ● kerosene (C9–C14) and ▲ diesel (> C14)] in the products at various H₂/ feed ratio (nL/L) (Pressure 70 bar; LHSV 1.0; temperature 598 K)

The distribution of hydrocarbon types (alkanes, cycloalkanes, aromatics, PAH, residue, and unreacted feed) in hydroprocessed products at various space velocities (LHSV) (pressure, 70 bar; H_2 /feed ratio, 1000; temperature, 648 K) are seen in Fig. 6. The alkanes yield decreases rapidly from 65% (at 0.25 LHSV) to 20% (at 1.25 LHSV) when LHSV is reduced. Simultaneously, the unreacted compounds increase from 0% to 70% as the LHSV increases from 0.25 to 1.25. The results indicate that very low space velocity is required for complete conversion of the compounds present in the aqueous phase of bio-oil. The residues in the product decrease from 30% to 10% with an increase in LHSV from 0.25 to 1.25. The PAH formation remains below 5% at all studied space velocities, while the formation of aromatics and cycloalkanes is negligible.

Figure 7 shows the distribution of hydrocarbon types (alkanes, cycloalkanes, aromatics, PAH, residue, and unreacted compounds) in the hydroprocessed products at various temperatures (pressure, 70 bar; LHSV, 1.0; H_2 /feed ratio 1000). Maximum conversion of feed (75%) is observed at 573 K, but the formation of undesired PAH (10%) and residues (20%) are very high. Maximum alkane formation (50%) is observed at 597 K. The results indicate that the feed conversion is maximum in a very narrow temperature range around 573 K.

Figure 8 shows the distribution of hydrocarbon types (alkanes, cycloalkanes, aromatics, PAH, residue, and unreacted compounds) in hydroprocessed product at various H_2 /feed ratios (pressure 70 bar; LHSV 1.0; temperature 598 K). The figure shows that at 1500 and higher H_2 /feed ratios, the conversion is very low (> 80% unreacted compounds). Only at 1000 H_2 /feed ratio, the conversion is ~ 65%. As the catalyst is coated inside microchannels, the flow conditions are not completely plug-flow type, and hence hydrogen flow increase (higher H_2 /feed ratio) would reduce the effective utilization of catalyst for conversions (Sinha and Rai, 2018).

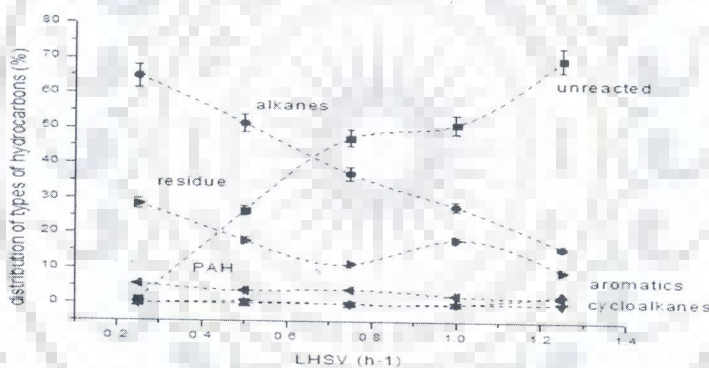


FIG. 6: Distribution of hydrocarbon types (● alkanes, ▲ cycloalkanes, ▼ aromatics, ◀ PAH ▶ residue and ■ unreacted) in hydroprocessed products (pressure 70 bar; H_2 : feed 1000; temperature 648 K) at various LHSV

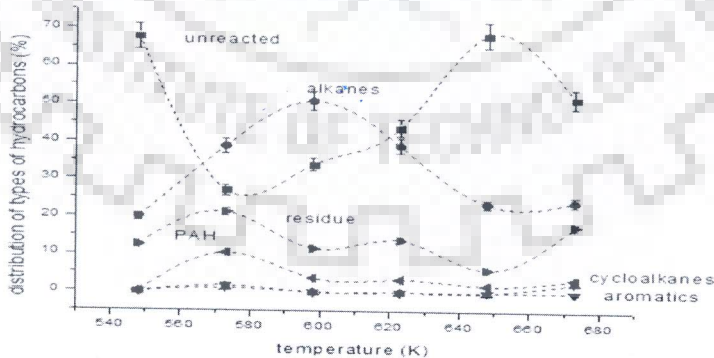


FIG. 7: Distribution of hydrocarbon types (● alkanes, ▲ cycloalkanes, ▼ aromatics, ◀ PAH ▶ residue and ■ unreacted) in hydroprocessed products (pressure 70 bar; LHSV 1.0 H_2 : feed 1000;) at various temperatures

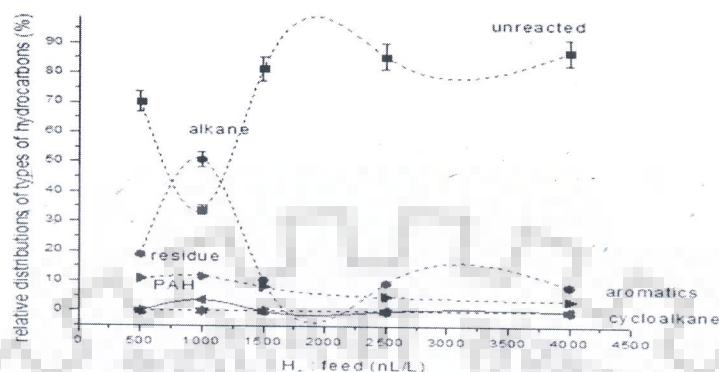


FIG. 8: Distribution of hydrocarbon types (■ alkanes, ▲ cycloalkanes, ● aromatics, ▼ PAH ◀ residue and ▶ unreacted) in hydroprocessed (pressure 70 bar; LHSV 1.0; temperature 598 K) at various H₂/feed ratios

4. CONCLUSIONS

Hydroprocessing of the aqueous phase of bio-oil (BO) obtained from pyrolysis of de-oiled jatropha curcas seeds cake (JCC) with sulfided NiMo catalyst supported on mesoporous silica-alumina and coated in a microchannel reactor is a promising route for producing transportation fuels. Complete deoxygenation of the organics in the aqueous phase was achieved. The water obtained after hydroprocessing contained < 5% organics, indicating that > 95% of organics in the aqueous phase of bio-oil was converted into useful products.

Products obtained from hydroprocessing contained 5%–45% gasoline (< C₉), 5%–60% kerosene (C₉–C₁₄), 15–40% diesel (> C₁₄), with 15–65% alkanes, 0–5% polyaromatic hydrocarbons (PAH), negligible cycloalkanes and aromatics, with 30%–75% unreacted, and residues under reaction condition of temperature 523–673 K, LHSV 0.25–1.25, H₂:feed ratio 500–4000, and at fixed pressure of 70 bar. Maximum hydrocarbon yield (~ 65%) was obtained at 648 K, 0.25 LHSV, and 70 bar, with 35% undesired residues and PAH.

ACKNOWLEDGMENTS

The authors are thankful to the Institute Instrumentation Center (IIC) of IIT, Roorkee, India for TEM analysis. We are also thankful to the hydroprocessing laboratory of CSIR-IIP for help in experimental and analytical works.

REFERENCES

- Anand, M. and Sinha, A.K., Temperature-Dependent Reaction Pathways for the Anomalous Hydrocracking of Triglycerides in the Presence of Sulfided Co–Mo-Catalyst, *Bioresour. Technol.*, vol. 126, pp. 148–150, 2012.
- Baldauf, W., Balfanz, U., and Rupp, M., Upgrading of Flash Pyrolysis Oil and Utilization in Refineries, *Biomass Bioenergy*, vol. 7, pp. 237–244, 1994.
- Bhutto, A.W., Qureshi, K., Abro, R., Harijan, K., Zhao, Z., Bazmi, A.A., Abbas, T., and Yu, G., Progress in the Production of Biomass-to-Liquid Biofuels to Decarbonizes the Transport Sector—Prospects and Challenges, vol. 6, pp. 32140–32170, 2016.
- Bridgwater, A., Czernik, S., Diebold, J., Meier, D., Oasmaa A., and Peacocke, C., *Fast Pyrolysis of Biomass: A Handbook*, Berkshire, U.K.: CPL Press, 1999.
- Chheda, J.N., Huber, G.W., and Dumesic, J. A., Liquid-Phase Catalytic Processing of Biomass-Derived Oxygenated Hydrocarbons to Fuels and Chemicals, *Angew. Chem., Int. Ed.*, vol. 46, pp. 7164–7183, 2007.
- Demirbas, A., Progress and Recent Trends in Biofuels, *Prog. Energy Combustion Sci.*, vol. 33, pp. 1–18, 2007.
- Desavath, V.N., Vimal, K., Basheshwar, P., Mukesh, K.P., Babita, B., Rajaram, B., Om, P.K., Dilip, K.A., and Madhukar, O.G., Catalytic Cracking of Jatropha-Derived Fast Pyrolysis Oils with VGO and Their NMR Characterization, *RSC Adv.*, vol. 5, pp. 389, 2015.

- Diebold, J.P.A., Chemical and Physical Mechanisms of the Storage Stability of Fast Pyrolysis Bio-Oils: A Review, NREL/SR-570-27613, Colorado, USA, 2000.
- Elliott, D.C. and Baker, E.G., Upgrading Biomass Liquefaction Products through Hydrodeoxygenation, *Biotechnol. Bioeng. Symp. Suppl.*, vol. **14**, pp. 159–174, 1984.
- Elliott, D.C. and Huamin, W., Hydrocarbon Liquid Production via Catalytic Hydroprocessing of Phenolic Oils Fractionated from Fast Pyrolysis of Red Oak and Corn Stover, *ACS Sustainable Chem. Eng.*, vol. **3**, pp. 892–902, 2015.
- Fogassy, G., Thegarid, N., Toussaint, G., Van, A.C., Schuurman, Y., and Mirodatos, C., Biomass Derived Feedstock Co-Processing with Vacuum Gas Oil for Second Generation Fuel Production in FCC Units, *Appl. Catal. B.*, vol. **96**, pp. 476–485, 2010.
- Forson, F.K., Oduro, E.K., and Hammond-Donkoh, E., Performance of Jatropha Oil Blends in a Diesel Engine, *Renewable Energy*, vol. **29**, pp. 1135–1145, 2004.
- Furimsky, E. and Massoth, F.E., Deactivation of Hydroprocessing Catalysts, *Catal. Today*, vol. **52**, pp. 381–495, 1999.
- Gloria, E., Rai, A., Paulino, B., and Sinha, A.K., Selective Poly-Aromatics Saturation and Ring Opening During Hydroprocessing of Light Cycle Oil over Sulfided Ni-Mo/SiO₂-Al₂O₃ Catalyst, *Fuel*, vol. **219**, pp. 270–278, 2018.
- Huber, G. and Corma, A., Synergies between Bio- and Oil Refineries for the Production of Fuels from Biomass, *Angew. Chem., Int. Ed. Engl.*, vol. **46**, no. 38, pp. 7184–7201, 2007.
- Mariefel, V.O., Alan, H.Z., Asanga, B.P., Sarah, D.B., Heather, M.J., Teresa, L.L., Marie, S.S., Leslie, J.R., Gary, N.N., John, G.F., and Douglas, C.E., Stabilization of Softwood-Derived Pyrolysis Oils for Continuous Bio-oil Hydroprocessing, *Topics Catal.*, vol. **59**, pp. 55–60, 2016.
- Mercader, F.M., Groeneveld, M.J., Kersten, S.R.A., Way, N.W.J., Schaverien, C.J., and Hogendoorn, J.A., Production of Advanced Biofuels: Co-Processing of Upgraded Pyrolysis Oil in Standard Refinery Units, *Appl. Catal. B.*, vol. **96**, pp. 57–66, 2010.
- Mercader, M.D., Groeneveld, F.K., Venderbosch, S.R.A., and Hogendoorn, K., Pyrolysis Oil Upgrading by High-Pressure Thermal Treatment, *Fuel*, vol. **89**, pp. 2829–2837, 2010.
- Miguel, M.F.D., Groeneveld, M.J., Kersten, S.R.A., Way, N.W.J., Schaverien, C.J., and Hogendoorn, J.A., Production of Advanced Biofuels: Co-Processing of Upgraded Pyrolysis Oil in Standard Refinery Units, *Appl. Catal.*, vol. **26**, pp. 57–66, 2010.
- Otterstedt, J.E., Gevert, S.B., Jaras, S.G., and Menon, P.G., Fluid Catalytic Cracking of Heavy (residual) Oil Fractions, *Appl. Catal.*, vol. **22**, no. 2, pp. 159–179, 1986.
- Pankaj, K.K., Desavath, V.N., Deependra, T., Raghuvir, S., Mukesh, K.P., Siva, L.N.K., and Yogendra, K.S., Pyrolysis of Jatropha Curcas Seed Cake Followed by Optimization of Liquid-Liquid Extraction Procedure for the Obtained Bio-Oil, *J. Analyt. Appl. Pyrolysis*, vol. **118**, pp. 202–204, 2016.
- Poddar, M.K., Rai, A., Maurya, M.R., and Sinha, A.K., Co-Processing of Bio-Oil from De-Oiled Jatropha Curcas Seed Cake with Refinery Gas–Oil over Sulfide CoMoP/Al₂O₃ Catalyst, *RSC Adv.*, vol. **6**, pp. 113720, 2016.
- Rai, A., Anand, M., Farooqui S.A., Gloria, E., and Sinha, A.K., Hydroprocessing of Light Cycle Oil and Gas Blends over Sulfided Ni-Mo/SiO₂-Al₂O₃ Catalyst in Microchannel and Fixed Bed Reactions Catalysis, *Green Chem. Eng.*, vol. **1**, no. 1, pp. 1–9, 2018.
- Samolada, M.C., Baldauf, W., and Vasalos, I.A., Production of a Bio-Gasoline by Upgrading Biomass Flash Pyrolysis Liquids via Hydrogen Processing and Catalytic Cracking, *Fuel*, vol. **77**, pp. 1667–1675, 1998.
- Sinha, A.K., Anand, M., Rana, B.S., Kumar, R., Farooqui, S.A., Sibi, M.G., Kumar, R., and Joshi, R.K., Development of Hydroprocessing Route to Transportation Fuels from Non-Edible Plant-Oil, *Catal. Surveys Asia*, vol. **17**, pp. 1–13, 2013.
- Sinha, A.K., Sibi, M.G., Naidu, N., Farooqui, S.A., Anand, M. and Kumar, R., Process Intensification for Hydroprocessing of Vegetable Oils: Experimental Study, *Ind. Eng. Chem. Res.*, vol. **53**, pp. 19062–19070, 2014.
- Sinha, A.K. and Rai, A., *Intensification of Bio-Based Processes*, RSC Green Chemistry Series, 2018.
- Wildschut, J., Melian-Cabrera, I., and Heeres, H.J., Catalyst Studies on the Hydrotreatment of Fast Pyrolysis Oil, *Appl. Catal. B.*, vol. **99**, pp.298–306, 2010.



ELSEVIER

Contents lists available at ScienceDirect

Biomass and Bioenergy

journal homepage: www.elsevier.com/locate/biombioe

Research paper

Hydroprocessing of lipids extracted from marine microalgae *Nannochloropsis* sp. over sulfided CoMoP/Al₂O₃ catalyst

M.K. Poddar^{a,b}, M. Anand^a, S.A. Farooqui^a, G.J.O. Martin^c, M.R. Maurya^b, A.K. Sinha^{a,*}^a CSIR-Indian Institute of Petroleum, Dehradun, India^b Indian Institute of Technology, Roorkee, Chemistry Department, India^c Algal Processing Group, Department of Chemical Engineering, The University of Melbourne, Parkville, Victoria, 3010, Australia

ARTICLE INFO

Keywords:

Marine microalgae
Lipid
Hydroprocessing
Hydrocarbons kinetics
Activation energy

ABSTRACT

Hydroprocessing of neutral lipids extracted from *Nannochloropsis* sp. algal biomass was studied over sulfided cobalt molybdenum phosphorus/aluminium oxide (CoMoP/Al₂O₃) catalyst in a batch reactor at 300–375 °C with H₂ at 50–120 bar. A clear light yellowish green product was obtained, containing 6–26% gasoline, 35–50% kerosene, 8–40% diesel, with 10–80% alkanes, 1–10% cycloalkanes, and 5–35% aromatics, with a maximum of 10% char formation in the process. Power law kinetic model was validated with experimental results. A kinetic study shows a pseudo 1st order reaction with respect to the neutral algae lipids oil concentration, with the activation energy for algal oil conversion over CoMoP/Al₂O₃ catalyst was 14.96 kJ/mol. Activation energies for the formation of diesel (125 kJ/mol) and kerosene (146 kJ/mol) were higher than for the heavy hydrocarbons such as PAH (7 kJ/mol) and alkanes (64 kJ/mol) products.

1. Introduction

There is much continued interest in the sustainable production of renewable biofuels to displace fossil fuels. These renewable biofuels are being developed broadly considering two key factors: 1) minimizing competition with food production and 2) compatibility with current infrastructure [1,2]. First generation biofuels, i.e., ethanol and biodiesel from sugar or starch and vegetable oils respectively, requires the cultivation of crops on land that could be otherwise used for food production [2]. In contrast, second generation biofuels can be produced either from crops or food wastes. These include biodiesel from waste oil or tallow and lignocellulosic ethanol from forestry or crop wastes. More recently, algae have been considered as a promising feedstock for third generation biofuels, as they can be produced at high productivity on otherwise non-arable land. Moreover, many algal biomasses can be cultivated to have high oil (triacylglyceride) content, and can produce oil at much higher productivity than other land-based oil-crops [3,4]. These are a hydrophyte containing chlorophyll without stems and roots and are categorized into two varieties, based on size, i.e., macroalgae (seaweed) and microalgae [5]. Algae can be cultivated in the non agricultural land by using any kind of water (brackish, salty, west water, open ponds or in closed photobioreactors) with ample nutrients. They grow rapidly compared to other crops and plants, and its volume and size get double in just 24 h by consuming CO₂ as a feed [4–6].

Unfortunately, the conventional biofuels produced from these crops, ethanol, and biodiesel, require engine modification for their use in present vehicular engines. There is a need to develop second and third generation biofuels that are compatible with current infrastructure.

Currently, mainly three approaches are being used to produce algae based biofuels. The first process involves extracting lipids from algal biomass cell, followed by the transesterification of triglycerides (TAGs) and alcohol into fatty acids alkyl esters (biodiesel). The second technique employs hydrothermal liquefaction (HTL) at high pressure (50–200 bar) and temperature (250–450 °C) to produce water-insoluble bio-crude oil [7]. The third technique is pyrolysis, which thermally degrades algae biomass at 300–700 °C in the absence of oxygen, resulting in the production of bio-oils (aqueous and organic phase), solid residue (char/coke), and gases (bio-gas). These processes require the final bio-oil/crude to be upgraded using hydrogen, before being used in conventional transportation engines. Hydroprocessing of the bio-oil/crude may produce drop-in biofuels which are compatible with engines and can be used directly without any upgrading.

Many researchers have studied the hydroprocessing of bio-crude produced via hydrothermal liquefaction of algae over various catalysts including sulfided CoMo/γ-alumina, HZSM-5 at temperatures between 400 and 500 °C. Transportation oil produced between 55 and 85%, however, yield decreases on increasing temperature. The highest reported yield was achieved using a combination of Ru/C and Raney/Ni

* Corresponding author.

E-mail address: asinha@iip.res.in (A.K. Sinha).

catalysts [8–11].

Today, the direct conversion of algae lipids to drop-in fuels has yet to be investigated. In comparison to hydrothermal liquefaction, the extraction of algae lipids allow the other valuable biomass components, in particular, the proteins, pigments, and long-chain polyunsaturated fatty acids, to be recovered [12]. The direct conversion of these lipids to a drop-in fuel would be a major improvement over the conventional approach of conversion to biodiesel via transesterification.

The lipids extracted from microalgae using a wet extraction process are predominantly triacylglycerides, but also contain waxes, sterols, free fatty acids, monoglycerides, diglycerides, phospholipids, glycolipids and chlorophyll as impurities. It is therefore of interest to determine whether a catalytic process can be developed, that can successfully convert this complex feedstock to suitable drop-in fuels. This study investigates for the first time the hydroprocessing of crude lipids extracted from the commercially relevant marine microalga *Nannochloropsis* sp. over a sulphided form of CoMoP/Al₂O₃ catalyst [13].

2. Experimental details

2.1. Catalyst preparation

The catalyst CoMoP/Al₂O₃ was prepared by conventional wet impregnation method on commercial mesoporous extrudates of γ -Al₂O₃ (BET surface area = 298 m² g⁻¹, BJH pore size = 6.1 nm, pore volume = 1.1 ml g⁻¹). 1.89 g of (NH₄)₆Mo₇O₂₄·4H₂O, as molybdenum precursor, 1.55 g Co (NO₃)₂·6H₂O as cobalt precursor and 0.16 g of 85% aqueous H₃PO₄ as Phosphorous precursor were used during catalyst synthesis. An ammonical solution of molybdenum precursor, an aqueous solution of cobalt precursor, were added over 7.9 g of moisture free γ -alumina to prepare 16%Mo, 4%Co, 1%P. Each metal precursors were added sequentially after overnight drying at 120 °C. After drying the final prepared catalyst was calcined at 550 °C for 6 h in a muffle furnace with a heating rate of 1 °C min⁻¹ [13]. All precursors, toluene and dimethyl disulphide (DMDS) were purchased from (Sigma Aldrich). Refinery gas oil was taken from Indian Oil Corporation, Mathura refinery. High performance liquid chromatography (HPLC) grade water was taken as a solvent for synthesis [13].

The surface area of the catalyst was measured using the Brunauer–Emmett–Teller (BET) method with nitrogen (N₂) adsorption isotherm at –196 °C using BELSORP-max Microtrac (Japan) apparatus. Before analysis, the catalyst sample was degassed at 250 °C under vacuum. The pore size was calculated from the desorption isotherm using the Barrett, Joyner, and Hallender (BJH) method. The Sample for transmission electron microscopy (TEM) was prepared by deposition of the catalyst, suspended in isopropanol, on a copper grid. TEM images were recorded using a Tecnai G2 (FEI) Instrument, operating at 200 kV. Deposited metals (Co 4%, Mo 16%, and P 1%) were determined using an inductively coupled plasma atomic emission spectroscopy (ICP-AES) method on a PS 3000 UV (DRE) (Teledyne Leeman Labs, Inc., USA) [13].

2.2. Lipid (TAGs) extraction from ruptured microalgae biomass

The feed for the reaction was a neutral lipid extract, obtained from multiple batches of *Nannochloropsis* sp. algal biomass [14]. The fatty acid composition of the saponifiable lipids in the extract was mostly palmitic acid (C16:0) and palmitoleic acid (C16:1) and included some longer chain polyunsaturated fatty acids including eicosapentaenoic acid (C20:5n3) as previously presented. The biomass was produced and concentrated to ca. 25% w/w solid as previously described [14]. The cultures were deprived of nitrogen for approximately 10 days to allow accumulation of TAG in the algae. Before lipids extraction, the microalgal cells were weakened by incubated at 37 °C for approximately 24 h and then ruptured by a single pass through a GEA Panda 2K NS1001L

high pressure homogenizer (GEA NiroSoavi, Parma, Italy) at 1000 bar previously described [14]. The neutral lipids were preferentially extracted by twice contacting with hexane, and the lipids containing hexane was recovered from the de-lipidated biomass by centrifugation, the hexane was removed from the lipids by evaporation, and the lipids stored at –20 °C [14].

2.3. Lipid conversion

The lipids extract was hydroprocessed in stainless steel (SS) cylindrical reactor of 25 ml capacity, with a magnetic drive stirrer (model 4590, Parr Instrument Co., Moline, IL, US), heated by an electric heater and the temperature controlled using a PID controller (Model 4848, Parr Instruments, IL, US). 7 g of the lipids feedstock was added along with 10 wt% of the sulfided catalyst CoMoP/Al₂O₃ into the reactor. Sulfidation was done in same reactor prior to the reaction, using 2.5 wt % of dimethyl disulphide (Sigma-Aldrich) mixed in refinery gas oil, at a H₂ pressure of 40 bar, by gradually raising the temperature from 100 °C to 350 °C temperature (at 10 °C min⁻¹) which was then maintained for 12 h with constant stirring at 680 rpm [13]. Prior to commencing the reaction, high purity hydrogen gas was used to purge the reactor vessel five times, and build up a pre-set initial pressure of 10 bar at room temperature. During the reaction, the liquid sample was drawn in every 2 h and cooled before analysis for the kinetic calculation. After the reaction, the reactor was cooled to ambient temperature. The overall material balance was recorded, which confirmed minimal loss occurred during the experimental measurement and the formation of a different type of solid (char/coke)/liquid/gases products. Based on the material balance, an estimated experimental and measurement uncertainty of 10% has been included in the results as an error bar.

The final reaction temperatures (300 °C, 325 °C, 350 °C, and 375 °C) were achieved by heating gradually (10 °C min⁻¹) while the reaction pressure (50, 75 and 120 bar) was achieved by the addition of external hydrogen gas pressure to maintain desired reaction condition. The temperature and pressure were increased to the desired reaction condition after sample collection. The quantity of liquid feed (lipids), liquid products, catalyst, and coke/char, were measured using a weight balance with a precision of ± 0.01 g. Catalyst and coke/char deposited on the catalyst surface were measured after rinsing with toluene to remove the unreacted feed and deposited hydrocarbons. The amount of char formed was measured after subtraction of the catalyst amount loaded in the reactor. The amount of gases formed/consumed were determined from the difference in the weight of the reaction vessel, containing the reaction mixtures, before and after the reactions.

Liquid products obtained during the reaction were filtered using cellulose membrane (pore size 220 μ m) and then analyzed and quantified using gas chromatography and simulated distillation by GC (Varian 3800 GC, with a J&W VF-5ms column (Agilent; 30 m · 0.25 mm, 0.25 mm) and flame ionization detection (qFID). Simulated distillation was done in accordance to ASTM D 2887 to quantify wt% of different boiling range compounds of product. GC was calibrated by using standard hydrocarbon sample for equipment calibration and retention time and concentration accuracy. The yield of various liquid product components was calculated on a relative basis considering the entire range of liquid products formed as 100%. The relative yield has been reported based on the relative amount of gas, liquid, and char produced. Liquid products distribution were quantified on the basis of hydrocarbon chain length: gasoline (< C9 hydrocarbons), kerosene (C9–C14 hydrocarbons), diesel (C15–C18 hydrocarbons) and heavy oil (> C18 hydrocarbons).

Detailed hydrocarbons analysis (alkanes, cycloalkanes, aromatics and polyaromatic hydrocarbon) were done using an Agilent 7890B 2D-GC (GC × GC; first dimension – nonpolar, DB-5 ms column, 30 m × 0.25 mm, 0.25 μ m; second dimension polar, PAC column, 5 m × 0.25 mm, 0.15 μ m), with FID, MS, capillary flow modulator and ZOEX software. Two column systems were used to separate various

components present in the product. 2D-GC*GC-qFID was calibrated using standard gravimetric blend standard from Analytical Controls by PAC (PNA in AVTUR reference, Part No 00.02.717 Lot No. Lot-001), which helped in qualitatively as well as quantitatively establishing different classes of product formed, i.e., alkanes, cycloalkanes, aromatics and polyaromatics in different products. GC/MS has been done, Model No. Agilent Technologies 5977 A MSD, shows the highest selectivity towards pentadecane and hexadecane in the liquid products. Hydrogen consumption was calculated based on gas phase analysis using refinery gas analyzer (Agilent technologies 7890A gas chromatography) results. The gas analysis was done after the completion of reaction (after 6 h), twice for confirmation and repeatability. The RGA was calibrated using a calibration standard provided by M/s Hydrocarbon Solutions (India) Pvt. Ltd. (Sample Code C4339, Cylinder No M1607003022) prior to analysis.

Kinetic evaluations were carried out using the power law kinetic model, and the Arrhenius equation was then used for calculation of activation energy [15–18]. Considering the pseudo first order of the reaction for lipids conversion [15,16], rate equations for the conversion of lipids into different products were made. Rate constants were then evaluated by plotting the logarithmic plot of concentration vs. time at a particular reaction temperature. The slope of the graph gave the rate constant value at different temperatures, which was then used to find the activation energy according to the Arrhenius equation [15–18].

3. Results and discussion

3.1. Catalyst characterization

The BET surface area and pore volume of the sulphided catalyst were found to be $298 \text{ m}^2/\text{g}$ and 0.5 ml g^{-1} respectively. BJH analysis (mean pore size) showed a narrow pore size distribution with a mean pore size of 7.0 nm (Supporting Fig. 1).

Many researchers have identified the monolayer morphology of MoS_2 slabs with 5–8 nm length visible in micrographs of sulphided $\text{CoMo}/\text{Al}_2\text{O}_3$ catalyst [16,17]. This indicates that monolayer of CoMoS clusters exists in the active phase, with a slab-like morphology of MoS_2 on Al_2O_3 support [17]. In our case, after doping P on $\text{CoMo}/\text{Al}_2\text{O}_3$, a multi-layered (3–5 layers) morphology of CoMoS with a 10–50 nm length and $\sim 0.6 \text{ nm}$ interlayer spacing can be observed in the TEM image in Fig. 1 [13]. Our earlier work has also showed that $\text{CoMoP}/\text{Al}_2\text{O}_3$ catalyst was more active than $\text{CoMo}/\text{Al}_2\text{O}_3$ catalyst [13]. Hence, we have used a $\text{CoMoP}/\text{Al}_2\text{O}_3$ catalyst in the current study due to its better performance.

The catalyst modified by P works in two ways: there is an increase in active sites by enhanced metal dispersion, and there is an increase in the Brønsted acidity. Mo interacts preferentially with the P–OH group on P-added γ -alumina, and additionally, the other surface hydroxyl become more reactive with Mo in the presence of P [18–20]. It was also observed that the catalyst prepared by impregnating P on $\text{CoMo}/\text{Al}_2\text{O}_3$, was more active than the P-free catalyst [21]. $\text{MoP}/\text{Al}_2\text{O}_3$ was tested for

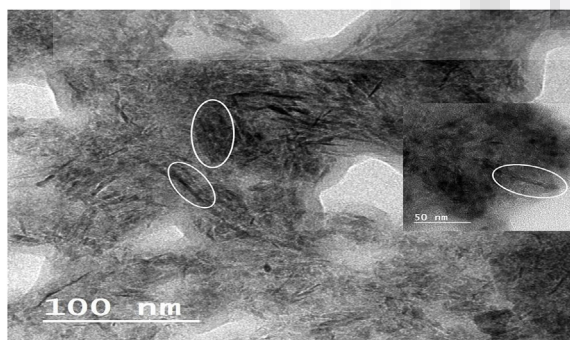


Fig. 1. TEM image of the S-CoMoP/ Al_2O_3 catalyst.

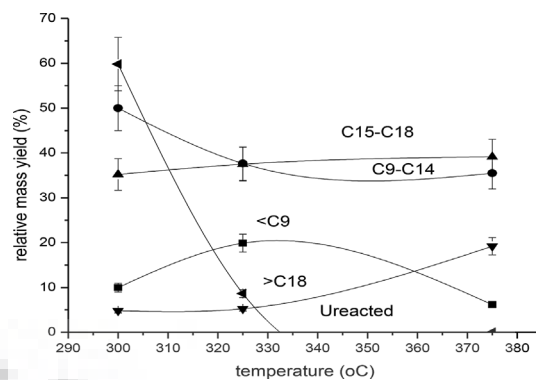


Fig. 2. Distribution of hydrocarbons [■ gasoline (< C9), • kerosene (C9–C14), ▲ diesel (C15–C18), and ▼ heavy residue (> C18)] in the products at various temperatures (cat: feed ratio 1:10; pressure 50 bar).

the catalytic activity in the HDN reaction for some model compounds; it was found that the intrinsic HDN activity of the surface Mo atom was about 6 times higher than that of Mo edge atom in $\text{MoS}_2/\text{Al}_2\text{O}_3$ [21,22]. Deposition of P metal forms Lewis and Brønsted acid sites on the catalyst surface, making the compound accessible for easy reducibility and sulfidation. It increases the Mo dispersion due to enhanced solubility of molybdate by the formation of phosphomolybdate complexes, and it increases the stacking of MoS_2 crystallites and changes their morphology [18,19].

3.2. Catalytic studies

The hydroprocessed product was obtained as a clear transparent light yellowish green liquid after hydroprocessing of the opaque algal oil/Lipids (Supporting Fig. 2.). Fig. 2 shows the influence of reaction temperatures on the lipids conversion and relative yield of various hydrocarbons. The unconverted lipids were nearly 60% in the liquid products for the reaction at 300°C . However the concentration of unconverted lipid rapidly decreased to zero at a reaction temperature of 375°C .

Fig. 3 shows the products (liquid, solid and gases) distribution (yield %) as a function of H_2 pressure (50–120 bar) over S-CoMoP/ Al_2O_3 , at a reaction temperature of 375°C for which the lipid conversion was always > 99%. The liquid products yield decreased linearly with pressure, with a maximum liquid yield (78%) obtained at 50 bar H_2 pressure. This yield decreased to 9% at the higher pressure of 120 bar. The hydrocarbon gases yield increased exponentially from 22% to 80% with an increase in pressure from 50 bar to 120 bar. These results, clearly indicate that lower pressure (around 50 bar) are favorable for maximizing liquid hydrocarbon/hydrogenation, while higher pressure favors cracking at 375°C of reaction Temperature.

The influence of pressure on cracking was also observed in the distribution of hydrocarbon, as shown in Fig. 4. The gasoline (< C9)

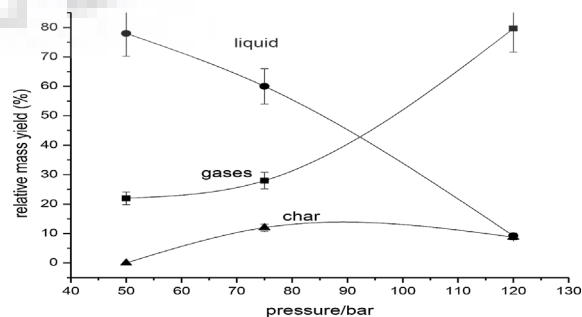


Fig. 3. Yield (%) of the products (liquid, gases and solid char) at various H_2 pressures at 375°C (reaction time of 6 h; cat: feed ratio of 1:10).

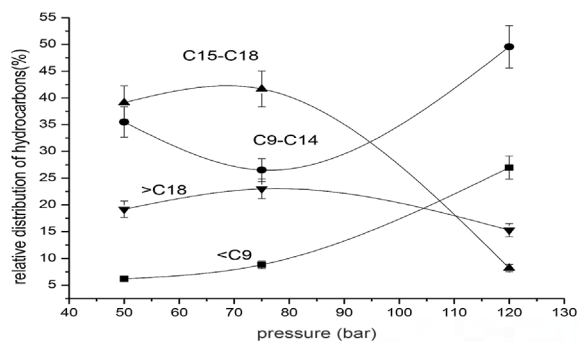


Fig. 4. Distribution of hydrocarbons [■ gasoline (< C9), ● kerosene (C9–C14), ▲ diesel (C15–C18), and ▼ heavy residue (> C18)] in the products at various H₂ pressures (temp. 375 °C; cat: feed ratio 1:10; reaction time 6 h).

yield increased exponentially from 6 to 27% on increasing the pressure from 50 bar to 120 bar. The kerosene (C9–C14) yield changed parabolically from 36 to 50% on increasing the pressure. Minima (at 27%) can be observed in the kerosene (C9–C14) yield at around 75 bar. The diesel (C15–C18) and heavier hydrocarbon (> C18) yield increased linearly from 39 to 42% and from 19 to 23%, respectively, on changing the pressure from 50 to 75 bar. The diesel (C15–C18) and heavier (> C18) hydrocarbon yield decreased sharply from 42 to 8% and 23 to 15% respectively, indicating that severe hydrocracking occurs with an increase in pressure.

Varying the pressure had a significant impact on the hydrocarbon types in the liquid product (Figs. 4 and 5). The alkane component was > 80% at or below 75 bar and then decreased rapidly above this pressure, decreasing to 8% at 120 bar (Fig. 4). Polyaromatics and Aromatics yields were constant at 5% at or below 75 bar, but increased rapidly to 60% and 36%, respectively at 120 bar. This trend for the polyaromatics and aromatics was similar to that of the < C9 and C9–C15 yield above 75 bar (Fig. 3). The increase in aromatics may be correlated with the increase in cracking activity, which favors aromatization at higher pressure. The cycloalkanes yield was slightly higher than that of the aromatics and polyaromatics at or below 75 bar pressure, but it decreased to 1% at 125 bar from 10% at 75 bar (Fig. 4). Based on results presented in Figs. 3–5, it may be concluded that the reaction at 50 bar and 375 °C was the best for product formation; to minimize undesired coking and to prolong the catalyst life. Simulated distillation results indicated that 6% of the compounds were formed in the gasoline range (IBP–135 °C), 65% of the compounds were formed in kerosene range (135–260 °C) and 29% of compounds were in the diesel range (260 °C - FBP) at 375 °C and 50 bar H₂. 2D-GCXC results indicated the formation of 87.47% alkanes, 9.67% cycloalkanes, 0.18% aromatics and 2.48% polyaromatics under similar conditions.

Table 1 Indicates the gas phase analysis of products at 350 °C, 375 °C, and 50 bar H₂. Hydrogen consumption, at 50 bar H₂ pressure,

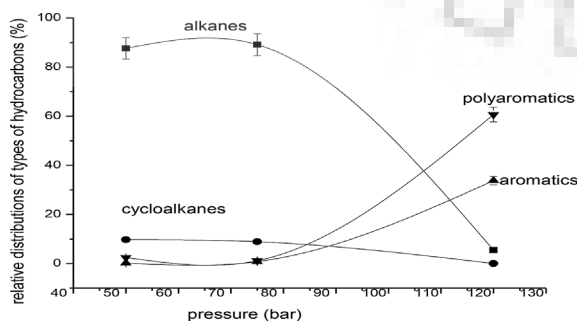


Fig. 5. Distribution of hydrocarbon types [■ alkanes, ● cycloalkanes, ▲ aromatics, and ▼ polynuclear aromatics] in hydroprocessed products at various H₂ pressures (temp. 375 °C; cat: feed ratio 1:10; reaction time 6 h).

Table 1

RGA data for Hydroprocessing of algae Lipids at 350 °C and 375 °C at 50 bar H₂.

Reaction Condition	% gases					
	Consumed			Evolved		
Temp. (°C)	H ₂ (bar)	H ₂ (± 5)	CO ₂ (± 5)	CO ((± 5))	C ₃ H ₈ (± 5)	C1–C5 (except C ₃ H ₈) (± 5)
350	50	15	4.79	0.30	2.18	12.1
375	50	30	19.01	0.61	5.41	14.2

was found to be approximately 15 ± 5% at 350 °C, while on increasing temperature to 375 °C, the consumption increased to 30 ± 5%. The increase in hydrogen consumption at higher temperatures indicates increasing in hydrocracking reactions, also evident from increasing C1–C5 hydrocarbons under these conditions Table 1 Increase in CO/CO₂ concentration at 375 °C temperature as compared to 350 °C temperature indicates an increase in C–C cracking reactions as compared to C–O bond cracking reaction on increasing reaction temperatures (Table 1).

Based on the above results, the mechanism for removal of oxygen content in the lipids are cracking (catalytic cracking), hydrodeoxygenation (HDO), and decarboxylation/decarbonylation (removal of oxygen to form CO₂/CO). First C=C bond in the alkyl chain gets hydrogenated, and then C=O of fatty acids, propane (Table 1) are produced through the hydrogenolysis of saturated triglycerides followed by the hydrodeoxygenation of fatty acids to alkanes [18,23]. The degree of hydrocracking/hydrotreating of the feed into pure hydrocarbons was always > 99% in this study which was confirmed by GC/MS analysis, which showed the absence of oxygen and nitrogen containing compounds. GC/MS shows the highest selectivity towards pentadecane and hexadecane in the liquid hydrocarbons without any oxygen or nitrogen containing product hydrocarbon.

A study of hydroprocessing of lipids extracted from *Botryococcus braunii* algae over CoMo/Al₂O₃ catalyst (without P promoter) showed that only 15% kerosene (jet fuel) (C9–C14) was obtained even at higher temperature and pressure (400 °C and 200 bar respectively) [24]. Catalyst life is dependent on char/coke deposition rate. Catalyst deactivation was mainly due to the deposition of coke on the catalyst. Char/coke formation over the P promoted catalyst was nearly 10 times lower than that over catalyst without P as a promoter, which indicates that the P promoted catalyst has better catalyst life [20].

In the mechanism for direct deoxygenation, vacant sites are created by the removal of hydrogen sulphide in the presence of H₂. Hydrogen, activated by heterolytic dissociation forming one S-H and one Mo-H group; with oxygen in the feed material adsorbing onto the vacant sites. An adsorbed carbocation is formed after the donation of a proton from the S-H group. This intermediate undergoes direct C–O bond cleavage and generates a deoxygenated product. The vacant sites are recovered by the formation of H₂O from the adsorbed OH and H group [18].

The distribution of hydrocarbon types (gasoline, kerosene, diesel and heavy hydrocarbons) at 325 °C and 50 bar H₂ (Fig. 6), shows that kerosene (C9–C14) yield increased as the reaction time progressed, reaching a maximum (up to 56%) after 8 h. However, the gasoline yield formed maxima (24%) at a reaction time of 4 h, while the diesel range hydrocarbon formed minima (~20%) at 5 h and the heavy hydrocarbon yield continuously increased with time of reaction. This happened because, the conditions were not severe enough for cracking, slight cracking leading to the formation of the kerosene range of hydrocarbon.

The hydrocarbons distribution at 350 °C and 50 bar H₂ at various reaction time are shown in Fig. 7. It can be seen that at a reaction time of 6 h the gasoline (< C9) product formed minima (46%). It can also be seen that the gasoline yield was doubled by increasing the reaction temperature by 25 °C (325–350 °C). However, the kerosene (C9–C14)

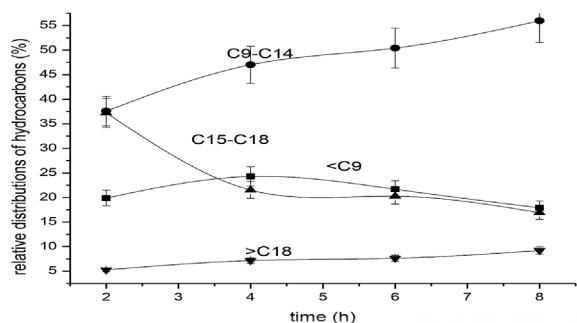


Fig. 6. Distribution of hydrocarbons [■ gasoline (< C9), • kerosene (C9–C14), ▲ diesel (C15–C18), and ▼ heavy residue (> C18)] in the products at various reaction times (temp. 325 °C; cat: feed ratio 1:10; pressure 50 bar).

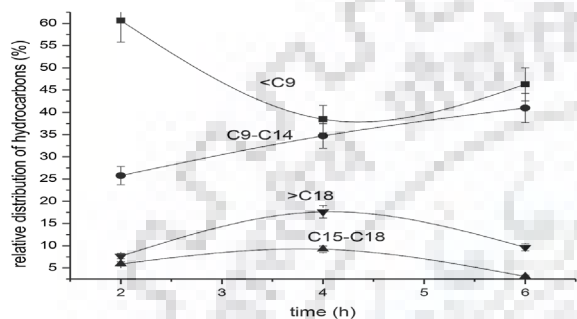


Fig. 7. Distribution of hydrocarbons [■ gasoline (< C9), • kerosene (C9–C14), ▲ diesel (C15–C18), and ▼ heavy residue (> C18)] in the products at various reaction times (temp. 350 °C; cat: feed ratio 1:10; pressure 50 bar).

yield increased linearly to 41% after a reaction time of 6 h. The higher hydrocarbon (> C18) and diesel (C15–C18) yield, form maxima of 18% and 9% respectively. The higher hydrocarbon yield decreased by almost 4% on increasing the temperature from 325 to 350 °C in Figs. 6 and 7. It may be concluded that a reaction time 4–6 h is optimal.

3.3. Kinetic studies

The apparent activation energy for the conversion of algae oil (Lipids) and its hydroprocessed product was calculated by Arrhenius plot [25]. The activation energy signifies the amount of energy required for conversion of lipids. Lower activation energy indicates reduced conversion temperatures and in-turn less energy requirement. Algal oil (neutral lipids) has a lower activation energy (14.96 kJmol⁻¹) as compared to that for *Jatropha* oil (26 kJmol⁻¹) [15–18] over CoMoP/Al₂O₃ catalyst, indicating improved conversion of algal oil lipids at low temperature, and less energy requirements when compared to *Jatropha* oil lipids [15,16].

The apparent activation energy for the formation of diesel (125 kJmol⁻¹) is less than kerosene (146 kJmol⁻¹), while apparent activation energy for the formation alkanes and polyaromatics hydrocarbons are 64 kJmol⁻¹ and 7 kJmol⁻¹ respectively. In comparison, the reported activation energy for *Jatropha* oil hydroprocessing over CoMoP/Al₂O₃ catalyst was 26 kJmol⁻¹, and those for kerosene, diesel, and heavier hydrocarbons formation were 83, 127 and 47 kJmol⁻¹ respectively [15].

4. Conclusions

Algal lipid was successfully hydroprocessed over sulfided CoMoP/Al₂O₃ catalyst. The results show that almost complete conversion of neutral lipids was achieved (375 °C and 50 bar H₂), by forming 6% of gasoline, 35% of kerosene, and 87% of alkanes. Pressures of 50 bar and temperatures of 375 °C were the best for minimizing undesired coking, and to prolong the catalyst life. Increased formation of aromatics (35%)

and cycloalkanes (10%) during the hydroconversion of marine microalgae *Nannochloropsis* sp. was observed indicating a new alternative renewable source for the petrochemical industry. Algal oil neutral lipids followed a pseudo 1st order kinetics and required less energy (14.96 kJmol⁻¹) when compared to *Jatropha* oil lipids for hydroconversion over CoMoP/Al₂O₃ catalyst.

Acknowledgments

We are thankful to the Hydroprocessing Laboratory of CSIR-IIP to support and help in experimental and analytical work. We are also thankful to CSIT-IIP for funding the research work under OLP 134919 (OLP- 0893).

Appendix A. Supplementary data

Supplementary data related to this article can be found at <https://doi.org/10.1016/j.biombioe.2018.08.011>.

References

- [1] Simon Jegan Porphy, Mohammed M. Farid, Feasibility study for production of biofuel and chemicals from marine microalgae *Nannochloropsis* sp. based on basic mass and energy analysis, *Renew. Energy* 11 (2012) 1–11.
- [2] Xiaowei Liu, Benjamin Saydah, Pragnya Eranki, Lisa M. Colosi, B. Greg Mitchell, James Rhodes, Andres F. Clarens, Pilot-scale data provide enhanced estimates of the life cycle energy and emissions profile of algae biofuels produced via hydrothermal liquefaction, *Bioresour. Technol.* 148 (2013) 163–171.
- [3] Zhou Dong, Liang Zhang, Shicheng Zhang, Hongbo Fu, Jianmin Chen, Hydrothermal liquefaction of macroalgae *Enteromorpha prolifera* to bio-oil, *Energy Fuels* 24 (2010) 4054–4061.
- [4] Yusuf Chisti, Biodiesel from microalgae, *Biotechnol. Adv.* 25 (2007) 294–306.
- [5] John J. Milledge, Benjamin Smith, Philip W. Dyer, Patricia Harvey, Macroalgae-Derived biofuel: a review of methods of energy extraction from seaweed biomass, *Energies* 7 (2014) 7194–7222.
- [6] T.J. Lundquist, I.C. Woertz, N.W.T. Quinn, J.R. Benemann, A. Realistic, Technology and Engineering Assessment of Algae Biofuel Production, Energy Biosciences Institute University of California Berkeley, California, October 2010.
- [7] Simon Jegan Porphy, and Mohammed M. Farid. Microalgae as a Renewable Source of Energy, a Niche Opportunity, Department of Chemical and Materials Engineering The University of Auckland, New Zealand.
- [8] Patrick Biller, Brajendra K. Sharma, Bidhya Kunwar, Andrew B. Ross, Hydroprocessing of bio-crude from continuous hydrothermal liquefaction of microalgae, *Fuel* 159 (2015) 197–205.
- [9] D.C. Elliott, T.R. Hart, A.J. Schmidt, G.G. Neuenschwander, L.J. Rotness, M.V. Olarte, Process development for hydrothermal liquefaction of algae feedstocks in a continuous-flow reactor, *Algal Res.* 2 (2013) 445–454.
- [10] Z. Li, P.E. Savage, Feed stocks for fuels and chemicals from algae: treatment of crude bio-oil over HZSM-5, *Algal Res.* 2 (2013) 154–163.
- [11] X. Bai, P. Duan, Y. Xu, A. Zhang, P.E. Savage, Hydrothermal catalytic processing of pretreated algal oil: a catalyst screening study, *Fuel* 120 (2014) 141–149.
- [12] R. Halim, P.A. Webley, G.J.O. Martin, The CIDES Process: fractionation of concentrated microalgal paste for co-production of biofuel, nutraceuticals, and high-grade protein feed, *Algal Res.* 19 (2016) 299–306.
- [13] Mukesh Kumar Poddar, Aditya Rai, Mannar Ram Maurya, Anil Kumar Sinha, Co-processing of bio-oil from de-oiled *Jatropha curcas* seed cake with refinery gas-oil over sulfided CoMoP/Al₂O₃ catalyst, *RSC Adv.* 6 (2016) 113720.
- [14] I.L.D. Olmstead, S.E. Kentish, P.J. Scales, G.J.O. Martin, Low solvent, low temperature method for extracting biodiesel lipids from concentrated microalgal biomass, *Bioresour. Technol.* 148 (2013) 615–619.
- [15] M. Anand, A.K. Sinha, Temperature-dependent reaction pathways for the anomalous hydrocracking of triglycerides in the presence of sulfided Co-Mo-catalyst, *Bioresour. Technol.* 126 (2012) 148–155.
- [16] F. Trejo, J. Ancheyta, Kinetics of asphaltenes conversion during hydrotreating of Maya crude, *Catal. Today* 109 (2005) 99–103.
- [17] M. Anand, S.A. Farooqui, R. Kumar, R. Joshi, R. Kumar, M.G. Sibi, Hari Singh, Anil K. Sinha, Kinetics, thermodynamics, and mechanisms for hydroprocessing of renewable oils, *Appl. Catal., A* 516 (2016) 144–152.
- [18] S. Zhang, Y. Yan, T. Li, Z. Ren, *Energy Sources* 31 (2009) 639–645.
- [19] Guoran Li, Wei Li, Minghui Zhang, Keyi Tao, Morphology and hydrodesulfurization activity of CoMo sulfide supported on amorphous ZrO₂ nanoparticles combined with Al₂O₃, *Appl. Catal. Gen.* 273 (2004) 233–238.
- [20] Yukio Sakashita, Yasuhiro Araki, Kosaku Honna, Hiromichi Shimada, Orientation and morphology of molybdenum sulfide catalysts supported on titania particles, observed by using high-resolution electron microscopy, *Appl. Catal. Gen.* 197 (2000) 247–253.
- [21] Changyan Yang, Rui Li, Chang Cui, Shengpeng Liu, Qiu Qi, Yigang Ding, Yuanxin Wu, Bo Zhang, Catalytic hydroprocessing of microalgae-derived biofuels: a review, *Green Chem.* 18 (2016) 3684.

- [22] Kwaka Chan, Mi Young Kima, Kyungil Choib, Sang Heup Moona, Effect of phosphorus addition on the behavior of CoMoS/Al₂O₃ catalyst in hydrodesulfurization of dibenzothiophene and 4,6-dimethyldibenzothiophene, *Appl. Catal. Gen.* 185 (1999) 19–27.
- [23] Jenny M. Lewis, Ronald A. Kydd, The MoO₃-Al₂O₃ interaction influence of phosphorus on MoO₃ impregnation and reactivity in thiophene HDS, *J. Catal.* 136 (1992) 478–486.
- [24] C. Stinner, R. Prins, Th Weber, Formation, structure, and HDN activity of unsupported molybdenum phosphide, *J. Catal.* 191 (2000) 438–444.
- [25] Kwaka Chan, Mi Young Kima, Kyungil Choib, Sang Heup Moona, Effect of phosphorus addition on the behavior of CoMoS/Al₂O₃ catalyst in hydrodesulfurization of dibenzothiophene and 4,6-dimethyldibenzothiophene, *Appl. Catal., A* 185 (1999) 19–27.

